

Extensible Modular Landing Systems for Human Moon and Mars Exploration

by
Wilfried Hofstetter

Master Thesis (Diplomarbeit) written at the
MASSACHUSETTS INSTITUTE OF TECHNOLOGY

in partial fulfillment of the requirements for the degree of
Diplomingenieur Maschinenwesen

at the
TECHNISCHE UNIVERSITÄT MÜNCHEN

December 2004

RT-DA 04/08

Supervision by
Prof. Olivier de Weck
Assistant Professor

Department of Aeronautics & Astronautics and
Engineering Systems Division, MIT

and

Prof. Ulrich Walter

Institute of Astronautics, TU Munich



Author.....

Cambridge, Massachusetts,
December 13, 2004

Certified by.....

Prof. Olivier de Weck

Hiermit bestätige ich, dass ich diese Arbeit eigenständig und nur mit den angegebenen Hilfsmitteln angefertigt habe.

I hereby certify that I completed this thesis on my own, using only the works quoted.

Author.....

Cambridge, Massachusetts,
December 13, 2004

Contents

1.	Introduction.....	12
1.1	Motivation and Context - The Vision for Space Exploration.....	12
1.2	Flexible and Extensible Systems	16
1.2.1	Design for Changeability	17
1.2.2	Flexibility	19
1.3	Thesis Objectives and Outline	21
1.4	Thesis Roadmap.....	25
1.5	Summary of Chapter 1	26
2.	Landing System Architecture and Conceptual Manned Spacecraft Modeling.....	27
2.1	Existing and Proposed Moon and Mars Exploration System architectures	27
2.1.1	The Apollo System	27
2.1.2	The Mars Design Reference Mission of NASA	29
2.1.3	Systematical Architecture Generation	31
2.2	Conceptual Manned Spacecraft Modeling.....	39
2.2.1	Empirical Model	39
2.2.2	Scaling Model.....	51
2.3	Summary of Chapter 2.....	54
3.	Moon and Mars System Architectures Point Designs	55
3.1	Mission Type Network	55
3.2	Architecture Point Designs	61
3.2.1	Results for Mars Missions	62
3.2.2	Results for Lunar Missions	66
3.2.3	Preferred Missions and Architectures	70
3.3	Trade Analysis	74
3.3.1	Lunar Staging Orbit and Continuous Surface Abort Options.....	74
3.3.2	Crew Size and Mission Duration For Lunar Missions.....	76
3.3.3	Mars Free Return, Mars Staging Orbit and Mars Orbit Insertion.....	79
3.3.4	Number and Size of Propulsion Stages in the Landing System.....	82
3.4	Baseline Moon and Mars Exploration Architectures.....	86
3.5	Summary of Chapter 3.....	88
4.	Commonality and Modularity in Manned Moon and Mars Landing System Architectures.....	89
4.1	Two Approaches to Extensible Design.....	89
4.2	Modular Crew Compartments and Habitats	91
4.3	Propulsion Stage Commonality – “Mars Back”	96
4.4	Extensibility Through Modularization of Fuel Management Systems and Rocket Engines	101
4.5	Extensibility Through Modularization of the Life-Support and Electrical Power Subsystems for the CEV	106
4.6	Summary of Chapter 4.....	109
5.	Results, Conclusions, Further Work	110
5.1	Results, Conclusions, Further Work: Modeling	110
5.1.1	Architecture Modeling / Generation (Section 2.1)	110
5.1.2	Empirical and Scaling Models of Individual Spacecraft (Section 2.2)...	111

5.2	Results, Conclusions, Further Work: Moon and Mars Exploration System Point Designs.....	112
5.2.1	Point designs (Sections 3.1 & 3.2).....	112
5.2.2	Trades.....	114
5.3	Results, Conclusions, Further Work: Commonality and Modularity	116
5.3.1	Modularization of Pressurized Volumes for Crew Compartments and Habitats (Section 4.1).....	116
5.3.2	Commonality Between Propulsion Stages (Section 4.2)	118
5.3.3	Modularization of Propulsion Stages (Section 4.3)	120
5.3.4	Modularization of ECLSS and EPS Equipment (Section 4.4).....	121
5.4	Thesis Overall Summary.....	122
6.	Bibliography	124
7.	Appendices.....	128
7.1	Appendix A: Systematical Architecture Generation.....	128
7.1.1	Architectures with Crew Transfers in Orbit and on the Surface.....	128
7.1.2	Architectures with Crew Transfers in Transit.....	144
7.2	Appendix B: Δv Values, C_3 Energy, and Trip Times for Moon and Mars Transportation.....	154
7.2.1	The Patched-Conics Approximation.....	154
7.2.2	Transportation in the Earth-Moon System.....	157
7.2.3	Mars Transportation.....	161
7.3	Appendix C: Point Design Architecture Data.....	165
7.3.1	Architecture Results for In-Situ Propellant Production (ISPP)	165
7.3.2	Baseline point design Moon and Mars architectures	167
7.4	Appendix D: Vehicle Propulsion Stages with Equal Tank Sizes (i.e. Propellant Masses)	172
7.4.1	Two Approaches to the Modeling of Propulsion Stages	172
7.4.2	Vehicles with Two Identical Propulsion Stages	173
7.5	Appendix E: Commonality and Modularization.....	177
7.5.1	Reference Data for Moon and Mars Architectures and Vehicles with Modularized Pressurized Volumes	177
7.5.2	Modular Building Blocks for the CEV Electrical Power Subsystem Equipment.....	181

List of Figures

Figure 1-1: Overview of the President’s Vision for Space Exploration [Bush, 2004]	12
Figure 1-2: Overview of the transformed organizational structure of NASA [www.nasa.gov, 2004]	14
Figure 1-3: a, NASA budget 1958-1976, in 2004 \$ [Nadir, 2004]	15
Figure 1-4: Comparison of point designs (A) to designs with a high degree of extensibility (B)	17
Figure 1-5: Classification of a system’s changeability [Schulz, Fricke, 1999]	18
Figure 1-6: Aspects of flexibility [Crawley, de Weck, 2003]; DSM = Design Structure Matrix.....	20
Figure 1-7: Selection of operations for extensible system change	21
Figure 1-8: Top-level operational sequence for a Moon or Mars landing; operational steps shaded are specific to a Mars landing	22
Figure 1-9: The Doctrine of Successive Refinement [NASA, 1995]	23
Figure 1-10: Visualization of the two approaches to commonality and modularity in the context of Moon and Mars exploration system hierarchy	23
Figure 1-11: Thesis roadmap	25
Figure 2-1: Elements of the Apollo system	28
Figure 2-2: Overview of the Apollo mission operation sequence	29
Figure 2-3: Manned vehicles for the NASA Mars design reference mission	30
Figure 2-4: Operational overview of the Mars design reference mission (1 st mission); for every vehicle inserted towards Mars, two heavy lift launches are necessary: one for the vehicle, and one for the nuclear TMI propulsion stage.....	30
Figure 2-5: Four early test architectures for definition of CEV vehicle requirements [MIT, 16.981 Course 2004]	31
Figure 2-6: Definitions and nomenclature for schematic architecture representation	32
Figure 2-7: Top-level architectural option space for manned operations in the vicinity of Moon or Mars	33
Figure 2-8: Combined habitat and landing vehicles and their qualitative decomposition (right-hand side).....	34
Figure 2-9: “Legal” design vectors according to Rules 1-12.....	37
Figure 2-10: Architecture overviews for Apollo (left), and Apollo with a dedicated long- duration surface habitat (right).....	37
Figure 2-11: Architecture diagrams for the NASA Mars Design Reference Mission (left), and a 1-vehicle architecture (right)	38
Figure 2-12: Overview of empirical crew compartment computational model.....	39
Figure 2-13: Logarithmic model for the pressurized volume per crewmember as a function of mission duration [Larson, Pranke, 2000]	40
Figure 2-14: habitable volume required per crewmember as a function of mission duration [Larson, Pranke, 2000]	41
Figure 2-15: Crew compartment mass as a function of $N_{Crew} \cdot \Delta t_{Mission} \cdot V_{Pressurized}$ for short mission durations and / or small crew sizes.....	42
Figure 2-16: Crew compartment mass as a function of $N_{Crew} \cdot \Delta t_{Mission} \cdot V_{Pressurized}$ for medium mission durations and / or crew sizes	43

Figure 2-17: Crew compartment mass as a function of $N_{Crew} \cdot \Delta t_{Mission} \cdot V_{Pressurized}$ for long mission durations and / or large crew sizes crew size	43
Figure 2-18: Habitat masses as a function of argument for various resupply fractions ...	45
Figure 2-19: Engine weight to thrust over absolute thrust for various engines	46
Figure 2-20: Overview of NASA's RLL spacecraft and subsystems [Wingo, 2004]	52
Figure 2-21: Crew compartment masses generated with a model based on the NASA RLL (red dots); the blue dots represent the empirical NASA model of section 2.2.1 with 125%, 100%, and 75% values.....	53
Figure 3-1: Distinction between mission and architecture	55
Figure 3-2: Network of conceivable manned Moon and Mars landing missions; mission durations based on [MIT 16.89 Course 2004, Walberg 1993]	56
Figure 3-3: Reorientation of polar lunar orbits with the respect to the Earth due to the Moon's orbital motion (not to scale)	57
Figure 3-4: Two possible opposition class Mars mission geometries with Venus flybys [NASA, 1994], [Walberg 1993].....	58
Figure 3-5: Conjunction class Mars mission overview.....	59
Figure 3-6: Architecture IMLEO results for 30-day short Mars mission	62
Figure 3-7: Architecture IMLEO results for a 60-dya short Mars mission	63
Figure 3-8: Architecture IMLEO results for a conjunction class Mars mission.....	64
Figure 3-9: Architecture IMLEO results for a fast conjunction class Mars mission	65
Figure 3-10: Architecture IMLEO results for a 3-day lunar landing mission (Apollo)....	66
Figure 3-11: Architecture IMLEO results for a 14-day lunar landing mission	68
Figure 3-12: Architecture IMLEO results for a 30-day lunar landing mission	69
Figure 3-13: Architecture IMLEO results for a 180-day lunar landing mission	70
Figure 3-14: Preferred mission type network for further trade analysis.....	71
Figure 3-15: Overview of preferred lunar architectures, numbers are vehicle designations	72
Figure 3-16: Preferred Mars architectures, numbers are vehicle designations.....	73
Figure 3-17: Hardware elements of the preferred Moon and Mars architectures (TMI / TLI stages not shown); commonality and modularity are not yet considered (point designs). The numbers besides the vehicles are the designations of these vehicles in the architecture diagrams from Figure 3-15 and 3-16	73
Figure 3-18: Results for lunar staging and abort trade	75
Figure 3-19: Total TEI velocity change including a 90° plane change maneuver of a HELO before returning to Earth	75
Figure 3-20: Pareto front for mass-effectiveness over IMLEO for lunar landing missions with varying crew size and duration	77
Figure 3-21: Diagram of mass-efficiency over cumulative lunar surface stay time for varying crew size and mission duration.....	78
Figure 3-22: Habitable volume requirements and saving	78
Figure 3-23: Mission geometry in the vicinity of Mars for staging operations	79
Figure 3-24: Systematical overview of operations in Mars vicinity in the form of a so-called Object-Process-Diagram [Dori, 2002]	80
Figure 3-25: Results of the trajectory and staging operations trade for the 'Blend' architecture.....	82

Figure 3-26: Operational architecture for landing on the Moon with equally sized propulsion stages; the spacecraft on the left were planned (and built) for the Soviet lunar landing	83
Figure 3-27: Trade results for the lunar surface habitat and the lander ascender vehicle	84
Figure 3-28: Trade results for Mars landing vehicles	85
Figure 3-29: Hardware elements of the baseline Moon and Mars architectures (TMI / TLI stages not shown)	86
Figure 3-30: Concepts of operation for lunar and Mars CEVs	87
Figure 4-1: Two approaches to extensible design: design reuse (commonality), and modularization	89
Figure 4-2: Pressurized volume requirements for crew compartments and surface habitats	91
Figure 4-3: Pressurized surplus volume for building blocks between 10 and 25 m ³ [pictures from www.astronautix.com , 2004]; the Apollo CM accommodated 3 crew, the Soyuz 2 or 3 crew	92
Figure 4-4 Pressurized volume surplus for habitat building blocks between 80 and 360 m ³	93
Figure 4-5: New operational scenarios for the CEV due to the modularization of crew compartments	95
Figure 4-6: Long Mars mission hardware; heat shields and TMI stages not shown	98
Figure 4-7: 180 day Moon mission (the lander and orbiter are the hardware for the 3-day mission); TLI stages not shown	98
Figure 4-8 Short Mars mission hardware; heat shields and TMI stages not shown	99
Figure 4-9: Notional hardware development roadmap for commonality and design reuse of propulsion stages	99
Figure 4-10: Modularized hardware for a long Mars mission	102
Figure 4-11: Modularized hardware for a 180-day lunar mission; the orbiter and the lander / ascender are the hardware needed for a 3-day lunar landing mission	103
Figure 4-12: Modularized hardware for a short Mars mission	103
Figure 4-13: Notional hardware development roadmap for modular Moon and Mars exploration systems	104
Figure 4-14: Possible arrangement of subsystem modules in the CEV (horizontal cross-section); the crew sizes and durations are arbitrary and not directly related to the architectures proposed above; scalability for up to six crew is assumed	107
Figure 4-15: Modularization of life support equipment dry mass for 3- and 6-crew; based on the scaling model developed in Subsection 2.2.2	108
Figure 4-16: Modularization of life support equipment dry mass for 3-, 4- and 6- crew; based on the scaling model developed in Subsection 2.2.2	108
Figure 5-1: Preferred architectures and missions, and associated IMLEO values; please note: for the three-day lunar mission, actually an Apollo-architecture without surface habitat is employed, which is a subset of the Apollo + surface habitat architecture	114
Figure 5-2: Baseline architectures (result of trade analysis) and associated IMLEO values; please note: for the three-day lunar mission, actually an Apollo-architecture without surface habitat is employed, which is a subset of the Apollo + surface habitat architecture	115

Figure 5-3: Process for the design of extensible systems, consisting of two sub-processes: (1) point design as a basis for (2) design for extensibility (for all elements / subsystems / components).....	117
Figure 5-4: Rationale for the selection of approach one or approach two for the extensible design of elements, subsystems, or components.....	122
Figure 7-1: Illustration of the concept of the Sphere of Influence (SOI) in the Earth-Moon system	154
Figure 7-2: C_3 energy in the context of planetary arrival	156
Figure 7-3: Lunar C_3 arrival energy and velocity change in Earth orbit as a function of the time of flight between perigee and Moon encounter	159
Figure 7-4: Lunar arrival energy to velocity change in LLO conversion table	160
Figure 7-5: Lunar arrival energy as a function of the inclination of the transfer orbital plane to the Moon's orbital plane	161
Figure 7-6: Departure and arrival energies, as well as heliocentric orbital periods for Earth-Mars transfers as a function of transfer time	162
Figure 7-7: Departure and arrival energies, as well as heliocentric orbital periods for Mars-Earth transfers as a function of transfer time	163
Figure 7-8: Departure / arrival energy to velocity change conversion table for Mars and Earth.....	163
Figure 7-9: Architecture IMLEO requirements for a fast conjunction class mission with free-return for the case of 'ideal' ISPP	166
Figure 7-10: Architecture IMLEO requirements for a 30-day lunar landing mission for the case of 'ideal' ISPP	166
Figure 7-11: Qualitative comparison of the two modeling approaches.....	172
Figure 7-12: Velocity changes for two sequentially used propulsion stages with equal propellant masses (sizes) as a function of the total velocity change (for liquid methane / liquid oxygen propulsion)	174
Figure 7-13: Payload mass fraction for two sequentially used propulsion stages with equal propellant masses (sizes) as a function of the total velocity change (for liquid methane / liquid oxygen propulsion) compared to the optimal payload fraction (equal velocity changes)	174
Figure 7-14 Velocity changes for two sequentially used propulsion stages with equal propellant masses (sizes) as a function of the total velocity change (for liquid hydrogen / liquid oxygen propulsion).....	175
Figure 7-15: Payload mass fraction for two sequentially used propulsion stages with equal propellant masses (sizes) as a function of the total velocity change (for liquid hydrogen / liquid oxygen propulsion) compared to the optimal payload fraction (equal velocity changes)	175
Figure 7-16: Velocity changes for two sequentially used propulsion stages with equal propellant masses (sizes) as a function of the total velocity change (for hypergolic propulsion)	176
Figure 7-17: Payload mass fraction for two sequentially used propulsion stages with equal propellant masses (sizes) as a function of the total velocity change (for hypergolic propulsion) compared to the optimal payload fraction (equal velocity changes)	176

Figure 7-18: Normalized modularization mass penalty for the electrical power equipment dry mass due to interface masses and surplus functionality for a 3-, and a 6-crew CEV	182
Figure 7-19: Normalized modularization mass penalty for the electrical power equipment dry mass due to interface masses and surplus functionality for a 3-, a 4-, and a 6-crew CEV	182

List of Tables

Table 2-1: Pressurized and habitable volumes per crewmember of existing or proposed spacecraft designs	41
Table 2-2: Arguments and reference masses for existing or proposed manned spacecraft designs.....	44
Table 2-3: Resupply fractions and mass flows for various loop closures in the life support system [Messerschmid, 1997].....	45
Table 2-4: Structural factors for spacecraft propulsion stages [Wingo, 2004; Gavin, 2002]	46
Table 2-5: Apollo 17 LM characteristics [NASA, 1972; Gavin, 2002].....	49
Table 2-6: Component masses calculated with the empirical model in comparison the Apollo 17 LM [NASA, 1972; Gavin, 2002]	50
Table 2-7: Sensitivity analysis of the Apollo LM for perturbations of the input parameters	50
Table 2-8: Conversion of RLL subsystem masses into mass fraction or specific masses for modeling purposes [NASA, OASIS, 2004; Wingo, 2004]	52
Table 3-1: Reference data for velocity changes and mission phase durations used in the analysis of point designs in Section 3.2	58
Table 3-2: Reference data for opposition-class Mars missions, adapted from [Walberg 1993]	59
Table 3-3: Reference data for conjunction class missions, according to [Walberg 1993], and for a reference mission based on ideal coplanar Hohmann transfers (see Appendix B).....	60
Table 3-4: Vehicle design variables unspecified by the top-level architecture model; these variables apply to all architectures.....	61
Table 3-5: Architecture ranking for a 30-day short Mars mission.....	63
Table 3-6: Architecture ranking for a 60-day short Mars mission.....	64
Table 3-7: Architecture ranking for a conjunction class Mars mission	65
Table 3-8: Architecture ranking for a fast conjunction class Mars mission	66
Table 3-9: Architecture ranking for a 3-day lunar landing mission.....	67
Table 3-10: Architecture ranking for a 14-day lunar landing mission.....	68
Table 3-11: Architecture ranking for a 30-day lunar landing mission.....	69
Table 3-12: Architecture ranking for a 180-day lunar landing mission.....	70
Table 3-13: Staging options for the realization of the continuous surface abort option for polar landing sites	74
Table 3-14: Crew size and cumulative surface time options	76
Table 3-15: Option space for Earth-Mars trajectory and Mars staging operations trade; options underlined and italic are undesirable and disregarded for the analysis.....	81
Table 3-16: Reference data for a fast-conjunction class mission with a two-year free-return trajectory (see Appendix B)	81
Table 3-17: Propulsion stage trade space for Moon and Mars landing systems.....	82
Table 3-18: Mass multipliers or ‘growth factors’ for parachutes, heat shields, TMI and TLI for the individual vehicles in the baseline architectures	87
Table 4-1: Mass overheads for architectures with modularized crew compartments and habitats	95

Table 4-2: Impulse and thrust for liquid methane / liquid oxygen propulsion stages.....	97
Table 4-3: Mass overhead and deviations for propulsion stage design reuse in addition to habitat and crew compartment commonality (see Section 4.2)	100
Table 4-4: Sensitivity of the tank and engine building block values to perturbations in various parameters	105
Table 4-5: Building block sizes for modularization with and without the short Mars mission	106
Table 4-6: Equipments mass for life support and electrical power systems as a function of crew size (according to the scaling model of Section 2.2)	106
Table 7-1: Sample architectures from literature for the (0, 1, L, N, N, N, N) architecture	130
Table 7-2: Sample architecture from literature for the (1, 2, L, S, N, N, N) architecture	131
Table 7-3: Sample architectures from literature for the (2, 2, L, S, S, N, N) architecture	134
Table 7-4: Sample architectures from literature for the (2, 2, O, L, O, N, N) architecture	135
Table 7-5: Sample architecture from literature for the (2, 3, L, S, O, N, N) architecture	137
Table 7-6: Sample architectures from literature for the (4, 3, O, L, S, S, O) architecture	143
Table 7-7: Radii of the SOI for solar system bodies.....	155
Table 7-8: Reference data from literature on Earth-Moon transportation	157
Table 7-9: Three reference conjunction class Mars missions, as well as for Mars descent and ascent, used for trade studies and baseline architectures in Sections 3.3 and 3.4	164
Table 7-10: Reference data for the 3-day lunar lander and orbiter, and for the 14-day surface habitat	168
Table 7-11: Reference data for the 30-day, and 180-day surface habitats.....	169
Table 7-12: Reference data for a fast-conjunction class Mars mission with free return (see Appendix B, Section 3.3).....	170
Table 7-13 Reference data for a 60-day short Mars mission with a Venus-flyby on the way back to Earth (see Section 3.3).....	171
Table 7-14: Reference data for the 30-day and 180-day lunar surface habitats employing the modularized habitat structure (“plugs” + end cones).....	177
Table 7-15: Reference data for the lunar lander, the lunar orbiter, and the 14-day lunar surface habitats employing the modularized habitat structure (“plugs” + end cones), and the CEV structure (22 m ³).....	178
Table 7-16 Reference data for a fast-conjunction class Mars mission architecture employing a free return, and using the modularized habitat structure (“plugs” + end cones), and the CEV structure (22 m ³)	179
Table 7-17: Reference data for a 60-day short Mars mission architecture employing a Venus flyby, and using the modularized habitat structure (“plugs” + end cones), and the CEV structure (22 m ³).....	180

List of Acronyms

ATV	Automated Transfer Vehicle
CEV	Crew Exploration Vehicle
CM	Command Module
CSM	Command & Service Module
DAV	Descent / Ascent Vehicle
DRM	Design Reference Mission
ELV	Expendable Launch Vehicle
EM-L1	Earth-Moon Libration point 1
ERV	Earth Return Vehicle
ESA	European Space Agency
FLO	First Lunar Outpost
HLLV	Heavy Lift Launch Vehicle
HMM	Human Mars Mission
ISPP	In-Situ Propellant Production
ISPR	International Standard Payload Rack
ISRU	In-Situ Resource Utilization
ISS	International Space Station
LM	Lunar Module
MAV	Mars Ascent Vehicle
NASA	National Aeronautics and Space Administration
NEA	Near Earth Asteroid
NEO	Near Earth Object
NTP	Nuclear Thermal Propulsion
OTV	Orbital Transfer Vehicle
TEI	Trans-Earth Insertion
TLI	Trans-Lunar Insertion
TMI	Trans-Mars Insertion

Nomenclature

α	Mass fraction, sensitivity
β	Scaling parameter
δ	Design distance
η	Normalized mass overhead
ζ	Normalized volume overhead
a	Functional requirement value
A	Area
g	Local gravity
I	Specific impulse
m	Subsystem / component mass
n	Number of....
p	Impulse
r	Radius
Δt	Duration
T	Thrust
v	Velocity
V	Volume
W	Weight force

For Astrodynamics nomenclature in Appendix B please refer to [Bate, Mueller, White, 1971].

1. Introduction

1.1 Motivation and Context - The Vision for Space Exploration

On January 14, 2004, President George W. Bush announced a new United States Vision for Space Exploration for the coming years and decades. After the loss of Space Shuttle Columbia on February 1, 2003, a presidential directive on the future of the United States manned space program had been widely expected. The Vision for Space Exploration gives an overview of the goals and objectives for unmanned and manned US space exploration over the next years and decades.

According to the vision, the Space Transportation System (STS) will resume flights after the implementation of the recommendations made by the Columbia Accident Investigation Board (CAIB). The STS will be launched only on flights to the International Space Station (ISS), which will be completed by the year 2010, thereby fulfilling treaties and agreements with international partners. The STS will be retired after the completion of ISS assembly around the year 2010 [Bush, 2004].

In parallel to the continuing assembly of the ISS, a new manned Crew Exploration Vehicle (CEV) will be developed. The purpose of the CEV is to succeed the Space Shuttle in providing the US with a manned space flight capability, as well as serving as the core vehicle for future manned space exploration beyond Low Earth Orbit (LEO). The CEV is to be flight-tested in 2008, and the first operational manned flights are planned for 2014.

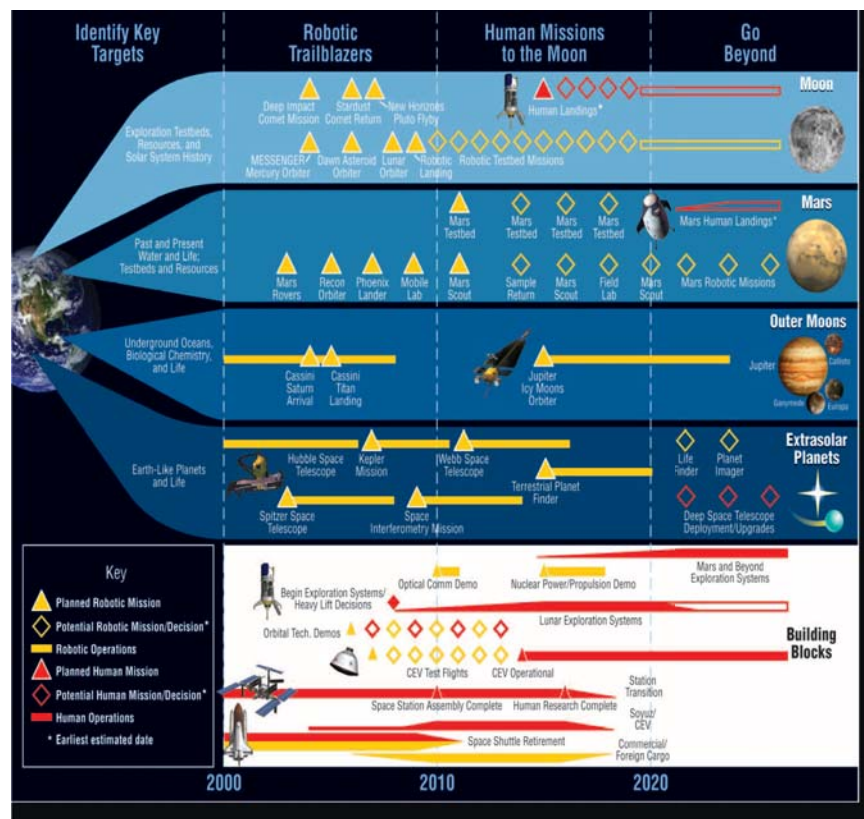


Figure 1-1: Overview of the President's Vision for Space Exploration [Bush, 2004]

Apart from these statements, which address the immediate future of US manned space flight in the wake of the Columbia accident, the presidential vision is centered around four themes (see Figure 1-1):

1. Robotic and human exploration of the Moon: according to the vision, robotic lunar exploration is to be resumed by a mission in 2005, and is to eventually lead up to a manned return to the lunar surface not later than 2020. Objectives for lunar exploration are the investigation of lunar resources, research into solar system history, and the use of the Moon as an operational testbed for more complex Mars missions.
2. Robotic and human Mars exploration: the manned exploration of the Martian surface is one of the long-range goals of the Vision for Space Exploration. It will be preceded by a number of unmanned missions, which will establish science, resource and operational knowledge needed for the manned missions.
3. Exploration of the Solar System: unmanned visits to other planets in the Solar System and their moons remain an important exploration goal. Besides the ongoing Cassini / Huygens Mission to the planet Saturn and its moons, the Jupiter Icy Moons Orbiter is base-lined for the 2010 to 2020 time frame. This mission is assumed to carry a nuclear reactor for power generation.
4. Astronomical research: the scientific observation of objects outside the Solar System is another major pillar of the exploration efforts in the coming years and decades. The search for extrasolar planets, especially Earth-like planets with conditions favorable to the development of life, is of special interest. After the retirement of the Hubble Space Telescope (HST), a number of satellite observatories, e.g. the Spitzer and the James Webb telescopes, are planned for the coming years (see Figure 1-1).

The foundation for the exploration activities described above is the development of key technologies, which will either enable new missions in the first place or significantly enhance exploration capabilities. The technology development activities are shown as fifth line of development in Figure 1-1. With the retirement of the STS and the development of the CEV, an important paradigm shift is established in the launch strategy: crew and cargo transportation will be separated as far as possible, instead of being combined, as in the STS. This will enable the use of non-man-rated launchers for most components of the exploration architecture, and is thereby also intended to provide opportunities for commercial participation in future US space exploration activities.

A large part of the research on board the ISS will be directed at the biological and physiological challenges posed by long-term manned space flight, thereby providing operational knowledge and experience for later missions to the Moon and Mars.

In addition, new technologies such as optical communications and nuclear power generation in space will be developed as well as new space vehicles, e.g. interplanetary transfer vehicles, planetary rovers, or spacecraft for planetary landing. This thesis will focus on the development of manned planetary landing systems.

In the weeks and months after publication of the presidential Vision for Space Exploration, the National Aeronautics and Space Administration (NASA) underwent a process of structural transformation to better meet the different exploration goals and objectives posed by the vision (see Figure 1-2).

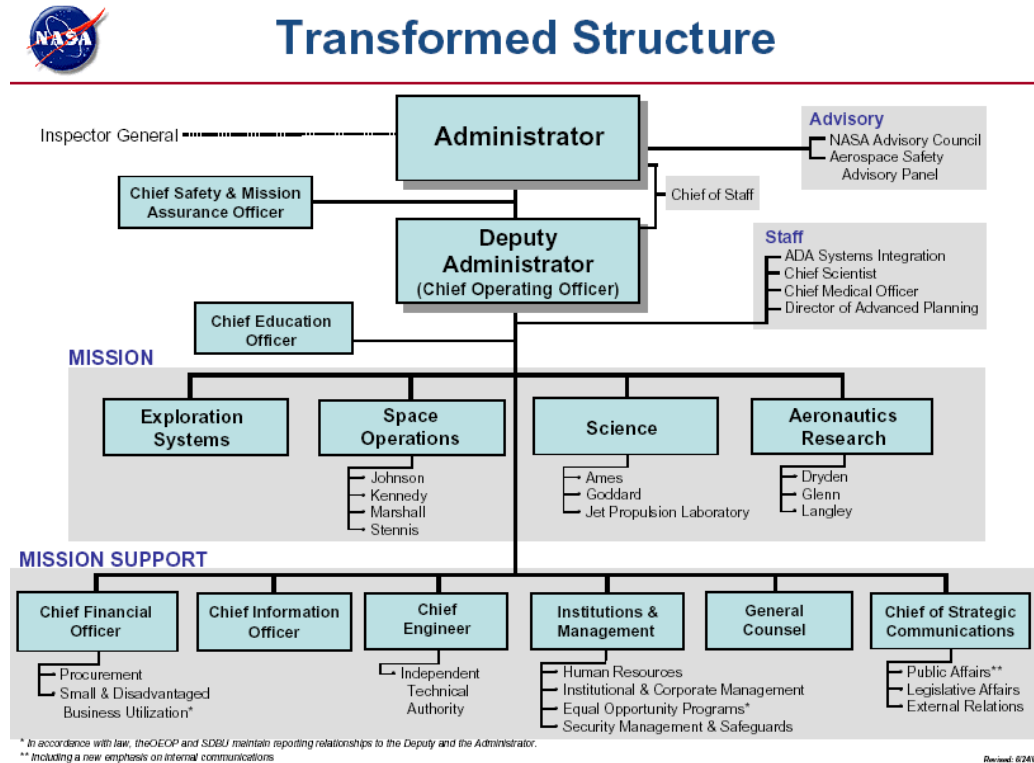


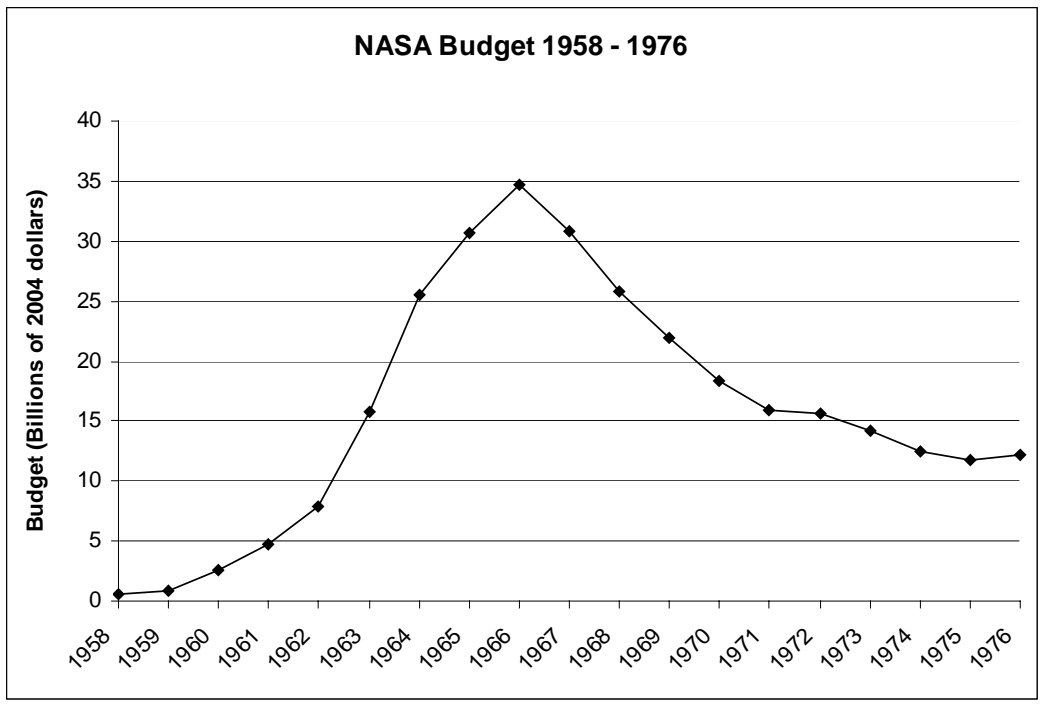
Figure 1-2: Overview of the transformed organizational structure of NASA [www.nasa.gov, 2004]

The agency is now organized in four main directorates:

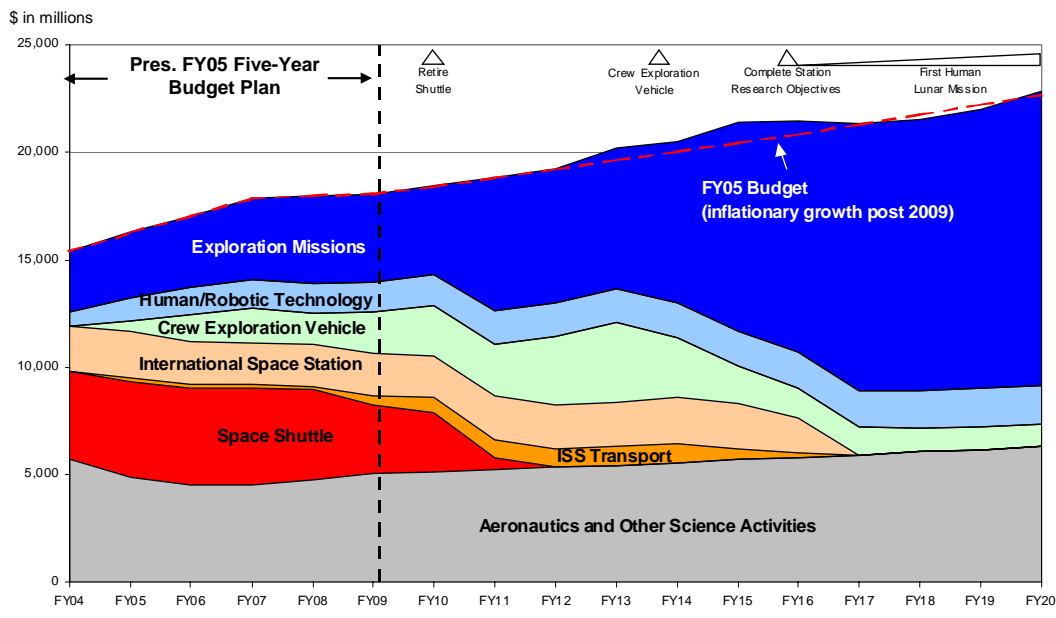
1. The Space Operations Directorate, focused on launch and in-space operations, e.g. for the STS and the ISS
2. The Science Directorate, focused on robotic missions and remote sensing of the Earth, the Solar System and the known universe (e.g. extrasolar planets)
3. The Aeronautics Research Directorate, focused on advanced vehicle development for atmospheric flight
4. And the newly created Exploration Directorate, dedicated to the development of technology and systems needed for sustained human and robotic exploration over the next decades.

The activities detailed in the President's Vision for Space Exploration span a time-frame of over 25 years, from the return to flight of the STS in 2005 until a proposed human Mars landing around 2030. The realization of this exploration program will thus depend on the approval of many future administrations and Congresses. In order not to commit future administrations to providing funding for programs and decisions taken decades ago, the vision proposes a stepping-stone approach for the realization of the exploration goals: exploration capabilities will be built up one at a time, thereby leaving room for flexible decisions and developments at any point in time. This approach is intended to make long-term space exploration affordable and sustainable by requiring moderate resource allocations at any particular time instead of major resource commitments upfront for large projects as in the case of the Apollo program (see Figure 1-3a).

This stepping-stone approach for sustainable and affordable space exploration is illustrated by the proposed budget allocations for NASA in the near future. Figure 1-3b shows a budget overview published with the Vision for Space Exploration:



a,



b,

Figure 1-3: a, NASA budget 1958-1976, in 2004 \$ [Nadir, 2004]
b, NASA's near- and long-term budget plan, inflation corrected [Bush, 2004]

According to the President's five-year budget plan, the NASA budget will be increased by about 1 billion \$ from 2005 to 2009, and will then retain its buying power over the following years. Figure 1-3b shows that the retirement of the Space Shuttle around 2010 and the transitioning of ISS leadership around 2017 will open up resources needed for the development of new systems for lunar, and later Mars missions and for the operation of these missions.

As the total NASA budget has a fixed upper boundary, an increase in the cost of a particular development project will directly cause a delay in the schedule of the associated exploration activity: in the triangle of cost, scope and schedule, only the latter can give way, when the first two are fixed. Each new system that has to be developed represents a new major project, and therefore decreases the probability of staying within, or close to the envisioned exploration schedule. Also, due to the tight budget constraints shown in Figure (1-3b), it is unlikely that several point design architectures for manned Moon and Mars exploration could be developed at all. At the height of the Apollo program, the annual budget allocated to NASA was on the order of several percent of the GDP (see Figure 1-3a, [Godwin, 2000]); the exploration budget planned for the coming years is well below the 1 percent mark.

In light of these observations, the ability to reuse systems and components designed for early lunar missions on later and more demanding lunar and Mars missions will be a key factor for the success of NASA's exploration mission. The following section gives a brief overview of design principles and methodology associated with flexible and extensible design and illustrates them for the example of manned landing systems. For additional information about the Vision for Space Exploration see reference [Bush, 2004].

1.2 Flexible and Extensible Systems

Reusing¹ systems and components (both hardware and software) from early manned lunar landing missions on longer Moon and Mars missions has a variety of effects on the development of these systems or components: the same design will have to deliver its functionality under changing conditions. These changes can be internal to the system, as well as in the operating environment of the system. For Moon and Mars landers, the different velocity changes required and the associated differences in propellant mass would cause a change internal to the system; the different radiation (electromagnetic and charged particles) conditions in lunar and Mars orbit [Larson, Pranke, 2000] would be an example of a change in the operating environment.

If a system or component design has to provide functionality under varying conditions, the number of conditions or requirements for the design will in most cases be higher than for a point design like a lander with the sole purpose of executing a short lunar landing mission. An increased number of requirements will, however, generally increase the complexity and risk of the development associated with the design, thereby increasing the cost of the project. Why is it then beneficial to design a system for delivering value under changing conditions? Figure 1-4 illustrates the answer to this question:

¹ Please note: the term "reuse" is employed in the sense of using a system or component of identical design, not necessarily the same physical specimen of the system or component.

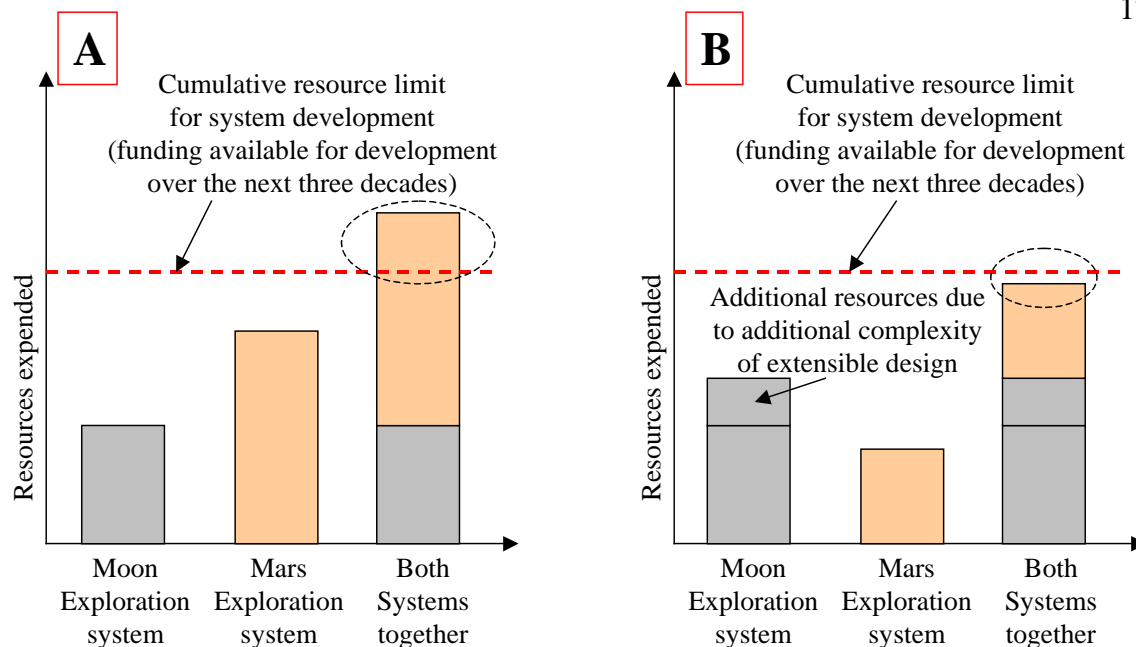


Figure 1-4: Comparison of point designs (A) to designs with a high degree of extensibility (B)

In scenario A, both systems represent point design, e.g. one system solely for lunar exploration, and another one devoted to Mars missions. The amount of spending available is limited to a certain amount per year, which prohibits the parallel development of both systems. The systems therefore have to be developed sequentially. During the development phase of system two, however, expenses for recurring costs caused by the operation of system 1 have to be made. With limited funds available, and a project as complex as a manned Mars mission, it is likely that the non-recurring development costs for system number 2 would exceed the spending threshold.

A possible solution to this problem is also illustrated in Figure (1-4): if the non-recurring development cost of system 1 is not exceeding the spending limit, the remaining resources can be used to increase commonality between systems 1 and 2, and thereby reduce the non-recurring cost for system 2 (scenario B). This is only possible, if the two systems employ a certain degree of common technology; for manned Moon and Mars mission this will, however, be quite likely.

It is important to mention that for every subsystem the penalties of commonality, apparent in Figure 1-4 as additional resources required for system 1, will have to be weighted against the possible gains for the development of system 2.

1.2.1 Design for Changeability

The design of systems for changing conditions and requirements is not an altogether new concept: in 1999, E. Fricke, A. Schulz, et al. proposed a framework and guiding principles for a methodology called “Design for Changeability” (DFC). They suggest two basic characteristics to capture the “changeability” of systems (see Figure 1-5):

1. The orientation of the system’s changes, i.e. whether the system adapts to intrinsic changes (i.e. changes in structure and functionality), or to changes in environmental conditions external to the system
2. The ease with which a system is able to react to changing conditions.

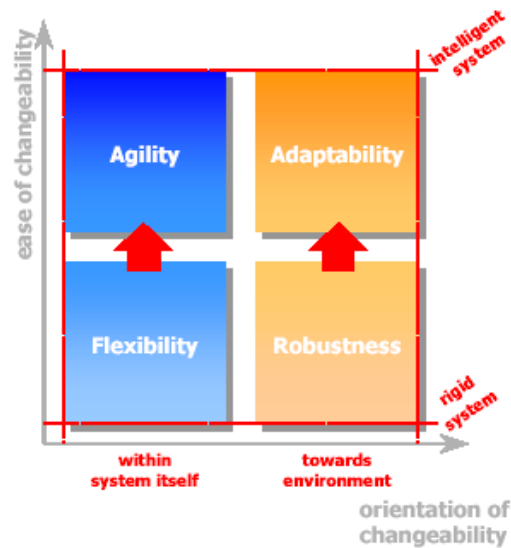


Figure 1-5: Classification of a system's changeability [Schulz, Fricke, 1999]

Employing these two aspects, [Schulz, Fricke, et al., 2000] define four basic properties of changeable systems:

“Flexibility represents the property of a system to be changed easily and without undesired effects.

Agility represents the property of a system to implement necessary changes rapidly.

Robust systems deliver their intended functionality under varying operating conditions without being changed.

Adaptability characterizes a system's capability to adapt itself towards changing environments to deliver its intended functionality”.

Together with these characterizations of system types, Fricke, Schulz et al. propose a set of enabling principles, derived from various sources, to achieve design for changeability: the principles of ideality / simplicity, of independence, of modularity / encapsulation, of integrability, of autonomy, of scalability / self-similarity, of non-hierarchical integration, and of decentralization. These principles can be grouped into basic principles, which support all the four aspects of changeability, and into extending principles, which apply only to some of these aspects. Also, this list of principles is not considered to be complete, but still growing. For some of the principles, simultaneous application yields negative results [Schulz, Fricke, et al., 2000].

It is important to note that the analysis of system changeability by [Schulz, Fricke, et al., 2000] was conducted in the context of a hyper-competitive business environments with relationships to fast-growing markets. Therefore it is by no means evident that the principles and methods suggested for design for changeability can be transplanted unmodified to the development of space exploration systems. On the basis of Figure 1-3, however, it can be assumed that the stringent budget constraint for NASA acts as a ‘virtual competitor’ in the decade-spanning exploration activities: if NASA is not able to keep the cost of system acquisition and operation below the spending limit, the United

States Congress is likely to stop or at least reduce the exploration activities. This situation bears a strong resemblance to system development in a very competitive business environment.

For the case of manned Moon and Mars landing systems, the most desirable system properties are flexibility and robustness: a lunar lander that is to be reused for landings in the different environment of Mars needs to be easily changed without undesired effects (e.g. guidance instability during powered descent). As Mars missions are planned for about a decade after the first Moon landings, it is not of particular importance that these changes can be accommodated rapidly (agility). Equally, the systems will be changed on Earth before launch, and do not have to adapt during the mission (adaptability). There will certainly be marked differences in the environmental conditions encountered by a Mars lander and a Moon lander (radiation environment, gravitational field, atmospheric and surface conditions, [Larson, Pranke, 2000]); however, the lunar lander design will not have to work in the Martian environment without prior refitting and reconfiguration (robustness) on Earth. Therefore, the most important property desired for lunar and Mars landing systems will be **flexibility**.

According to [Schulz, Fricke, et al., 2000], the design principles supporting design for flexibility are: the principle of ideality / simplicity, of independence, of modularity / encapsulation, of integrability, of autonomy, of scalability, of non-hierarchical integration, of decentralization, and of redundancy. The principles of integrability and decentralization exhibit of course a strongly negative mutual effect; they cannot be employed at the same time [Schulz, Fricke, et al., 2000]. Due to the modular nature of propellant storage, thrust generation, etc., the principle of modularity will be of special importance. The above-mentioned design principles will be indicated in this thesis when employed.

As indicated in Figure 1-5, design for changeability is associated with more upfront design expenditure, which will have to be offset by future saving in the development of follow-on systems. In order to enable informed decisions where and to what extent to introduce flexibility, agility, robustness and adaptability into a design, quantitative metrics have to be used to measure penalties in effectiveness and cost. For manned Moon and Mars landing systems these metrics will be mainly mass and mass-effectiveness (see Chapter 3); mass is used as a surrogate metric for cost. As spacecraft mass directly influences launch cost, and indirectly coupled to the development, assembly and test costs, this seems to be an acceptable metric for initial architectural analysis. Mass-effectiveness will be dependent on the actual function of the module or component that is being analyzed in Chapter 3.

1.2.2 Flexibility

As was discussed above, planetary landing systems are expected to be flexible systems in order to accommodate the changes induced during the lifetime of the system design. The concept of flexibility, however, is still not very specific, and encompasses several other system characteristics. Figure 1-6 shows three aspects that flexibility is commonly thought to represent [Crawley, de Weck, 2003]:

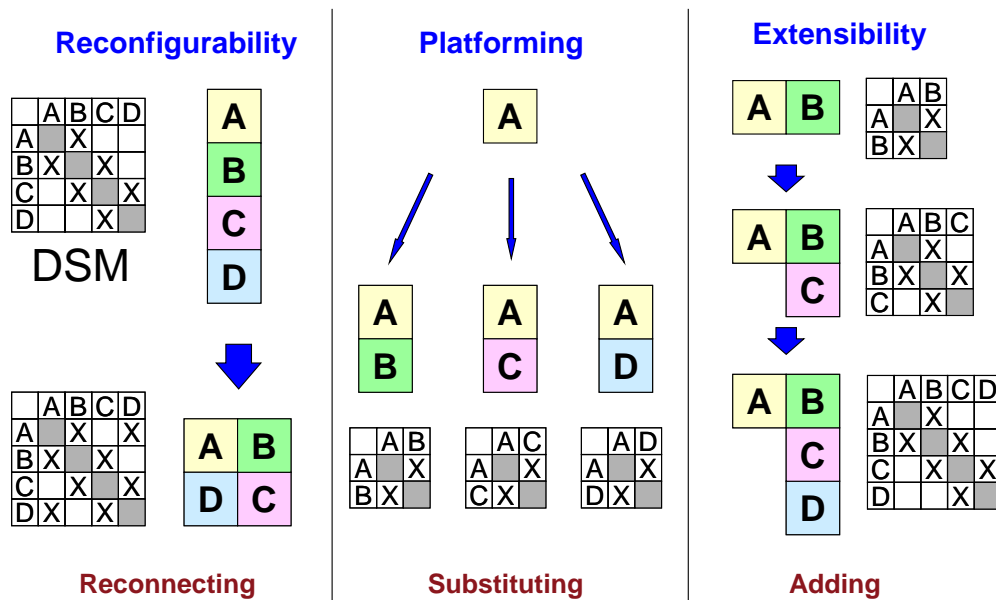


Figure 1-6: Aspects of flexibility [Crawley, de Weck, 2003]; DSM = Design Structure Matrix

The aspect of **reconfigurability** represents the possibility of rearranging and reconnecting a system's elements during its operational phase in order to provide changing functionality. In purely reconfigurable systems, the number of elements remains constant. A common example of reconfigurable systems is modern business office furniture, where shelves, tables etc can be easily arranged in different ways [de Weck, 2004]. Reconfigurability can be applied both to hardware and software.

Platforming refers to the fact that several systems with different overall functionality have a set of common core elements (in this case element A) that provides basic functionality. The platform design shown in Figure 1-6 necessitates a common interface between the core element A and the various additional elements B, C and D. Platform design is regularly employed in the automotive industry, where several different car designs have the same engines, gearboxes, etc., but a different chassis and exterior design [Simpson, 2003].

A system is called **extensible** if additional elements can be added in order to provide additional functionality. The key characteristic of an extensible design is the uncertainty if the additional elements will be connected; the system is able to deliver a certain functionality without them. The best intuitive example of a highly extensible design might be a system of LEGO-blocks: they can be easily reconnected, added, removed, reattached, swapped, etc [de Weck, 2004].

The number of different interfaces is generally higher for extensible systems than for platform-based systems. This is due to the fact that in the latter a limited number of core elements provide all the interfaces, whereas in extensible systems every additional element provides new interfaces for new elements.

Also, extensible systems cannot only accommodate the addition of elements, but also element subtraction and element swapping, and combinations of all these operations. Figure 1-7 illustrates these operations:

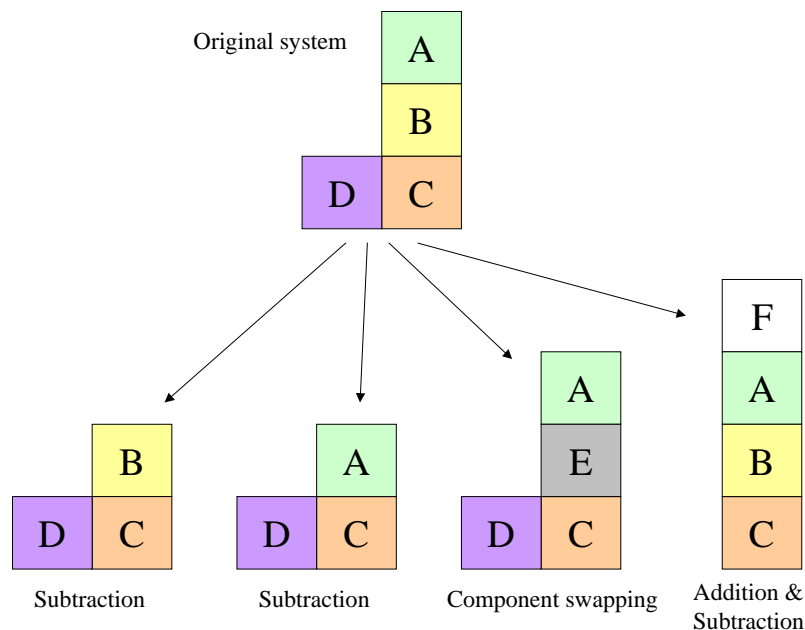


Figure 1-7: Selection of operations for extensible system change

Reconfigurability, platforming, and extensibility all involve changes in the relationships between their components, i.e. changes in the system's connectivity. For complex systems these components are modules that are in turn made up of less complex elements. The elements are grouped into modules so that the connectivity between a module's elements is high, and the number of relationships to elements of other modules is small. This operation of grouping elements into modules is also called clustering.

Modularity is one of the enabling factors of flexible design (see also principles of changeability above). The reverse statement, however, is not necessarily true: not all modular designs are automatically flexible. The ISS, for example, was designed in a highly modular fashion, due to the mass constraints posed by present launch technology (about 25 t of maximum payload to LEO). Though modules are added in stages during ISS assembly, thereby providing additional functionality, the ISS is not an extensible design: with every additional module, the guidance software has to undergo a redesign in order to accommodate the new dynamic characteristics of the station in orbit. Also, for the ISS, a strict assembly sequence has to be followed, whereas for a flexible system multiple pathways for adding functionality exist in order to accommodate uncertainty in future developments. The ISS, however, is reconfigurable to a certain degree, e.g. concerning the attachment of the solar power units [Messerschmid, 1997].

1.3 Thesis Objectives and Outline

For manned missions to the surface of the Moon and of Mars, the operations in the vicinity of the destination planet exhibit strong similarities concerning the required velocity changes, the operational phases (see Figure 1-8), staging options, and the expected duration of landing, ascent and rendezvous activities.

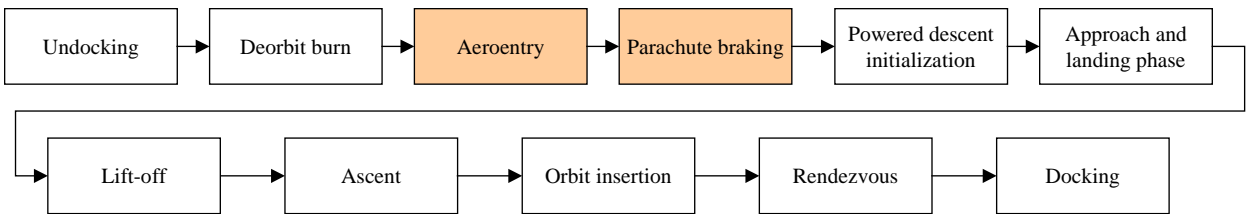


Figure 1-8: Top-level operational sequence for a Moon or Mars landing; operational steps shaded are specific to a Mars landing

Moon and Mars landing systems are therefore likely candidates for extensible design. The objectives for the work in this thesis are based on the assumption that landing systems are going to be made extensible, at least to a certain degree:

It is the goal of this thesis to develop and exercise a design process for modular extensible manned space systems, by

- 1. Analyzing instances of existing or proposed manned system architectures (Apollo, NASA Mars DRM, NASA First Lunar Outpost, Soviet Lunar Landing Architecture, etc.),**
- 2. Developing qualitative and quantitative models of manned space system architectures and individual manned spacecraft,**
- 3. Providing preliminary designs for customized Moon and Mars exploration systems as a starting point for extensible design,**
- 4. Exercising the process on customized manned Moon and Mars landing systems,**

Using a “cost”-function to capture the penalty of modularization and commonality, while also demonstrating that the design process is generalizable to generic design of modular extensible systems.

In order to carry out a successful and systematic conceptual design of customized Moon and Mars exploration systems, rigorous design methodology as described in Pahl, Beitz [Pahl, Beitz, 1997], and by NASA’s Doctrine of Successive Refinement [NASA, 1995] (see Figure 1-9) shall be employed. This encompasses the steps of requirements and functional analysis (‘Identify and quantify goals’), design space setup (‘Create concepts’), designs space and systems analysis (‘Do trade studies’), and an informed selection of the best alternatives (‘Select design’) to proceed to the next spiral with increased system resolution.

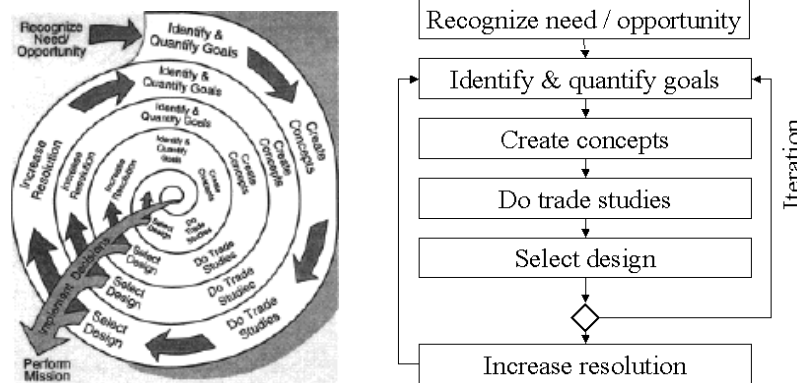


Figure 1-9: The Doctrine of Successive Refinement [NASA, 1995]

The customized architectures serve as the starting point for extensible design, which is based on identifying options for modularity and commonality on different systems levels. In this thesis, two different approaches to identifying options for extensibility are discussed (see Figure 1-10): the first is based on the reuse of propellant stage and rocket engine point designs for the Mars exploration architecture in the Moon architecture, and vice versa. This means that no extra development cost arises for the design that is reused in a different architecture. This approach couples the Moon and Mars exploration architectures at a very early stage in the design process: any later changes jeopardize the reusability of the designs.

The second approach is focused on the modularization and commonality of subsystems and components, i.e. on the lower levels of system hierarchy. In order to modularize successfully, the modular quanta with the smallest performance penalty have to be selected. This approach decouples the design of the Moon and Mars exploration system architecture, if the selection of the modular quanta is robust against minor changes in requirements that inevitably occur in the process of design. A certain level of robustness seems to be achievable, and is visualized in Chapter 4.

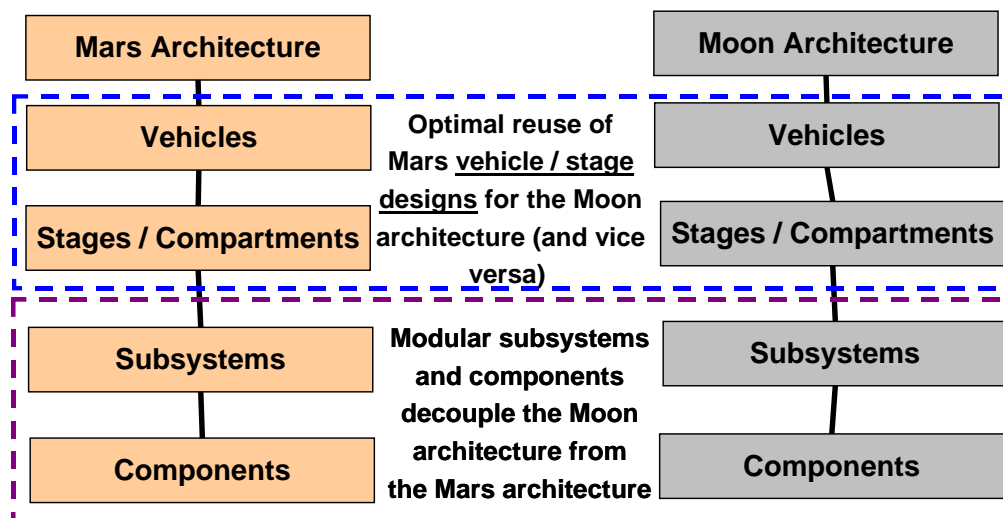


Figure 1-10: Visualization of the two approaches to commonality and modularity in the context of Moon and Mars exploration system hierarchy

The two approaches are not unrelated, and are not mutually exclusive. The difference between them is due to a relative weighting of the architectures: if a point design for the Mars architecture is reused in the Moon architecture, then the Mars architecture is weighed higher than the Moon architecture, because its requirements are satisfied exactly. If subsystems and components are modularized, then both architectures are weighed equally.

Design processes with qualitative similarities to the process outlined for the extensible system design in this thesis have been proposed before, e.g. for the platforming of unmanned science missions in the Solar System in [Gonzalez-Zugasti, Otto, Baker, 1998]. The process above, however, strives to systematically generate and evaluate exploration system architectures, and to quantify the performance penalties and the resulting “cost” caused by the introduction of commonality and modularity into these architectures. The quantification of performance penalties, or the “cost” of modularity is important, because the “economic” viability of modular design is determined by differences between savings in development, assembly and testing costs, which are counteracted by an increase in launch cost and by performance reduction [Enright, Jilla, Miller, 1998]. The penalty function can therefore serve as a decision-making tool for commonality and modularity (see Chapter 4).

Exact cost estimation for spacecraft is beyond the scope of this thesis; therefore, Injected Mass in LEO (IMLEO) will be used as a surrogate metric for cost. This appears to be appropriate, because IMLEO is directly related to launch cost, and to performance and effectiveness (crew-days on the destination surface / IMLEO). Also, the surplus in functionality, e.g. engine thrust, pressurized volume, tank volume, etc., generated by modularization can be perceived as a penalty, which is directly related to the “cost” of modularity. Both metrics will be used to evaluate the effect of introducing modularity into Moon and Mars exploration architectures (see Chapter 4).

It should be noted that, in some situation, functional surplus is actually useful, because it provides redundancy. An example for this would be a fuel cell for electrical power generation. If one unit fails, the surplus functionality of another unit could be used to recompense for the loss. Margins for redundancy, however, are assumed to be incorporated in the models, so that the surplus in functional attributes that is calculated below is a “real”, undesirable surplus.

The work presented in this thesis is part of the Massachusetts Institute of Technology’s Space Systems Laboratory’s contribution to the NASA Concept Evaluation & Refinement (CER) study for the development of requirements for the Crew Exploration Vehicle and for Human Lunar Exploration (HLE) architectures. Therefore, outlines of top-level CEV requirements are included in the architecture descriptions where appropriate.

1.4 Thesis Roadmap

This section gives an overview of the information flow in the thesis; Figure 1-11 documents this in the form of a so-called “thesis roadmap”:

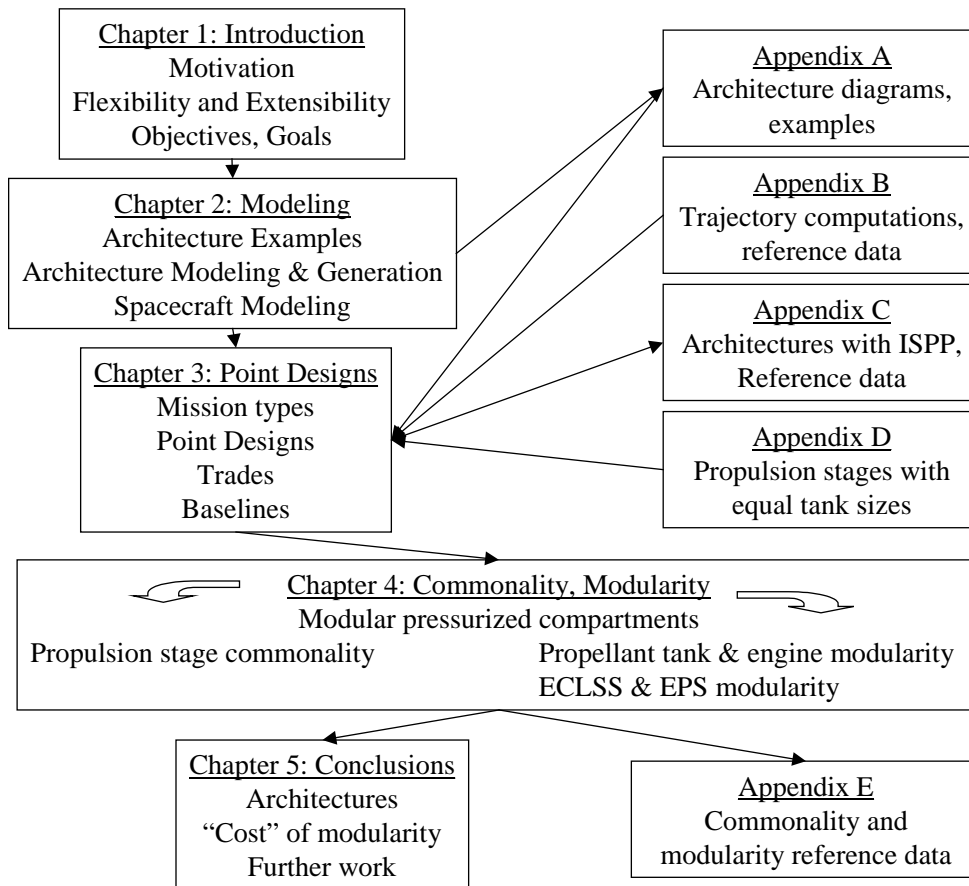


Figure 1-11: Thesis roadmap

The roadmap for this thesis is rather complex, because the flow of information branches at several points, and there are several sources for information input for different steps in the design process. This complexity is mainly due to the fact that the systematical design of customized architectures necessitates thorough mission analysis of Moon and Mars missions, and that many results have to be documented for reuse later in the thesis.

Chapter 1 provides an overview over the new Space Exploration Initiative and its budgetary background as a motivation for extensible design for manned Moon and Mars exploration architectures. In Chapter 2, models are derived for exploration architectures and for individual manned spacecraft, and are benchmarked against reference data. The architecture model enables the systematical generation of manned exploration system architectures in the vicinity of the destination planet. The resulting architectures and associated examples of existing or proposed architectures are documented in Appendix A. These architectures serve as basis for the systematical design in Chapter 3. Preferred architectures for Moon and Mars are selected based on IMLEO and abort considerations, and are then subjected to trades concerning various design parameters. The best trade options are selected, and with these, the preferred architectures are augmented. This leads

to so-called “baseline” architectures documented in Appendix C. Additional information input to the systematical design and trade studies is provided by Appendix B (trajectory data), and Appendix D (velocity changes for equally sized propulsion stages).

In Chapter 4, the two approaches to extensible design described above (one at the vehicle / stage level, one at the subsystem / component level) are exercised on the baseline architectures in order to identify options for commonality and optimal modular quanta for pressurized volumes, propellant tanks, rocket engines, life support and electrical power systems. The resulting modular architectures are documented in Appendix E.

Chapter 5 summarizes the methods and results developed in the preceding chapters, provides conclusions drawn from these results, and outlines interesting directions for possible future work on the subject of extensible design for manned spacecraft.

1.5 Summary of Chapter 1

The Vision for Space Exploration by President G. W. Bush set clear objectives and goals for US manned and unmanned space exploration in the next years and decades: a return of humans to the Moon no later than 2020 and manned missions to Mars around 2030. With the stringent budget constraints imposed on NASA, these exploration goals will only be affordable and sustainable (key requirements of the Space Exploration Initiative) if the necessary exploration systems will be flexible and modular, thereby enabling the reuse of component and module designs for different missions. Manned Moon and Mars landing systems are very promising for extensible design, because they exhibit many similarities in their operational scenarios and functional attributes. This thesis provides a systematical process to identify options for extensible design and quantify the performance penalties introduced by the realization of these options. NASA’s Doctrine of Successive Refinement will be applied to ensure a methodical, retraceable, and thorough design of customized Moon and Mars exploration systems.

2. Landing System Architecture and Conceptual Manned Spacecraft Modeling

2.1 Existing and Proposed Moon and Mars Exploration System architectures

A manned landing system for Moon and Mars exploration is always part of a larger Moon and Mars exploration architecture. The landing system and other elements of the architecture generally exhibit strong interrelations with other vehicles during the operational life of the exploration system. Also, it is conceivable that one vehicle serves as in-space transportation device, as well as landing craft [Hoffman, Kaplan, 1997; Zubrin, 1997]. Before commencing the design of modular extensible landing systems, it is therefore important to provide a systematic overview of existing or proposed exploration system architectures in order to understand and define what can be regarded as a manned landing system. For a definition of the exploration system hierarchy, please refer to Figure 1-10. Also, a generic model will be presented that is able to reproduce the sample architectures and generate new ones; the model attempts to span a wide space of architectural options with few parameters. Two sample architectures are presented below in more detail:

1. The **Apollo** architecture: the Apollo spacecraft is the only system for manned planetary landing ever flown.
2. The **NASA Mars Design Reference Mission** architecture

Additional proposed architectures for manned Moon and Mars exploration are described in Appendix A, along with the corresponding architecture diagrams (see section 2.1.3). Among them is also the architecture for the Soviet Moon Landing mission, which provides several interesting features. The hardware for the Soviet lunar missions was actually built and partially flown [Harford, 1997].

2.1.1 The Apollo System

NASA used the Apollo system in the 1960s and the early 1970s to conduct manned explorations of several locations on the lunar nearside. In the so-called Apollo program, 11 manned missions were conducted: two in Earth orbit (Apollo 7 and Apollo 9), 2 in lunar orbit (Apollo 8 and Apollo 10), six lunar landings (Apollo 11 – 12 and Apollo 14 - 17), and one aborted lunar mission (Apollo 13). Also, later, parts of the Apollo system were used for the Skylab orbital workshop program, and for the Soviet–American Apollo-Soyuz test project [www.spaceflight.nasa.gov, 2004]. The landing system, the so-called Lunar Module, performed flawlessly on every mission.

The Apollo lunar landing system is the only system ever flown successfully in a manned planetary landing mission; the Soviet lunar landing hardware was built and also partially tested; however, it has never been flown in a manned landing [Harford, 1997]. Apollo is therefore the prime benchmark for any architectural or vehicle models developed in this thesis, and is described in particular detail. The benchmarking only refers to the individual spacecraft, not the Apollo architecture.

Figure 2-1 provides an overview of the space-borne elements of the Apollo system:

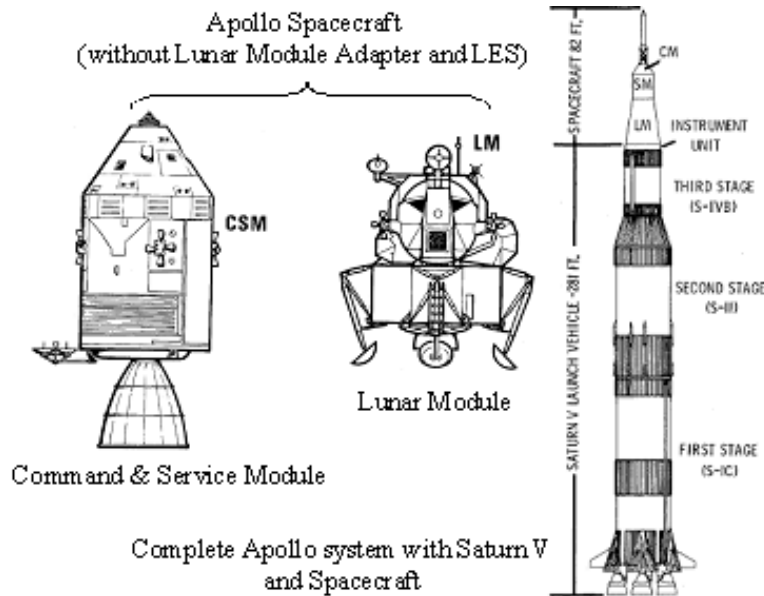


Figure 2-1: Elements of the Apollo system

The Apollo system can be decomposed into two main components: the launch rocket, and the so-called Apollo spacecraft. The launcher lifts the system into Earth orbit, and later inserts the Apollo spacecraft towards the Moon. The Apollo spacecraft at launch consists of the Launch Escape System (LES), the Command & Service Modules (CSM), the Lunar Module (LM), and the Lunar Module Adapter (LMA). The LES provides abort capability for the crew anytime from before launch to a certain height and velocity during launch, when it can no longer be accelerated along with the other elements and is dropped. The LMA covers the LM and transmits the thrust force to the CSM during launch, and is jettisoned after Trans-Lunar Injection (TLI) [NASA, 1969].

Figure 2-2 illustrates the operational profile of an Apollo lunar landing mission. During the ascent into LEO, the first two stages of the Saturn V rocket are burnt to depletion and then dropped; part of the propellant in the third stage (S IV-B) is also expended. In orbit, the remaining stack is tested and checked out, before being inserted on a trajectory towards the Moon by burning the remaining fuel in the S IV-B. After completion of the burn, the CSM separates from the stack, docks with and extracts the LM and moves away from the S IV-B and the jettisoned LMA panels [NASA, 1969, 1972].

The combined CSM and LM coast until a burn of the Service Propulsion System inserts them into an elliptical lunar orbit (LOI-1). The orbit is circularized after several revolutions (LOI-2) into a 110 km Low Lunar Orbit (LLO). After LM activation and checkout, two crewmembers undock the LM from the CSM, which performs a small orbit adjustment burn to put itself into a slightly different orbit (the “mini-football”), to stay clear of the LM. The LM performs a short Descent Orbit Insertion (DOI) burn that places the periselenium over the destined landing site. After one more revolution, the LM starts the Powered Descent (PD) near the periselenium, descends to the lunar surface, and lands. All the burns and maneuvers described above are performed either by the LM Reaction Control System (RCS), or the descent stage engine [NASA, 1969, 1972].

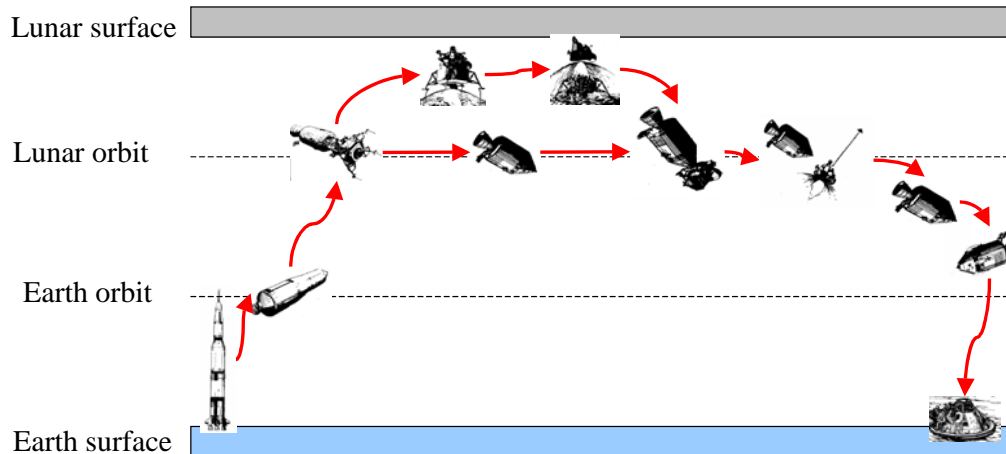


Figure 2-2: Overview of the Apollo mission operation sequence

After completion of the assigned crew surface operations, the LM ascent stage lifts off the lunar surface and ascends into an elliptical lunar orbit. Performing several small burns, the LM achieves rendezvous with the orbiting CSM, and the CSM (active) docks with the LM (passive). After transferring crew and samples into the CM, the LM is jettisoned and inserted either on a trajectory to a heliocentric orbit, or on a collision course with the Moon. The CSM stays for several more revolutions in LLO, and then performs the Trans Earth Insertion (TEI) burn that sends it back to Earth. Shortly before Earth entry, the CM and SM separate: the SM burns up in the atmosphere, and the CM with crew and samples performs a splashdown in one of the Earth's oceans [NASA, 1969, 1972].

2.1.2 The Mars Design Reference Mission of NASA

The NASA Mars Exploration Study Team at Johnson Space Center, Texas published the Mars Design Reference Mission (DRM) in 1997. The study represents a completely new approach to manned Mars exploration compared to the plans published in the 90-day report prepared for the Space Exploration Initiative in 1990 by President George Bush senior. The changes are largely due to the publication of the "Mars Direct" [Zubrin1997] mission plan several years earlier, which suggested extensive use of In Situ Propellant Production (ISPP) on the Martian surface to reduce propellant mass, and thereby overall mission mass. The DRM incorporates ISPP, albeit to a lesser extent than planned for "Mars Direct".

Figure 2-3 gives an overview of the vehicles used in the reference mission, and Figure 2-4 illustrates the mission operations. One Mars launch window before the manned mission, three vehicles are sent towards Mars: a Mars Ascent Vehicle (MAV), which starts generating propellant (CH_4 / LOX) out of imported hydrogen and CO_2 indigenous to the Martian atmosphere. A nuclear power plant provides the energy for this process. Also, an Earth Return Vehicle (ERV) is delivered to LMO; it will take the crew home after completing their surface mission several years later. The third vehicle sent to Mars is a transit & surface habitat identical to the one used by the crew 2 years later, which is positioned on the surface of Mars as a backup resource for crew survival, in case other

elements of the architecture fail. All vehicles are injected towards Mars with nuclear propelled insertion stages, and either aerocapture or perform aeroentry at Mars [Hoffman, Kaplan, 1997].



Figure 2-3: Manned vehicles for the NASA Mars design reference mission

In the next Mars launch window, approximately two years later, a manned transit and surface habitat is launched by a nuclear-propelled insertion stage towards Mars. After aerocapturing into Mars orbit and surveying the landing site, the crew begins descent to the Martian surface. They land in the immediate vicinity of the MAV and the prepositioned spare surface & transit habitat. After completion of the surface mission, and provided the ISPP for the MAV went well, the crew ascends to Mars orbit and docks with the waiting ERV. This, in turn injects them towards Earth, and sustains the crew during the 200-day journey. Shortly before entering the Earth's atmosphere, the crew separates from the ERV in a reentry capsule called ECCV (a scaled-up version of the Apollo CM), which has been attached to the ERV since Earth launch. The ECCV lands on the continental United States and brings the crew and samples back to Earth [Hoffman, Kaplan, 1997].

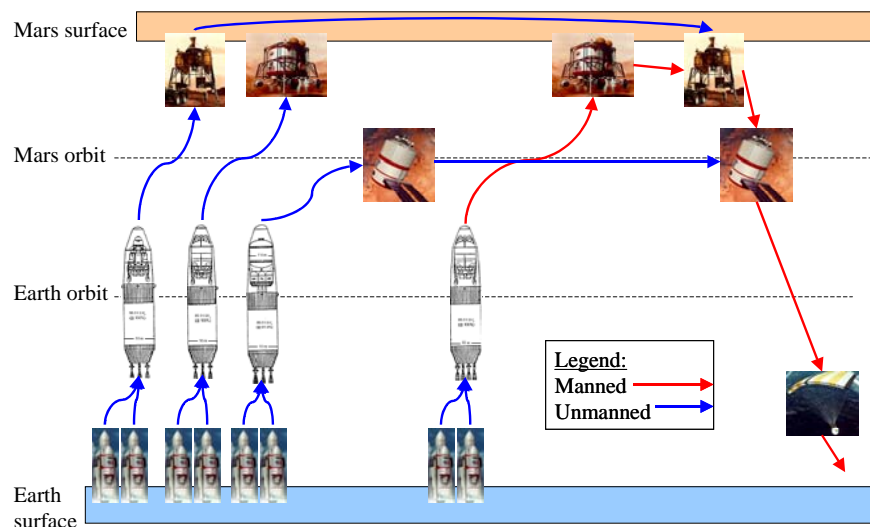


Figure 2-4: Operational overview of the Mars design reference mission (1st mission); for every vehicle inserted towards Mars, two heavy lift launches are necessary: one for the vehicle, and one for the nuclear TMI propulsion stage

2.1.3 Systematical Architecture Generation

For the extensible design of modular manned landing systems, it is necessary to define what exactly a manned landing system is. At first sight, this appears to be straightforward: a landing system is comprised of all the vehicles that sustain manned operations on the surface, and in transit to or from the surface. In any case, a manned landing vehicle has to make contact with the planetary surface while the crew is in the vehicle. The architectures presented in the preceding section, however, suggest that there are a variety of conceivable overall system architectures that can lead to manned Moon or Mars landings. All architectures are only possible under certain conditions, and have various advantages and disadvantages, especially concerning performance and risk (see Appendix A). It is therefore by no means evident, which architecture will be chosen for future Moon and Mars exploration.

In this section, an attempt will be made to generate and qualitatively describe a wide range of architectures, including the sample architectures, with a very limited range of variables. The idea for this approach is based on a practice used during early architectural studies in the MIT 16.981 space systems architecting course (research for the NASA CE&R project). The architectures shown in Figure 2-5 employ the categories of Earth Orbit Rendezvous (EOR), Lunar Orbit Rendezvous (LOR), and Lunar Surface Rendezvous (LSR) that were used during studies for Apollo [Houbolt, 1961]:

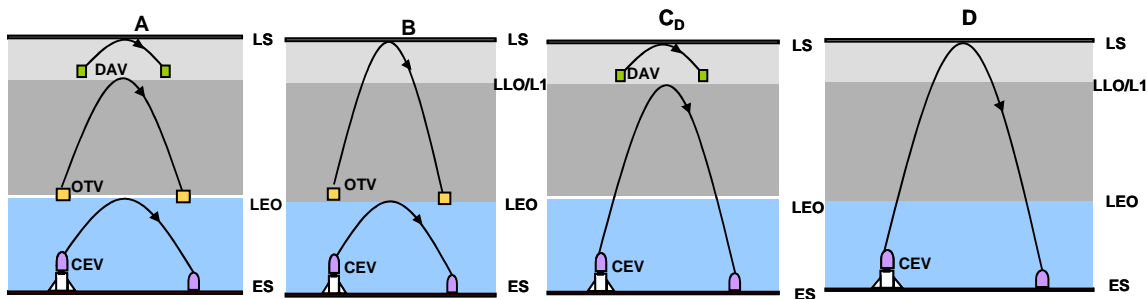


Figure 2-5: Four early test architectures for definition of CEV vehicle requirements [MIT, 16.981 Course 2004]

The test architectures shown in Figure 2-5 were derived by mapping out the manned operations, specifying the number of manned vehicles and the start and ending point of the manned operation of each vehicle. For architecture A, for example, three vehicles are employed: the first brings the crew to LEO, and back to the surface of the Earth. The second transports the crew from LEO to an unspecified lunar orbit, and back. The third craft lands the crew on the Moon, and lifts them back to orbit. All architectures appear to be “symmetrical” in the manned usage of spacecraft. From the perspective of the crew, the sequence of events is:

1. Ascend to LEO in vehicle 1
2. Switch to vehicle 2
3. Transfer to lunar orbit in vehicle 2
4. Switch to vehicle 3
5. Land on the lunar surface in vehicle 3

6. Surface activities
7. Ascend to LLO in vehicle 3
8. Switch to vehicle 2
9. Transfer to LEO in vehicle 2
10. Switch to vehicle 1
11. Land on Earth in vehicle 1

The underlined words and expressions contain all the information necessary to describe the architecture on a high level. The key parameters of a landing mission architecture are therefore the number of vehicles, the number of crew changes between these vehicles, the sequence of changes as well as where they take place, and the position of the crewed landing in the sequence of events.

Figure 2-5 also shows that every manned vehicle leaving Earth orbit necessarily enters the vicinity of the target planet (in this case, the Moon). Therefore there is a conservation law for manned vehicles, which decouples the Earth orbital operations from those in the vicinity of the target planet: only a vehicle inserted to the target planet can influence the operational architecture in the vicinity of the planet. As for manned landing systems, only operations in the vicinity of the target planet or in transit are of interest, we can neglect any changes between vehicles in Earth orbit for a top-level analysis of manned systems in the vicinity of the Moon and Mars.

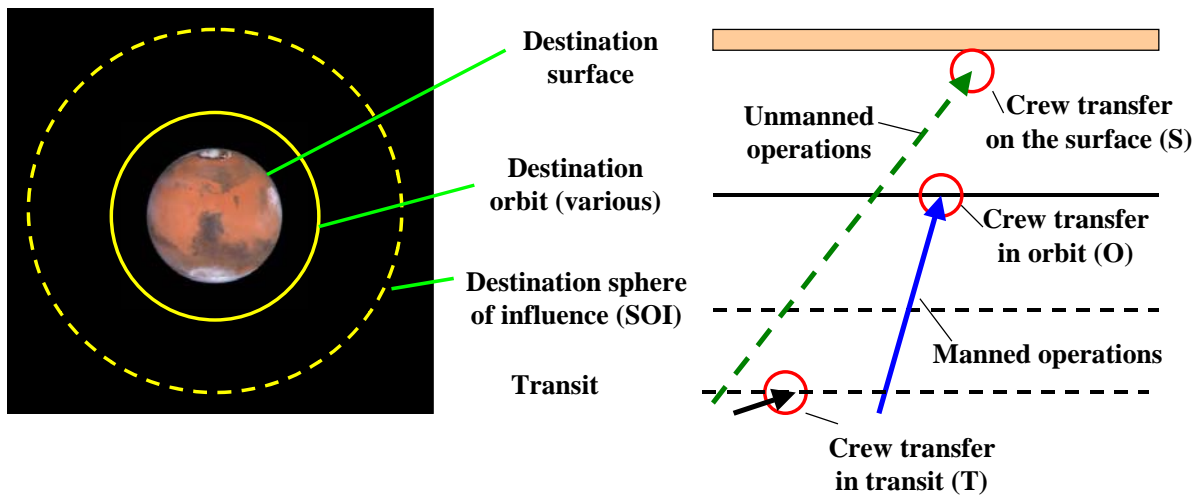


Figure 2-6: Definitions and nomenclature for schematic architecture representation

Due to this decoupling, the variables for describing planetary landing system architectures are:

1. The number of vehicles inserted towards the destination (Moon or Mars)
2. The number of crew transfers between these vehicles
3. The sequence of changes / switches, and where they take place (orbit / surface)
4. The position of the crew landing in the sequence of events

Figure 2-6 provides an overview of the syntax for schematically describing a Moon or Mars exploration architecture. Different colors represent different vehicles. Unmanned operations are indicated by a dashed arrow, manned by a solid arrow. A red circle represents crew transfers from one vehicle to another. “L” stands for landing on the surface of the destination planet, “O” for crew transfers in orbit, “S” for crew transfers on the surface, “T” for crew transfers in transit, and “N” for non applicable. Vehicle one is represented by a blue line, vehicle two by a green, and vehicle three by a black line.

Figure 2-7 shows the architecture variables arranged in a Morphological Matrix [Pahl, Beitz, 1997], in which the rows list the options for the design variables:

Number of crew transfers between vehicles	0	1	2	3	4
Number of vehicles	1	2	3		
Event 1	O	L	T		
Event 2	S	O	L	T	N
Event 3	S	O	L	T	N
Event 4	S	O	L	T	N
Event 5	S	O	L	T	N

Figure 2-7: Top-level architectural option space for manned operations in the vicinity of Moon or Mars

Going through the rows of the matrix and selecting one option generates one particular set of design variables describing one particular landing system. This can be visualized by a so-called design vector: the components are the selected options for the design variables. In Figure 2-7, the process is shown for the design vector $(1, 2, L, S, N, N, N)^T$; this is the “Mars Direct” architecture proposed by [Zubrin, 1997], which is discussed in more detail in Appendix A, Section 7.1.1.

It is important to mention that there are many characteristics of an exploration architecture that are, on purpose, not determined by the variables in the Morphological Matrix. For example, it is not determined

1. If vehicles travel together or separately (abort options, second pressurized volume available)
2. What propellants the individual vehicles use (storable / cryogenic)
3. If ISRU / ISPP is employed or not (drives surface power needs)
4. If aerocapture is used for Mars Orbit Insertion (MOI) or not; etc.

This leaves room for variations and design trades of the individual Moon and Mars architectures during detailed design (see Chapter 3). The Morphological Matrix in Figure 2-7 only provides information about the manned and unmanned usage of a vehicle, i.e. a top-level view of the architecture captured with few variables.

Not every design vector generated with the Morphological Matrix from Figure 2-7 contains a viable set of options; some options cannot be realized without others, and some are contradictory. We therefore have to provide a number of rules for the generation of useable (“legal”) design vectors. These rules are as follows:

Rule 1: Only manned vehicles are modeled (i.e. spacecraft with both a crew compartment and propulsion stages)

This rule was implicitly introduced above, and is based on the assumption that crew and cargo will be separated to a maximum extent; this is supported by the Vision for Space Exploration [Bush, 2004]. Also, during the course of the NASA CE&R study, it became clear that surface operations’ architectures (rovers, equipment, etc.) are of a level of complexity comparable to the in-space transportation architecture [Hoffman, 2004]; it is therefore beyond the scope of this thesis to model the surface architectures. Cargo for surface operations is assumed to be predeployed unmanned and is not modeled here.

A manned vehicle is defined as a vehicle that has exactly one crew compartment, and one or more propulsion stages. In several studies for manned Mars missions, however, vehicles have been proposed that exhibit two crew compartments (see Figure 2-8, [Goodwin, 2001], [ESA, 2004]): one crew compartment is located in the ascent stage of the vehicle, and provides a habitable environment for the crew during ascent and descent. The other crew compartment is located in the descent stage, and serves as habitat during the stay on the surface. In this case, the crew does not actually change or transfer between vehicles, but between habitats or crew compartments. On the right side of Figure 2-8, it is shown that these configurations are qualitatively equivalent to a landing system that consists of a lander for crew transport to and from the surface, and of a surface habitat: the ascent stage and the surface habitat can both be regarded as being the payload of a common landing stage, which can then be split into two landing stages which deliver the ascent stage and the habitat separately to the surface. The quantitative discussion of propulsion stages in section 2.2 shows that in a first-order approximation, both the combined and the separate system have the same mass.

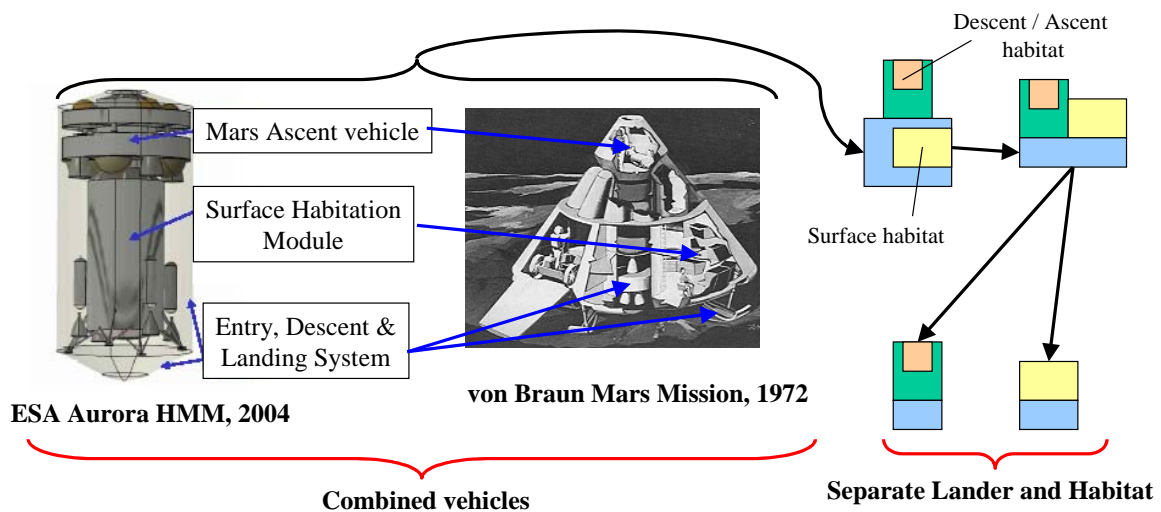


Figure 2-8: Combined habitat and landing vehicles and their qualitative decomposition (right-hand side)

The combination of a surface habitat and a lander / ascender spacecraft in one integrated vehicle has advantages and disadvantages. The advantages are that there is no need for surface rendezvous, and that there are small mass savings by integrating vehicles rather than having separate ones (only one landing gear, etc.). The disadvantages, however, are that the combined vehicle can be too heavy to be launched (>100 tons), that the extension of a short-term surface habitat into a long-term habitat will necessitate a complete redesign (also of the ascending stage), that the surface habitat cannot be predeployed on a low-energy trajectory or by electric propulsion, and that in the event of an abort to orbit the descent stage with the habitat is dropped and lost. This list of advantages and disadvantages is by no means complete; nevertheless it appears that separate vehicles are more desirable. This question will be answered during the trade studies in Chapter 3.

Rule 2: Every manned vehicle has to be used at least once

Redundant vehicles are provided in some architectures to reduce mission risk, for example for Mars Direct [Zubrin, 1997], and for the NASA Mars DRM [Hoffman, Kaplan, 1997]. In order to ensure a design vector that points uniquely to one architecture, however, we need to exclude redundant vehicles. Backup vehicles and abort strategies will be discussed during architecture selection in Chapter 3.

Rule 3: For n crew transfers, the number of vehicles must be below (n+1)

This rule is directly related to Rule 2: if for n changes the number of vehicles exceeds (n+1), then the crew cannot use all vehicles during the mission unless the crew is split at some point during the mission. This is prohibited by Rule 8 (see below.)

Rule 4: A vehicle that the crew has used and then abandoned rests at the location where the crew last used it

It is assumed in this model that all manned vehicles, except the one the crew rides in the beginning, are predeployed to their respective crew transfer locations. The crew then transfers to these vehicles and is transported to another location. Additional autonomous maneuvers of vehicles beyond predeployment, however, are excluded, because they inflict additional operational risk on the mission. As every vehicle plays a vital role for the success of the mission, the failure of an autonomous maneuver would automatically lead to mission loss. Therefore it is desirable to have all the vehicles in place before the crew sets out [Hoffman, Kaplan, 1997; Zubrin, 1997].

Rule 5: Crew transfers on the surface can only occur after landing

The crew has to land on the destination surface, before they can access and change to another vehicle prepositioned there, i.e. design vectors containing the sequence (... , S, ... , L, ...)^T are invalid. It is assumed that pinpoint landing capabilities next to predeployed assets are developed.

Rule 6: The crew goes to the surface only once per (nominal) mission, and does not return

Event sequences that have the crew land, go back to orbit and land again, i.e. design vectors containing the sequence (... , L, ... , L, ...)^T are excluded; the crew only lands once on the surface.

Rule 7: The vehicles are numbered in sequence of crew occupancy

This is more of an arbitrary convention than a rule. The vehicle that the crew sets out in is vehicle 1, the next vehicle the crew transfers to is vehicle 2, etc.

Rule 8: The entire crew always stays together

Enabling the crew to split up and rejoin later on would apply a strong constraint on the feasibility of a landing system design; architectures like the NASA Mars DRM, for example, would no longer be possible. Also, in the case of Mars, the cost of transporting a human being to Mars would seem too high to not land him on Mars [Hoffman, 2004]. It is recognized, however, that especially for early lunar landing missions, operational scenarios where crewmembers stay in orbit are conceivable. Designs enabling this are still contained in the design space; they are treated as an exception for architectures where one vehicle is abandoned in orbit and later picked up again (see Apollo architecture below).

Rule 9: No dedicated destination orbital space stations

This rules out all design vectors containing the sequence $(\dots, O, O, \dots)^T$. The rule also includes space stations at non-orbital locations which remain in a certain position relative to the destination planet, e.g. libration points.

Rule 10: No dedicated space stations in transit (to the Moon or to Mars)

This rules out all design vectors containing the sequence $(\dots, T, T, \dots)^T$.

Rule 11: Only one dedicated surface habitat is provided in every mission

This rules out all vectors containing the sequence $(\dots, S, S, S, \dots)^T$.

Rule 12: Crew transfers in transit can only be the first and / or last crew transfer in an architecture.

Design vectors containing the sequence $(\dots, O, T, \dots, L, \dots)^T$ or $(\dots, L, T, \dots, O, \dots)^T$ are excluded.

All the design vectors contained in the matrix of Figure 2-7 that comply with these rules (“legal” design vectors) are shown in Figure 2-9. Manual analysis reveals that there are 30 altogether, out of 28125 possible combinations contained in the matrix. Manual analysis of this problem is possible, because the above rules allow for a fast screening of the design vectors.

The number of different manned vehicles is limited to 3, and the number of switches between these vehicles does not exceed 4; both these assumptions are very probable, as every additional manned vehicle point-design is going to be a considerable investment, and as every additional transfer of the crew between vehicles increases mission risk. Four crew transfers allow for the use of an additional dedicated surface habitat for an Apollo-style mission. The 30 options shown in Figure 2-9 contain the sample designs presented in section 2.1.2. Appendix A provides a description and examples (if existing) for all the architectures presented in Figure 2-9.

- (0, 1, L, N, N, N, N)
- (1, 2, L, S, N, N, N)
- (1, 2, L, O, N, N, N)
- (1, 2, O, L, N, N, N)
- (2, 2, L, S, S, N, N)
- (2, 2, O, L, O, N, N)
- (2, 3, L, S, S, N, N)
- (2, 3, L, S, O, N, N)
- (2, 3, O, L, S, N, N)
- (2, 3, O, L, O, N, N)
- (3, 3, L, S, S, O, N)
- (3, 3, O, L, S, S, N)
- (3, 3, O, L, S, O, N)
- (4, 3, O, L, S, S, O)
- (1, 2, L, T, N, N, N)
- (1, 2, T, L, N, N, N)
- (1, 2, T, L, T, N, N)
- (1, 2, L, S, T, N, N)
- (2, 3, L, O, T, N, N)
- (2, 3, O, L, T, N, N)
- (2, 3, T, L, S, N, N)
- (2, 3, T, L, O, N, N)
- (2, 3, T, L, T, N, N)
- (3, 3, L, S, S, T, N)
- (3, 3, O, L, O, T, N)
- (3, 3, T, L, S, S, N)
- (3, 3, T, L, S, T, N)
- (3, 3, T, L, O, T, N)
- (4, 3, T, L, S, S, T)
- (4, 3, T, O, L, O, T)

Figure 2-9: “Legal” design vectors according to Rules 1-12

Architectures with crew transfers in transit on the way back to Earth have a significantly higher risk than those with crew transfers only in orbit or on the surface: if the insertion into the exact trajectory of the transiting spacecraft is not possible, there is no second try. Transfers in transit on the way to the destination planet usually (for exception, see Appendix A) means abandoning the vehicle in transit.

Figure 2-10 shows a schematic architectural diagram for the Apollo architecture, and one for an Apollo mission with an additional long-duration surface habitat. Please note that in the Apollo architecture, actually, the crew split up: one astronaut stayed in orbit, and two landed on the lunar surface; they joined again in orbit before TEI. In Figure 2-10 this is indicated by the solid blue arrow in “destination orbit”. For the Apollo architecture with an additional habitat, it is assumed that the entire crew lands on the Moon.

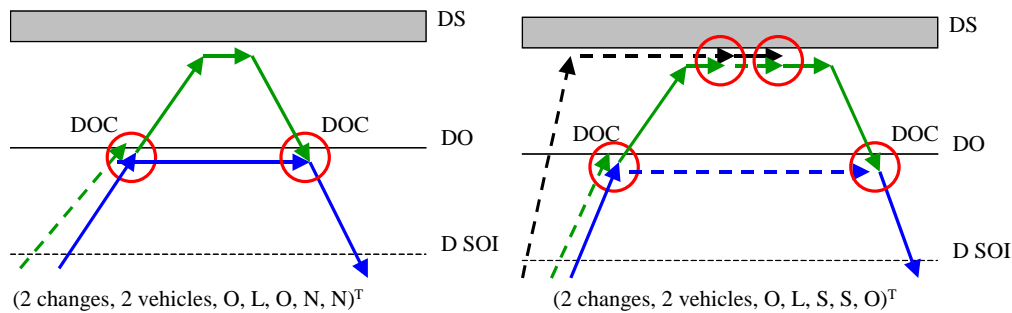


Figure 2-10: Architecture overviews for Apollo (left), and Apollo with a dedicated long-duration surface habitat (right)

These architectures exhibit several special features. Firstly, the starting and the ending points of the manned operations for a vehicle are always the same: the LM descends from LLO to the lunar surface, and ascends again to LLO. In the case of the added surface habitat, the crew enters the habitat and also leaves it on the lunar surface. Secondly, the architectures exhibit a certain symmetry concerning the sequence of vehicle switches: $(\dots, O, L, O, \dots)^T$, $(\dots, O, L, S, S, O, \dots)^T$. These two characteristics signify that the manned operations of vehicles are decoupled from each other: the LM and CSM crewed

operations have a clear interface in LLO, and only there. The LM only has the functionality to sustain the crew in transit to and from, and on the lunar surface (for a short time), whereas the CSM sustains the crew during transit to and from Earth, and in lunar orbit.

Figure 2-11 shows architecture diagrams for the NASA Mars Design Reference Mission, and for a 1-vehicle mission without any vehicle changes.

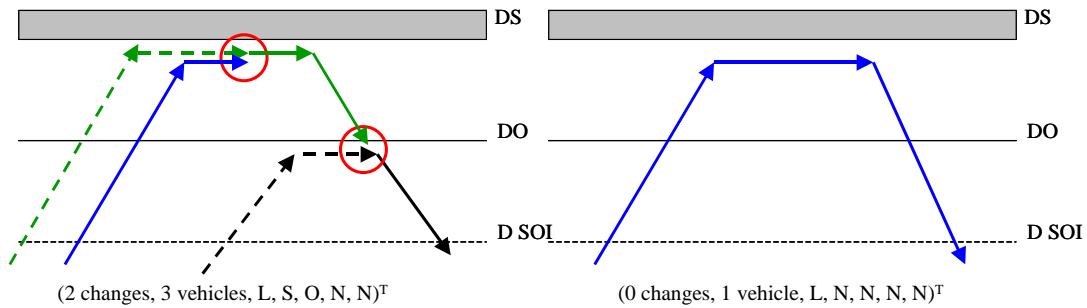


Figure 2-11: Architecture diagrams for the NASA Mars Design Reference Mission (left), and a 1-vehicle architecture (right)

In the case of the NASA Mars DRM, two crew transfers occur: one on the surface of Mars from the transfer habitat to the MAV, and one in LMO from the MAV to the ERV (see section 2.1.2). The DRM architecture does not exhibit the symmetry of the Apollo architecture: all vehicles have different starting and ending points for the manned operation phases of vehicles. In this case, the function of sustaining the crew during interplanetary travel is coupled with the function of landing the crew on Mars. This means that vehicle 1 always lands and stays on Mars, thereby enabling accumulation of hardware on the surface. This characteristic could be very interesting in terms of building a Mars surface base

The 1-vehicle scenario is a completely coupled design: one vehicle provides all the functionality for interplanetary travel, landing, ascent, and return to Earth. Architectures of this kind are conceivable for lunar missions of short duration, and even then only with very large launch rockets or extensive assembly operations in Earth orbit. For manned Mars missions, 1-vehicle architectures are considered non-viable if ISPP is unavailable, because all equipment and consumables needed for the months-long journey back to Earth would have to be landed in and accelerated out of the Martian gravitational field; this would result in prohibitive propellant masses (for details, see Chapter 3).

2.2 Conceptual Manned Spacecraft Modeling

In the course of the detailed architectural analysis of the landing system design space, hundreds of possible landing system combinations can arise when parameters like the number of vehicle stages, propellant combinations and the number of vehicles are varied. On the subsystem level, technologies for specific functions like electrical power generation can be varied, which also leads to a great number of spacecraft design options. In order to meaningfully assess the potential designs at every stage, models have to be provided which enable the computation of objective metrics with the information available at that particular point in the design process. As the information available about the design solution generally increases as the design progresses, the corresponding models also become more complex.

In this section, two models for the mass of the manned crew compartment are presented: firstly, an empirical model that has few input parameters, and serves to provide a first-order approximation for the mass and pressurized volume of the crew compartment. Secondly, a parametric model that allows detailed design of certain subsystems, whereas the mass of others is handled as a fraction of the total mass. The second model is based upon data from NASA's Reusable Lunar Lander Design [Wingo, 2004]. It can also be used without any subsystem design input as purely a scaling model.

2.2.1 Empirical Model

Crew Compartments

The empirical model for the crew compartment utilized in this thesis was published by NASA in 1994, and is cited here from [Larson, Pranke, 2004]. It provides the mass of the crew compartment as a function of crew size, pressurized volume, and time spent in the crew compartment. The crew compartment represents in this context all the spacecraft subsystems except propulsion, parachutes, and landing gear. Qualitatively, the crew size and the mission duration (or time spent in the crew compartment) are the main design drivers for many subsystems: the duration largely determines the technologies viable for electrical power and life support systems and the amount of crew gear needed, and the crew size serves as the scaling factor which sizes the absolute mass of these subsystems. The pressurized volume is also determined by the crew size, and the mission duration. Figure 2-12 shows a black-box diagram for the flow of information in the empirical model.

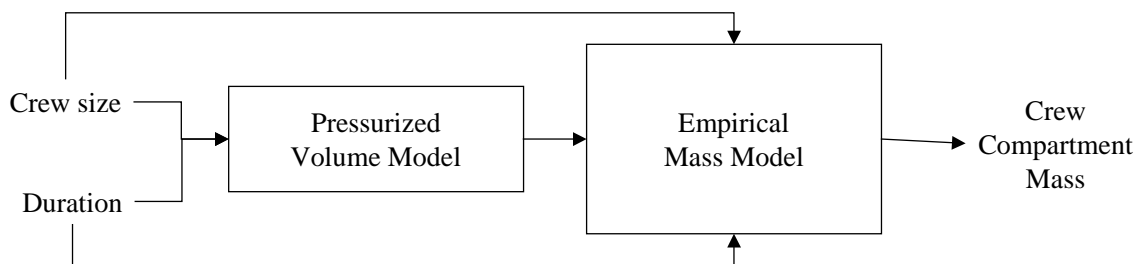


Figure 2-12: Overview of empirical crew compartment computational model

Before we can start computing the crew compartment mass, we have to provide a model for the pressurized model needed for a certain crew size and mission duration. In [Larson, Pranke, 2000], two diagrams are published that allow the approximation of pressurized and / or habitable volume per crewmember. Figure 2-13 shows the first, a logarithmic approximation:

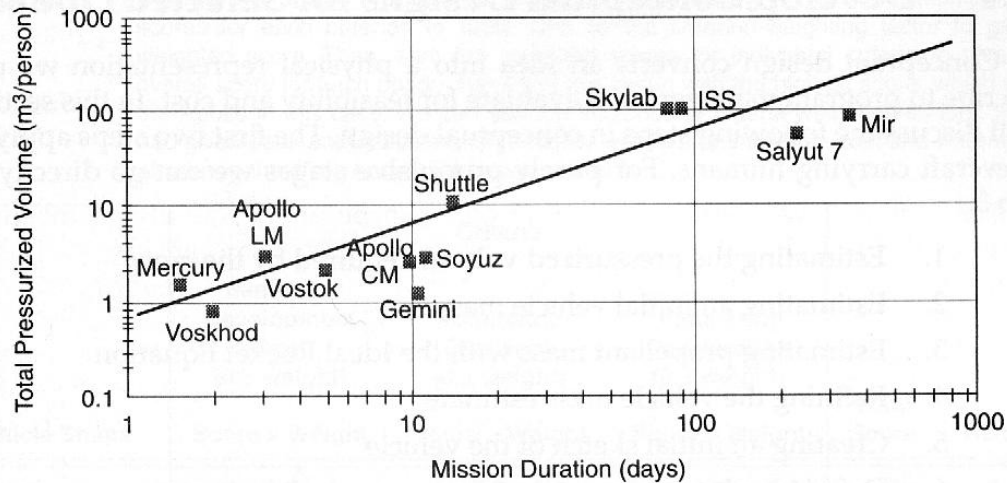


Figure 2-13: Logarithmic model for the pressurized volume per crewmember as a function of mission duration [Larson, Pranke, 2000]

The logarithmic model has two substantial drawbacks: first, in logarithmic diagrams, many trends can be perceived as obeying a linear law, while they actually exhibit different characteristics. For example, the logarithmic model states that the pressurized volume required is a strictly monotone function of mission duration, and is always increasing with mission duration. This, however, appears to be unlikely, because from a certain mission duration on, the volume is expected to be constant: a crewmember does not need more volume for a 500 day mission than for a 400 day mission. The second drawback is that the model also includes space station volumes; these are generally larger than needed for transport habitats, because extra room is required for experiments and logistics operations.

Figure 2-14 illustrates the second model suggested for the habitable volume required per crewmember as a function of mission duration. Three curves are shown: the first is a curve for the ‘tolerable limit’ of habitable volume that is absolutely essential for the well being of the crewmember. The pressurized volume of a spacecraft should always be above this curve. The second is curve labeled ‘performance limit’, the third ‘optimal’. If the crew has to carry out complex operations, as it is expected for long-duration Moon and Mars missions, the habitable volume per crewmember should lie between these two lines; for longer durations, on the order of several months or more, it should lie close to the ‘optimal’ curve [Larson, Pranke, 2000]. For long duration space flight, the habitable volume required per crewmember reaches a plateau. Due to this characteristic, the model of Figure 2-14 will be used in this thesis to determine habitable and pressurized volumes.

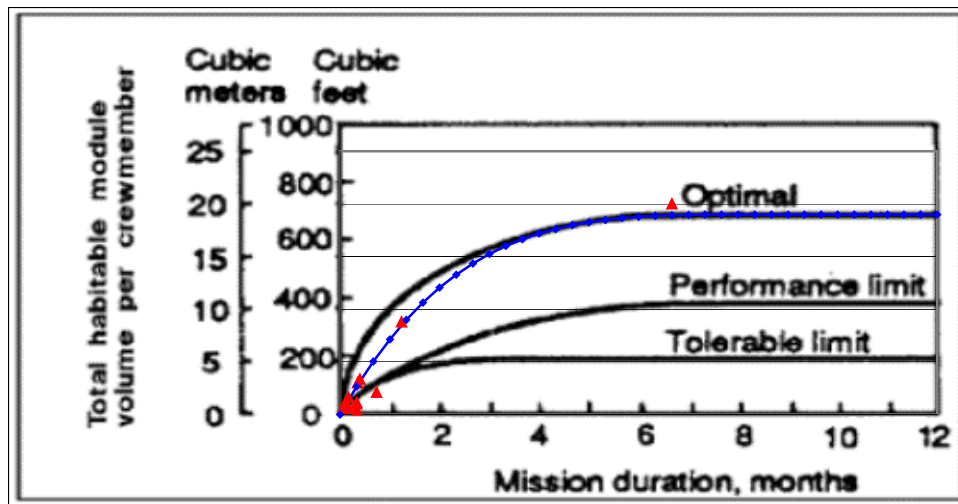


Figure 2-14: habitable volume required per crewmember as a function of mission duration [Larson, Pranke, 2000]

The red triangles in Figure 2-14 represent the habitable volumes per crewmember of existing and proposed manned spacecraft designs; the reference values are shown in Table 2-1. Three conclusions can be immediately drawn from the diagram: firstly, if we exclude space stations (see above), few data points exist for long-duration missions. Secondly, for short duration missions (up to 2 months), the reference points lie close to the “performance limit” curve, or between the “optimal” and “performance limit” curves. Thirdly, for long mission durations, the reference point indicates good agreement with the plateau value of 19 m³.

Spacecraft	Pressurized volume / crew [m ³]	Habitable volume / crew [m ³]	Duration [d]
Mercury	1.7	0.56	1.5
Gemini	1.275	0.425	10
Apollo CM	3.0	1.0	10
Apollo LM	3.35	1.116	3
Vostok	2	0.67	5
Soyuz	3.33	1.11	10
Shuttle orbiter	10	3.33	12
CTV	6.25	2.08	22
NASA RLL	9	3	10.7
ESA HMM MAV	4.9	1.62	5
ESA HMM Hab	26.3	8.8	37
NASA Mars DRM ERV	60	20	200

Table 2-1: Pressurized and habitable volumes per crewmember of existing or proposed spacecraft designs

In order to express the two latter observations with a mathematical model, it is necessary to find a function that lies between the “optimal” and “performance limit” curves for

short durations, and reaches the optimal plateau for long durations. This can be achieved by dividing the duration axis into two intervals (below and above 270 days), and assigning the following functions to the intervals:

$$V_{Habitable}(\Delta t_{Mission} < 270d) = \left(19 - \left(\frac{19}{270^4}\right) \cdot (\Delta t_{Mission} - 270)^4\right) m^3 \quad \text{Equation 2-1}$$

$$V_{Habitable}(\Delta t_{Mission} > 270d) = 19m^3 \quad \text{Equation 2-2}$$

These functions are indicated by the blue curves in Figure 2-14. With the required habitable volume known, the total pressurized volume for a particular mission with a given crew size can then be computed by a rule of thumb given in [Larson, Pranke, 2000]:

$$V_{Pressurized} = 3 \cdot N_{Crew} \cdot V_{Habitable} \quad \text{Equation 2-3}$$

The effect of sharing of common volume between crewmembers is included into the habitable volume function modeled after Figure 2-14. The total pressurized volume allows us to compute the mass of the crew compartment by using an empirical equation of NASA [Larson, Pranke, 2000]:

$$m_{CrewCompartment}(\Delta t_{Mission} < 200d) = 592kg \cdot (N_{Crew} \cdot \Delta t_{Mission} \cdot V_{Pressurized})^{0.346} \quad \text{Equation 2-4}$$

The mass of the crew compartment hereby includes the mass for all subsystems except propulsion and entry, descent & landing. Figures 2-15 to 2-17 show data for the empirical mass model in relation to reference data points of existing or proposed manned spacecraft designs:

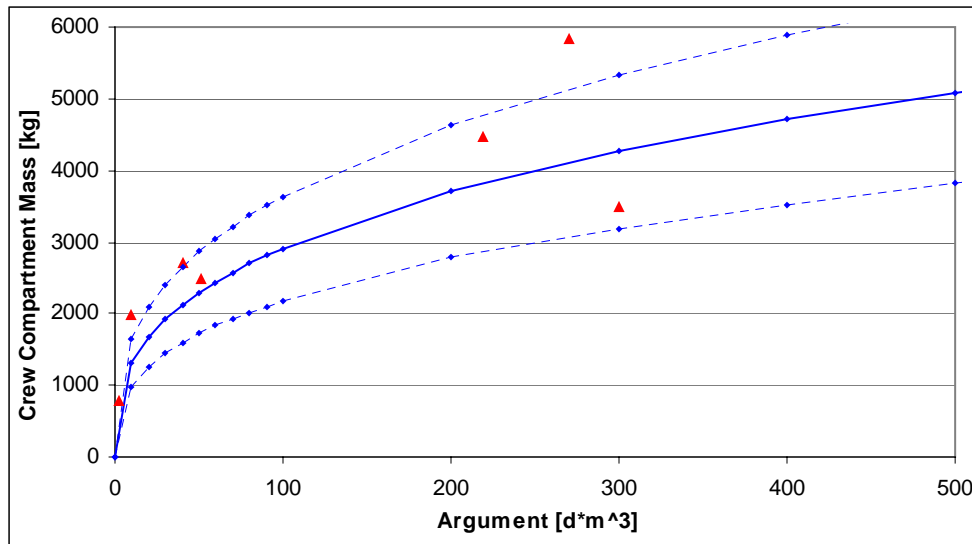


Figure 2-15: Crew compartment mass as a function of $N_{Crew} \cdot \Delta t_{Mission} \cdot V_{Pressurized}$ for short mission durations and / or small crew sizes

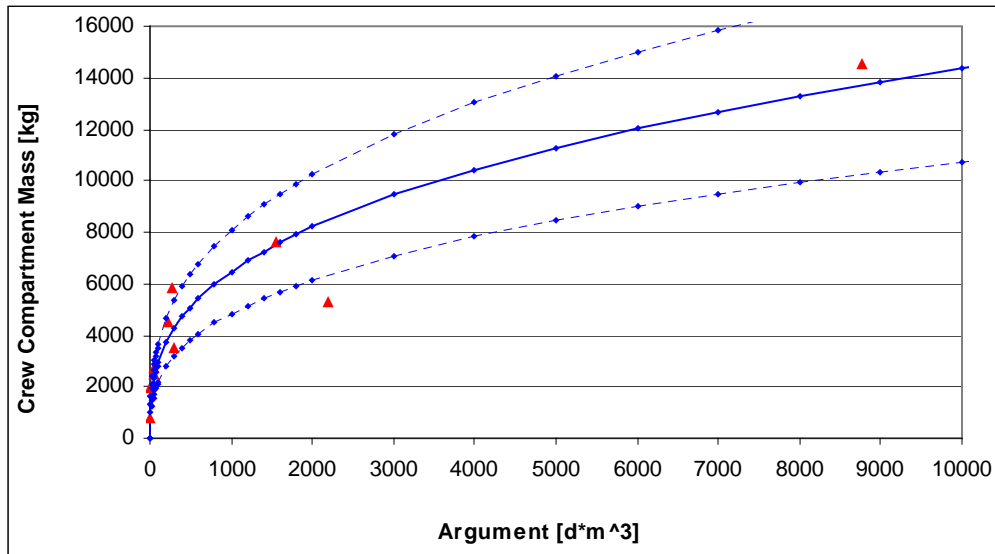


Figure 2-16: Crew compartment mass as a function of $N_{Crew} \cdot \Delta t_{Mission} \cdot V_{Pressurized}$ for medium mission durations and / or crew sizes

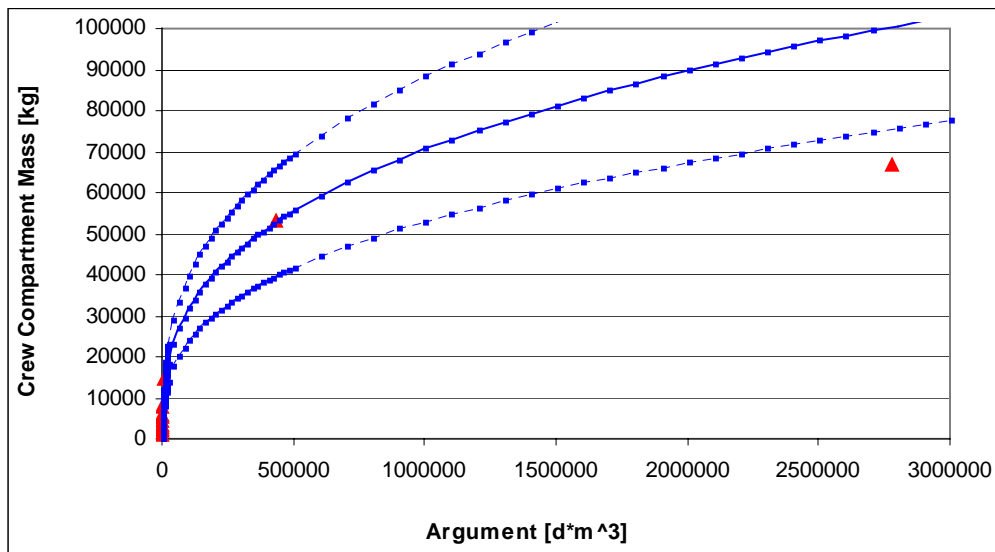


Figure 2-17: Crew compartment mass as a function of $N_{Crew} \cdot \Delta t_{Mission} \cdot V_{Pressurized}$ for long mission durations and / or large crew sizes crew size

The crew compartment masses are shown as a function of the argument of the power function ($N_{Crew} \cdot \Delta t_{Mission} \cdot V_{Pressurized}$). The triangles in the diagrams represent reference points of the existing or proposed manned spacecraft in Table 2-2. For arguments below 500000, the reference data points are within 20 % of the values predicted by the empirical model. Noticeable deviations occur in the case of Gemini and Apollo, where the pressurized volumes are substantially lower than required by the model presented above.

Spacecraft	Argument [d*m ³]	Crew compartment mass [kg]
Mercury	2.55	774
Gemini	51	2480
Apollo CM	270	5844
Apollo LM	40.2	2698
Vostok	10	1968
Soyuz	299.7	3480
CTV	2200	5274
NASA RLL	1540.8	7626
ESA HMM MAV	219	4473
ESA HMM Hab	8769	14513
NASA Mars DRM ERV	432000	53400
ESA HMM interplanetary hab	278200	67000

Table 2-2: Arguments and reference masses for existing or proposed manned spacecraft designs

For the data point at argument 2750000 (ESA HMM interplanetary transfer habitat), the NASA model is off by more than 20 %. This indicates, that the empirical model is assuming very conservative technology with very limited loop closure for life support. As loop closure of some sort is assumed to be a given for long duration space flight, it is necessary to model the crew compartment / habitat mass as a function of loop closure.

For the following, it is assumed that after 200 days the dominant source for crew compartment mass increase is life-support consumables. This is justified by the fact that the pressurized volume required per crewmember is very close to the plateau value of 19 m³ for a duration of 200 days; crew compartment mass increase due to structural mass of the pressure shell can be neglected. The habitat mass for missions with durations over 200 days can then be modeled using the following **Equation 2-5**:

$$m_{CrewCompartment}(\Delta t_{Mission} > 200d) = m_{CC}(200days) + (\Delta t_{Mission} - 200d) \cdot N_{Crew} \cdot 9,5 \frac{kg}{d} \cdot \alpha \cdot \eta$$

The first term is the mass of a habitat with a duration of 200 days for the mission crew size computed with the empirical model of NASA discussed; this mass is also the starting point (with an argument of about 400000) for the curves in Figure 2-18. It is the “interface” point between the two models. α is the resupply fraction (the ratio of the resupply mass needed for the partially closed system to the resupply mass for an open-loop system), and η is a structural factor for the additional equipment and storage mass required for the consumables (η is assumed to be 1.0 for the calculations in Chapter 3). The open-loop mass rate of 9.5 kg / person-day is based on the Apollo life support system [Messerschmid, 1997]. Table 2-3 shows resupply fractions and the resulting mass flows for various loop closures in the life support system; alone by closing the water loop, the resupply fraction can be reduced to below 50 % [Messerschmid, 1997].

Figure 2-18 shows the habitat mass for a six-person habitat as a function of the argument used for the empirical model. It appears that the NASA empirical model assumes a resupply fraction of about 0.8 for the life-support system. The two available data points

lie close to the 0.32 (water and carbon dioxide closure) and 0.175 (water, carbon dioxide and oxygen closure) resupply fractions. It is noticeable that additional loop closure will have smaller and smaller benefits in terms of additional habitat mass; this is due to the high initial investment necessary to at all enable missions of this duration. For the calculations in this thesis, the 0.32 resupply fraction will be assumed for the life-support system, because it only requires technology that has already been flown on Skylab, the Russian space stations, and the ISS. The additional benefits for closure of the oxygen loop are comparatively small and are, when available, not expected to necessitate any changes in the architecture.

Loop Closure	α	Resupply mass / crew day
Open loop system (Apollo)	1.0	9,5 kg/d
Waste water regeneration	0.45	4.275 kg /d
+ Regenerative CO ₂ filtering	0.32	3.04 kg/d
+ O ₂ loop closure	0.175	1.6625 kg/d

Table 2-3: Resupply fractions and mass flows for various loop closures in the life support system [Messerschmid, 1997]

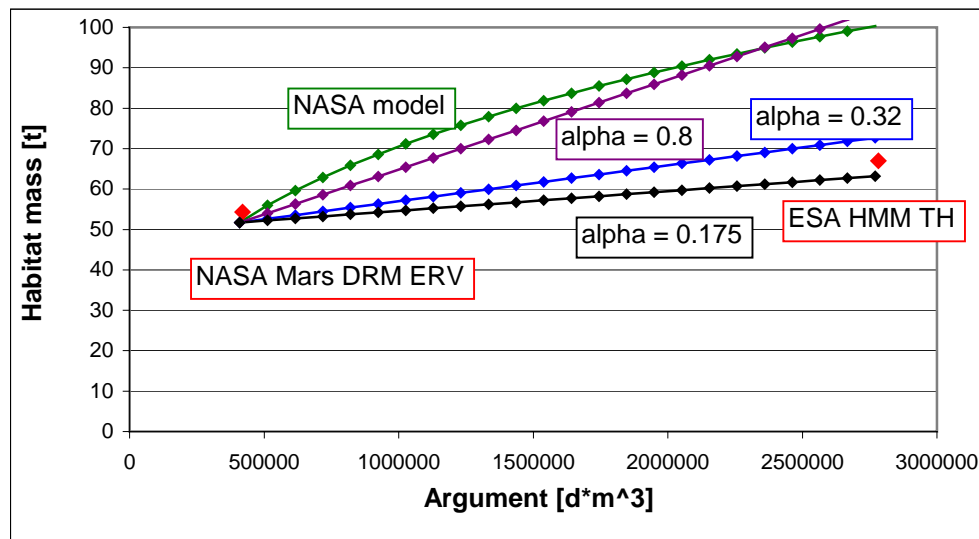


Figure 2-18: Habitat masses as a function of argument for various resupply fractions

Propulsion Stages

The crew compartment models in the preceding section provide masses for all the subsystems except propulsion, and entry, descent & landing. If a vehicle has to provide velocity changes, a propulsive stage needs to be connected to the crew compartment, which can be regarded as a “payload” for the stage. The propulsion stage consists of fuel and the oxidizer, the tanks (also thermal control) and plumbing for the propellants, the pressurizing system (if needed), the rocket engines, and of structural interconnections between all the former elements. The sum of engine, tank and plumbing, and interconnection mass is commonly referred to as “structural mass”.

There are two ways to calculate the dry (structural) mass of a propulsion stage at a conceptual level: to assume that it is a certain fraction of the propellant mass, or to assume that it is a certain fraction of the total vehicle mass. The former convention is

commonly applied for manned spacecraft and satellites, the latter for launch vehicles [Messerschmid, 2000; Larson, Pranke, 2000]; the relationship between the two views is discussed in Appendix D. For the conceptual design of spacecraft, the structural mass of a propulsion stage is assumed to be a fixed fraction of the propellant mass of the stage. The rule of thumb for structural mass is about **15 %** of the propellant mass of the stage (this value is specified in [Larson, Pranke, 2000] for conceptual design purposes). The values in Table 2-4 show that this is in good agreement the proposed RLL of NASA and the LM descent stage. For the LM ascent stage it is a conservative estimate; as the LM ascent propulsion system was highly integrated into the crew compartment, however, it is expected to have a lower mass than a separate stage.

Spacecraft stage	Propulsion system mass [kg]	Propellant mass [kg]	Ratio [-]
Apollo LM ascent stage	213	2372	0.090
Apollo LM descent stage	1161	8848	0.131
NASA RLL (one stage)	3772	26375	0.143

Table 2-4: Structural factors for spacecraft propulsion stages [Wingo, 2004; Gavin, 2002]

The rule of thumb stated above is sufficient for calculations of overall vehicle masses; for the modularization of rocket engines, propellant tanks and associated masses, however, it is necessary to know what the individual components weigh.

As the masses of many engines with widely different thrust are known, an empirical interpolation can be used to determine the engine mass for a given maximum thrust. Figure 2-19 shows thrust-to-weight (T/W) ratios for several engines with different propellants, as well as the interpolation function; the maximum thrust is given in [N]. As intuitively expected, the engine weight-to-thrust ratio (W/T) drops with increasing thrust.

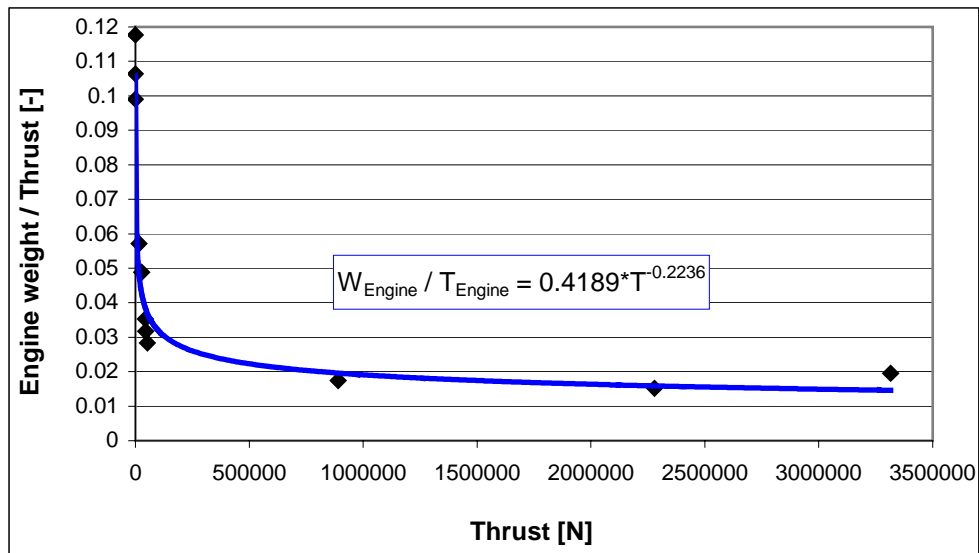


Figure 2-19: Engine weight to thrust over absolute thrust for various engines

If not stated differently, all engines for propulsion stages other than TMI / TLI stages are assumed to be deeply throttleable (down to 10 % thrust). The model presented here is assumed to cover this case.

The interpolation function shown in Figure 2-19 takes the following form:

$$m_{Engine} [kg] = \left(\frac{T_{max} [N]}{g_0} \right) 0.4189 \cdot (T_{max} [N])^{-0.2236} \quad \text{Equation 2-6}$$

With this interpolation function, we can compute the mass of any engine, given its thrust. It is important to mention that this model is a top-level approximation, which does not take into account design differences for different propellant combinations. The model, however, gives a qualitatively correct trend for the engine mass: with increasing thrust, the ratio of engine weight to thrust decreases. Also, for very small thrust engines, the mass rises steeply, following a power law; this is intuitively clear, because even for very small thrust, there will be a considerable mass needed for the nozzle, the burning chamber, the plumbing, etc. The constants for this qualitatively correct model have been determined by using data of existing engines [Gavin, 2002]; the model therefore should be sufficiently detailed for conceptual analysis.

With the engine mass known, we can compute the structural mass remaining for the propellant management system (tanks, plumbing and associated structural mass) of a propulsion stage. This mass can then be related to the propellant mass in order to compute a mass fraction. The reference data for this computation are taken from the Apollo Lunar Module descent stage, which is a good example of a propulsion stage [Gavin, 2002]:

$$\frac{m_{PropellantManagement}}{m_{propellant}} = \frac{1470 + 1089 - 348}{19507} \approx 0.113 \quad \text{Equation 2-7}$$

If the thickness of a propellant tank is small compared to the radius of the tank, the mass of a spherical tank scales proportionally to the volume of the tank:

$$m_{tank} = A_{SurfaceTank} \cdot d_{Tank} \cdot \rho_{Tank} \sim r_{Tank}^3 \sim \frac{4}{3} \cdot \pi \cdot r_{Tank}^3 \cdot \rho_{Propellant} = m_{Propellant} \quad \text{Equation 2-8}$$

As the plumbing and associated structural mass of a propellant management system is generally assumed to be a fraction of the tank mass [Larson,], the scaling law indicates that we can use the above mass fractions to scale up and down propellant management systems.

With the empirical model for engine mass, and the mass for propellant management systems, all the tools necessary for modularization of propulsion stages have been introduced.

Heat Shield, Parachutes, Landing Gear

For a landing on Mars, a heat protection system, as well as a drogue parachute is required [Larson, Pranke, 2000]; for both Moon and Mars landings, landing gears are required. The masses of these subsystems / components are generally computed on the conceptual level by using mass fractions. These fractions can be calculated with the data published

for missions executed in the past, or for proposed mission designs. In the case of the landing gear, the influence of the local gravity has to be captured by a scaling law.

For thermal protection during atmospheric entry, the heat shield mass is commonly considered to be between 15 – 20 % of the protected mass of the vehicle entering the atmosphere [Larson, Pranke, 2000; Messerschmid, 2000]; this model is for ablative heat shields of the same type as those used for the Apollo CM. Inflatable heat shields would enable significant mass savings; as this technology is still in the development phase, this is a topic for future research.

$$m_{HeatShield} = \alpha_{HS} \cdot m_{Protected}, 0.15 \leq \alpha \leq 0.2 \quad \text{Equation 2-9}$$

The exact value depends strongly on the technology selected (capacitive, ablative, inflatable, etc.). As we are considering Earth entry velocities of up to 17 km/s (see Chapter 3), the upper boundary of 20 % will be used for Earth entry, and 15 % for Mars entry.

Mars entry of manned spacecraft has been studied in great detail in various mission concepts proposed; we will refer here to the concept employed in the NASA Mars DRM and reflected in [Hoffman, Kaplan, 1997]: after using the heat shield to protect the spacecraft from the intense heat during high-velocity entry, a drogue parachute will be deployed that slows the spacecraft down to a velocity of under 1 km/s relative to the Mars surface. This parachute is then separated, and the remaining descent until landing is accomplished with rocket propulsion. The drogue parachute mass is assumed here to be proportional to the mass suspended under the parachute:

$$m_{DrogueParachute} = \alpha_{DP} \cdot m_{Suspended} \quad \text{Equation 2-10}$$

From mass values given in [Larson, Pranke, 2000] for a case study of a Mars landing habitat, we can compute the mass fraction:

$$\alpha_{DP} = \frac{600kg}{57754kg} \approx 0.01 \quad \text{Equation 2-11}$$

The mass of the landing gear is also assumed to be proportional to the mass that is landed, i.e. to the weight that rests on the landing gear. There is, however, another factor to be taken into account: the influence of the local gravity of the destination planet. The following equation states a scaling law for the mass of one landing leg; the leg is assumed to have the same length and to consist of the same material for Moon and Mars landers; the cross-sectional area, however, varies:

$$m_{Leg} = L_{Leg} \cdot \rho_{Leg} \cdot A_{Leg} = L_{Leg} \cdot \rho_{Leg} \cdot \frac{m_{PerLeg}}{\sigma_s} \cdot g_{Planet} \quad \text{Equation 2-12}$$

The structural mass of a landing leg therefore is proportional to the local gravity of the target planet. For a lunar landing gear, we can compute the mass fraction from data given for the LM in [Gavin, 2002]:

$$m_{LG,Moon} \approx 0.03 \cdot m_{Landed} \quad \text{Equation 2-13}$$

For a Mars landing gear, the mass fraction can be scaled up from the Moon value with the ratio of the local gravities:

$$m_{LandingGear} = \frac{g_{Mars}}{g_{Moon}} \cdot 0.03 \cdot m_{Landed} = \frac{0.38}{0.17} \cdot 0.3 \cdot m_{Landed} \approx 0.07 \cdot m_{Landed} \quad \text{Equation 2-14}$$

Validation and Sensitivity Analysis for the Apollo LM

The empirical model is intended to be a tool for the conceptual design of manned spacecraft. Before we use it as such, it is necessary to assess the accuracy of the model, and the sensitivity to perturbations of the input parameters.

The accuracy of the model will be assessed here by comparing component, stage, and vehicle masses calculated with the model to actual masses of the Apollo 17 LM. The Apollo 17 LM was characterized by the following input parameters:

Characteristic	Value
Crew Size	2
Crew Mass (2 crew)	160 kg
Mission duration (habitated duration)	4 days
Sample mass to orbit, returned upon ascent	95 kg
Payload mass to surface	557 kg
Specific impulse of ascent / descent engines	311 s
Ascent velocity change	1874 m/s
Descent velocity change	2045 m/s
Descent velocity change with 20 % margin for hovering	2454 m/s
Maximum thrust / weight ratio descent	0.33
Maximum thrust / weight ratio ascent	0.5

Table 2-5: Apollo 17 LM characteristics [NASA, 1972; Gavin, 2002]

The actual duration of independent flight, i.e. the time from undocking to docking in LLO was 3.313 days for the Apollo 17 LM. The LM was powered up, however, during translunar coast, and also had spare lifetime for the event of a contingency in lunar orbit. The mission duration of 4 days therefore seems to be a realistic assumption. The sample and payload masses, as well as crew size and crew mass are well documented in [NASA, 1972]. The thrust / weight ratios were calculated with the values for thrust given in [NASA, 1972].

With these input parameters, we can calculate the masses of various LM components and compare them to the actual data of the Apollo 17 LM:

The deviation in Table 2-6 was based on the LM component masses published in [Gavin, 2002]. The deviation for the entire vehicle, as well as for the ascent stage is about 3 %, which indicates excellent agreement with the existing design. The only components that are overestimated by over 20 % in mass are the ascent and descent stage engines. This overestimation is due to the empirical model for engine mass as a function of engine thrust. Most of the engines selected for landing system design in this thesis have to be restartable, and, in the case of cryogenics, will also feature propellant pumps. A conservative engine mass estimation model therefore seems to be appropriate.

Component [kg]	Mass computed with model [kg]	Apollo 17 mass [kg]	Normalized deviation [-]
Crew compartment	2336	2427	-0.037
Ascent stage propellant	2538	2372	0.070
Ascent engine mass	114	91	0.253
Ascent stage (including crew)	5275	4960	0.064
Descent stage propellant	8968	8848	0.014
Descent engine mass	197	158	0.247
Landing gear	218	220	-0.009
LM total mass	16228	16430	0.012

Table 2-6: Component masses calculated with the empirical model in comparison the Apollo 17 LM [NASA, 1972; Gavin, 2002]

In addition to the accuracy of the model, we can also determine the sensitivity of the total mass to variations of the input parameters. The sensitivities are especially interesting for technology selection and development: if a large and very expensive improvement regarding one technology has little effect on the overall vehicle mass, whereas a less expensive enhancement of a different technology has a substantial impact on the overall mass, the latter option should be selected. It is important to mention that technology selection contributes to the risk of system failure; in order to take an informed decision, a similar sensitivity analysis for risk would have to be done. As a comprehensive risk assessment is beyond the scope of this work, we only perform a sensitivity analysis for the overall LM mass.

Parameter	Perturbed value	Original value	Perturbed total mass	Original total mass	Sensitivity
Mission duration	5 d	4 d	18476	16228	0.554
Crew size	3	2	20645	16228	0.544
Structural factor ascent stage	0.14	0.113	16639	16228	0.101
Structural factor descent stage	0.14	0.113	16926	16228	0.180
Specific impulse ascent engine	320	311	15897	16228	-0.705
Specific impulse descent engine	320	311	15747	16228	-1.024
Velocity change ascent	2000	1874	17059	16228	0.762
Velocity change descent	2600	2454	17311	16228	1.122
Landing gear factor	0.04	0.03	16431	16228	0.038
Sample mass	110	95	16273	16228	0.018
Payload mass	600	557	16347	16228	0.095

Table 2-7: Sensitivity analysis of the Apollo LM for perturbations of the input parameters

The sensitivities of the LM mass to perturbations of the input parameters are shown in Table 2-7 as partial differential coefficients of the LM mass, normalized with the values

of the original design point (see Table 2-5). The following equation demonstrates the calculation of the sensitivity for the specific impulse of the ascent stage:

$$\alpha_{I_{sp,Ascent}} = \frac{\Delta m_{total}}{\Delta \alpha_{I_{sp,Ascent}}} \cdot \left(\frac{\alpha_{I_{sp,Ascent}}}{m_{total}} \right)_{original} \quad \text{Equation 2-15}$$

Large values (positive or negative) for sensitivities indicate strong influence of the corresponding parameters on the overall spacecraft mass. Positive sensitivity signifies that the total mass increases with an increase of the parameter; negative means that the total mass decreases with a positive difference in the parameter.

In the case of the LM, the parameters with the biggest influence on total mass are the velocity changes for ascent and descent, as well as the specific impulse of the ascent and descent stages. This indicates that in terms of mass savings, it will be very interesting to trade different propellant combinations and trajectories. The parameters with the next biggest influence are the crew size and the duration of the mission. These parameters are also going to be subject to trades in Chapter 3. The structural factors of the descent and ascent stages and the payload mass have a significantly smaller influence than the crew size and the duration; the landing gear structural factor as well as the sample mass have very little influence on the overall mass.

2.2.2 Scaling Model

The empirical model presented in the preceding section provides the basis for conceptual design of Moon and Mars architectures and allows for the modularization of pressurized compartment structures, propellant management systems and rocket engines. For modularization of subsystems such as electrical power and life-support, however, a model with higher resolution is required.

The full design of a manned spacecraft on the subsystem level, however, is beyond the scope of this thesis. The solution to this dilemma is to design subsystems that are interesting for modularization in more detail, and to determine the mass of the remaining subsystems by using scaling relationships and / or mass fractions (see Chapter 4).

This approach requires a sample spacecraft design that serves as the basis for scaling up or down. In this thesis, the sample spacecraft is the NASA Reusable Lunar Lander (RLL) that was studied in detail in the context of the NASA OASIS framework [Wingo, 2004].

The reasons for this choice are as follows:

1. The Reusable Lunar Lander is a spacecraft designed for landing on a planetary surface, in this case, the Moon.
2. A detailed mass breakdown for the subsystems, as well as information about the subsystem technology is available for the RLL [NASA, OASIS, 2004; Wingo, 2004].
3. The Apollo LM is the only landing spacecraft ever designed and flown successfully; it is however a 30-year-old design, that does not represent present technology. The RLL design incorporates present technology.
4. The RLL design is reusable; a model based on the RLL will therefore be conservative for non-reusable designs, and appropriate for reusable designs.

Figure 2-20 gives an overview of the NASA RLL spacecraft design, and the allocation of crew compartment mass to the various subsystems. The mass for “Growth” represents a mass margin that is expected to be consumed gradually during further refinement and detailed design of the spacecraft.

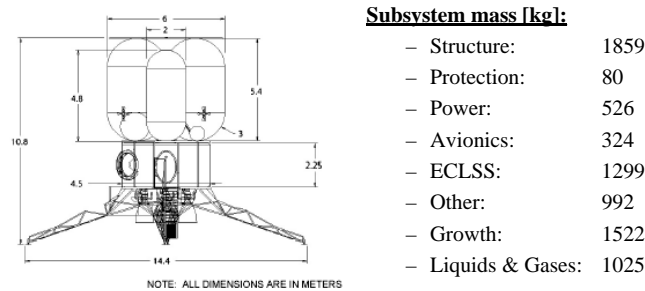


Figure 2-20: Overview of NASA’s RLL spacecraft and subsystems [Wingo, 2004]

In order to convert the data of the RLL into a usable model, the subsystem masses have to be either converted into specific values (volume-, crew-, or crew-day specific), or to percentages of total crew compartment mass. Table 2-8) shows the results of this process:

<u>Crew Size</u>	<u>Duration [d]</u>	<u>Pressurized volume [m³]</u>	<u>Pressurized volume (Model) [m³]</u>		
4	11	36	35		
<u>Subsystem</u>	<u>Mass [kg]</u>	<u>Scaling law</u>	<u>Specific Mass β</u>	<u>Unit</u>	<u>Mass Fraction α</u>
Structure	1859	$\frac{m_{Structure}}{V_{Pressurized}} = const$	53.19639	[kg / m ³]	-
Protection	80	-	-	-	0.010489
Power	526	$\frac{m_{Power}}{n_{Crew}} = const$	131.5	[kg / crew]	-
Avionics	324	-	-	-	0.042481
ECLSS (dry)	1299	$\frac{m_{ECLSS}}{n_{Crew}} = const$	324.75	[kg / crew]	-
Other Subsystems	992	-	-	-	0.130064
Growth	1522	-	-	-	0.199554
Liquids & Gases	1025	$\frac{m_{Liquids\&Gases}}{n_{Crew} \cdot \Delta t_{Mission}} = const$	23.29545	[kg / crew-day]	-
Total:	7627	-			

Table 2-8: Conversion of RLL subsystem masses into mass fraction or specific masses for modeling purposes [NASA, OASIS, 2004; Wingo, 2004]

With the specific masses for structure, power, ECLSS, and liquids & gases presented in Table 2-8, the total mass of a crew compartment can be calculated:

$$m_{CrewCompartment} = \frac{m_{Structure} + m_{Power} + m_{ECLSS} + m_{Liquids\&Gases}}{1 - (\alpha_{Protection} + \alpha_{Avionics} + \alpha_{Other} + \alpha_{CGrowth})} \quad \text{Equation 2-16}$$

The masses for the subsystems in the numerator can be generated either by the following scaling relationships or by detailed subsystem design or by a mix of both approaches:

$$\begin{aligned} m_{Structure} &= \beta_{Structure} \cdot V_{Pressurized} \\ m_{Power} &= \beta_{Power} \cdot n_{Crew} \\ m_{ECLSS} &= \beta_{ECLSS} \cdot n_{Crew} \\ m_{Liquids\&Gases} &= \beta_{Liquids\&Gases} \cdot n_{Crew} \cdot \Delta t_{Mission} \end{aligned} \quad \text{Equations 2-17}$$

Figure 2-21 shows crew compartment masses calculated by using the scaling model with the above scaling laws for crew sizes from 3 to 6 and for mission durations from 5 d to 20 d. The results are plotted as a function of the argument used for the empirical model of Section 2.2.1. For reference, the empirical NASA model is shown with 125 %, 100 % and 75 % mass. The diagram indicates good agreement with the empirical model. The scaling model will be used in Chapter 4 for the modularization of the ECLSS, Structure and Power subsystems between Moon and Mars landers.

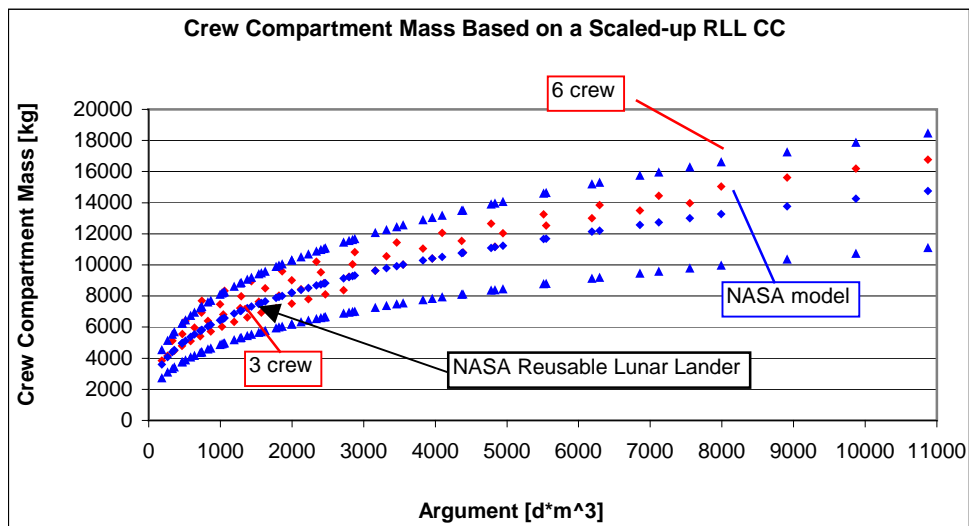


Figure 2-21: Crew compartment masses generated with a model based on the NASA RLL (red dots); the blue dots represent the empirical NASA model of section 2.2.1 with 125%, 100%, and 75% values

2.3 Summary of Chapter 2

Chapter 2 introduces all the basic models and descriptions used throughout the thesis. The chapter first discusses two architectures: the Apollo architecture, representative for manned Moon mission architectures, and the NASA Mars Design Reference Mission architecture, which represents NASA's baseline approach to manned Mars exploration from 1997 - 2000. They serve to introduce important concepts and terms and to provide reference points for mission architectures. Additional architectures for Moon and Mars exploration are presented in Appendix A.

After this introduction to mission architecture, a generic way to describe and systematically generate top-level manned mission architectures in the vicinity of the target planet, i.e. Moon or Mars, is presented. This is necessary to ensure that interesting architectures have not been overlooked. By applying certain rules, 30 architectures are generated out of several thousand possible architectures (see Appendix A). The architecture down-selection could be accomplished manually with the rules described in Section 2.1. These architectures will be applied to different Moon and Mars mission scenarios in Chapter 3.

Systematic conceptual models are not only needed to generate architectures, but also to compute the properties and characteristics of manned spacecraft. Two models for spacecraft design are introduced in Section 2.2: an empirical one, which is based on empirical correlations for crew compartment and engine mass, and on mass fractions and scaling laws for propellant management, heat protection, parachutes, etc. For validation, the model is compared to existing spacecraft designs, namely the Apollo 17 LM. Also, a sensitivity analysis is performed to identify the main drivers of LM design. The empirical model will be used in Chapter 4 for the modularization of pressurized structures, propellant management systems and rocket engines.

Another model is presented that provides more detail on the subsystems used in the crew compartment: based on the data given for NASA's reusable lander, a model is devised which allows to scale up (or down) the masses for the structure, ECLSS and EPS subsystems, and also to compute other subsystem masses by mass percentages. This model will be used in Chapter 4 for the modularization at the subsystem level.

3. Moon and Mars System Architectures Point Designs

3.1 Mission Type Network

In Chapter 2, models for systematical architecture generation as well as for individual spacecraft (empirical and scaling models for mass estimation) were introduced. In this chapter, the models will be used to determine the most desirable system architectures for custom-designed Moon and Mars exploration systems, and to trade various design options.

An important distinction needs to be made between the term ‘Mission’ and ‘Architecture’: architectures are usually proposed for specific mission types. An architecture consists of a specific concept of operations for a specific number of vehicles with certain assigned functions. A mission concept represents trajectories and durations envisioned for a flight opportunity. The two concepts are usually uncoupled.

The NASA Mars Design Reference Mission architecture, for example, was designed for a fast-conjunction class mission [Hoffman, Kaplan, 1997]. This does not preclude the NASA Mars DRM architecture from being used for an opposition class mission with a Venus flyby on the outbound leg: most architectures are not specifically limited to one mission type; particularly not the architectures described in Appendix A. Figure 3-1 illustrates this for three different architectures and four different missions. The red marks indicate that an architecture can be used to execute the mission

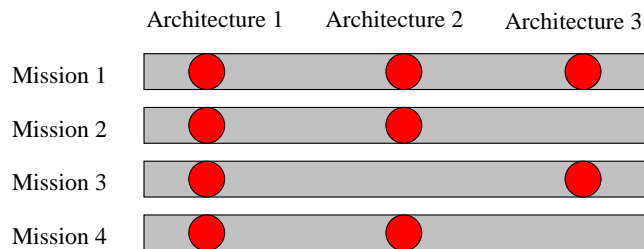


Figure 3-1: Distinction between mission and architecture

For the analysis in this chapter, we only include missions with crew transfers in destination orbit or on the destination surface (see Chapter 2, Appendix A). Crew transfer in transit is not included for two reasons: firstly, it is very risky to have crew transfer in transit on the way back to Earth, because the orbit of the craft one needs to rendezvous with is not in a bound orbit; therefore there is only one opportunity to rendezvous. Secondly, crew transfer in transit before entering destination orbit means abandoning an asset in interplanetary space which could be potentially used for contingency operations and which was very expensive to insert towards the destination. The mass savings obtained by not braking the assets into orbit could potentially offset both of these disadvantages. Apollo 11 astronaut Buzz Aldrin and others proposed cycler architectures that would allow rendezvous with a spacecraft previously abandoned in transit [McConaghy, 2002]. A conclusive analysis of this topic is, however, beyond the scope of this thesis.

The exclusion of crew transfers in transit leaves us with 14 remaining candidate architectures (see Appendix A), which will be analyzed for various Moon and Mars missions. All 14 architectures are eligible for a mission, as long as orbit can be achieved around the destination planet. This is possible for both the Moon and Mars.

Eight mission types will be investigated here: four Moon missions and four Mars mission types. Only landing missions are considered. Mars flybys and missions to Phobos or Deimos or NEOs are not included in the network. This is because the architectures are not to be designed for these missions. It does not preclude the use of the Moon and Mars architectures for such missions; this represents another direction of extensibility.

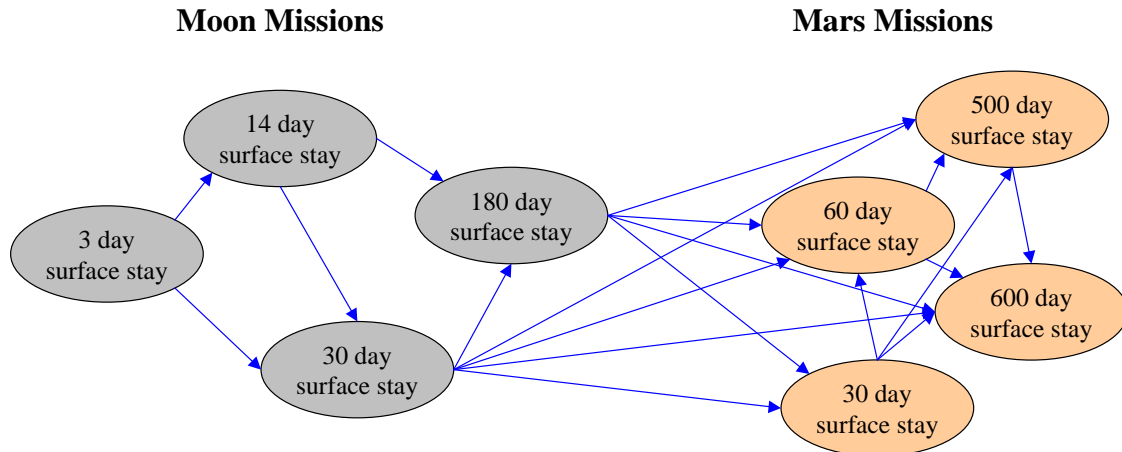


Figure 3-2: Network of conceivable manned Moon and Mars landing missions; mission durations based on [MIT 16.89 Course 2004, Walberg 1993]

In Figure 3-2 eight missions are shown in the form of a network. The network only shows mission types, not how often each mission is executed. This implies that a mission could also be executed 0 times. The arrows in the network indicate what follow-on missions are possible once a certain mission type has been successfully flown. From Figure 3-2, it can be seen that there are many possible paths through the network. This is a token for the uncertainty that is in the nature of an extensible, sustainable space exploration program: as the information (“knowledge”, see [MIT 16.89 course 2004]) gathered during a particular mission influences the decision how to carry on and where to go next, it is impossible to predict the actual path through the network at the outset of the program [MIT 16.89 Course 2004]. This observation underlines the crucial need for extensible systems to meet changing requirements.

What can be assumed, however, is that every mission will be at least as demanding as its predecessor. This is in accordance with the principle of building up capabilities through a sequence of flights. This principle was established during the early days of space flight, and was especially apparent during the Apollo program (G, H, and J missions [NASA, 1969]). Therefore the arrows always point to missions with increasing surface stay duration, or to missions involving a change of destination from Moon to Mars.

The durations of the surface stays for lunar missions were chosen for the following reasons: the initial 3-day lunar landing mission is essentially a 21st-century Apollo mission demonstrating point-landing, surface EVA and other operational capabilities in

lunar vicinity. The landing site is not necessarily constrained; we will assume, however, that it will be close to one of the lunar poles.

After a successful 3-day mission, two other mission types with surface stays of 14 days and one month are enabled. The 14-day mission would also land close to one of the poles and always stay in sunlight. The 30-day mission would demonstrate lunar overnight stay capability (if it lands far from the sunlit pole) and pave the way (in terms of surface operations) for a 30-day surface stay Mars mission. In order to prepare for the very long surface stays possible on Mars, a 180-day lunar mission could be executed. The 180 days were chosen because, at the lunar poles (excluding ‘peaks of eternal light’), it is possible to stay in perpetual sunlight for exactly half a year; to stay in the sunlight is crucial, however, for thermal control and electrical power reasons.

For the following quantitative analysis, it will be assumed that all four lunar missions are executed exactly once. As it is desirable to be able to abort at any given point during the mission, all architectures that require a crew transfer in orbit are assumed to utilize an Earth-Moon L1 halo orbit. The reason for this choice is that the Earth-Moon L1 or L2 points are accessible from any point on the lunar surface at any time, and from these points, it is always possible to return to Earth. A polar lunar orbit is also accessible at any given time; however, due to the Moon’s orbital motion, the polar orbital plane that an orbital asset needed for return is in might not be aligned correctly for an immediate return to Earth, because the plane is fixed in space while the Moon is moving along its orbit. This would necessitate a waiting period of 10 – 14 days in lunar orbit, until the Moon is exactly at the opposite position in its orbit with the respect to the Earth (see Figure 3-3).

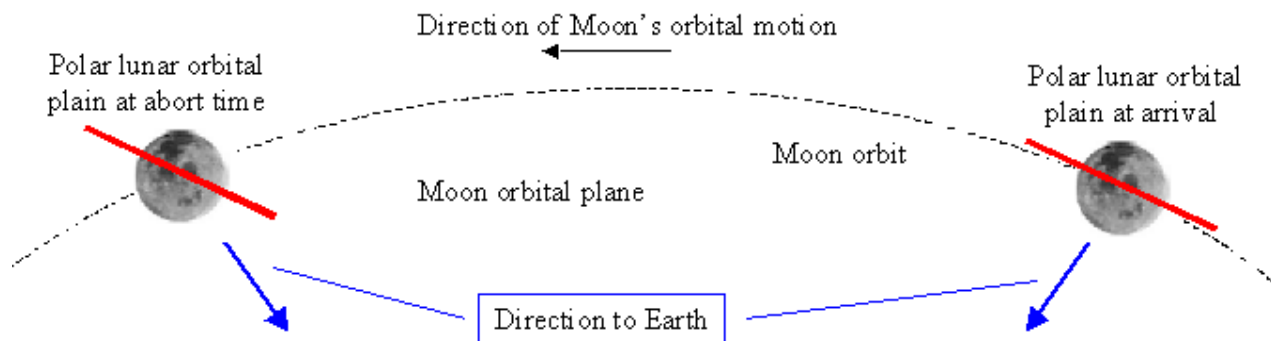


Figure 3-3: Reorientation of polar lunar orbits with the respect to the Earth due to the Moon’s orbital motion (not to scale)

Table 3-1 provides data on velocity changes, and durations of various mission phases for lunar missions via the Earth-Moon L1 point. Please note: crew transfers are executed only at the Earth-Moon L1 point, i.e. vehicles that are abandoned by the crew in orbit are left there. It is assumed, however, that vehicles going to the surface (directly or from the L1 point) make a stopover in LLO before the actual powered descent to the surface. This is a reasonable assumption, because the savings due to a direct landing are small, and the stopover allows for visual inspection of the landing site, and provides an additional controlled abort point. Also, from LLO, a rescue is conceivable, which is impossible on the surface. The Apollo LM also went into a low LLO before powered descent to the surface [NASA, 1972].

Lunar landing missions from L1	
Trans-lunar insertion velocity change in LEO to EM-L1	3100 m/s
Velocity change for insertion into EM-L1 halo orbit	750 m/s
Transfer duration between LEO and EM-L1	3.5 d
Velocity change to go from EN-L1 Halo orbit to LLO	(248+632) m/s
Velocity change for descent to lunar surface from LLO	2083 m/s
Velocity change to land from L1 directly	2745.5 m/s
Velocity change to go from LEO to LLO	3150 m/s
Velocity change from Apollo flyby hyperbola to LLO	850 m/s
Duration landing from LLO	1 d
Velocity change to ascend into LLO from lunar surface	1871 m/s
Duration of transfer between EM-L1 and LLO	3 d
Lunar surface stay durations	3 d, 14 d, 30 d, 180 d

Table 3-1: Reference data for velocity changes and mission phase durations used in the analysis of point designs in Section 3.2

The Mars mission types shown in the network above (see Figure 3-2) fall into two big categories: short missions with stay times in Mars vicinity from 30 to 60 days, and long missions with stay times in Mars vicinity in excess of 400 days.

The short mission types need to pass through the inner Solar System during transit to Mars, or on the way back from Mars, or on both legs. For certain opportunities, these passes through the inner Solar System can be augmented in terms of trip time and velocity changes by Venus flybys. Figure 3-4 illustrates two possible mission geometries:

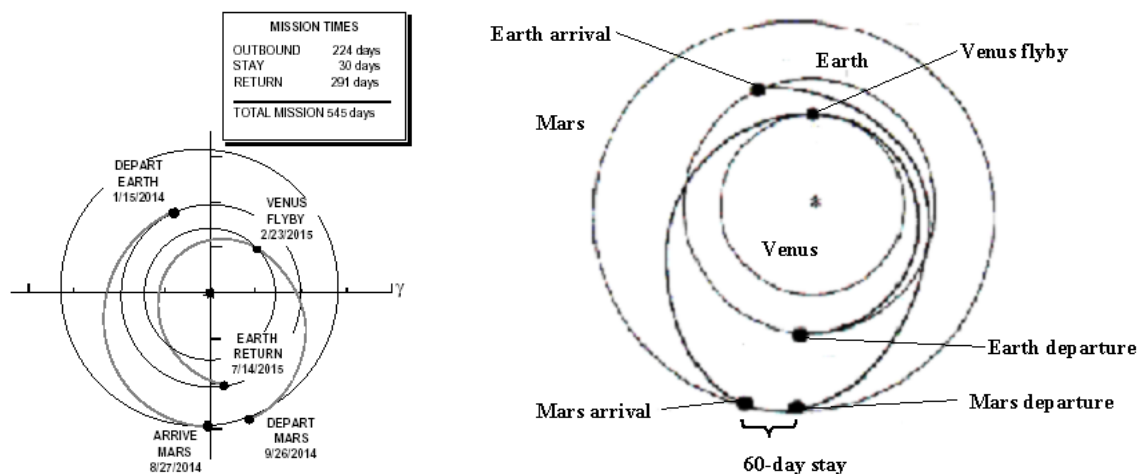


Figure 3-4: Two possible opposition class Mars mission geometries with Venus flybys [NASA, 1994], [Walberg 1993]

The mission on the left-hand side has a near-Hohmann transfer on the way to Mars, and a Venus-flyby on the return trip to Earth; the stay time in Mars vicinity is about 30 days. The mission on the right-hand uses a Venus flyby on the trip to Mars, and a regular

elliptic trajectory on the way back. Due to the particular phasing constraints, the return trajectory also needs to pass through the inner Solar system. Passing through the inner Solar System is, in general, difficult from a radiation shielding and thermal control point of view.

Table 3-2 provides reference data for a 30-day stay Mars mission with a Venus flyby on the way to Mars, and a 60-day stay mission with a Venus flyby on the trip back to Earth [Walberg 1993]. The velocity changes for Mars orbit insertion (MOI) and trans-Earth insertion (TEI) given in the original source [Walberg 1993] were adapted for a 500 km high LMO.

Opposition class mission, Venus flyby outbound, 1983	
Trans-Mars insertion velocity change	7360 m/s
Earth-Mars transit duration	250 d
Velocity change for Mars orbit insertion	4290 m/s
Mars vicinity stay time	30 d
Trans-Earth insertion velocity change	3720 m/s
Earth Entry velocity	16540 m/s
Mars Earth transit duration	210 d
Total duration	495 d
Opposition class mission, Venus flyby inbound, 2015	
Trans-Mars insertion velocity change	4893 m/s
Earth-Mars transit duration	220.6 d
Velocity change for Mars orbit insertion	5076 m/s
Mars vicinity stay time	60d
Trans-Earth insertion velocity change	4442 m/s
Earth Entry velocity	12811 m/s
Mars Earth transit duration	249.9 d
Total duration	535.3 d

Table 3-2: Reference data for opposition-class Mars missions, adapted from [Walberg 1993]

The two long Mars mission types are illustrated in Figure 3-5:

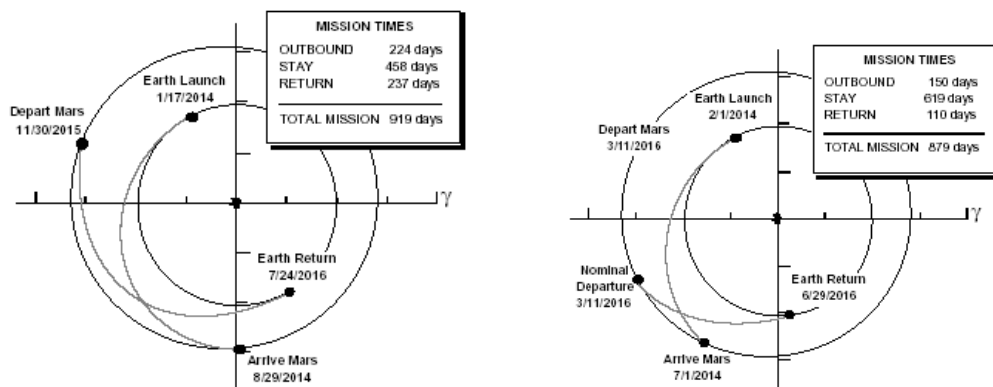


Figure 3-5: Conjunction class Mars mission overview

On the left-hand side of Figure 3-5 mission where both transfer trajectories have a transfer angle close to 180 degrees (near-Hohmann transfer). The stay time in Mars vicinity is between 400 and 500 days, and the velocity changes required as well as the Earth entry velocity are modest (see Table 3-3). On the right-hand side, a long Mars mission with fast transits between Earth and Mars is shown. The transfer angles are closer to 90 degrees, and the transfer times between Earth and Mars are below 180 days, i.e. they are below typical increment stay times for the International Space Station, and therefore in the US micro gravity database [Hoffman, Kaplan, 1997]. Due to the fast transfers between Earth and Mars, fast conjunction-class missions are especially interesting in terms of limiting micro gravity exposure, and because they don't require transfers through the inner Solar System with the associated radiation and thermal control challenges (see above).

Conjunction-class mission, 2018	
Trans-Mars insertion velocity change	3506 m/s
Earth-Mars transit duration	235.1 d
Velocity change for Mars orbit insertion	2344 m/s
Mars vicinity stay time	515.4 d
Trans-Earth insertion velocity change	2412 m/s
Earth Entry velocity	11263 m/s
Mars Earth transit duration	191.2 d
Total duration	946.7 d
Fast conjunction class mission, 2016	
Trans-Mars insertion velocity change	3687 m/s
Earth-Mars transit duration	150 d
Velocity change for Mars orbit insertion	4968 m/s
Mars vicinity stay time	635 d
Trans-Earth insertion velocity change	2845 m/s
Earth Entry velocity	13097 m/s
Mars Earth transit duration	120 d
Total duration	910 d
Standard Hohmann Mission (ideal)	
Trans-Mars insertion velocity change	3600 m/s
Earth-Mars transit duration	260 d
Velocity change for Mars orbit insertion	2115 m/s
Mars surface stay	500 d
Trans-Earth insertion velocity change	2115 m/s
Earth Entry velocity	11215 m/s
Mars Earth transit duration	260 d
Total duration	1020 d

Table 3-3: Reference data for conjunction class missions, according to [Walberg 1993], and for a reference mission based on ideal coplanar Hohmann transfers (see Appendix B)

Table 3-3 provides reference data for conjunction class missions. The velocity changes for Mars orbit insertion (MOI) and trans-Earth insertion (TEI) given in the original source [Walberg 1993] were adapted for a 500 km high LMO. Also, reference data are given for a mission based on ideal coplanar Hohmann transfers assuming a circular Mars orbit (see Appendix B). This transfer will serve as reference mission for cargo transport and pre-deployment, which can be perceived as the “logistics” operations of the mission.

3.2 Architecture Point Designs

The objective of this section is to identify preferred system architectures for the mission types described above. The figures of merit, or metrics, to measure the value of a mission are IMLEO (quantitative), as well as mission risk and extensibility towards other architectures in the mission type network of Figure 3-2 (qualitative).

As mentioned above, the architecture model developed in Section 2.1 leaves considerable design freedom for vehicle design variables. Table 3-4 provides an overview of the vehicle design variables that are not specified by the architecture model:

Design variable	Value / Option
Mars staging orbit	Low Mars orbit (LMO)
Mars orbital capture	Aerocapture or direct entry
In Situ Propellant Production	No
Crew size for lunar missions	3
Crew size for Mars Mission	6
TMI / TLI propulsion	LH ₂ , LOX / Nuclear
All remaining maneuvers	LCH ₄ , LOX (low boil-off)
LMO to surface duration	2.5 d
LLO to surface duration	1 d
Mass Earth Entry Capsule	12000 kg

Table 3-4: Vehicle design variables unspecified by the top-level architecture model; these variables apply to all architectures

The staging orbit around Mars is a Low Mars Orbit (LMO) of about 500 km height; the velocity change necessary to de-orbit is below 100 m/s, and is assumed to be provided by several short maneuvers with the reaction control system. For abort reasons, the staging orbit for the lunar missions is assumed to be the Earth-Moon L1.

Capture into the Mars staging orbit is achieved by aerocapture; for the unmanned repositioning of ground assets, direct aeroentry is conceivable, if the weather-conditions prove favorable (no dust-storms).

ISPP is not used for the analysis of the preferred architectures. Extensibility towards easy incorporation of ISRU / ISPP into the architecture is one of the qualitative selection criteria. Also, Appendix C provides the results for calculations of architectures that incorporate ISPP of the propellant used to ascend from the Moon, or Mars. This ISPP is assumed to be ideal: the propellant is ready on the planetary surface, and is just picked up and used by the crew.

The crew size for lunar missions is assumed to be 3, and 6 for Mars missions. For Mars missions, this choice is driven by the need for key qualifications in the team [Hoffman, Kaplan, 1997].

The TMI / TLI propulsion stages use either liquid hydrogen / liquid oxygen (two sequential stages), or nuclear thermal propulsion (one stage).

The duration for the descent to the surface and ascent from it to a low orbit is assumed to be about 2.5 days for Mars [ESA, 2004], and one day for the Moon. The actual powered flight phases last, of course, only minutes, but additional time for rendezvous and docking and for contingencies has to be provided.

For Mars missions, it is assumed that the vehicle returning to Earth carries an Earth Entry Capsule for direct entry and descent of the crew to the surface of Earth out of the interplanetary trajectory. The mass of this capsule is assumed to be 12 tons [Hoffman, Kaplan, 2004]. For lunar missions, it is assumed that the manned vehicle the crew uses to return to Earth has a heat shield and performs direct Earth entry.

With these assumptions, and the trajectory information given in the preceding section and Appendix B, we can start the calculation of IMLEO for the architectures. The models used for the computations in this section are the empirical crew compartment / habitat model, the conceptual propulsion stage model (15 %-rule for tanks and engines, see Section 2.2), and the equation for heat shields. Parachutes and landing gears are neglected to simplify the calculations, i.e. make analytical solutions possible. For a top-level screening of many architectures, this approach provides enough resolution.

3.2.1 Results for Mars Missions

Figure 3-6 shows the IMLEO results of the 14 architectures for a short Mars mission with a 30-day surface stay, and a Venus swing-by on the way to Mars (see Figure 3-4).

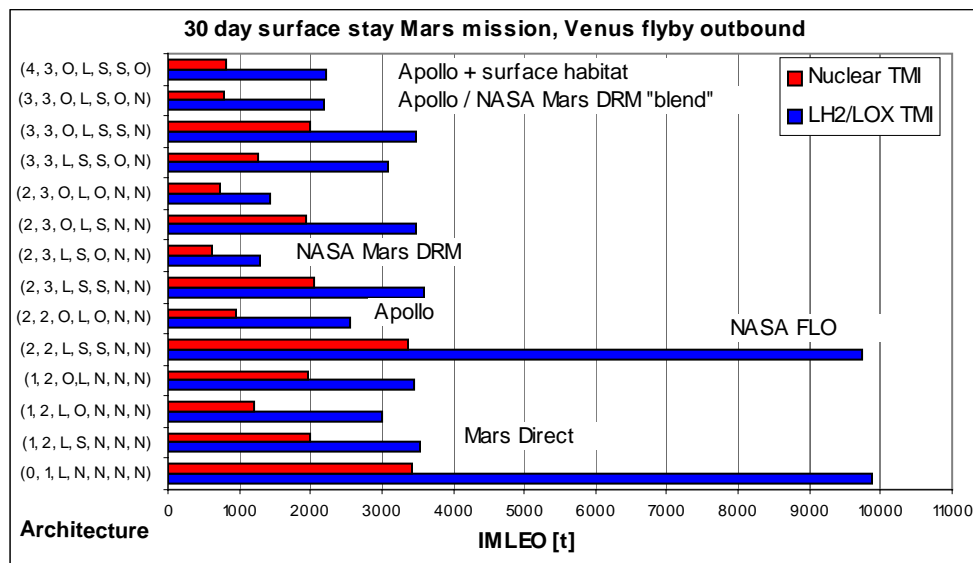


Figure 3-6: Architecture IMLEO results for 30-day short Mars mission

Table 3-5 shows the IMLEO results in the form of a ranking. The five best architectures are: NASA Mars DRM, $(2, 3, O, L, O, N, N)^T$, Apollo / DRM Blend, Apollo + surface habitat, and Apollo. These architectures fall into two broad groups: the first has a dedicated surface habitat, which is not brought back to orbit (DRM, Blend, Apollo + surface hab); the second has a combined descent / ascent and surface hab, that is brought back to orbit ($(2, 3, O, L, O, N, N)^T$, Apollo). The architecture of choice would be the NASA Mars DRM or the $(2, 3, O, L, O, N, N)^T$ architecture. For detailed descriptions of the architectures, please refer to Appendix A.

Architecture	IMLEO [t], TMI with LH2 / LOX
(2, 3, O, L, S, N, N), NASA Mars DRM	1292
(2, 3, O, L, O, N, N)	1430
(3, 3, O, L, S, O, N), DRM / Apollo "blend"	2199
(4, 3, O, L, S, S, O) Apollo + surface hab	2227
(2, 2, O, L, O, N, N) Apollo	2551
(1, 2, L, O, N, N, N)	3014
(3, 3, L, S, S, O, N)	3091
(1, 2, O, L, N, N, N)	3441
(3, 3, O, L, S, S, N)	3489
(2, 3, O, L, S, N, N)	3490
(1, 2, L, S, N, N, N), "Mars Direct"	3525
(2, 3, L, S, S, N, N)	3591
(2, 2, L, S, S, N, N)	9729
(0, 1, L, N, N, N, N)	9880

Table 3-5: Architecture ranking for a 30-day short Mars mission

Figure 3-7 shows the IMLEO results of the 14 architectures for a short Mars mission with a 60-day surface stay, and a Venus swing-by on the way back to Earth.

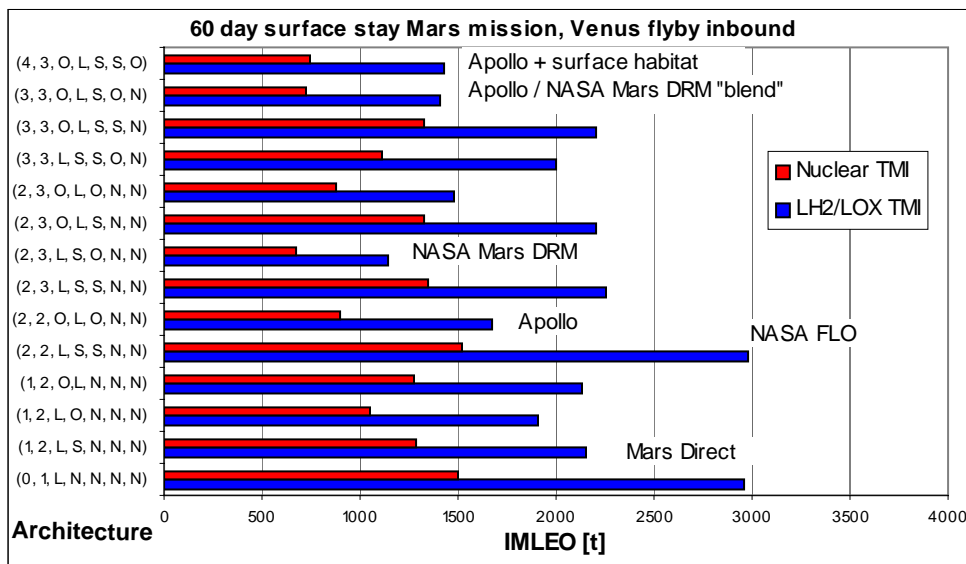


Figure 3-7: Architecture IMLEO results for a 60-dya short Mars mission

Table 3-6 shows the IMLEO results in the form of a ranking. The five best architectures are (as for the 30-day mission): NASA Mars DRM, Apollo / DRM Blend, Apollo + surface habitat, (2, 3, O, L, O, N, N)^T, and Apollo. The architecture of choice would be the NASA Mars DRM or the "Blend" architecture. It should be noted that the 60-day stay Mars mission with a Venus-flyby on the way back to Earth generally requires a lower IMLEO than the 30-day short Mars mission with the flyby on the way to Mars. Also, the architecture ranking is somewhat different.

Architecture	IMLEO [t], TMI with LH2 / LOX
(2, 3, O, L, S, N, N), NASA Mars DRM	1146
(3, 3, O, L, S, O, N), DRM / Apollo "blend"	1404
(4, 3, O, L, S, S, O) Apollo + surface hab	1433
(2, 3, O, L, O, N, N)	1474
(2, 2, O, L, O, N, N) Apollo	1675
(1, 2, L, O, N, N, N)	1911
(3, 3, L, S, S, O, N)	1997
(1, 2, O, L, N, N, N)	2128
(1, 2, L, S, N, N, N), "Mars Direct"	2149
(3, 3, O, L, S, S, N)	2205
(2, 3, O, L, S, N, N)	2207
(2, 3, L, S, S, N, N)	2252
(0, 1, L, N, N, N, N)	2958
(2, 2, L, S, S, N, N)	2980

Table 3-6: Architecture ranking for a 60-day short Mars mission

Figure 3-8 shows the IMLEO results of the 14 architectures for a minimum-energy conjunction class Mars mission with a 515-day surface stay.

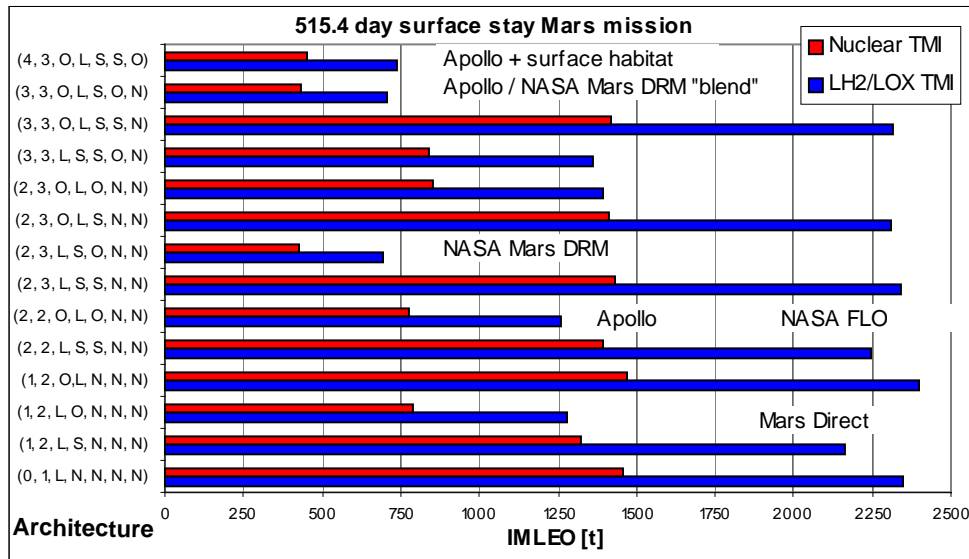


Figure 3-8: Architecture IMLEO results for a conjunction class Mars mission

Table 3-7 shows the IMLEO results in the form of a ranking. The five best architectures are: NASA Mars DRM, Apollo / DRM Blend, Apollo + surface habitat, Apollo, and (1, 2, L, O, N, N, N)^T. The architecture of choice would again be the NASA Mars DRM, the "Blend", or the Apollo + surface habitat architecture. The IMLEO requirement of the best architecture for the conjunction class Mars mission is a little more than half of that of a 60-day stay short Mars mission. The calculations here do not include the mass necessary for surface exploration operations (rovers, equipment); this mass is expected to be heavier for a 500-day Mars mission than for a 60-day Mars mission. However, it appears to be unlikely that the additional surface operations mass will close the gap of several 100 tons IMLEO between the conjunction class and the short Mars missions. The short-stay Mars missions are therefore more demanding in terms of IMLEO than the long-stay ones. This is mainly due to the larger velocity changes for TMI, MOI and TEI for the short-stay

missions. Other disadvantages of the short Mars mission include: long transit times between Mars and Earth due to the Venus flyby, and the associated close pass to the sun (radiation and thermal conditions). While an initial short-stay Mars mission could be desirable from a surface operations point of view, the results presented above suggest that as few of these missions as possible should be executed.

Table 3-7 shows that the architecture ranking is very different for short and for long Mars missions; the NASA Mars DRM architecture, however, always seems to be best. There is a noticeable gap between the three best architectures and the following ones.

Architecture	IMLEO [t], TMI with LH2 / LOX
(2, 3, O, L, S, N, N), NASA Mars DRM	694
(3, 3, O, L, S, O, N), DRM / Apollo "blend"	706
(4, 3, O, L, S, S, O) Apollo + surface hab	737
(2, 2, O, L, O, N, N) Apollo	1260
(1, 2, L, O, N, N, N)	1276
(3, 3, L, S, S, O, N)	1360
(2, 3, O, L, O, N, N)	1395
(1, 2, L, S, N, N, N), "Mars Direct"	2161
(2, 2, L, S, S, N, N)	2246
(2, 3, O, L, S, N, N)	2308
(3, 3, O, L, S, S, N)	2315
(2, 3, L, S, S, N, N)	2340
(0, 1, L, N, N, N, N)	2346
(1, 2, O, L, N, N, N)	2399

Table 3-7: Architecture ranking for a conjunction class Mars mission

Figure 3-9 shows the IMLEO results of the 14 architectures for a fast conjunction class Mars mission with a surface stay of 635 days.

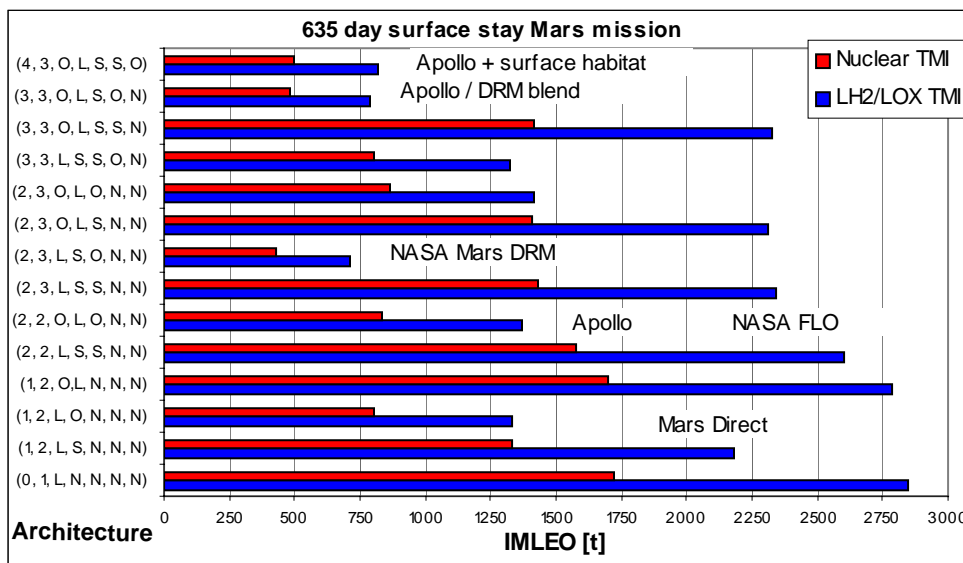


Figure 3-9: Architecture IMLEO results for a fast conjunction class Mars mission

Table 3-8 shows the IMLEO results in the form of a ranking. The five best architectures are: NASA Mars DRM, Apollo / DRM Blend, Apollo + surface habitat, (3, 3, L, S, S, O, N)^T, and (1, 2, L, O, N, N, N)^T. The architecture of choice would again be the NASA Mars

DRM, the “Blend”, or the Apollo + surface habitat architecture. Again, the IMLEO of the best architecture is significantly lower than the IMLEO requires for the best 60-day short Mars mission. The fast-conjunction class mission has interplanetary transfers in microgravity of below 180 days duration; this is comparable to a regular increment on the International Space Station [www.nasa.gov].

Again, there is a gap between the three best architectures, and the others. It should also be noted that the architecture ranking is slightly different than for the regular conjunction-class mission.

Architecture	IMLEO [t], TMI with LH2 / LOX
(2, 3, O, L, S, N, N), NASA Mars DRM	708
(3, 3, O, L, S, O, N), DRM / Apollo “blend”	789
(4, 3, O, L, S, S, O) Apollo + surface hab	820
(3, 3, L, S, S, O, N)	1323
(1, 2, L, O, N, N, N)	1330
(2, 2, O, L, O, N, N) Apollo	1366
(2, 3, O, L, O, N, N)	1415
(1, 2, L, S, N, N, N), “Mars Direct”	2179
(2, 3, O, L, S, N, N)	2309
(3, 3, O, L, S, S, N)	2323
(2, 3, L, S, S, N, N)	2340
(2, 2, L, S, S, N, N)	2605
(1, 2, O, L, N, N, N)	2719
(0, 1, L, N, N, N, N)	2846

Table 3-8: Architecture ranking for a fast conjunction class Mars mission

3.2.2 Results for Lunar Missions

Figure 3-10 shows the IMLEO results of the 14 architectures for lunar landing mission with a three-day surface stay.

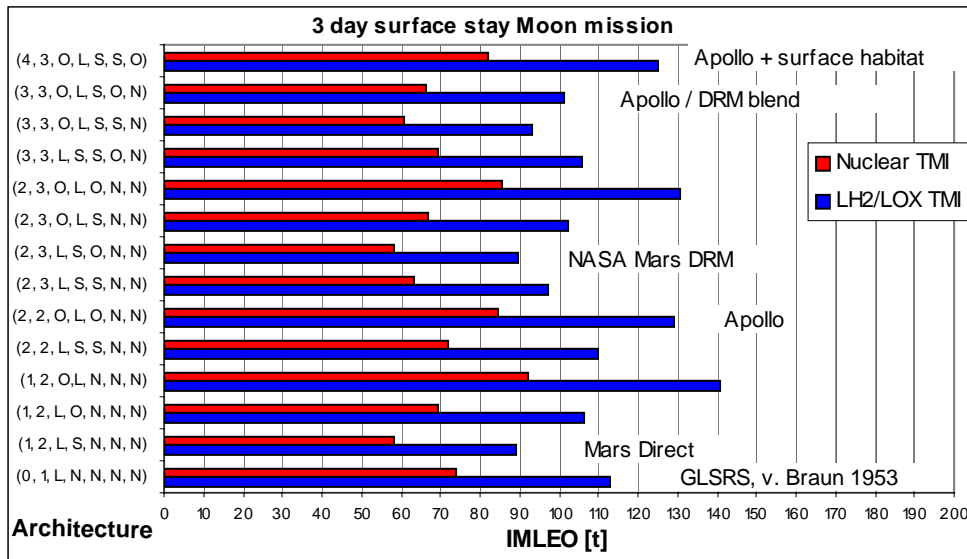


Figure 3-10: Architecture IMLEO results for a 3-day lunar landing mission (Apollo)

Table 3-9 shows the IMLEO results in the form of a ranking. The best architectures concerning IMLEO are those that do not require crew transfers at the Earth-Moon L1, but employ direct descent to or ascent from the lunar surface. This is understandable, because a stopover at the EM-L1 is costly in terms of velocity changes. It is also remarkable that for a lunar mission involving staging at EM-L1, there are many architectures that have lower IMLEO than the Apollo architecture. This is also the reason why the “Mars Direct” architecture is actually the optimal one, even better than the NASA Mars DRM architecture: the “Mars Direct” architecture does not involve any operations at the EM-L1, whereas for the NASA Mars DRM the crew has to ascend at the end of the mission to the EM-L1, and transfer there to the waiting Earth Return Vehicle. Introducing the EM-L1 point as staging point actually changes the architecture ranking substantially from that done LLO by [Houbolt, 1961]; rendezvous at the EM-L1 is no longer the preferred option but lunar surface rendezvous.

For the Moon, a selection criterion other than IMLEO applies: the ability to abort at any time during Earth-orbital operations, and during the transit to the Moon. This is only possible if the crew sets out in the same vehicle that is used for the return to Earth by direct entry. The only architectures fulfilling this condition are marked blue in Table 3-9. Of these, the NASA FLO, the Apollo + surface habitat, and the Apollo architectures are desirable. The one-vehicle architecture leads to a vehicle with over 110 tons even for the short 3-day lunar landing mission; this vehicle could probably not be launched, and would have to be assembled in orbit. For the other three architectures, each vehicle with the associated TLI stage weighs less than 110 tons, which shall be considered as the limit of the LEO capability of a future HLLV.

Architecture	IMLEO [t], TMI with LH2 / LOX
(1, 2, L, S, N, N, N), “Mars Direct”	89.1
(2, 3, L, S, O, N, N), NASA Mars DRM	89.6
(3, 3, O, L, S, S, N)	93.1
(2, 3, L, S, S, N, N)	97.2
(3, 3, O, L, S, O, N), DRM / Apollo “blend”	101.3
(2, 3, O, L, S, N, N)	102.2
(3, 3, L, S, S, O, N)	105.9
(1, 2, L, O, N, N, N)	106.3
(2, 2, L, S, S, N, N) NASA FLO	110.1
(0, 1, L, N, N, N, N), GLSRS, v. Braun 1953	113.0
(4, 3, O, L, S, S, O) Apollo + surface hab	125.1
(2, 2, O, L, O, N, N) Apollo	128.9
(2, 3, O, L, O, N, N)	130.3
(1, 2, O, L, N, N, N)	140.7

Table 3-9: Architecture ranking for a 3-day lunar landing mission

In Figures 3-11 to 3-13 and Tables 3-10 to 3-12, IMLEO results and architecture rankings are presented for lunar landing missions with surface stays of 14, 30, and 180 days. As it is always desirable to have an option for abort with direct Earth entry during Earth-orbital operations, and during the coast to the Moon, the same condition applies as described above. Again, only the four architectures which are highlighted in blue are available to choose from. And, again, the one-vehicle architecture is deemed undesirable. Therefore, for all the lunar missions, the NASA First Lunar Outpost, the Apollo + surface habitat,

and the Apollo architecture are most desirable. From these architectures, the best lunar architecture is chosen for each mission in the following section.

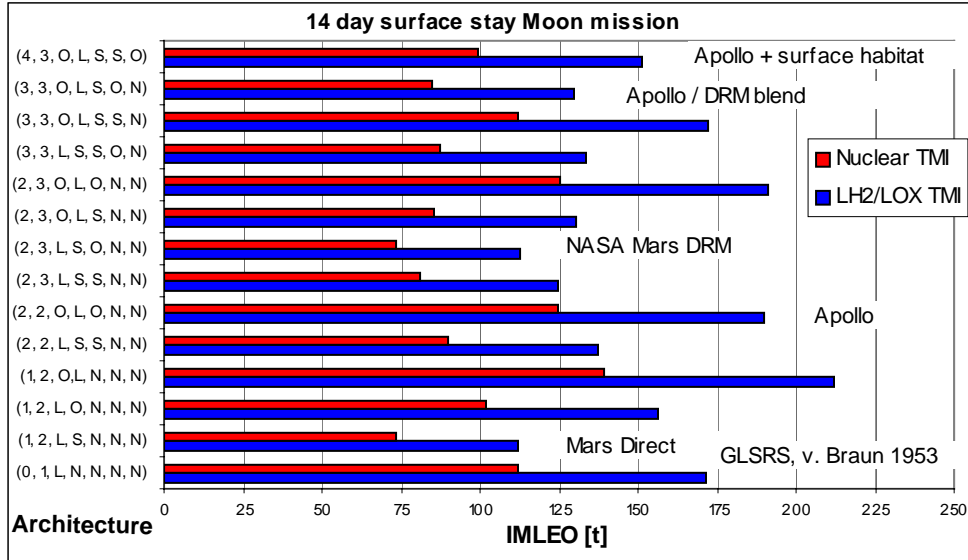


Figure 3-11: Architecture IMLEO results for a 14-day lunar landing mission

Architecture	IMLEO [t], TMI with LH2 / LOX
(1, 2, L, S, N, N, N), “Mars Direct”	112.2
(2, 3, L, S, O, N, N), NASA Mars DRM	112.7
(2, 3, L, S, S, N, N)	124.7
(3, 3, O, L, S, O, N), DRM / Apollo “blend”	129.5
(2, 3, O, L, S, N, N)	130.4
(3, 3, L, S, S, O, N)	133.4
(2, 2, L, S, S, N, N) NASA FLO	137.6
(4, 3, O, L, S, S, O) Apollo + surface hab	151.2
(1, 2, L, O, N, N, N)	156.2
(0, 1, L, N, N, N, N), GLSRS, v. Braun 1953	171.8
(3, 3, O, L, S, S, N)	171.8
(2, 2, O, L, O, N, N) Apollo	189.6
(2, 3, O, L, O, N, N)	191.0
(1, 2, O, L, N, N, N)	212.0

Table 3-10: Architecture ranking for a 14-day lunar landing mission

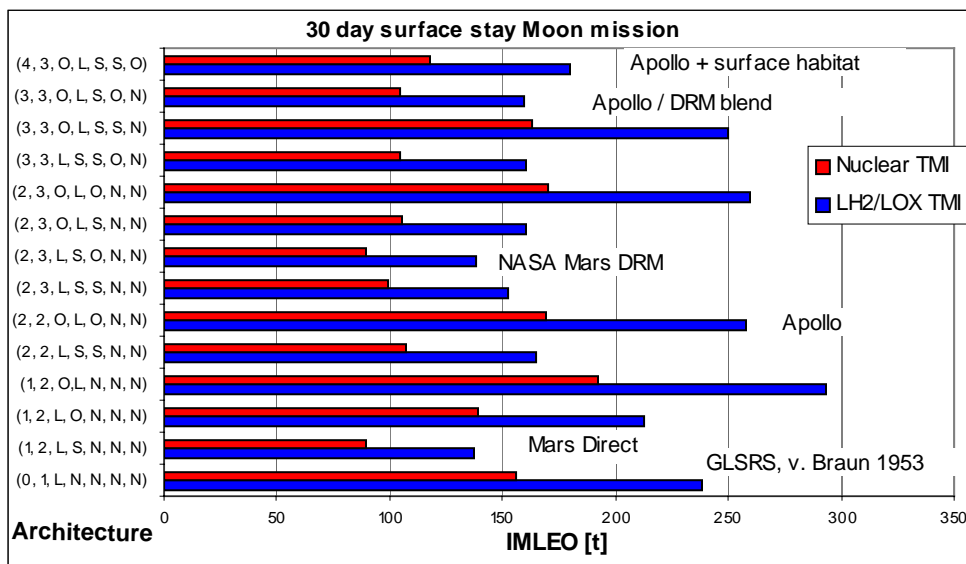


Figure 3-12: Architecture IMLEO results for a 30-day lunar landing mission

Architecture	IMLEO [t], TMI with LH2 / LOX
(1, 2, L, S, N, N, N), "Mars Direct"	137.3
(2, 3, L, S, O, N, N), NASA Mars DRM	137.8
(2, 3, L, S, S, N, N)	152.0
(3, 3, O, L, S, O, N), DRM / Apollo "blend"	159.8
(2, 3, O, L, S, N, N)	160.7
(3, 3, L, S, S, O, N)	160.8
(2, 2, L, S, S, N, N) NASA FLO	164.8
(4, 3, O, L, S, S, O) Apollo + surface hab	179.9
(1, 2, L, O, N, N, N)	212.8
(0, 1, L, N, N, N, N), GLSRS, v. Braun 1953	238.6
(3, 3, O, L, S, S, N)	250.0
(2, 2, O, L, O, N, N) Apollo	258.0
(2, 3, O, L, O, N, N)	259.0
(1, 2, O, L, N, N, N)	292.8

Table 3-11: Architecture ranking for a 30-day lunar landing mission

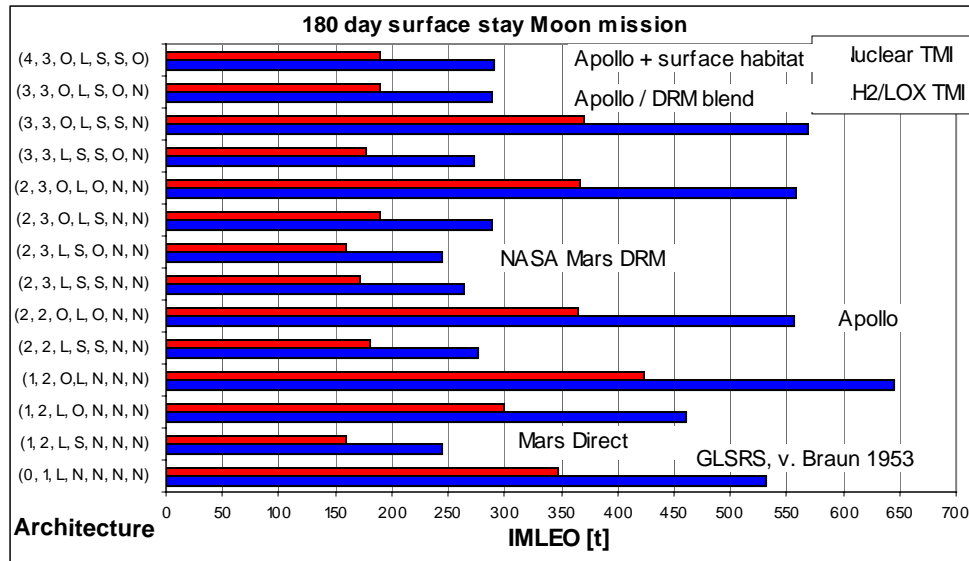


Figure 3-13: Architecture IMLEO results for a 180-day lunar landing mission

Architecture	IMLEO [t], TMI with LH2 / LOX
(1, 2, L, S, N, N, N), "Mars Direct"	243.9
(2, 3, L, S, O, N, N), NASA Mars DRM	244.4
(2, 3, L, S, S, N, N)	263.3
(3, 3, L, S, S, O, N)	272.0
(2, 2, L, S, S, N, N) NASA FLO	276.1
(3, 3, O, L, S, O, N), DRM / Apollo "blend"	288.3
(2, 3, O, L, S, N, N)	289.2
(4, 3, O, L, S, S, O) Apollo + surface hab	291.2
(1, 2, L, O, N, N, N)	460.2
(0, 1, L, N, N, N, N), GLSRS, v. Braun 1953	531.5
(2, 2, O, L, O, N, N) Apollo	556.1
(2, 3, O, L, O, N, N)	557.6
(3, 3, O, L, S, S, N)	568.9
(1, 2, O, L, N, N, N)	645.9

Table 3-12: Architecture ranking for a 180-day lunar landing mission

3.2.3 Preferred Missions and Architectures

Before trading options various design variables of the architectures, baseline missions and architectures need to be established as a reference for the trades.

Preferred Missions

The selection of the baseline Mars missions shall be based on the IMLEO values required for the best-ranked architectures. The selection for the lunar landing missions is straightforward: two of the interesting architectures permit to execute the longest (and

therefore heaviest) 180-day Moon mission with an IMLEO below 300 t. This appears to be acceptable; all four lunar mission types are therefore baselined.

The results shown for the Mars missions are only representative for specific opportunities; due to the eccentricity of the orbit of Mars around the sun, the needed velocity changes and hence the mission masses can be subject to considerable variations (see Appendix B). Nevertheless, certain conclusions can be drawn from the results shown above: short Mars missions are more demanding concerning IMLEO than long Mars missions (except for the length surface stay). Of the two short Mars missions, the 60-day stay mission has generally a lower IMLEO requirement, and twice the cumulative crew surface time than the 30-day mission. Therefore the former is selected as the baseline short mission type.

The IMLEO difference between the best alternatives of the two long Mars mission types is below 100 t; therefore, the fast-conjunction class mission appears to be more attractive. There is a drawback, however: the fast-conjunction class mission necessitates very high reentry velocities in excess of 16 km/s at Earth for some opportunities; this will have considerable implications on the design of the Earth entry capsule, and therefore on the CEV. As the Earth-Mars and Mars Earth transit trajectories are decoupled, however, the Earth entry velocity can be lowered by choosing a Hohmann-type Mars-Earth trajectory with entry velocities around 13 km/s. The baseline long Mars mission chosen for further analysis is therefore a hybrid between the conjunction class and fast-conjunction class missions: it has the propulsive capabilities and the life support on the surface to execute the fast-conjunction class mission, and the life-support capabilities to sustain the longer transfer times introduced by the regular conjunction class missions. With this choice, maximum flexibility is ensured.

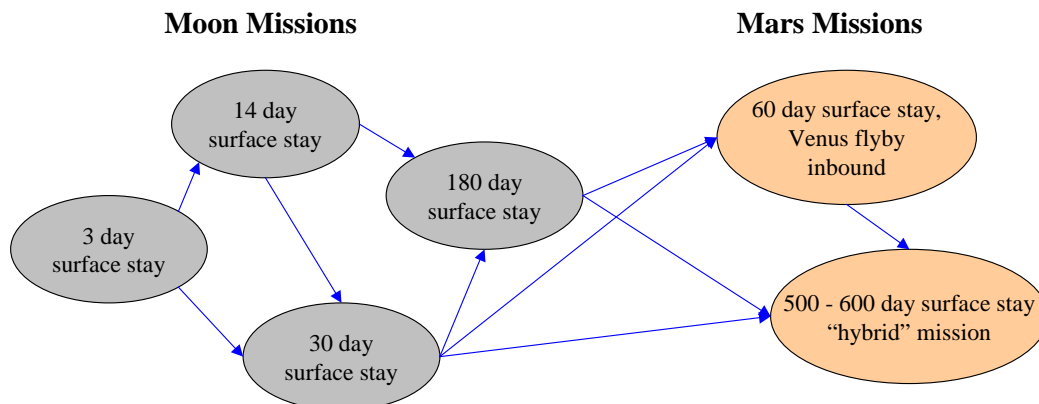


Figure 3-14: Preferred mission type network for further trade analysis

Preferred Lunar Architectures:

The preferred lunar architecture for the 14-, 30-, and 180-day lunar landing missions is the Apollo + surface habitat architecture (Figure 3-15), even though the quantitative analysis above revealed that it is not the most mass-effective. The reasons for this choice as opposed to the more mass-efficient NASA FLO are:

- Separate extension of the lunar surface habitat possible from 14 days to 180 days (as for the FLO); this is the dominant advantage, because it creates flexibility
- Low IMLEO, only moderately higher than for the NASA FLO

- More, but less massive vehicles than the NASA FLO
- If the lander and orbiter are sent to the Moon together, then two pressurized volumes are available in case of contingency situations similar to the one encountered during the Apollo 13 mission.

Especially the last argument makes the Apollo + surface habitat architecture appear more attractive than the NASA FLO.

For the 3-day lunar surface mission, an Apollo architecture was chosen. This architecture is a subset of the Apollo + surface habitat architecture, and employs only the orbiter and lander. In order to execute a three-day lunar surface mission with the lander, the lifetime has to be extended from two days to five days. This approach enables initial lunar missions with only the lander and orbiter, and extended lunar missions once the surface habitat is ready. Figure 3-15 illustrates the two architectures (see Appendix A).

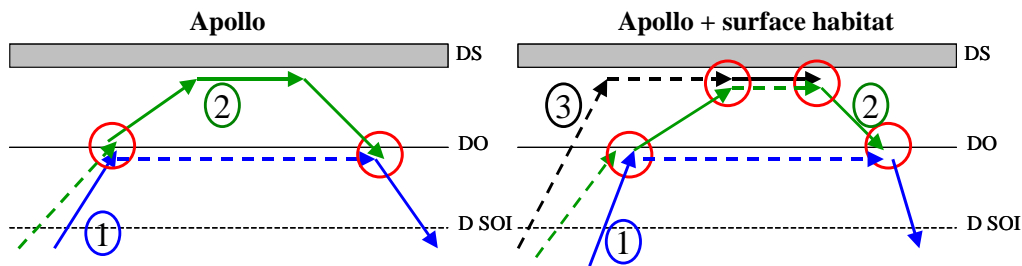


Figure 3-15: Overview of preferred lunar architectures, numbers are vehicle designations

Preferred Mars Architectures:

For the preferred Mars missions, three architectures are interesting: the NASA Mars DRM, the “Blend”, and the Apollo + surface habitat. The latter has the highest mass; its prime advantage is the fact that it offers the option of abort to orbit during descent, because it lands the crew in the ascent vehicle. There are several reasons why the abort to orbit option during descent is actually unattractive for Mars missions (as opposed to lunar missions!):

- In order to make the abort option work, all the consumables for the entire mission need to be provided in the orbiting spacecraft. As the calculations presented in this Chapter were carried out for nominal missions, this would further increase the IMLEO of the architecture beyond the values given above.
- The actual window in which the abort option is needed is very small compared to the overall mission duration: as it appears to be unlikely that a successful separation from the heat shield and the landing stage can be carried out at high Mach-numbers during the early portion of reentry, an abort to orbit is only possible relatively close to the surface, after parachute deployment.
- As it is conceivable that a Mars landing is possible with very little to no propulsive capability, the abort option would only be provided for the event of a parachute malfunction. This could be countered by carrying spare parachutes.
- If the crew lands too far from the surface habitat, they have to go back to Mars orbit after only a few days. One of the major topics of future work will be the analysis and comparison of abort options and scenarios for Moon and Mars missions

Therefore, the Apollo + surface habitat architecture is not considered for Mars missions. This leaves the two architectures depicted in Figure 3-16:

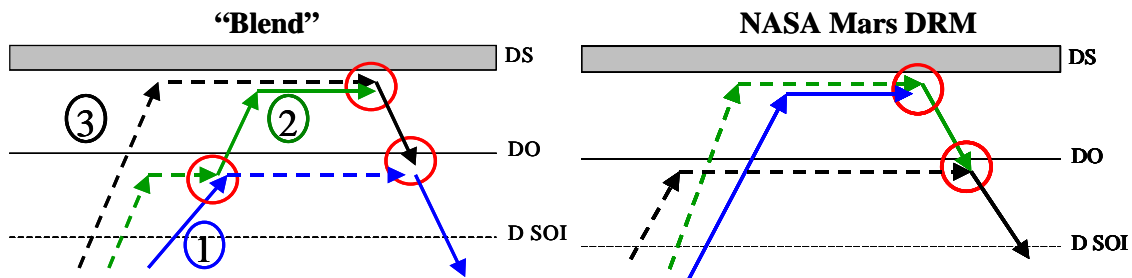


Figure 3-16: Preferred Mars architectures, numbers are vehicle designations

The “Blend” architecture is related to the NASA Mars DRM architecture, because it also features a predeployed Mars ascent vehicle, which could be used later for ISPP. The disadvantages of the “Blend” architecture are:

- Slightly higher IMLEO than the NASA Mars DRM
- Rendezvous / crew transfer in Mars orbit on the critical path for the mission.

Advantages are:

- One in-space habitat and one landing and surface habitat; subsystem design either for microgravity and partial gravity possible (weight reduction).
- Abort in orbit possible, because the crew first gains access to all consumables needed for the remainder of the mission, before they descend to the surface.
- Once the crew decides to land, pinpoint-landing capability is still required in order to return to orbit.

Despite the disadvantages, the “Blend” architecture is chosen as the favorite architecture for this thesis, partially also, because it has never been investigated before, and because it is easily possible to convert it into a NASA Mars DRM mission. The “Blend” architecture is used for both the long and short Mars missions.

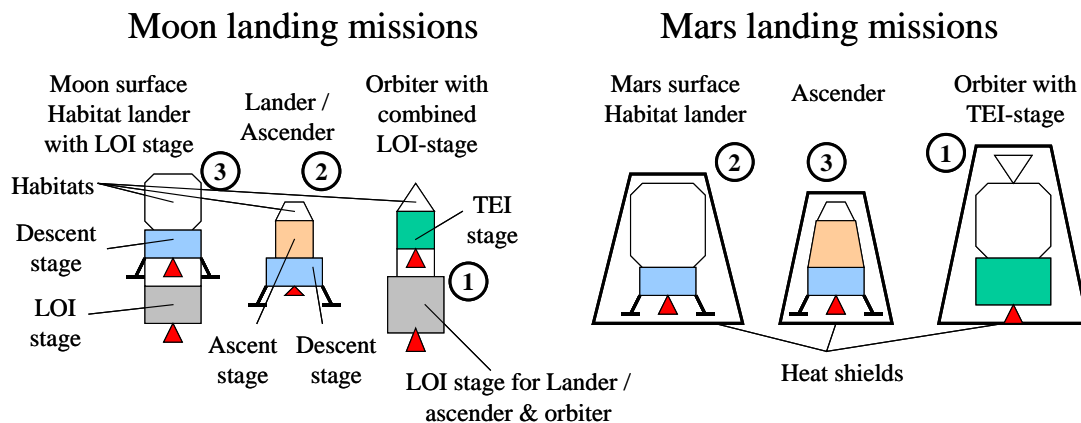


Figure 3-17: Hardware elements of the preferred Moon and Mars architectures (TMI / TLI stages not shown); commonality and modularity are not yet considered (point designs). The numbers besides the vehicles are the designations of these vehicles in the architecture diagrams from Figure 3-15 and 3-16

Figure 3-17 provides an overview over the hardware elements needed for both the lunar and Mars missions. The TMI / TLI stages for insertion towards the Moon and Mars are

not shown. Also, the short Mars mission employs two TEI stages due to its higher propulsive requirements.

3.3 Trade Analysis

The preferred architectures chosen in the preceding section represent single points in the design space created by the design variables of the architecture model, and those introduced at the beginning of Section 3.2. In order to explore the regions in the design space around the points, and in order to test the robustness of the assumptions made so far, a trade analysis is conducted for the following design options:

- Lunar staging orbits and continuous surface abort
- Crew size and mission duration for lunar missions
- Mars free return trajectories and Mars orbit operations
- Number and sizes of propulsion stages for landing vehicles

The options and results for these trades are described in the following sections. The calculations were carried out with the same models as those used for the architecture evaluation in Section 3.2

3.3.1 Lunar Staging Orbit and Continuous Surface Abort Options

This trade is concerned with the option of abort to Earth at any time during the operations in lunar vicinity, and especially for landing sites close to the poles. As explained above, this option is desirable for the Moon, because it is realizable and because a return to Earth is possible in comparatively short time (3-4 days). The availability of continuous surface abort depends on the staging strategy chosen. The options are (the thick line indicates the option chosen before the trade, the shading the one chosen after the trade):

Surface abort options	Staging orbit
Return to EM-L1, from there to Earth	EM-L1
Provide additional lifetime in LLO orbiter	Polar LLO
Provide additional lifetime in Lander / Ascender	Polar LLO
Plane change inbound in <u>Highly Elliptical Lunar Orbit (HELO)</u>	Polar LLO
Plane change outbound and inbound in HELO	Polar LLO

Table 3-13: Staging options for the realization of the continuous surface abort option for polar landing sites

The basic options are either to stage at the EM-L1 point (see above) or to put additional consumables into the orbiter or lander to wait until the return window to Earth opens again, or to go to LLO and perform one or more plane changes in lunar orbit. The EM-L1 option was chosen as default for the calculations presented above.

Quantitative analysis of the IMLEO masses for a 14-day lunar mission suggests that it is desirable to perform a plane change in a HELO before returning to Earth (see Figure 3-18). This eliminates the stopover in LLO and reduces the overall IMLEO compared to the results given in section 3.2.

For the analysis, the extra time required to execute the plane change in lunar orbit was assumed to be two days (worst case). The velocity change necessary to execute the plane

change increases the TEI velocity change from 850 m/s to about 1500 m/s (see Figure 3-19). The next best option would be to provide additional consumables in the orbiter. It should be noted that for some additional mass, it would also be possible to do the plane change maneuver on the way to polar lunar orbit; this would enable the use of free-return trajectories on the way to the Moon, and thereby increase safety. The calculations presented were done for lunar orbit insertion with cryogenic methane / LOX and hydrogen / LOX propellant combinations. As can be seen from Figure 3-18, using hydrogen would reduce the IMLEO, but would not change the ranking of the alternatives.

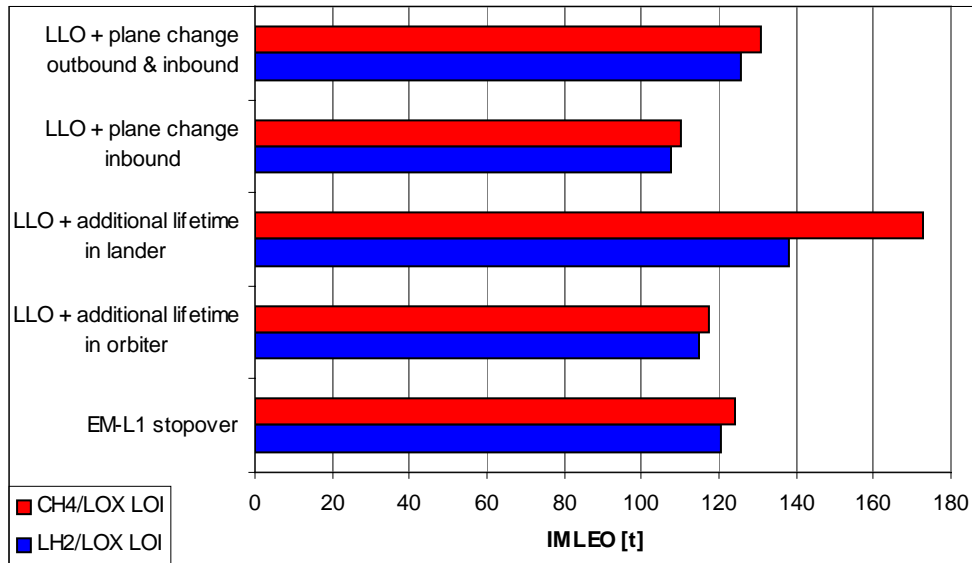


Figure 3-18: Results for lunar staging and abort trade

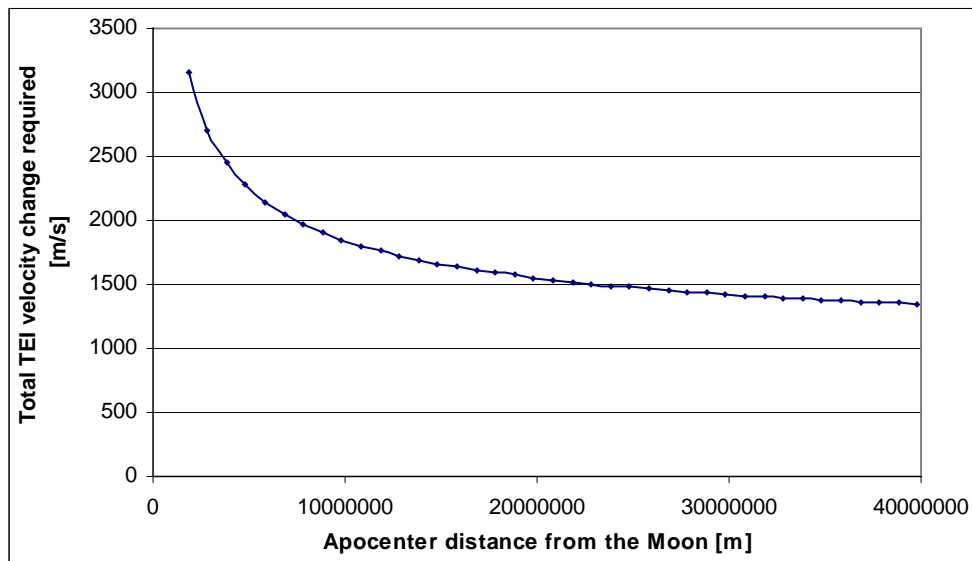


Figure 3-19: Total TEI velocity change including a 90° plane change maneuver of a HELO before returning to Earth

3.3.2 Crew Size and Mission Duration For Lunar Missions

For lunar missions, the surface duration is not constrained by orbital mechanics, but only by the lighting constraints of the landing site. For landing sites close to the poles, however, the lighted surface stays can be extended to 180 days. For a given requirement of cumulative man-hours on the surface, this makes it possible to trade crew size against surface stay duration. Crew sizes between 2 and 6 are considered, and cumulative surface stay times time between 60–180 crew days.

Trade Parameter	Range
Crew size	2, 3, 4, 5, 6
Cumulative crew time on the lunar surface	60 – 180 crew days
Crew size	Surface stay time [d]
2	30 – 90
3	20 – 60
4	15 – 45
5	12 – 36
6	10 – 30

Table 3-14: Crew size and cumulative surface time options

The calculations to assess the effect of crew size and duration are presented in the diagrams below. Two fundamental questions are interesting in this context:

- For a given IMLEO, what is the best number of crew and duration, to get the most cumulative surface days out of every unit mass invested?
- For a particular cumulative surface stay time, what is the best number of crew and duration to minimize IMLEO?

The effectiveness metric in this context is defined as mass / crew-days.

Best crew size, duration for given IMLEO

Figure 3-20 shows the answer to the first question. The blue points represent system designs with a certain crew size and surface stay time. The design points for a certain crew size visibly form a line.

The answer to the first of the above questions is provided in the form of a so-called Pareto front. The Pareto front is defined as the curve formed by the design points of non-dominated designs [de Weck, Chang, 2003]. In our case that means: if we hold the IMLEO constant, there is no design with a lower IMLEO per cumulative crew time on the surface. The Pareto front represents a ‘sound barrier’ for designs that cannot be crossed with present technology. In our case (see figure 3-20) the Pareto front states that if we reduce IMLEO, then we get less mass-efficient; if we increase the mass-efficiency, then we need more IMLEO.

The two end-points of the Pareto front can be used to define the so-called ‘Utopia point’, which represents an ideal design point that cannot be achieved, because it is on the infeasible side of the Pareto front (see Figure 3-20). The goal of technology development is to push the Pareto front into the direction of the Utopia point.

In our case, the designs with a crew size of two form the Pareto front; this indicates that lower crew sizes are always better to get the most cumulative surface time out of every mass unit invested in IMLEO. Also, it can be seen that if we were willing to invest more

IMLEO, we would be more mass-efficient, i.e. increase the cumulative surface time per mass unit (see Figure 3-20). This indicates that the initial investment to place the crew on the Moon (and similarly on Mars) is very high, but the additional investment for sustaining the crew becomes progressively less expensive (more efficient) for longer crew stays.

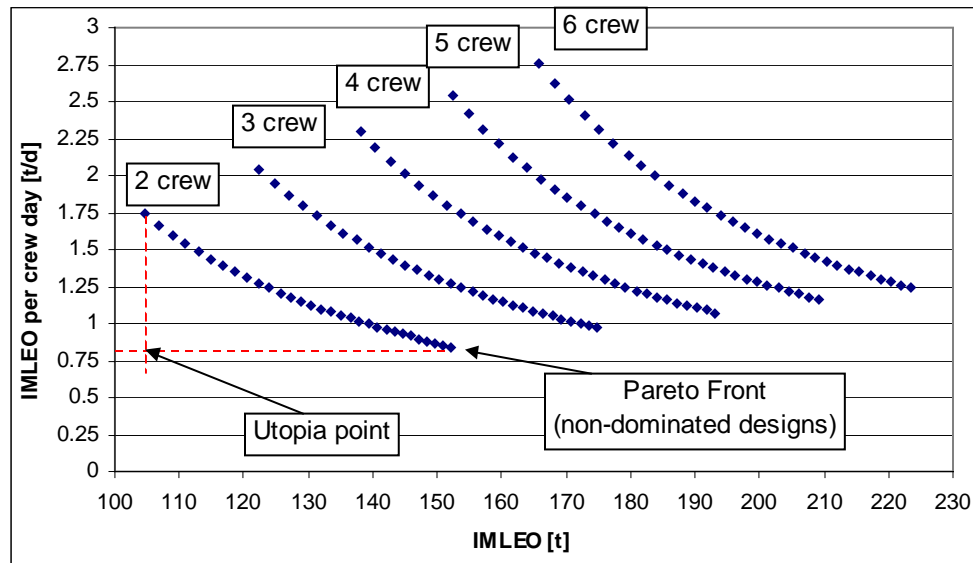


Figure 3-20: Pareto front for mass-effectiveness over IMLEO for lunar landing missions with varying crew size and duration

It should be noted that the definition of the Pareto front end point, and therefore also of the Utopia point is, to a certain degree, arbitrary. Nevertheless, the concept of the Utopia point and the front allow to qualitatively capture the nature of the trade and to indicate the direction for technology improvement.

Best crew size for given cumulative surface time

The second question is related to the first: for a given crew size, a longer cumulative surface stay time always necessitates a higher IMLEO and vice versa (more consumables for a longer stay). The second question is actually more interesting from an exploration point of view: the purpose of exploration is the accumulation of knowledge, concerning science, resources, operational capabilities, and technologies [MIT 16.89 course, 2004]. One of the factors determining the amount of knowledge gathered is the time (in man-hours) available for the process. For lunar landing missions, this would be the cumulative surface stay time of the crew on the surface. We could therefore rephrase the second question to: ‘in order to gather a certain amount of information / knowledge on the lunar surface, what is the best crew size and mission duration?’ Of course, it is assumed here that a crew of two for a long duration is as effective as a crew of six for a short duration, i.e. synergistic effects due to larger crew size are neglected. This assumption will have to be revisited and reassessed in future work.

The answer to the second question is presented again in the form of a diagram in Figure (3-21). The blue points again represent individual system designs. It can be seen, that for a given cumulative surface stay time, the system designs with 2 crewmembers again are most mass-efficient. The answer to the second question therefore is: in order to gather a certain amount of information / knowledge on the lunar surface, the most mass-efficient option is a small crew size for a long duration.

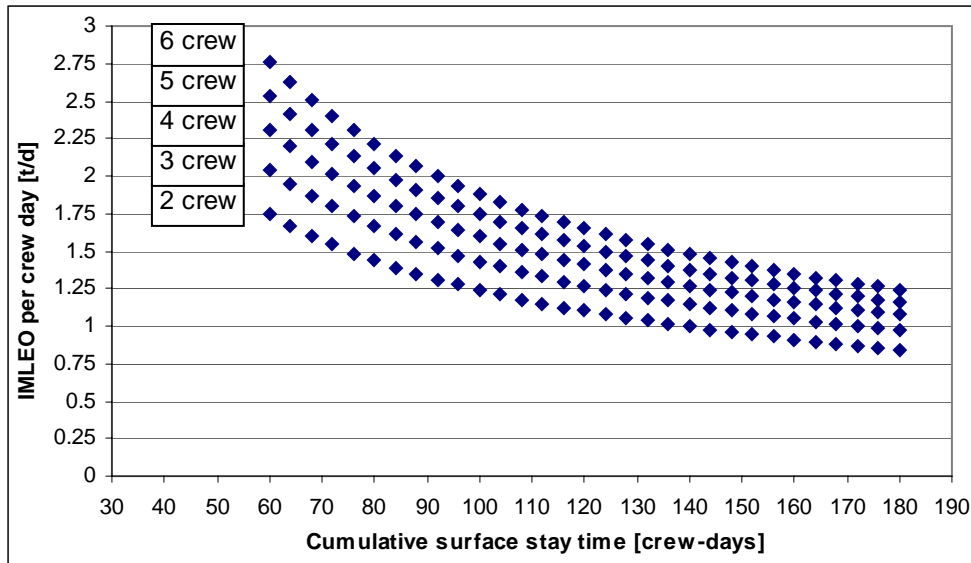


Figure 3-21: Diagram of mass-efficiency over cumulative lunar surface stay time for varying crew size and mission duration

Explanation of the mass efficiency for small crew sizes

A short explanation shall be presented here for the above results. The primary observation was that less mass is required to sustain a smaller crew for a longer time than a larger crew for a shorter time. In general, it is intuitively understandable that the initial investment of equipment mass per crewmember will be higher than the additional consumables needed in order to sustain fewer crewmembers for a longer time. This qualitative explanation shall be ascertained quantitatively by analyzing the effect of crew size onto the habitable and pressurized volume, and thereby on the structural mass of the crew compartment. Figure 3-22 shows the diagram for the habitable volume estimation presented in Section 2.2:

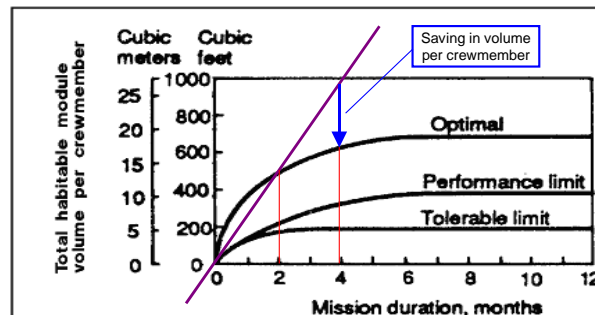


Figure 3-22: Habitable volume requirements and saving

Two missions are visualized in the diagram: one with a certain crew size that has a duration of four months, and one with exactly double the crew size, which lasts only two months; the cumulative duration for both is the same. It can be seen that, due to the curvature of the habitable volume model, the habitable volume (and therefore the pressurized volume) required by one crewmember for four months is smaller than the habitable volume required by two crewmembers, as indicated by the straight line through the origin. Therefore a smaller crew requires less habitable (and pressurized) volume, which translates into less structural mass, and causes the observed saving effect.

For the lunar landing missions considered in this thesis, we leave the crew size at three crewmembers, for the following reasons:

- A third crewmember is desirable for contingency situations in which two astronauts are stranded during EVA and need to be rescued by the third. This is especially important for longer missions, when the astronauts venture beyond walking distance from the surface habitat.
- A crew size of three is reasonably close to the minimum of two.
- By choosing a staged sleep-cycle, two crew-members are always awake, and work together (synergy).

3.3.3 Mars Free Return, Mars Staging Orbit and Mars Orbit Insertion

For the calculation of the point designs, it was assumed that spacecraft arriving at Mars would aerocapture into LMO, and then either stay in this orbit until TEI or land on the surface, and return to LMO. This trade is concerned with Mars staging options in case aerocapture is unavailable, and the impact of the Mars staging operations on the selection of interplanetary transfer trajectories. The most important interplanetary transfer trajectory in this context is a two-year free-return trajectory, which would bring the astronauts automatically back to Earth in case Mars orbit insertion is impossible. The disadvantage of the two-year free-return trajectory is that it features very high Mars arrival energies (see Appendix B).

Figure 3-23 provides an overview of the mission geometry in the vicinity of Mars:

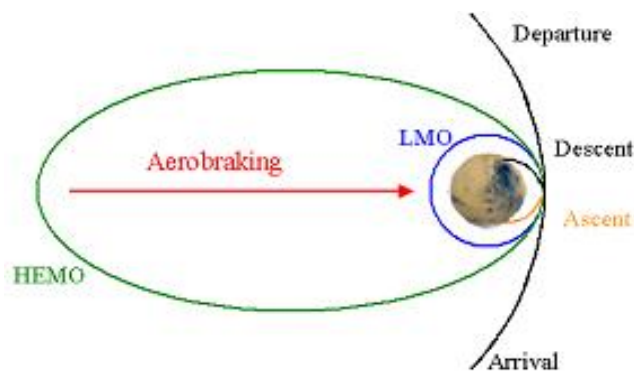


Figure 3-23: Mission geometry in the vicinity of Mars for staging operations

The major operational phases in the vicinity of Mars are: hyperbolic arrival, capture into either a LMO or Highly Elliptical Mars Orbit (HEMO), descent, surface stay, ascent, and departure. Commonly, it is assumed that the initial Mars staging orbit is identical to the final Mars staging orbit. It is, however, possible to modify the Mars staging orbit during the stay on the Martian surface, for example by aerobraking (see Figure 3-23), or by propulsive means.

In this section, a systematical analysis of staging operations in Mars vicinity is carried out for different types of Earth-Mars interplanetary trajectories. Figure (3-24) provides a systematic overview of the operations and maneuvers in Mars vicinity, created by using the Object-Process-Methodology of [Dori, 2002]. The major objects are the interplanetary arrival and departure trajectories, the initial and the rendezvous & TEI Mars orbits, and the orbit insertion and modification maneuvers. The last two of these can be in several states (rectangular boxes inside the objects). Not all combinations of states are viable: for example, it is physically impossible to modify a LMO to a HEMO by aerobraking.

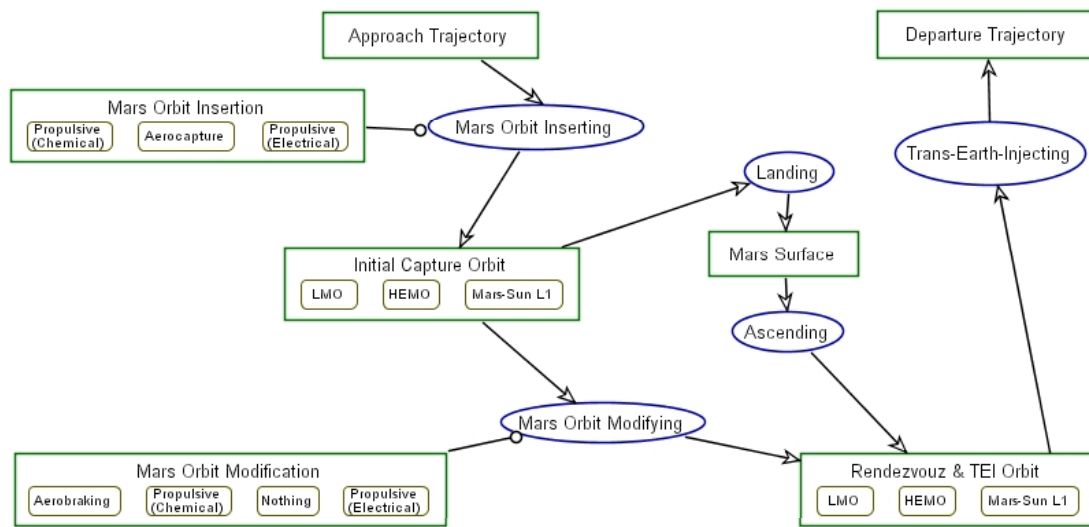


Figure 3-24: Systematical overview of operations in Mars vicinity in the form of a so-called Object-Process-Diagram [Dori, 2002]

Table 3-15 summarizes the options for Earth-Mars trajectories, and Mars staging operations. For long Mars missions, free-return trajectories are considered. The free-return represents a special type of fast conjunction class mission that employs an Earth-Mars transfer trajectory that has a heliocentric orbital period of exactly two years, and therefore reencounters the Earth.

Staging operations at the Mars-Sun libration points are not investigated in this trade study, nor are propulsive maneuvers with electrical propulsion. As in previous trades, the options chosen for the analysis of point design architectures in Section 3.2 feature thick lines, and the options chosen after the trade study are shaded. Mars staging options marked red are uninteresting, because they necessitate more mass than a solely propulsive insertion into Mars orbit.

The Mars staging operations are described in the form of a sequence of events: ‘Aerocapture-LMO-Nothing-LMO’, for example means that the spacecraft is aerocaptured into LMO, no orbit modification is performed, and the spacecraft remains in LMO.

The option employed up to this point is Aerocapture-LMO-Nothing-LMO.

Trajectory options
Conjunction class / Hohmann mission
Fast conjunction mission (transfer durations < 180 days)
Fast conjunction with 2 year free return outbound
Mars orbit insertion and modification
Aerocapture – LMO – Nothing – LMO
Propulsive – LMO – Nothing – LMO
<u><i>Aerocapture – LMO – Propulsive – HEMO</i></u>
<u><i>Propulsive – LMO – Propulsive HEMO</i></u>
<u><i>Aerocapture – HEMO – Propulsive – LMO</i></u>
Aerocapture – HEMO – Aerobraking – LMO
<u><i>Propulsive – HEMO – Propulsive – LMO</i></u>
Propulsive – HEMO – Aerobraking – LMO
Aerocapture – HEMO – Nothing – HEMO
Propulsive – HEMO – Nothing – HEMO

Table 3-15: Option space for Earth-Mars trajectory and Mars staging operations trade; options underlined and italic are undesirable and disregarded for the analysis

Table 3-16 provides reference data for the fast conjunction class Mars mission with a two-year free-return trajectory; for detailed calculations please refer to Appendix B.

Conjunction Class Mars Mission with Free-Return	
Trans-Mars insertion velocity change	4272 m/s
Earth-Mars transit duration	130 d
Velocity change for Mars orbit insertion	6782 m/s
Mars surface stay	710 d
Trans-Earth insertion velocity change	2600 m/s
Earth Entry velocity	16000 m/s
Mars Earth transit duration	180 d
Total duration	1020 d

Table 3-16: Reference data for a fast-conjunction class mission with a two-year free-return trajectory (see Appendix B)

Figure 3-25 shows results of the trade analysis for the various trajectory and staging options. The main conclusions to be drawn are:

- Either aerocapture technology, or technology for rendezvous in a HEMO is required to execute short Mars missions with an acceptable IMLEO (below 1500 tons per mission).
- If aerocapture is available, it is possible to use free-return trajectories (very desirable !)

- If both aerocapture and rendezvous in HEMO are available, the minimum IMLEO can be reduced.
- If both aerocapture and rendezvous in HEMO are unavailable, only minimum-energy and fast conjunction class Mars mission can be executed with acceptable IMLEO.

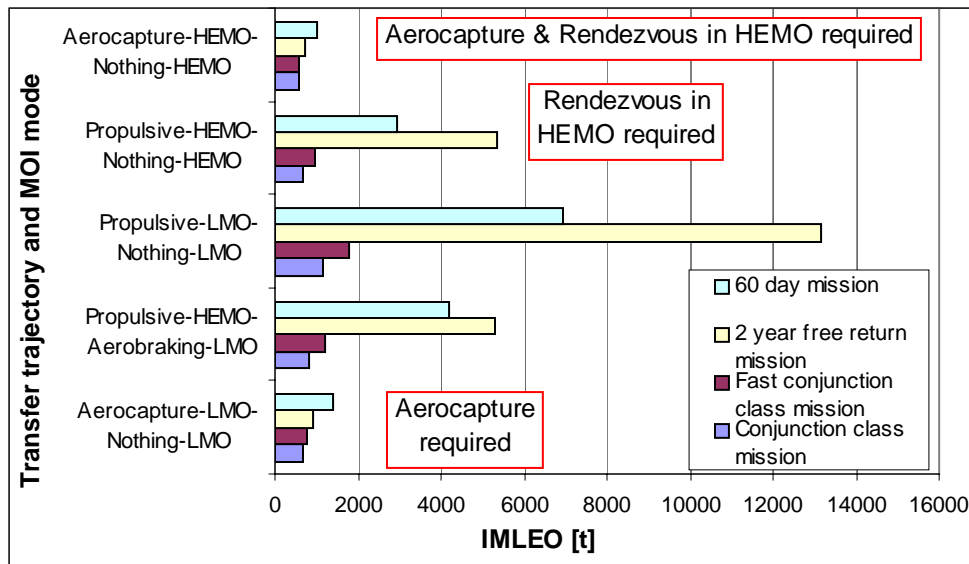


Figure 3-25: Results of the trajectory and staging operations trade for the 'Blend' architecture

On the basis of these observations, direct aerocapture into a LMO was chosen as the most desirable option; rendezvous in HEMO is considered desirable, but difficult, and is therefore not base-lined.

3.3.4 Number and Size of Propulsion Stages in the Landing System

For the point designs calculated in Section 3.2, it was assumed that for every major maneuver in the vicinity of the destination planet a dedicated propulsion stage is provided, and for the TLI / TMI maneuvers two propulsion stages. A lunar surface habitat therefore features two stages (besides TLI): one to brake into LLO, and one to land on the surface; analogous staging rules apply to all other vehicles.

It is the subject of this trade to investigate if other options of propulsion staging are advantageous. The trade space investigated is shown in Table 3-17. This trade is confined to the actual landing systems, i.e. the vehicles that go to the planetary surface.

Moon landing system				
Number of lander stages	1	2	2 (equal tank sizes)	3
Number of habitat lander stages	1	2	2 (equal tank sizes)	
Mars landing system				
Number of lander stages	1	2	2 (equal tank sizes)	3
Number of landers	1	2		
Number of habitat landers	1	2		

Table 3-17: Propulsion stage trade space for Moon and Mars landing systems

The stage numbers for the individual vehicles are based on the point design description given in Figure 3-17. Most of the trade options are self-explanatory, but one is quite unusual: generally, propulsion stages are either sized for one specific maneuver (e.g. lunar ascent), or, if several propulsion stages are used for one maneuver (launcher rockets), then it is assumed that they all provide the same velocity change. This is the optimal solution for minimal mass [Thomson, 1961], but yields very different stage sizes. It is also possible to assign velocity changes to propulsion stages so that they require the same amount of propellant (i.e. are of the same size). Thus, the need to develop several different stages is eliminated; as every stage design is a considerable investment, this could yield substantial cost savings. The implications of choosing stages with equal propellant masses (or tank sizes) are analyzed in Appendix D (see Section 7.4).

As the stages no longer share the optimal distribution of velocity changes, the overall mass of the system (payload + propulsion stages) is somewhat higher than for the stages with uniform velocity change. For high specific impulse propulsion (cryogenic methane or hydrogen + LOX), this mass overhead is very small, and can be neglected.

Choosing propulsion stages with the same amount of propellant has a significant impact on the operational architecture of Moon and Mars missions.

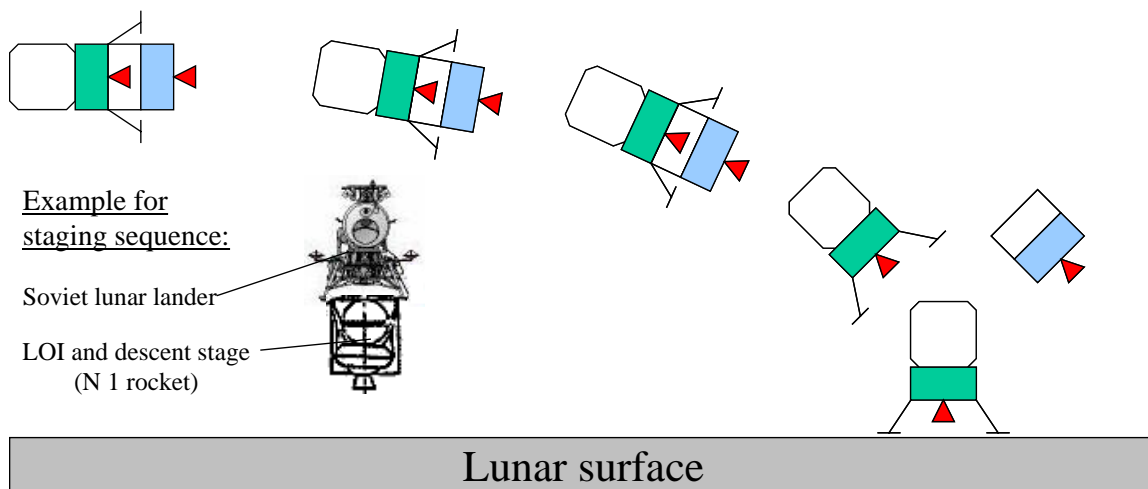


Figure 3-26: Operational architecture for landing on the Moon with equally sized propulsion stages; the spacecraft on the left were planned (and built) for the Soviet lunar landing

For a Mars landing, the velocity change required to land is small compared to that for the ascent. A Mars lander and ascender (Mars ascent vehicle) with two equal propulsion stages would therefore land and lift-off with the same propulsion stage, and drop this stage sometime during the ascent. The reason for this is that the upper stage of the lander does not provide enough velocity change to cover the complete ascent (see Appendix D).

For a lunar lander and ascender with two equal propulsion stages, the nominal operational sequence changes significantly compared to a Apollo LM-type design (see Figure 3-26): the lower stage (blue) provides not enough velocity change to cover the entire landing; it has to be dropped during descent, and the upper stage has to be used for the remainder of the descent; the same stage is used for the ascent back to orbit. The landing legs for this configuration have to be mounted to the upper stage.

At first sight, the inclusion of the operational steps of dropping a stage, igniting the upper stage, and landing with the upper stage seems to significantly increase the mission risk. However, exactly these three steps were crucial for an abort to orbit during the descent of the Apollo LM to the lunar surface. For a two-stage lunar lander, there is therefore no marked difference concerning risk between the optimal-mass lander design and the design with two equal propulsion stages. For a one-stage lunar lander, however, the dropping of a stage and the ignition of another rocket engine do not have to occur during the descent, which leads to lower risk; if the only stage malfunctions, however, there is no abort capability.

Dropping a stage during descent to the lunar surface is not an entirely new idea: this descent profile was planned for the Soviet lunar landing mission (see Figure 3-26, [Harford, 1997; www.astronautix.com, 2004]). The lower stage used to provide initial deceleration from orbit was also used for the lunar orbit insertion maneuver.

Figure 3-27 shows the trade study results for the Moon landing system. The mass values for the habitat lander are for the configuration on a hyperbolic arrival trajectory relative to the Moon; the values for the lander / ascender are for the configuration in LLO before landing.

For the habitat lander, the use of two propulsion stages with equal propellant masses creates only a very small mass overhead. The use of only one propulsion stage, however, necessitates a mass increase of below 10 %. Both options require the design of only one propulsion stage (as opposed to two in the original configuration); the one-stage solution, however, does not need to drop a stage before landing, and is therefore less susceptible to malfunctions. The one-stage configuration is the option of choice for all lunar surface habitats.

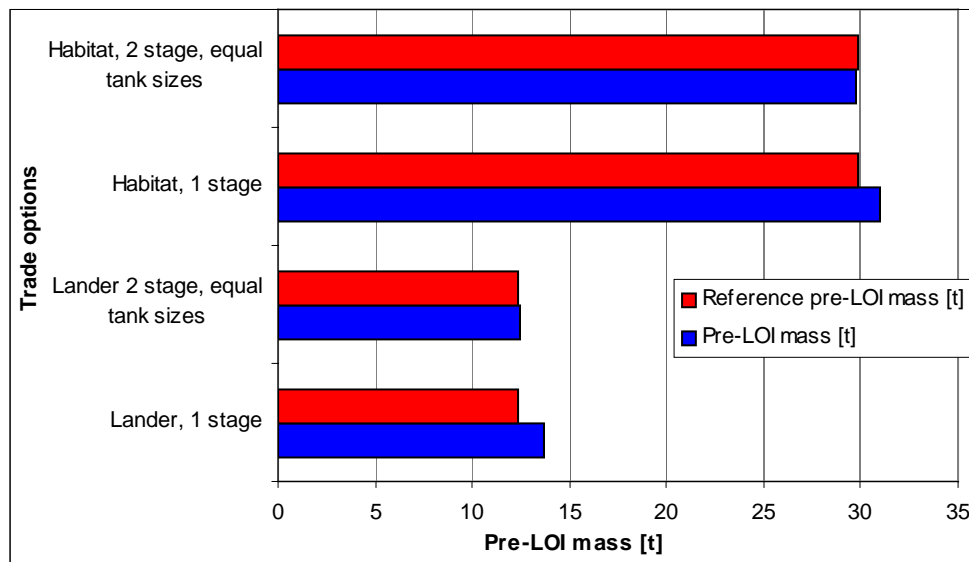


Figure 3-27: Trade results for the lunar surface habitat and the lander ascender vehicle

For the lunar lander, the trade analysis returns the same qualitative results as for the lunar surface habitat. The use of two propulsion stages with equal tank sizes creates a negligible mass overhead compared to the point design from Section 3.2; the use of a one-stage vehicle, however, causes only a comparatively small mass penalty, and does

not necessitate the ignition of a new stage. The one-stage option is therefore the option of choice for the lander / ascender, too.

As the crew size for the lunar landing missions is odd (3), the crew cannot be split into two teams which land separately, using two identical landing vehicles. For the Mars landing system, however, the crew size is even (6); therefore the trade includes the option to use two identical smaller vehicles.

Figure 3-28 provides an overview of the trade results for Mars landing vehicles:

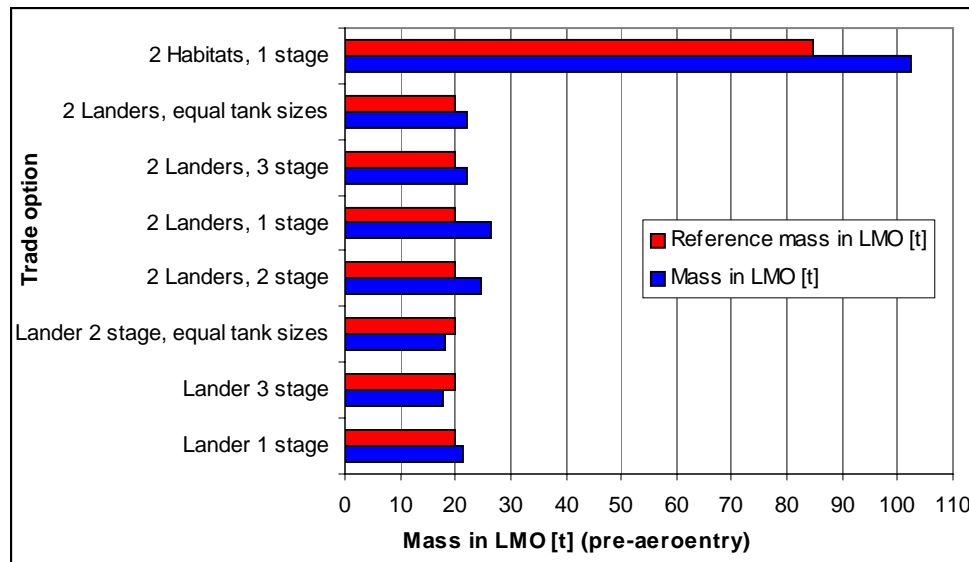


Figure 3-28: Trade results for Mars landing vehicles

From Figure 3-28 it can be seen that all options involving two identical smaller vehicles instead of one require more mass in LMO than those with only one vehicle; these options are regarded as uninteresting. The landing and surface habitat therefore stays unaltered.

The lander with two equally sized stages has actually a lower mass than the one from the preferred architecture. The reason for this lies in the very different velocity changes for the descent and ascent stage, as opposed to the optimum of equal velocity changes per stage. The use of equally sized propulsion stages actually brings both stages closer to the optimum. The one-stage option for the Mars lander and ascender does not require substantially more mass than the reference configuration.

For the Mars lander and ascender, the two-stage reference configuration is chosen, because

- The mass savings for other configurations are not substantial
- This configuration leaves open the possibility of using the same descent stage as the landing and surface habitat. Together with the ascent stage, which is lighter than the surface habitat, additional cargo / equipment could be landed with this stage.

3.4 Baseline Moon and Mars Exploration Architectures

The trade analysis in the preceding section confirmed the choices for certain design vectors, and uncovered superior options for others. The incorporation of these new design options into the favorite architectures yields refined architectures, which shall be called ‘baseline architectures’. Figure 3-29 gives an overview of the hardware elements of the baseline Moon and Mars architectures; TMI / TLI stages are not shown. Again, the short Mars mission features two TEI stages (as opposed to one for the long mission). Only the lunar surface habitat and the lunar lander / ascender underwent changes compared to the preferred architectures.

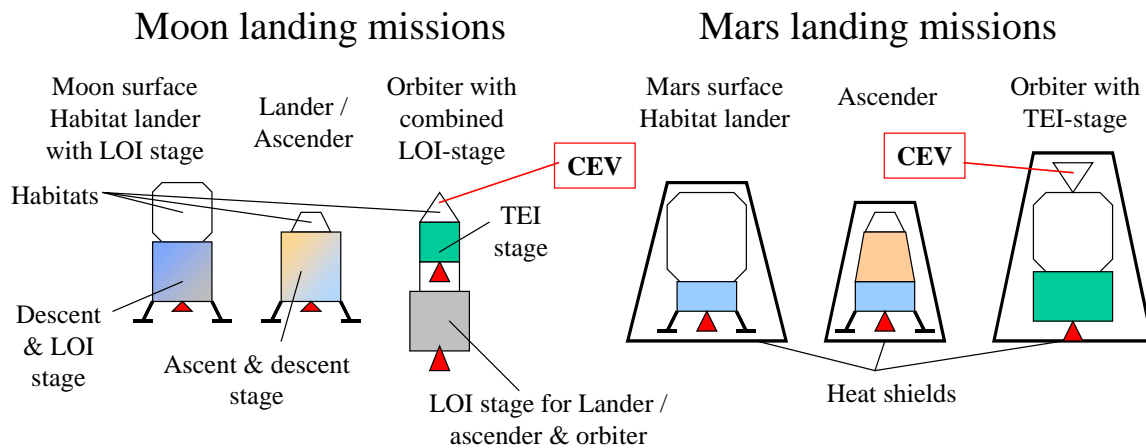


Figure 3-29: Hardware elements of the baseline Moon and Mars architectures (TMI / TLI stages not shown)

For the baseline architectures, detailed computations of the masses for crew compartments, habitats, propellant management systems, engines, parachutes, landing gears, and heat shields were carried out; the results of these computations are documented in Appendix C, Subsection 7.3.2 in the form of tables.

From these results, mass multipliers or ‘growth-factors’ can be calculated for the TMI and TLI maneuvers; given the post-TLI / TMI mass, these multipliers can be used to determine the IMLEO required to send a vehicle towards the Moon or towards Mars. This simplifies the calculation process significantly. Table 3-18 provides an overview of the mass multipliers for TMI, TLI, heat shields and parachutes. The only information needed in order to calculate the IMLEO of an architecture in addition to these multipliers is the mass of the individual vehicles.

It should be noted that the calculation of IMLEO via mass-multipliers is an approximation, because the actual engine and structural mass for the TMI / TLI stages is a function of the payload mass attached. This problem can only be solved iteratively. The differences between the approximation with mass multipliers and the iterative solution is, however, very small and will be neglected. Also, it is highly likely that all TMI / TLI stages will have the same size, i.e. will be of the same design; as this thesis is concerned with the design of extensible landing systems, however, this will not be investigated in

more detail, and is regarded as an important topic for future research. The methods for extensible design presented in Chapter 4 can be employed for this task.

On the basis of the baseline architectures, initial CEV requirements can be defined (see Figure 3-30). Reference data regarding the active lifetime, the volume and the mass of the Moon and Mars CEV are provided in Appendix C, Subsection 7.3.2. The dormant lifetime is determined by the duration of the individual operational phases of the missions in the mission type network. For a 180-day Moon mission, for example, the CEV will stay dormant in LLO for 180 days.

Vehicle(s)	Parachutes	Aerocapture	TMI / TLI	Total
Moon CEV & Lander	-	-	2.322	2.322
14 day lunar surface hab	-	-	2.320	2.320
30 day lunar surface hab	-	-	2.313	2.313
180 day lunar surface stay	-	-	2.302	2.302
Interplanetary transfer hab & CEV	1.01	1.15	3.128	3.633
Mars ascent vehicle	1.01	1.15	2.615	3.037
Surface habitat	1.01	1.15	2.595	3.014
Interplanetary transfer habitat + CEV	1.01	1.15	3.679	4.273
Mars ascent vehicle	1.01	1.15	2.595	3.014
Surface habitat	1.01	1.15	2.604	3.024

Table 3-18: Mass multipliers or ‘growth factors’ for parachutes, heat shields, TMI and TLI for the individual vehicles in the baseline architectures

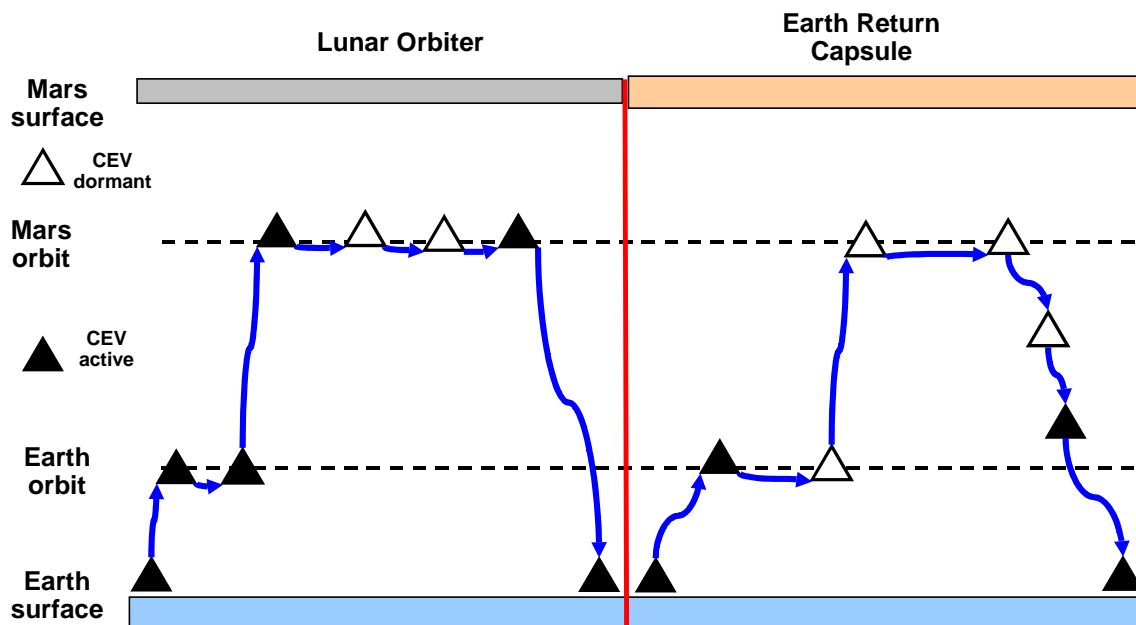


Figure 3-30: Concepts of operation for lunar and Mars CEVs

For the lunar missions, the CEV serves as the vehicle that delivers the crew from the surface of the Earth to lunar orbit and back. During the lunar surface stay, the CEV remains dormant in orbit, and is reactivated later by the crew, before the return to Earth. The lunar CEV essentially has the same functionality as the Apollo CM, except that it is also going to operate unmanned in lunar orbit.

The CEV for Martian missions delivers the crew to the interplanetary transfer vehicle in Earth orbit. After the docking and crew transfer, the CEV is powered down. The dormant CEV travels with the interplanetary transfer habitat to Mars orbit, remains in Mars orbit during surface operations, and inserts back towards Earth at the end of the stay in Mars vicinity. Shortly before Earth entry, the CEV is powered up, and serves the crew as the Earth reentry vehicle. Also, the CEV can be used as a second pressurized volume in the case of a contingency during interplanetary transit from the Earth to Mars, and back.

3.5 Summary of Chapter 3

In Chapter 3, the architectures generated with the systematical model introduced in Chapter 2 were analyzed quantitatively. For lunar and Mars missions, preferred architectures were chosen, based on IMLEO requirements, risk and safety characteristics, and their extensibility towards longer and more advanced missions possibly incorporating ISRU / ISPP was also assessed (see Appendix C, Subsection 7.3.1).

In accordance with systems engineering best practice, these favorite architectures were subjected to trade analysis to establish robust choices for the individual design variables. The trade analysis generated so-called baseline architectures based on the preferred architectures.

For the baseline architectures, detailed calculations of crew compartments, habitats, engines, propellant management structures, parachutes, landing gears, and heat shields were carried out (see Appendix C); these serve as the basis for the extensible design in Chapter 4.

From the baseline architecture descriptions, initial functional requirements for the CEV can be derived. For the lunar missions, the CEV is essentially an Apollo CM that has the capability to operate autonomously in lunar orbit. For the Mars missions, the CEV delivers the crew to Earth orbit, and is then only active again before Earth reentry to serve as an entry capsule for the crew. The CEV goes, however, all the way to Mars orbit and back, albeit dormant.

The main differences between a Mars and a Moon CEV are:

- The Mars CEV has a much higher dormant lifetime than the Moon CEV: from 180 days (longest lunar surface stay, CEV stays in orbit) to 3 years for the long Mars mission. This will have implications for the electrical power system (battery lifetimes are much shorter), the heat shield design (cold soak), storage of liquids and gases, etc.
- The Mars CEV experiences much higher velocities at Earth entry at the end of the mission: up to 14-16 km/s compared to 11-12 km/s for lunar missions.
- In case of a contingency situation during interplanetary coast both from and to the Earth, which makes the main pressurized compartment uninhabitable, the CEV has to serve as a “lifeboat”.

4. Commonality and Modularity in Manned Moon and Mars Landing System Architectures

This Chapter is focused on extensible design of manned spacecraft for Moon and Mars exploration. Section 4.1 outlines two approaches to identify options for extensible design, and in Sections 4.2 to 4.5 these two approaches are exercised on the design for commonality and modularity of pressurized volumes, propellant management systems, engines, and CEV ECLSS and EPS systems. This chapter can therefore be considered as one iteration through a process for extensible design.

4.1 Two Approaches to Extensible Design

The baseline architecture calculations from Chapter 3 (see Appendix C, Subsection 7.3.2) provide a host of requirements regarding pressurized volumes, propellant masses or volumes, engine thrusts, etc. So far, it was assumed that all these requirements would be fulfilled by point design solutions, thereby necessitating a great number of customized designs for propulsion stages, engines, crew compartments, etc. For reasons stated above (see Chapter 1), it appears to be unlikely that Moon and Mars exploration using these customized architectures would be affordable, and therefore sustainable.

If the same technological solution (“physical effect”, [Pahl, Beitz, 1997]) is employed to provide the functionality in different customized designs, then there is an opportunity for exercising extensible design through commonality and modularization. This section describes two approaches to identify and implement options for extensible design.

The first approach is based on **reusing a design** that was customized for the most stringent requirement encountered in the mission type network to provide the functionality for all other requirements, too. This is the concept of a so-called “design envelope” [de Weck, 2004]. Figure 4-1 (left-hand side) provides a visual explanation of the concept:

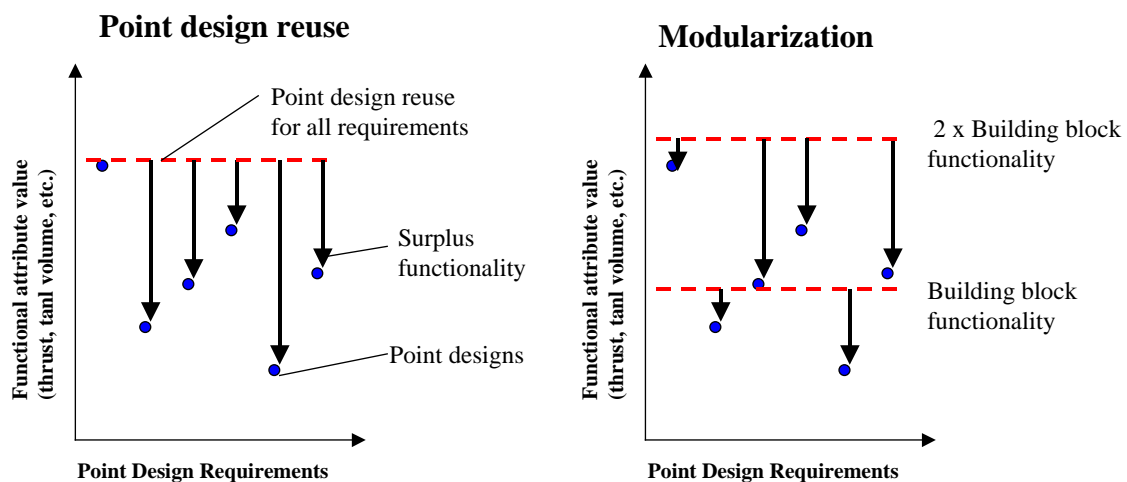


Figure 4-1: Two approaches to extensible design: design reuse (commonality), and modularization

The filled circles represent functional requirements imposed by the baseline architectures. The functional requirements all have different values of the functional attribute (e.g. pressurized volume for surface habitats), which is indicated by the ordinate. It is assumed that the functionality is in all cases provided by the same technology (e.g. aluminum or composite structures). For the first approach, we select one customized design and reuse it for all the other requirements. Thereby, we can satisfy one requirement exactly, and only one design needs to be developed.

As we have to satisfy all requirements, however, we have to select the point design with the largest functional attribute as our building block (see Figure 4-1); this creates substantial surplus of functionality for all other designs. This surplus represents the penalty of extensibility: it translates to higher system mass, and therefore higher “cost” and / or reduced performance of the system. The penalty can be reduced to acceptable levels by introducing additional building blocks, i.e. reusing another point design (see Section 4.3); this, however, increases the number of different elements that have to be developed, and therefore the total development cost. Please note: for element commonality, every building block is used instead of a point design, not in a modular arrangement (see below); therefore no additional interface costs arise.

The first approach to extensibility is exercised in Section 4.3 on in-space propulsion stages.

Approach two also starts with the point design functional requirements visualized in Figure 4-1 (right-hand side). However, approach two is not focused on reducing the number of point designs by reusing one of them for all requirements, but by providing a **modular solution**. One module provides a certain functionality that suffices to satisfy part of the requirements (see Figure 4-1). For requirements with a higher functional attribute, several modular building blocks are used to provide the functionality.

Thus, only one modular building block has to be designed for all systems. However, as the modular system design has to be able to work with varying numbers of modules, interfaces have to be provided that allow for adding or taking away modules; this increases system “cost” (mass) and complexity. For a propulsion stage with modular engines, for example, structural, electrical, control, and fluid interfaces are required to use an engine’s functionality. As every module, regardless of its size, requires an interface, the interface “cost” (mass) is of significant importance to the choice of the optimal building block size (see Section 4.5).

None of the requirements is necessarily satisfied exactly. Nevertheless, Figure 4-1 suggests that the second approach necessitates a smaller surplus, and therefore a smaller penalty than the first approach, because it has one more degree of freedom: the size of the building block can be chosen to minimize the surplus of functionality. This statement is not generalizable: if the interface mass is high compared to the building block mass, this drives the minimization towards choosing a larger building block that is employed in fewer numbers. This could lead to an increased surplus compared to approach one.

For approach two, it is also possible to utilize two building blocks of different size; this is expected to further reduce the surplus functionality, because the individual requirements can be approximated more closely. Please note that both approaches require that the technologies used to provide the functionality are “elastic” concerning the functional attribute: a propellant tank has to be usable if it is only partially filled, an engine has to be

usable with lower thrust, and a pressurized volume has to be usable if it provides more space than needed. For throttleable engines and pressurized propellant tanks this assumption is valid.

4.2 Modular Crew Compartments and Habitats

The baseline architectures for manned Moon and Mars exploration require a multitude of pressurized structures for the transport of humans in space, to and from planetary surfaces, and to sustain humans on the surface. Figure 4-2 provides an overview of the pressurized volume requirements for the different habitats and crew compartments in the baseline architectures. The requirements for in-space habitats for the interplanetary transfer to Mars are the same as for the 660d surface habitat.

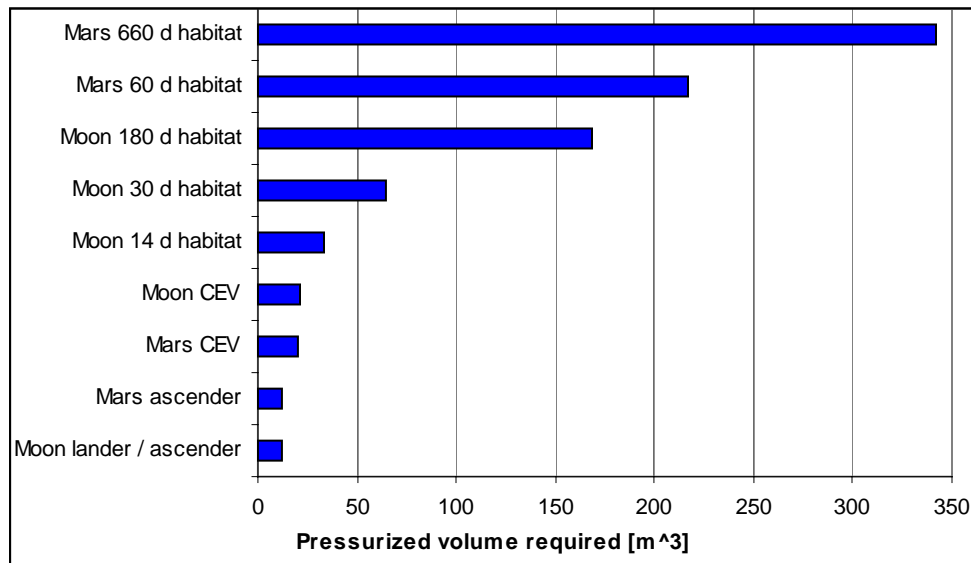


Figure 4-2: Pressurized volume requirements for crew compartments and surface habitats

Visually, the requirements can be grouped into two sets: the first contains the 660-day and the 60-day Mars habitats, and the 180-day Moon habitat ($> 150 \text{ m}^3$); all the remaining requirements belong to the second set ($< 100 \text{ m}^3$). It appears that this grouping would enable to choose two building blocks that create a small surplus.

However, the crew compartments and the surface habitats provide slightly different functionality: the crew compartments are used purely for transportation of crew, whereas the habitats primarily serve as living quarters and possibly also as an improvised laboratory. These differences have implications for the geometry of the pressurized volume building blocks: for crew compartments it is acceptable to choose a capsule-like building block, whereas for a habitat it is desirable to have a building block that permits astronauts to stand normally. Therefore, the 30-day and the 14-day lunar habitats are moved to the first set.

Crew Compartment Modularization

For the extensible design of crew compartments (second set), the modularization approach is employed. As the models for structural mass as a function of pressurized volume are not very detailed (especially for the long-term habitats, see Section 2.2), the

penalty of modularization shall not be measured by IMLEO impact, but directly by the surplus volume employed. The normalized volume surplus is defined by the following equation:

$$\zeta = \frac{V_{BuildingBlock} \cdot (n_1 + n_2 + n_3 + n_4) - (V_1 + V_2 + V_3 + V_4)}{V_1 + V_2 + V_3 + V_4} \quad \text{Equation 4-1}$$

The indices (1, 2, 3, 4) stand for the lunar lander / ascender, the Mars ascender, the lunar CEV and the Mars CEV. The multipliers “n” indicate how many building blocks are needed to satisfy the volume requirements for the individual crew compartments and $V_{BuildingBlock}$ is the pressurized volume of the building block chosen. This definition assumes that every mission is carried out exactly once. If the missions are carried out different times, then the volumes have to be multiplied with the number of missions. The total normalized surplus volume is then computed for all missions flown. By stepping through a range of building block values, the surplus volume generated can be calculated. Figure 4-3 shows the result for the crew compartments:

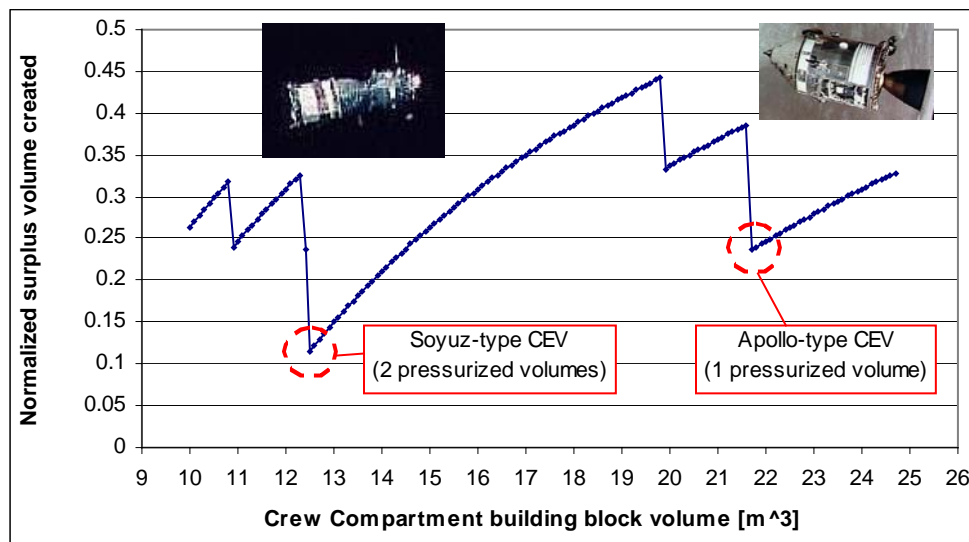


Figure 4-3: Pressurized surplus volume for building blocks between 10 and 25 m³ [pictures from www.astronautix.com, 2004]; the Apollo CM accommodated 3 crew, the Soyuz 2 or 3 crew

Building block volumes between 10 and 25 m³ were investigated; all the requirements lie in this interval. There are several drops in the surplus “curve” in Figure 4-3. These drops occur when the building block volume is contained as a multiplier in one of the requirements. Two “drops” or minima are of special interest for the modularization of the crew compartments: the minimum at 12.5 m³ is the global minimum for the space investigated; it produces a total surplus volume of a little over 10 % (see Figure 4-3). With this choice, however, two building blocks are needed to provide the necessary pressurized volume for the Moon and Mars CEV; this would lead to a Soyuz-like design [www.astronautix.com, 2004]. A Soyuz-like design requires an interface between the two modules, and is therefore more complex; however, it has the advantage that only one module needs to carry heat protection for reentry (mass saving), and that the second module could be used as an airlock (not in the actual Soyuz-design).

The second best minimum is at about 21.5 m³. It necessitates a pressurized volume overhead of about 23 %, but would allow for a one-module CEV like the Apollo CM (Figure 4-3); for the actual pressurized volume of the Apollo CM, please refer to Table 2-1. As the contribution of vehicles with crew compartments to the overall IMLEO is small, a volume surplus of about 25 % is acceptable; therefore, a pressurized building block volume of 22 m³ is chosen.

Habitat Modularization

The surplus volume for the pressurized volumes of the habitats is defined the same way as for the crew compartments. Figure 4-4 shows the resulting surplus curve; the structures shown adjacent to the minima represent cylindrical habitat configurations using different numbers of “plugs” and end cones at either end (not shown).

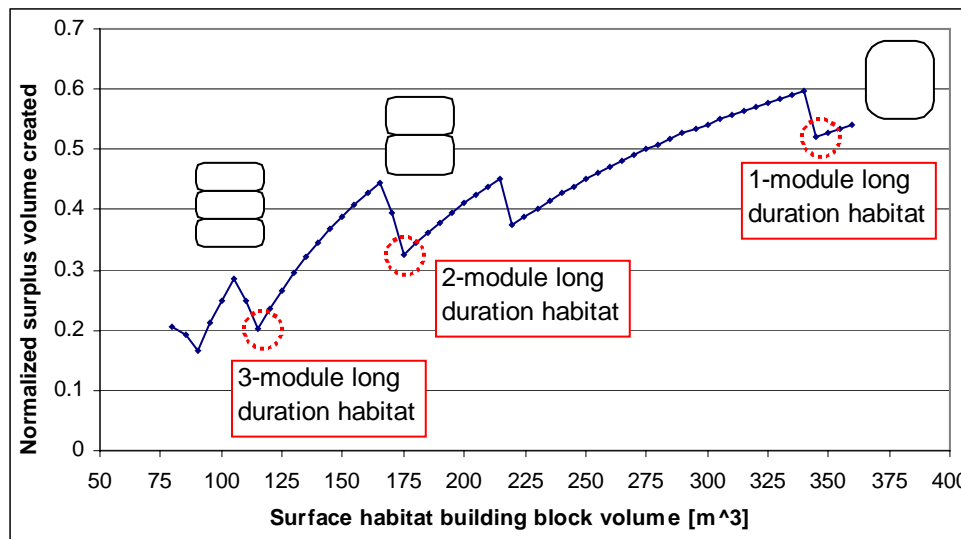


Figure 4-4 Pressurized volume surplus for habitat building blocks between 80 and 360 m³

Again, the surplus curve shows the characteristic “drops” when the building block is a multiplier contained in one of the requirements. The lowest normalized surplus volume of about 17 % can be achieved with a building block of about 90 m³. This would, however necessitate the use of four building blocks for the largest habitat with 342 m³ required volume. As every building block should have a height of at least 2 meters, so that the astronauts can stand upright, this would lead to an oblong habitat design, which is undesirable for Mars entry and landing. Therefore the next best minimum at 114 m³ is chosen; this leads to a three-module habitat for the long Mars mission (and also for all the in-space habitats, if the same building blocks are chosen).

Please note: as mentioned above, the modular arrangement envisioned consists of cylindrical “plugs”, and end cones. Every “plug” forms one story of the habitat. The stack of cylindrical “plugs” is closed on each side by end cones. The resulting structural design is similar to the SpaceLab or SpaceHab modules used on STS [www.astronautix.com, 2004], albeit in a vertical, not horizontal arrangement. Other geometrical shapes for the building blocks, e.g. truncated octahedral, should be investigated as part of future research.

IMLEO Overhead

The building block choices for the crew compartments and for the surface habitats make the manned vehicles heavier than the original point designs from the baseline architectures, except the vehicles where the building block is an exact multiplier of the requirement. This mass overhead affects the propellant management structures, the rocket engines, the parachutes, the heat shields and the landing gears for all the manned vehicles. Therefore, the detailed calculations for the mass breakdowns of the baselines architectures (see Appendix C, Subsection 7.3.2) were repeated for the vehicles with modularized crew compartments and habitats. As the modularization of the habitat and crew compartment volumes can be carried out independently of these calculations, and the pressurized volume building blocks serve as input parameters to the architecture calculation, no iterations are needed. The results are provided in tabular form in Appendix E, Subsection 7.5.1. The growth factors for TMI / TLI derived in Section 3.4 were used to determine the IMLEO; they are still valid because they are, in first-order approximation, invariant to the absolute mass (see Table 3-18, Section 3.4).

Table 4-1 shows the new IMLEO required for execution of the entire mission type network, and for individual missions, as well as the deviation. The deviation is defined as the mass overhead normalized with the total IMLEO for all missions using point designs only; the index i stands for the individual vehicles:

$$\eta = \frac{\sum_i m_{i, Modular Design} - \sum_t m_{i, Point Design}}{\sum_i m_{i, Point Design}} \quad \text{Equation 4-2}$$

The values presented in Table 4-1 indicate that the relative mass penalties are significantly larger (about one order of magnitude) for the lunar missions than for the Mars missions. This is understandable, because the building block choices cause a large pressurized volume surplus for the lunar surface habitats (see Figure 4-2). The overall IMLEO overhead of 4% is, however, very small.

Please note: the mass of interfaces was neglected for the modularization of the habitats, because they are assumed to be assembled on Earth, as the point designs; therefore there is no marked additional interface mass for the modular habitats compared to the point designed ones.

If launch cost is assumed to scale linearly with IMLEO, then this is also the launch cost deviation. For a specific launch cost of 10000 \$/kg (conservative assumption), the mass overhead for the execution of the entire mission network in relation to the point design solution translates into a launch cost penalty of about \$1.1 billion. However, instead of 12 crew compartment / habitat point designs, only two have to be developed. If we assume a development cost of about \$500 million per crew compartment / habitat, then the \$1.1 billion expenditure for additional launch cost enables a \$5 billion saving in development cost.

Please note: the calculations of launch and development cost in this Chapter are based on first-order approximations and serve the sole purpose to enable a top-level assessment of the feasibility (in terms of resource expenditure) of extensible design. The calculations can by no means substitute future detailed analysis of the launch and development costs.

The deviation for the entire mission type network is dependent on the number of times a mission is actually carried out. For the results given in Table 4-1 it was assumed that every mission is carried out exactly once. As the savings in development cost stay constant with time (non-recurring cost), the additional launch costs, however, are recurring costs, commonality and modularity actually become less attractive with each additional mission. However, if we choose the building blocks so that the missions that are executed frequently create minimal mass overhead (and hence additional launch costs), the break point between point designs and extensible designs lies at high mission numbers. This is the case for this modularization, if it is assumed that the long Mars missions are executed often, and the lunar missions once (see Table 4-1).

Mission (each executed exactly once)	Point design mass [kg]	Modularized mass [kg]	Deviation [-]
All missions	2716951	2825849	0.04
3 day Moon mission	75133	89034	0.185
14 day Moon mission	119151	156546	0.314
30 day Moon mission	146953	176498	0.201
180 day Moon mission	259622	293613	0.130
Long Mars mission	849642	865171	0.018
Short Mars mission	1229365	1244984	0.013

Table 4-1: Mass overheads for architectures with modularized crew compartments and habitats

The above modularization does not only affect the hardware needed for the baseline architectures, as well as the IMLEO, but also the operational scenarios for the CEV: as all the crew compartments use the same pressurized volume module, the CEV suddenly becomes a lunar lander / ascender, and a Mars ascender, in addition to being a lunar orbiter and an Earth reentry vehicle for return from Mars (see Section 3.4).

Figure 4-5 visualizes the new concepts of operations for the CEV (the lunar lander and Earth reentry scenario were described above):

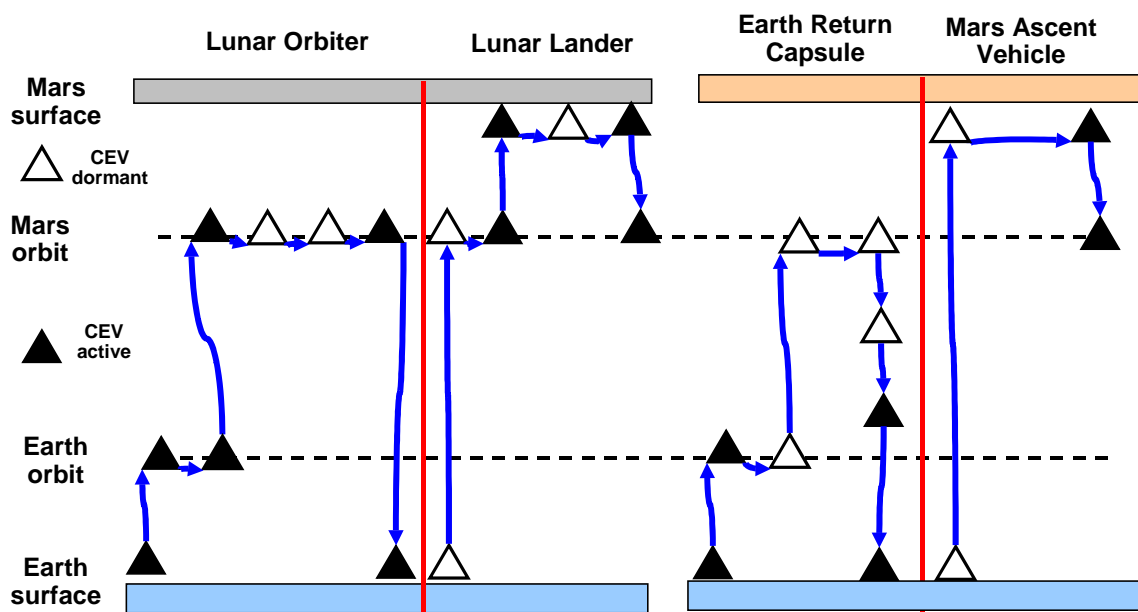


Figure 4-5: New operational scenarios for the CEV due to the modularization of crew compartments

The lunar lander CEV is deployed unmanned to LLO (possibly docked to the orbiter, as in Apollo [NASA, 1969]). There, the crew transfers to the vehicle, and lands on the surface. The lander is powered down (similarly as the Apollo LM, NASA 1969, 1972) during the lunar stay, and is powered up at the end of the stay. The crew then ascends to orbit and docks with the waiting orbiter. The lander is left in lunar orbit after departure of the crew.

The CEV that serves as crew compartment for the Mars ascent vehicle is predeployed unmanned to the Martian surface one opportunity before the human flight. It waits there until the end of the surface stay on Mars, is then powered up, and used for the ascent of the crew to Mars orbit. Afterwards, the vehicle is abandoned in Mars orbit.

For both of the new scenarios, the CEV does not necessarily need a heat shield; it is therefore recommended to design the CEV in such a way that the heat shield is not an integral part of the structure, and the vehicle can be used without it. One possible technical solution for this might be provided by inflatable heat shields.

If the Mars mission does not employ a free-return, it is conceivable that the CEV which is used to launch the crew is not brought to Mars orbit with the transfer vehicle, but that the Mars ascent CEV serves as an Earth reentry vehicle, as in the NASA Mars DRM [Hoffman, Kaplan, 1997]. This CEV would then have to have a heat shield.

In order to carry out all the operations described, the CEV will have to utilize different avionics; many subsystems like life support, electrical power, thermal control, etc. could, however, be the same. In Section 4.4, an initial conceptual analysis of the modularization of CEV ECLSS and EPS equipment dry masses is carried out; a comprehensive analysis of subsystem commonality and modularity is beyond the scope of this thesis, and has to be considered as future work.

4.3 Propulsion Stage Commonality – “Mars Back”

In this section, the extensibility of propellant management systems and engines is investigated for in-space propulsion (liquid methane / LOX), following approach one. The analysis is carried out for the system configuration with modularized crew compartments and habitats (see preceding section and Appendix E, Subsection 7.5.1).

The functional attributes used to identify options for commonality between the different point designs are

- The thrust for the liquid methane / liquid oxygen engines, and
- The impulse of the liquid methane / liquid oxygen propulsion stages

The impulse of a propulsion stage is defined as the propellant mass times the exhaust velocity of the engines:

$$P_{Stage} = m_{Propellant, Stage} \cdot v_{Exhaust} \approx m_{Propellant, Stage} \cdot I_{sp} \cdot g_0 \quad \text{Equation 4-3}$$

Table 4-2 provides the engine thrust and the impulse for all liquid methane / liquid oxygen stages used in the updated baseline architectures (Appendix E, Subsection 7.5.1):

Propulsion Stage	Impulse [10^6 kg*m/s]	Structural mass without landing gear [kg]	Thrust [kN]
Lunar missions			
Lunar lander ascender stage	47.96	1402	76019
Orbiter TEI stage	1.40	401	32500
Lander & orbiter LOI stage	29.62	866	114263
14 day habitat landing stage	59.82	1748	114199
30 day habitat landing stage	77.72	2272	148386
180 day habitat landing stage	182.67	5340	348732
Long Mars mission			
TEI stage	287.93	8418	447741
Mars ascent stage	46.14	1349	109001
Descent stage lander	13.71	400	116579
Descent stage habitat	46.61	1362	396225
Short Mars Mission			
Stage for 2 nd TEI	211.67	6188	368759
Stage for 1 st TEI	417.20	12197	726781
Habitat lander stage	23.21	678	197295

Table 4-2: Impulse and thrust for liquid methane / liquid oxygen propulsion stages

It is apparent that an impulse of around 48 M kg m/s is required for lunar descent and ascent, Mars ascent, and Mars landing of the 660-day habitat. The lunar lander and ascent stage therefore is chosen as one building block, named “propulsion stage one”. The engine for the lunar landing and ascent has a thrust of 76 kN; this is not enough for the Mars ascent and the habitat landing on the Martian surface. “Propulsion stage 1” therefore shall be designed to accommodate up to six engines with 76 kN each. With this configuration, the habitat can be landed on Mars.

The second propulsion stage chosen as building block is the TEI stage of the long Mars mission architecture (“propulsion stage 2”). With its impulse of about 290 M kg m/s and its thrust of 447.7 kN, it can serve as lunar landing stage for all the lunar surface habitats, and as one of several TEI stages for the short Mars mission (see Table 4-2). Also, the 447.7 kN engine could be mounted to propulsion stage one to land the 660-day Mars habitat (instead of the six engines proposed above). This would reduce the maximum number of engines for propulsion stage one to three, for the landing of the short Mars mission surface habitat.

The following Figures 4-6 to 4-8 show how the hardware for the long Mars mission, the 180 day lunar mission, and the short Mars mission would look, if only propulsion stage one and two and the associated engines were used. Please note: as the combined impulse for LOI and TEI for the lunar mission is below 48 M kg m/s, the functionality of these two stages has been assigned a single propulsion stage one. The TMI / TLI stages and the heat shields for Mars aerocapture / aeroentry are not shown.

Based on the pressurized volumes, and tank volumes, preliminary 3D CAD-models can be generated which are more detailed than the schematical diagrams presented here; this is, however, considered future work.

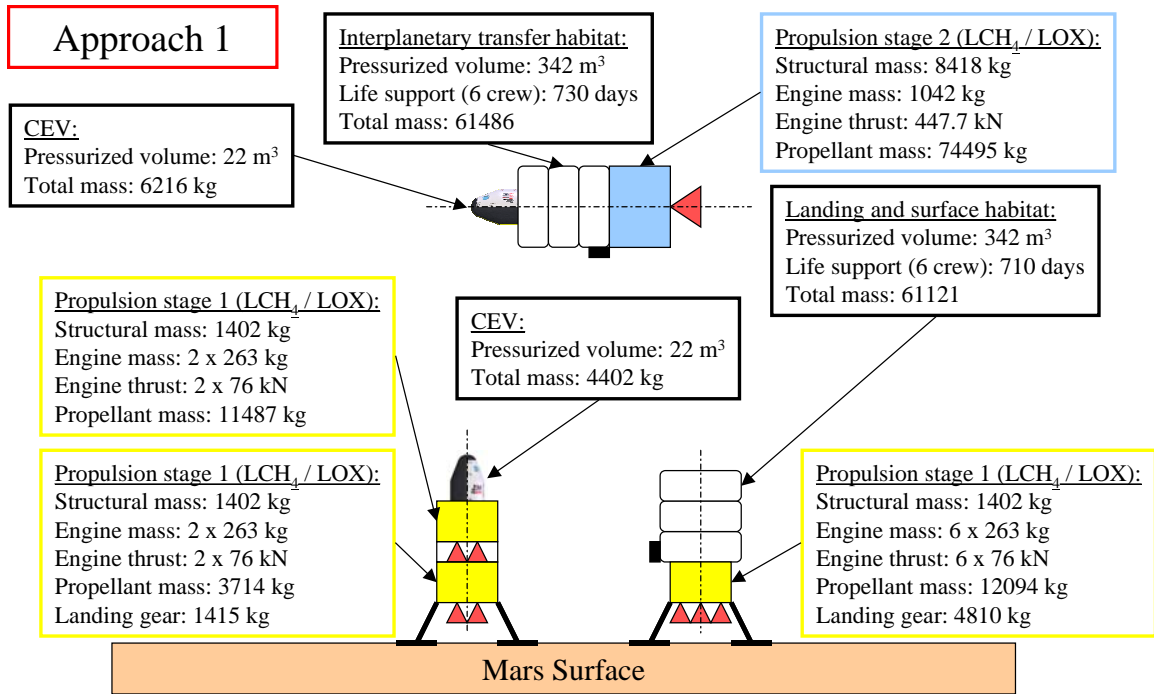


Figure 4-6: Long Mars mission hardware; heat shields and TMI stages not shown

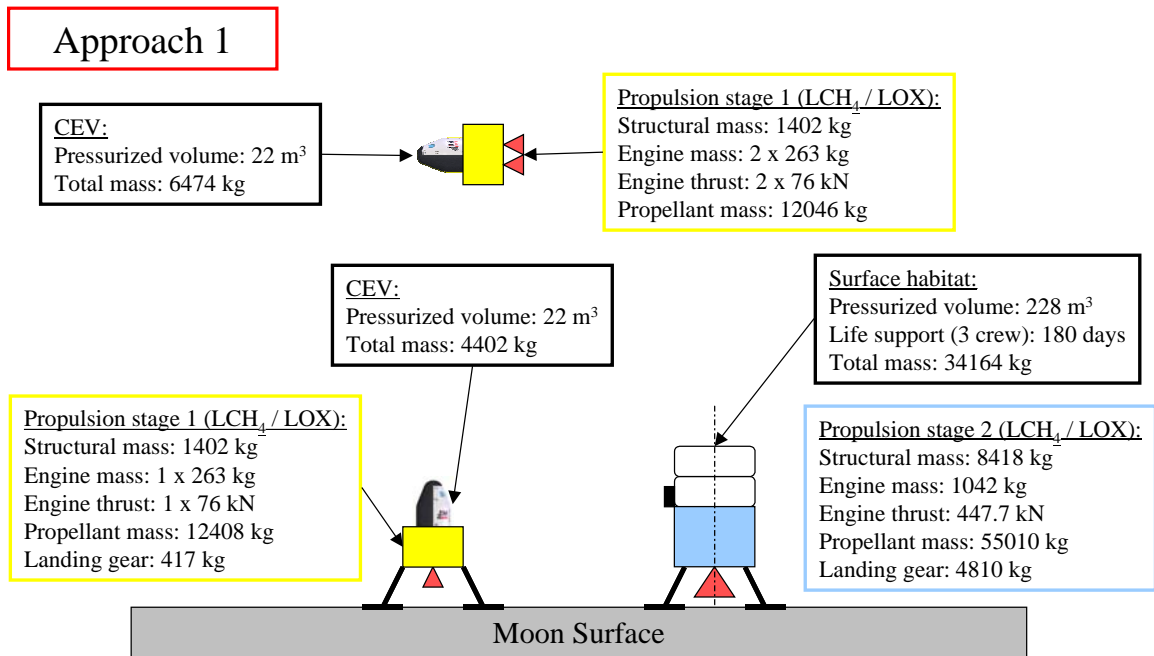


Figure 4-7: 180 day Moon mission (the lander and orbiter are the hardware for the 3-day mission); TLI stages not shown

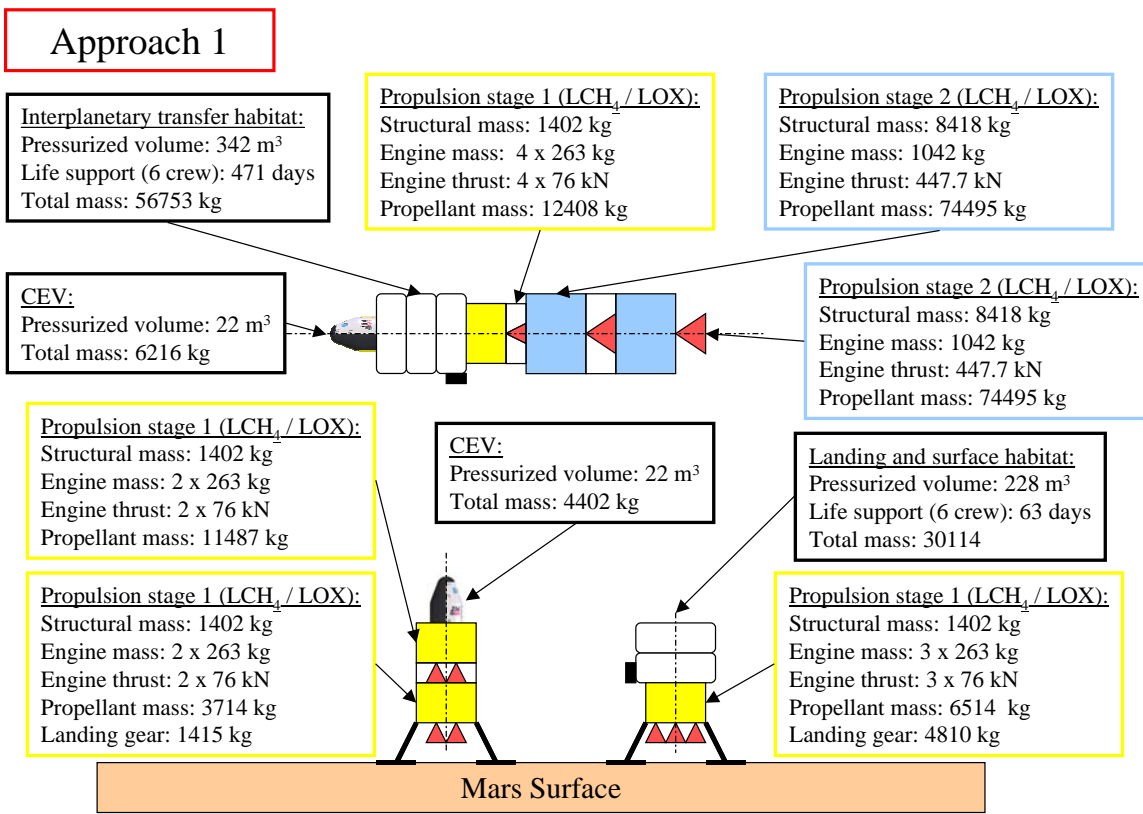


Figure 4-8 Short Mars mission hardware; heat shields and TMI stages not shown

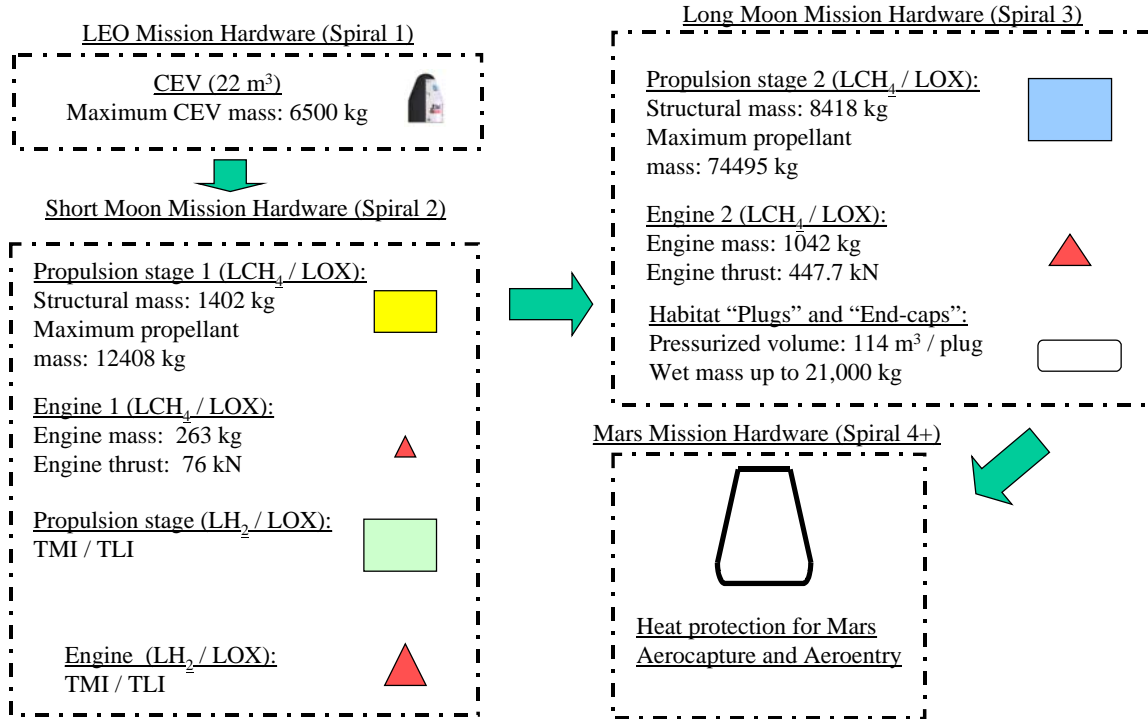


Figure 4-9: Notional hardware development roadmap for commonality and design reuse of propulsion stages

Figure 4-9 provides a top-level development roadmap for the hardware required to execute all the missions in the mission type network. The spiral organization is synchronized with NASA's development plan for the CEV and Human Lunar Exploration [www.exploration.nasa.gov], see Figure 1-1. In Spiral 1, the CEV is built and flown in LEO. In Spiral 2, propulsion stage one is built with the associated engine, and the liquid hydrogen / liquid oxygen stage that serves as TMI and TLI stage for all missions. Actually, two TMI / TLI stages are needed for most missions; these stages would have the same size. As this thesis is concerned with landing systems, the modularization for the TMI / TLI stages was not carried out (future research). The same approaches used to identify options for commonality and modularity of in-space propulsion stages can be applied to the modularization of TMI / TLI stages; this has to be coordinated with the launch vehicle choice, as well as with the potential development of new upper stages for launch vehicles: the Saturn IV B stage was used both as upper stage and as TLI stage. It is therefore justified to assume that the green TMI / TLI stage from Figure 4-9 represents this optimal stage. With those two propulsion stages available, 3-day lunar landing missions can be carried out.

In Spiral 3, propulsion stage two is developed with its associated engine, as well as the habitat "plug" with the end cones. With this hardware, long duration lunar landing missions can be carried out. In addition to that, several alternate missions are now possible: missions to Near-Earth-Objects, Mars flybys, and possibly a mission to Phobos (without aerocapture). The only hardware element that needs to be developed exclusively for manned Mars missions in Spiral 4 is the heat protection system for aerocapture at Mars. By the time this development is taking place, it appears likely that there will be technological heritage from robotic probes which accomplished aerocapture.

These preliminary results for Moon and Mars exploration system commonality clearly demonstrate that virtually all the hardware for lunar missions can be used for Mars missions. Therefore, there is no need for a multi-year technology development "gap" between Moon and Mars missions, which could jeopardize funding for the Mars exploration program. Also, as the same hardware is used for lunar missions and for Mars missions, lunar missions could continue at a lower frequency during the Mars exploration program. If Moon and Mars exploration missions are phased correctly, it is possible to almost continuously have astronauts either on the lunar or Martian surface during the 1.5-year Mars surface stay or the 180-day lunar stay.

Mission	Architecture mass with modular habitats [kg]	Architecture mass with propulsion commonality in addition to modular habitats [kg]	Deviation [-]
All missions	2825849	2998812	0.061
3 day Moon mission	89034	91347	0.0259
14 day Moon mission	156546	217096	0.3867
30 day Moon mission	176498	233275	0.3216
180 day Moon mission	293613	329475	0.1221
Long Mars mission	865171	870661	0.0063
Short Mars mission	1244984	1256956	0.0096

Table 4-3: Mass overhead and deviations for propulsion stage design reuse in addition to habitat and crew compartment commonality (see Section 4.2)

Table 4-3 shows the IMLEO mass deviations of individual missions, as well as of the entire mission type network for architectures with commonality regarding propulsion stages compared to the architectures with modularized habitats and crew compartments only. Again, the lunar missions have significantly higher deviations than the long and short Mars mission. The overall deviation compared to the architectures from Section 4.2 (see Appendix E, Subsection 7.5.1) is about 6 %; hence, the deviation compared to the point designs from Section 3.4 (see Appendix C, Subsection 7.3.2) is about 10 %.

Applying a specific launch cost of about 10000 \$ / kg (see above), we can compute the additional launch cost for executing the mission type network with modular crew compartments and common propulsion stages (in comparison to the point designs from Section 3.4) to be about 2.8 billion \$. In addition to the 5 billion \$ saving due to habitat and crew compartment modularization, the number of liquid methane / liquid oxygen propulsion stages is reduced from 13 to 2. If we assume an average cost of about \$200 million per propulsion stage, then the propulsion stage commonality creates an extra saving of \$2.2 billion in development cost. The \$2.8 billion additional launch cost would be easily offset by \$7.2 billion reduction in development cost. As above, more missions make the savings due to extensibility smaller; the long Mars mission, which is assumed to be carried out more than once (Mars back), has a very low mass overhead of 0.0063 %.

4.4 Extensibility Through Modularization of Fuel Management Systems and Rocket Engines

In this section, a modularization of the liquid methane / liquid oxygen propulsion stages is carried out following approach two (see above). The method for the identification of interesting building blocks is the same as used for the modularization of pressurized volumes in Section 4.2. The functional attributes are the fuel tank volume and the engine thrust; the oxidizer tank volume is coupled to the fuel tank volume by the fuel-to-oxidizer ratio [Messerschmid, 2000], which is assumed to be 1:4 (stoichiometric ratio).

The constraints for the functional attributes are as follows:

- Fuel tank volume: between 12.7 and 51 m³. The upper boundary is based on the largest fuel volume encountered, i.e. that of the first TEI stage for the short Mars mission (see Appendix E, Subsection 7.5.1). The lower boundary is one fourth of the maximum value; this constrains the maximum number of fuel and oxidizer tanks per propulsion stage to eight (one oxidizer tank per fuel tank).
- Engine thrust: between 121 and 727 kN. The upper limit is again based on the highest thrust required, i.e. that of the first TEI stage for the short Mars mission. The lower limit is exactly one-sixth of the upper boundary, in order to constrain the maximum number of engines per stage to six.

The actual modularization was carried out, as in Section 4.2 for the pressurized volumes, by stepping through the “legal” thrust and tank volume building block sizes, calculating the mass overhead per vehicle utilizing the empirical model from Section 2.2, and identifying the combination with the lowest mass overhead compared to the reference configuration in Appendix E, Subsection 7.5.1. The mass overhead is defined as in Section 4.2; the index *i* again denotes the individual vehicles:

$$\eta = \frac{\sum_i m_{i, \text{ModularDesign}} - \sum_t m_{i, \text{ReferenceDesign}}}{\sum_i m_{i, \text{ReferenceDesign}}}$$

Equation 4-4

The building blocks with minimal IMLEO overhead are (see also Table 4-4):

- A liquid methane / liquid oxygen engine with 185 kN thrust
- A methane fuel tank with a volume of 13 m³

This building block choice necessitates up to four oxidizer tanks and up to five engines; the modular propulsion stage therefore has to hold up to eight tanks (four fuel, four oxidizer), and up to five engines (see below).

The following Figures 4-10 to 4-12 provide an overview of the modularized system hardware for the long and short Mars missions, and a 180-day stay lunar mission. The TMI / TLI stages and the heat shields for Mars aerocapture and aeroentry are not shown.

Approach 2

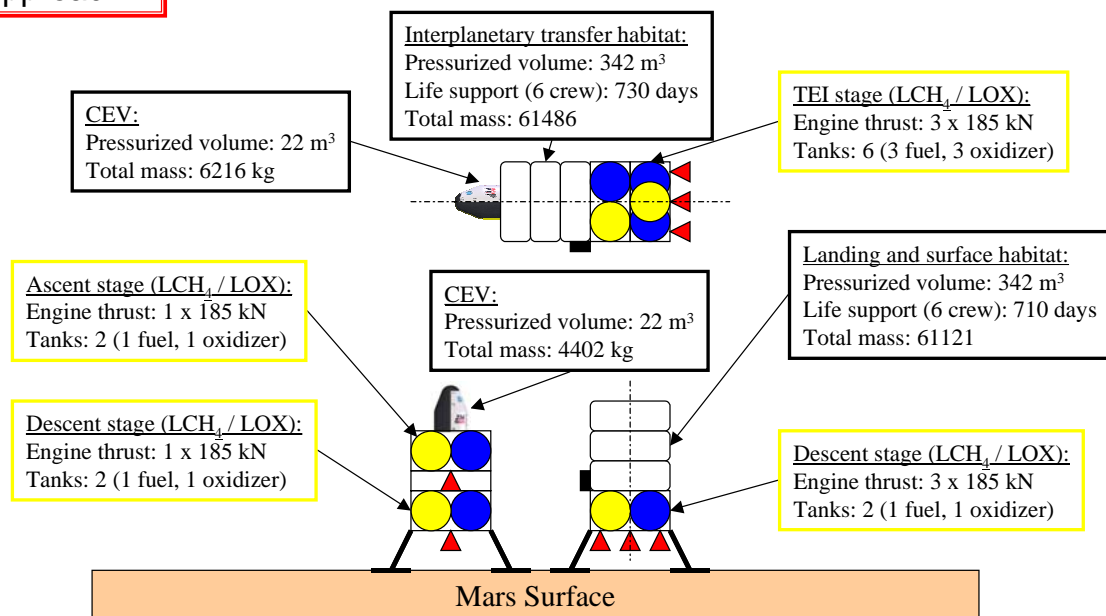


Figure 4-10: Modularized hardware for a long Mars mission

Approach 2

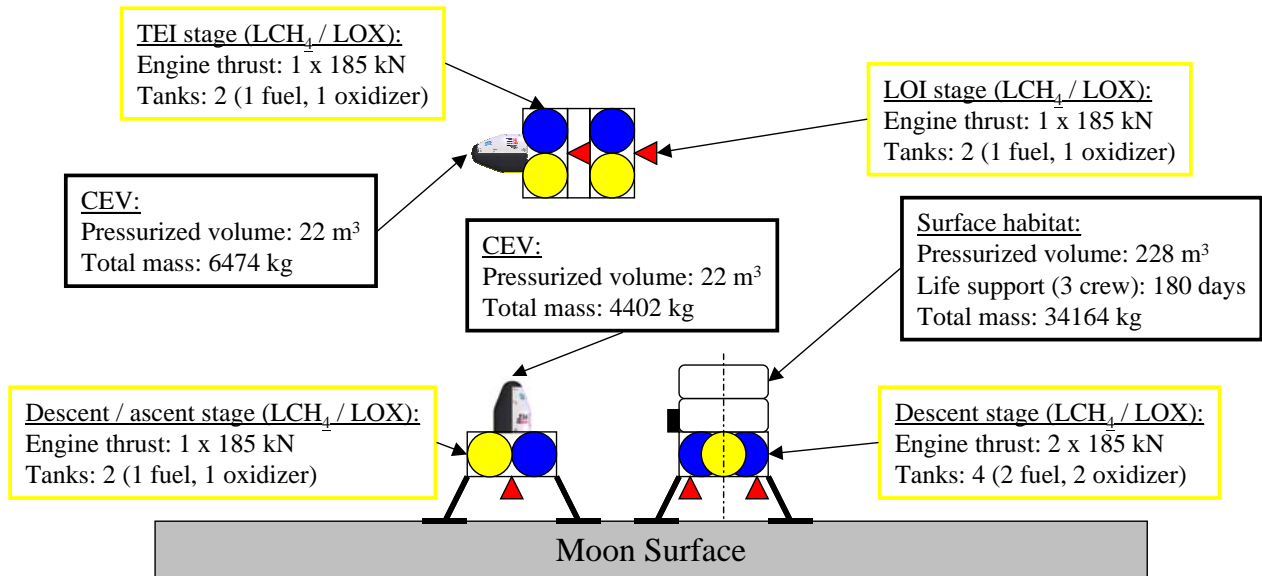


Figure 4-11: Modularized hardware for a 180-day lunar mission; the orbiter and the lander / ascender are the hardware needed for a 3-day lunar landing mission

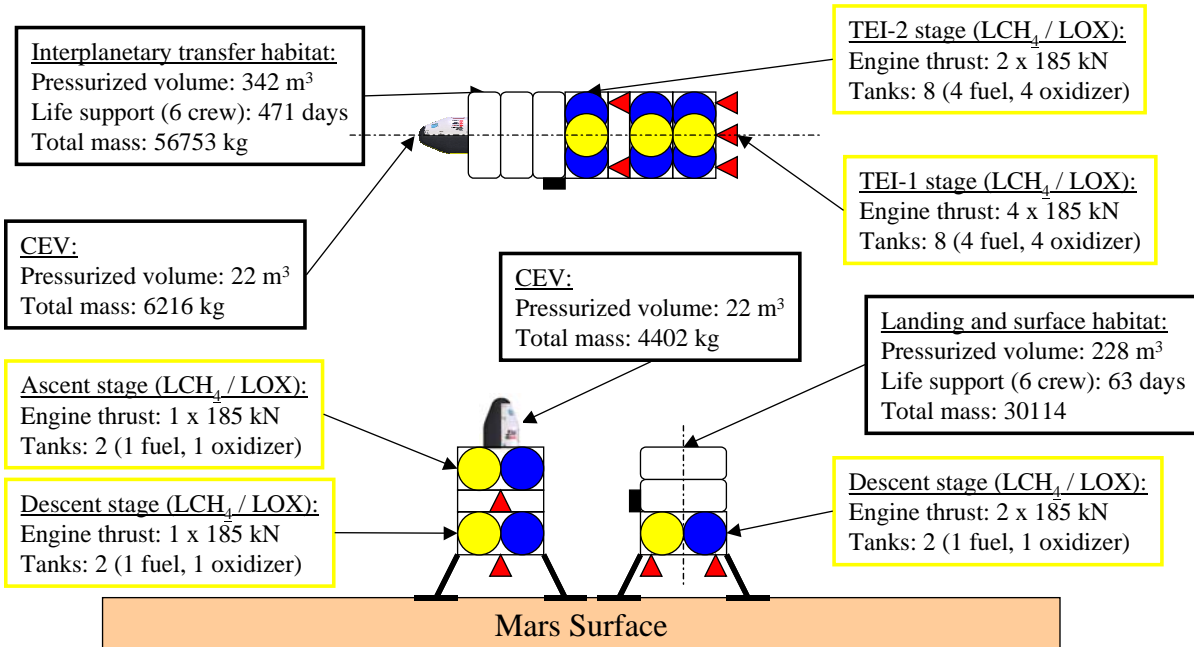


Figure 4-12: Modularized hardware for a short Mars mission

Approach 2

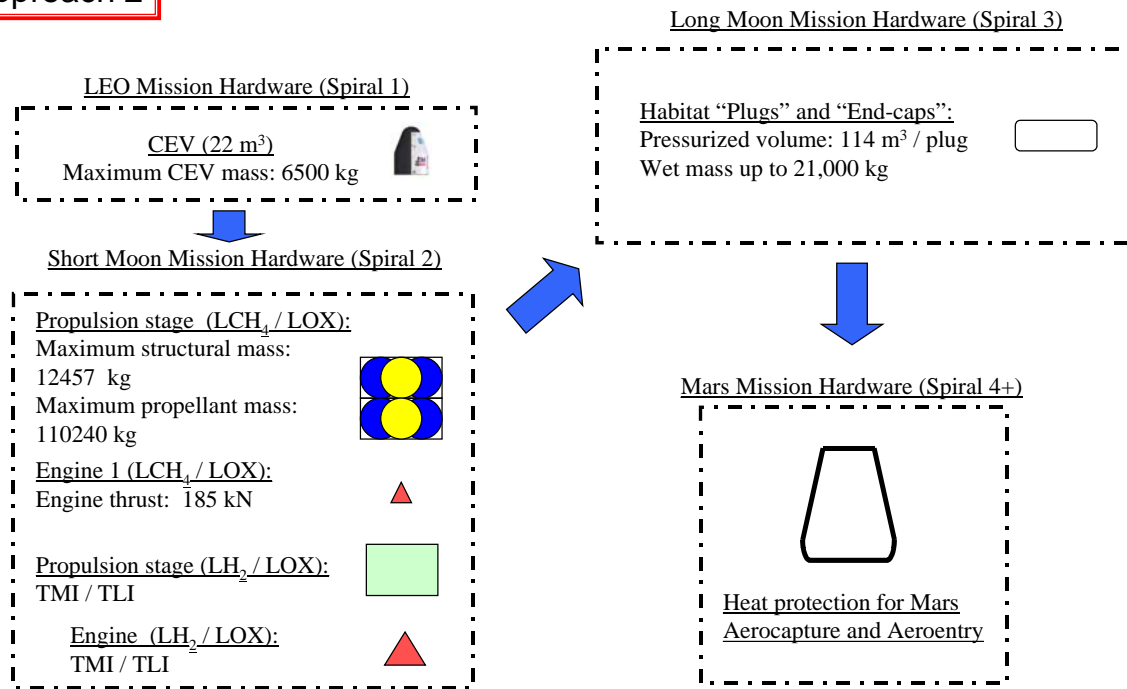


Figure 4-13: Notional hardware development roadmap for modular Moon and Mars exploration systems

Figure 4-13 provides a hardware development roadmap similar to that presented in Figure 4-9. This roadmap, however, is for the development of modular propulsion stages, as opposed to design reuse in Chapter 4.3.

The activities for Spiral 1 are the same as in Figure 4-9. In Spiral 2, the modular propulsion stage with eight propellant tanks and up to five engines is developed, as well as the liquid hydrogen / liquid oxygen stage used for TMI / TLI. With this hardware, initial lunar missions with surface durations of up to three days are possible. In Spiral three, only the habitat "plug" and the associated end cones need to be developed. As stated above, with this hardware, long duration lunar landing missions can be carried out. In addition to that, several alternate missions are now possible: missions to Near-Earth-Objects, Mars flybys, and possibly a mission to Phobos (without aerocapture). The only hardware element that needs to be developed exclusively for manned Mars missions in Spiral 4 is the heat protection system for aerocapture at Mars.

Again, a very small amount of hardware needs to be developed in order to carry out both the Moon and Mars landing missions. In comparison to the hardware development roadmap shown in Figure 4-9, it is apparent that only two propulsion stages need to be developed as opposed to three for the commonality solution. However, the modular propulsion stage proposed here are more complex than the propulsion stages proposed in Section 4.3, because the modular stage needs to work with tank numbers from two to eight, whereas the propellant management system for the reused point designs is always used in the exact same configuration.

Therefore, a more demanding initial (Spiral 2) development (and therefore funding) effort is expected for the modularization approach, than for the commonality approach. Spirals 3 and 4 will be less demanding for the modularization approach.

The modularization of in-space propulsion stages creates a mass overhead of about 10 % compared to the reference mass for the architectures with modularized habitats (see Appendix E, Section 7.5.1). Relative to the point design baseline architectures from Section 3.4, the mass overhead is about 14 %. This appears to be an acceptable mass penalty for the substantial reduction in the number of required hardware elements achieved through modularization.

With a specific launch cost of 10000 \$/kg, the 14 % mass overhead translates into an additional launch cost of \$3.8 billion. However, only one liquid methane / liquid oxygen propulsion stage needs to be developed as opposed to 13 for the point design solution. If, again, we assume that the average development cost for each propulsion stage of \$200 million, then a cost saving of \$2.4 billion can be achieved by modularizing the in-space propulsion stages. In addition to that, the \$5 billion development cost savings for the habitats apply. This brings the total cost savings to \$7.4 billion, which easily balances the \$3.8 billion additional launch cost.

As the calculations leading to the choice of the optimal tank volume and engine thrust building blocks are dependent on many parameters, a short sensitivity analysis of the building block sizes is included here (see Table 4-4):

Parameter	Reference value	Perturbed value	Sensitivity thrust building block [-]	Sensitivity tank building block [-]
Structural factor	0.113	0.13	0.133027	0.12804
Specific impulse	394 s	380 s	-1.271056	-2.041569
Coefficient in thrust model, see Eq. 2-6	0.43	0.4189	0.010206	0
Exponent of thrust model	-0.2236	-0.23	-0.037795	0
Number of long Mars missions	1	10	0.025422	0.000428

Table 4-4: Sensitivity of the tank and engine building block values to perturbations in various parameters

The building block values are very sensitive to changes of the specific impulse of the propulsion stages; this is expected, because the specific impulse is one of the main drivers of overall system mass.

The sensitivity of the building block choice to perturbations in the structural factor is an order of magnitude smaller than for changes in the specific impulse. For the calculations that lead to the building block choice, additional mass for the interfaces of the tank and engine modules to the rest of the stage were neglected, because the stages are assumed to be assembled on the ground, and are not reconfigured during their life-time. Therefore, the additional interface mass compared to a point designed stage is considered to be very small. The mass penalty of the modular stage only arises, because the modular stage is not completely filled with propellant, as opposed to a point-designed stage, which is completely filled. A small sensitivity to perturbations in the structural factor indicates that, even if the additional interface mass was more pronounced than assumed, building block sizes very close to the optimum ones presented here would be chosen.

This assumption is not necessarily valid if smaller launch vehicles are used, and the individual modules assembled on orbit.

The tank module displays no sensitivity to changes in the mass model for the rocket engines. The engine building block size has a low sensitivity to changes in the parameters of the engine mass model. Also, the number of long Mars missions (as well as the number of all the lunar landing missions) has only a very small influence on the building block sizes (although the mass overhead for lunar missions is large), because the overall mission mass (and hence the mass penalty) of a lunar mission is much smaller than that of a Mars mission. However, as the short Mars mission defines the constraints for the thrust and tank volume space available for the building blocks, an elimination of this mission has a large impact on the building block choice. For a mission type network without a short Mars mission, the optimal building blocks are (see Table 4-5):

	With the short Mars mission	Without the short Mars mission
Thrust	185 kN	90.2 kN
Fuel tank volume	13 m ³	8.885 m ³

Table 4-5: Building block sizes for modularization with and without the short Mars mission

Although the normalized mass overhead for a mission type network without a short Mars mission is reduced to about 8.7 %, it is recommended to modularize for a network including the short mission: thus, the option to execute such a mission without additional hardware development is preserved with only a small additional mass penalty.

Please note: the results presented in Sections 4.3 and 4.4 are based on concepts developed jointly by **Mr. Paul Wooster** of the MIT Space Systems Laboratory and the author of this thesis in the course of the NASA CE&R study during the fall and winter of the year 2004 at MIT.

4.5 Extensibility Through Modularization of the Life-Support and Electrical Power Subsystems for the CEV

In this section, a preliminary analysis of the nature and the penalties of CEV subsystem modularization is presented. Two subsystems are analyzed: the life support equipment and the electrical power equipment. Table 4-6 provides an overview of the mass requirements for life support and electrical power equipment masses as a function of crew size:

Crew size	Specific mass [kg / person]	Equipment mass [kg]
Life support equipment		
3	324.75	974.25
4	324.75	1299
6	324.75	1948.5
Electrical power equipment		
3	131.5	394.5
4	131.5	526
6	131.5	789

Table 4-6: Equipments mass for life support and electrical power systems as a function of crew size (according to the scaling model of Section 2.2)

The equipment masses for the two subsystems masses are assumed to scale linearly with the crew size. For the life support equipment, this is intuitively clear, because the in- and outputs are directly related to the crew, and hence to the crew size. The electrical power equipment (i.e. fuel cells for the case of the CEV) is sized by the peak power requirements. In first order, the peak power requirements are assumed to scale linearly with the crew size.

As the subsystems scale directly with the crew size, it appears to be very easy to modularize them without mass penalties due to surplus functionality by choosing one subsystem module for every crewmember. One possible way of arranging these subsystem modules would be in rack- or shelf-like structures that go along the walls of the crew compartment (see Figure 4-14):

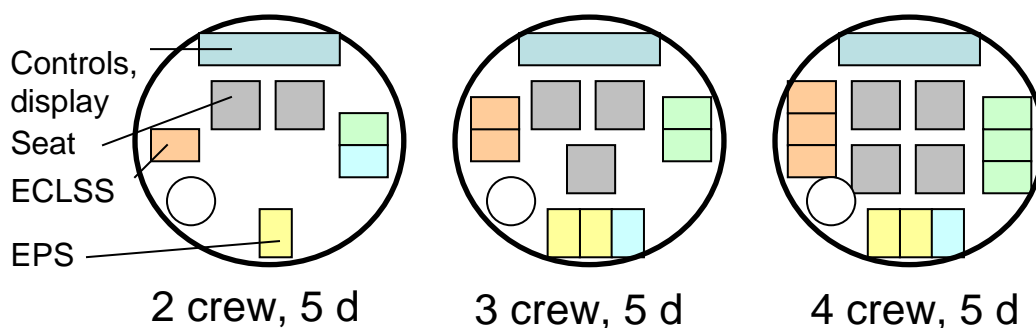


Figure 4-14: Possible arrangement of subsystem modules in the CEV (horizontal cross-section); the crew sizes and durations are arbitrary and not directly related to the architectures proposed above; scalability for up to six crew is assumed

Replaceable International Standard Payload Racks ISPR are / were used on SpaceHab, SpaceLab, the ISS, and the European ATV spacecraft [www.astronautix.com, 2004]. The racks have standardized electrical, structural, data and fluid connections [Messerschmid, 1997]. The use of racks has the advantage that modules can be exchanged easily, even in flight. Also, the racks would considerably reduce the effort for outfitting a CEV for the specific concept of operations required by the mission.

The modularization of subsystem equipment is not so easy as it appears at first sight. Though the equipment mass scales linearly with the crew size, interface masses, for example to connect a module to the CEV structure, can no longer be assumed to be negligible compared to the module mass.

Figure 4-15 shows the results of a modularization of the ECLSS equipment mass for the 3- and 6-crew CEVs proposed in the baseline architectures. The computation of the ECLSS and EPS dry masses is based on the scaling factors derived in Section 2.2. The diagram contains the characteristic curves for modularization penalties encountered in Section 4.2. The interface mass is varied by one order of magnitude from 10 kg per module, 50 kg, to 100 kg per module. Several immediate conclusions can be drawn from Figure 4-15:

- The lower the interface mass is, the more attractive are life support systems with many modular building blocks.
- The interface mass has only a small influence on the mass penalty for large building blocks, because few interfaces are needed.

- Even for low interface masses, the building block with about 1000 kg mass appears to be desirable. One of these building blocks would be needed for the 3-crew CEV, and two for the 6-crew CEV.

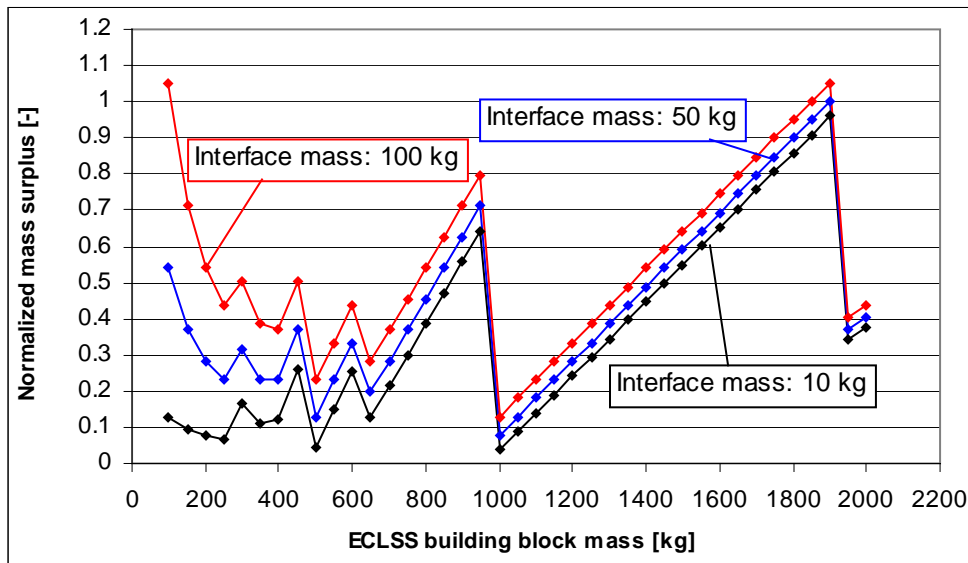


Figure 4-15: Modularization of life support equipment dry mass for 3- and 6-crew; based on the scaling model developed in Subsection 2.2.2

Figure 4-16 provides results for the modularization penalty, if the mass requirement for a 4-crew CEV is introduced in addition to a 3-crew CEV. The building block with 1000 kg is no longer the one with the lowest overall mass penalty due to interface mass and surplus functionality. It appears that a building block with a mass of about 500 kg is the optimum choice, because it creates a very low mass penalty in both the 3 / 6 crew and 3 / 4 / 6 crew cases. Thus, the option to use the CEV for missions with a crew size of 4 with a minimal mass penalty is preserved at a very low cost.

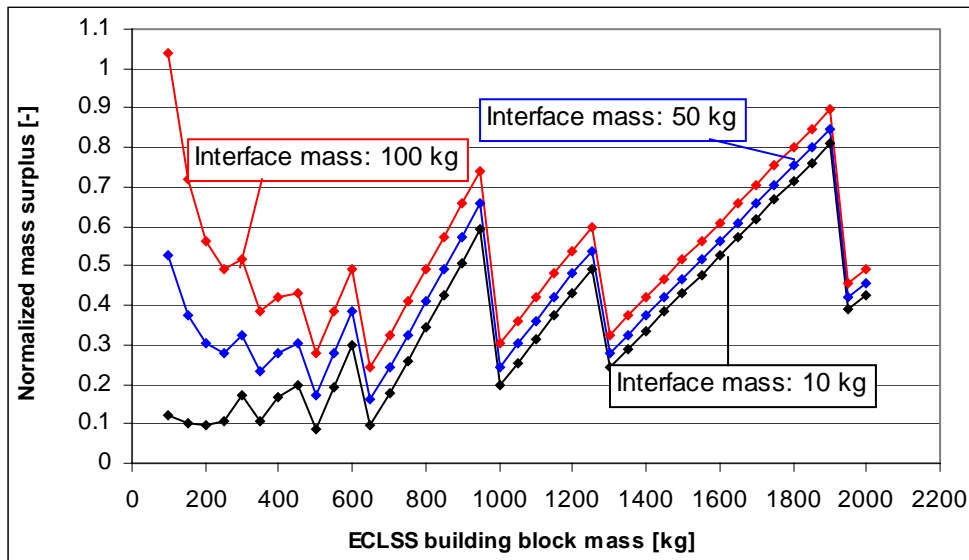


Figure 4-16: Modularization of life support equipment dry mass for 3-, 4- and 6- crew; based on the scaling model developed in Subsection 2.2.2

In Appendix E, Subsection 7.5.2, results for a similar analysis of the electrical power subsystem equipment is provided, also for the 3- / 6- crew and 3- / 4- / 6- crew cases.

4.6 Summary of Chapter 4

In Chapter 4, extensible design for manned Moon and Mars exploration architectures was demonstrated. A method for extensible design was outlined, which provides two approaches to identify options for extensibility and select the best one for given constraints. Both approaches were exercised on the modularization of pressurized volumes / structures, propellant management systems (tanks), and rocket engines. Chapter 4 therefore represents one iteration through this process for extensible design (see also Chapter 5).

Numerical values are provided for the building blocks for the CEV and surface habitats. Two complete strategies were laid out how to effect a high degree of extensibility between Moon and Mars exploration hardware, using the two approaches developed above. There appears to be ample opportunity for commonality and modularity between Moon and Mars exploration systems without creating unacceptable mass overheads compared to point designs. This enables the conclusion that there is **no need for a technology development 'gap' between Moon and Mars missions**, because most of the hardware that is needed for Mars missions is already used for lunar missions.

Both approaches for extensible design were exercised on various elements and subsystems of the Moon and Mars exploration architectures. During this application of the two methods, it was recognized that it is not possible to generally determine which one is better suited to achieve extensible design with very low penalties. Rather, it was observed that both approaches are desirable under certain conditions concerning the distribution of functional requirements that drove the modularization or commonality mapping; this is discussed in more detail in Chapter 5.

The normalized mass overheads given for the individual building block selections was converted into additional launch cost expenditures, and the reduction of the number of point designs into development cost savings. In the context of the very simple model assumed for the individual cost numbers, extensible design always pays off, if few Moon missions are conducted. Extensibility becomes progressively less attractive with the number of missions executed.

It should be noted, that the input parameters for the resource calculations carried out in this chapter are rather conservative concerning extensibility: the specific launch cost will probably be below 10000 \$/kg, whereas the development costs for crew compartments and in-space propulsion stages are likely to be in excess of \$500 million and \$200 million per unit. This would make the results even more favorable for extensible systems.

Nevertheless, a detailed assessment of the resource expenditures and savings for extensible systems compared to point designed one has to be carried out; this is, however beyond the scope of this thesis, and is considered future work.

5. Results, Conclusions, Further Work

This chapter summarizes all the results documented in this thesis; conclusions are drawn on the basis of these results, and suggestions for further work related to the particular issue or topic are provided.

5.1 Results, Conclusions, Further Work: Modeling

5.1.1 Architecture Modeling / Generation (Section 2.1)

Results:

- Two sample architectures for manned Moon and Mars landing were described: the Apollo architecture and vehicles, and the NASA Mars Design Reference Mission architecture and vehicles.
- A generic scheme for the qualitative modeling of top-level manned exploration architectures in the vicinity of the destination planet (Moon / Mars) was developed in the form of a “Morphological Matrix” [Pahl, Beitz, 1997].
- The design variables used for the modeling scheme are: the number of manned vehicles in the architecture, the number of crew transfers between these vehicles, the sequence and locations of the crew transfers, and the position of the destination surface landing in the sequence.
- A set of 12 rules has been provided to generate usable (“legal”) design vectors.
- With these, a set of 30 architectures has been (manually) generated, 14 with crew transfers only on the destination surface and / or in destination orbit, 16 with crew transfers also in transit.
- Among these 30 architectures there are numerous ones, which, to the best of the author’s knowledge, have not been proposed before.
- All 30 architectures have been analyzed qualitatively (Appendix A), the first 14 also quantitatively (see Chapter 3, Appendix C, Subsection 7.3.1).

Conclusions:

- It is possible to provide a top-level characterization of a broad class of manned Moon / Mars exploration architectures with very few parameters; this enables one single person to understand the nature of an architecture, without delving into excessive technological detail.
- The architecture model is sortie-based (single missions to the destination surface).
- The modeling scheme is oriented along the manned operations during the mission; unmanned vehicles are not modeled. This is justified, because the vehicles with crew compartments or habitats are expected to be the drivers of manned Moon and Mars exploration architectures.
- Considerable design freedom concerning technology (propulsion, life-support) and trajectory (minimum-energy, fast, spiral) choices is still available within one top-level architecture.
- The modeling scheme could potentially be extended to include Earth orbital operations, architectures without landing on a planetary surface, and potentially even surface operations architectures.

Further work:

- Extension of the architecture modeling scheme and philosophy to model individual propulsion stages and equipment needed for surface operations (pressurized rovers, tools, etc.). Initial work on a generic scheme for architecture modeling based on the model presented here has been done by **Mr. Willard Simmons**, a doctoral student at the MIT Space Systems Laboratory.
- Quantitative analysis of the 16 architectures with crew transfers in transit. It is conceivable that some of these architectures could provide significant mass savings, especially if ISPP is available, albeit at significantly increased mission risk.

5.1.2 Empirical and Scaling Models of Individual Spacecraft (Section 2.2)**Results:**

- Two quantitative models for crew compartment masses have been developed and described:
- The first is an empirical model for crew compartments developed by NASA that is based on past and existing manned spacecraft designs. The input parameters for this model are: the crew size, the duration of the stay in the compartment, and the pressurized volume needed for the stay. The results have been benchmarked against existing and proposed detailed designs.
- The second model is based on a subsystem breakdown of NASA's Reusable Lunar Lander given in [NASA OASIS, 2004; Wingo 2004]. Individual subsystem masses are determined by scaling laws, or by mass-percentages.
- For the modeling of propulsion stages, rocket engines, heat shields and landing gears, several models were developed based on information from literature.
- A sensitivity analysis was carried out to assess the impact of variations in parameters such as specific impulse, structural factors, velocity changes, crew size, mission duration, sample and cargo masses, etc.

Conclusions:

- Benchmarking of the first model in conjunction with the propulsion, heat shield and landing gear models showed excellent agreement (< 10 % for all components except the engines) with the masses given for the Apollo Lunar Module in [Gavin, 2002; NASA, 1972].
- Both models deliver masses within 25 % of available design data over a wide space of input values.
- The sensitivity analysis shows that velocity changes, the specific impulse, the crew size and the duration have the most significant influence on overall vehicle mass. It therefore is very desirable to choose a propulsion system with a high specific impulse and low boil-off; given these conditions, and the possible extensibility towards ISRU / ISPP, the choice is liquid methane / liquid oxygen.
- Benchmarking shows that the models used are conservative in mass estimation.

- The empirical mode allows quantitative analysis of architectures with very few design variables.
- The models allow for the identification of optimal modular quanta of propellant tanks, engines, pressurized volumes, life support and electrical power equipment.
- The models permit hardware design of propulsion stages to a level of detail that permits the analysis of design reuse for other missions and architectures (propulsion stage commonality).

Further work:

- Future analysis of commonality and modularity of within and between architectures on the subsystem and component level requires more detailed models, especially for habitats / crew compartments.
- The issue of launchability needs to be assessed in conjunction with modularity and commonality; this includes on-orbit assembly.
- The model for the propellant management systems is based on the assumption that the tank thickness is negligible compared to the radius of the propellant tank; this leads to a linear relationship between propellant mass and structural mass. While acceptable for the tank radii (> 1 m) used for the systems in this thesis, for very small tank radii (many modules), this assumption might no longer be valid.
- It needs to be examined if aerocapture and aeroentry require substantially different types and quantities of heat protection.

5.2 Results, Conclusions, Further Work: Moon and Mars Exploration System Point Designs

5.2.1 Point designs (Sections 3.1 & 3.2)

Results:

- The 14 architectures with crew transfers solely in destination orbit or on the destination surface were analyzed quantitatively.
- The architectures were analyzed for four different types of Moon, and four different types of Mars missions.
- The architectures were analyzed both for application and non-application of ISPP; results for ISPP are provided in Appendix C. ISPP represents “best-case” ISPP: all the propellant is available for free (in terms of mission mass) on the destination surface.
- The architectures were analyzed for TMI / TLI with cryogenic propulsion (liquid hydrogen / liquid oxygen), as well as nuclear thermal propulsion (NTP).
- Preferred architectures were selected based on the following two criteria: low IMLEO (quantitative), abort opportunities / risk (qualitative), and design simplifications through reduction of requirements.

Conclusions:

- There is a distinction between mission and architecture: architectures are usually proposed for specific missions, but can also be employed for other mission types.
- **For Mars missions**, abort to orbit during landing is undesirable, because:

- It is only possible at low velocities (< 1000 m/s), and close to the ground, i.e. not during to most dangerous portion of the descent: the high-speed reentry.
- Main parachutes might reduce the amount of velocity change required to that provided by retrorockets to cushion the impact.
- All the consumables for the entire mission have to be provided in orbit; therefore a considerable fraction of the consumables will be duplicated (launch window to Earth can be closed for up to 1.5 years).
- **For lunar missions**, abort to orbit is desirable, because it is practical for the whole duration of the descent, and also because it takes only 4 days to return to Earth.
- Based on these observations, the preferred architecture for manned Mars exploration (no ISPP) is the NASA Mars DRM / Apollo “Blend”. Reasons for this choice are (see Figure 5-1):
 - That this architecture is the second-best architecture concerning IMLEO, and very close to the best, the NASA Mars DRM.
 - That this architecture features one long-duration habitat that is only used in space, and one that is used for landing, and then only on the surface (design simplification).
 - That this architecture can be easily modified to include ISPP.
 - That this architecture can be changed to the NASA Mars DRM with comparatively few changes (flexibility during design).
 - That this architecture has not been proposed before.
- The favorite architecture for lunar missions is the Apollo + surface habitat architecture. Reasons for this choice are (see Figure 5-1):
 - This architecture enables, in case of a contingency, a direct return to Earth without rendezvous, crew transfer or orbit insertion, because the crew sets out from Earth orbit in the vehicle in which it returns to Earth.
 - If the orbiter and the lander travel together, and the surface habitat is prepositioned, the crew has a second crew compartment available for the largest part of the Earth-Moon coast. This is crucial for the survival of contingencies as encountered during the Apollo 13 mission [Goodwin, 2004].
 - This architecture includes an Apollo architecture, which is used for the short stay missions (up to 3 days surface stay); this is due to the decoupling of the surface habitat and lunar lander design.
 - For every mission, a different location can be chosen.
 - Direct abort to orbit during descent is available.
- The second-best choice for lunar missions would be NASA’s first lunar outpost architecture.
- If ISPP is available for Mars missions, the “Mars Direct” or the one-vehicle architectures are most desirable, because they have low IMLEO, and they reduce the number of manned vehicle designs. It should be noted that the crew compartment and habitat masses given in [Zubrin, 1997] appear to be very optimistic. The crew compartment masses used in this study are conservative and validated against proposed designs by NASA and ESA. With these conservative

- models, the “Mars Direct” architecture and concept of operations still appears to be very interesting, if large-scale ISPP is available.
- It appears that large-scale ISPP / ISRU almost certainly requires a surface nuclear reactor, which could be a significant hurdle to the realization of Mars missions. Options requiring large-scale ISRU, despite significant mass savings, therefore also have considerable drawbacks.
 - Small-scale ISRU might not require nuclear surface power, and could be used to provide fuel for rovers, and spare consumables for habitats.

Further work:

- Detailed assessment of the cost, benefit, and feasibility of ISRU / ISPP (especially concerning power requirements).

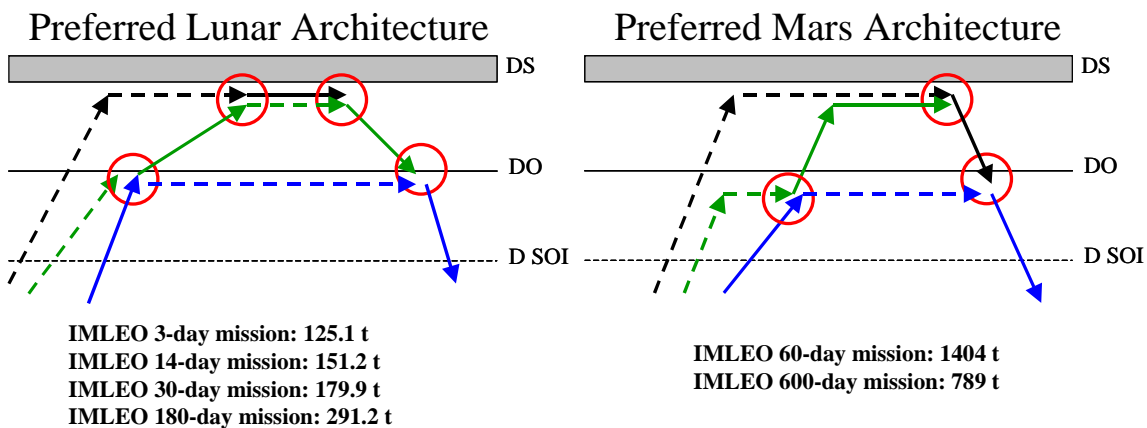


Figure 5-1: Preferred architectures and missions, and associated IMLEO values; please note: for the three-day lunar mission, actually an Apollo-architecture without surface habitat is employed, which is a subset of the Apollo + surface habitat architecture

5.2.2 Trades

Results:

- Preferred architectures were chosen from a wide variety of architectural options. They represent an initial best choice, which can be augmented and enhanced by trading options for various design variables, according to systems engineering best practice [NASA, 1995].
- The trades encompass a wide array of design variables. The following areas were subject to trades:
 - o Staging location in lunar vicinity and associated abort scenarios for a polar lunar landing site
 - o Crew size and surface mission duration for lunar missions (the surface duration can be chosen virtually arbitrarily only for lunar missions)
 - o Mars free-return trajectory and Mars orbit insertion and modification
 - o Number of vehicles
 - o Number and sizing of stages (optimal stages vs. stages with equal tank sizes)

- The architectures including the improvements identified through trades serve as baseline architectures for the extensibility analysis (see Figure 5-2).

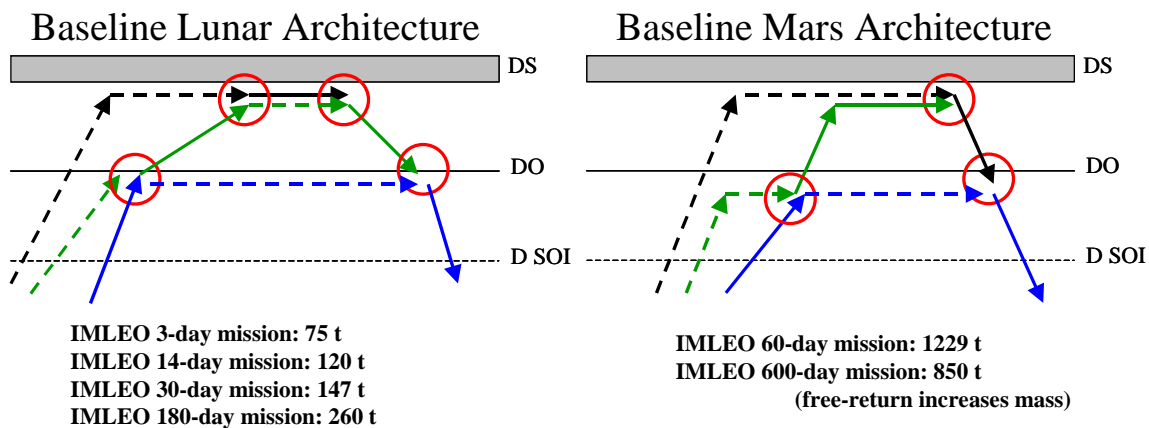


Figure 5-2: Baseline architectures (result of trade analysis) and associated IMLEO values; please note: for the three-day lunar mission, actually an Apollo-architecture without surface habitat is employed, which is a subset of the Apollo + surface habitat architecture

Conclusions:

- Performing a plane change from low (ca. 100 km) polar lunar orbit into near-equatorial lunar orbit is the best option for continuous surface abort from polar lunar landing sites. The operational concept consists of inserting into a highly elliptical lunar orbit, performing the plane change at the apocenter, and then inserting onto a trans-Earth trajectory that lies almost in the orbital plane of the Moon, rather than staging at the E-M L1 point.
- With additional propellant, it is conceivable to perform the same plane change on the way to polar lunar orbit; this would enable the use of a free-return trajectory on the way to the Moon.
- In terms of mass-effectiveness, smaller crew sizes and longer stay times on the lunar surface are better than larger crews and shorter stays. The reason for this is that the initial equipment and structural mass for a larger crew size is too large to be offset by the additional consumables needed to sustain a smaller crew for a longer time.
- The crew size of three was chosen, because, for long duration stays, it would be desirable to have one crewmember stay behind in the habitat for rescue purposes; extra vehicular activities are always carried out with at least two crewmembers.
- The crew size for Mars missions is assumed to be 6; the reason for this choice is that at least five crewmembers would be needed to provide all the skills needed for such a long and demanding mission [Hoffman, Kaplan, 1997].
- It is possible to modify the orbit of a spacecraft around Mars during the manned surface mission, for example from HEMO to LMO, by aerobraking. This can reduce overall mission mass, and might be interesting also for unmanned sample return missions.
- At least one of two operational capabilities has to be developed to carry out Mars missions with an acceptable IMLEO: aerocapture or rendezvous in HEMO. If

- rendezvous in HEMO is available, minimum energy and fast conjunction class missions can be flown; if aerocapture is available, fast conjunction class missions with a 2-year free-return trajectory outbound are possible.
- Combined lander / ascender and surface habitat vehicles have two disadvantages which make them undesirable: for long surface duration missions they are very heavy (> 100 t), and the surface habitat cannot be extended separately from the lander / ascender. For example, a mission with a cumulative surface stay time of 100 crew-days requires an IMLEO of 124 tons, if it is executed with a crew of 2 on a 50-day mission, but 160 tons, if it is executed with a crew of 4 on a 25-day mission.

Further work:

- A detailed analysis of the feasibility of rendezvous in highly elliptical orbits and / or aerocapture needs to be made.

5.3 Results, Conclusions, Further Work: Commonality and Modularity

5.3.1 Modularization of Pressurized Volumes for Crew Compartments and Habitats (Section 4.1)

Results:

- The penalty (or “cost”) of modularization of pressurized volumes was measured by the surplus volume the modularized designs create compared to the point designs.
- The analysis of surplus volumes was carried out for
 - o The crew compartments of the CEV, the Moon lander, the Mars Ascent Vehicle, and the Earth Entry Vehicle.
 - o The 14-, 30-, 180-day lunar surface habitats, the 60-day Mars landing and surface habitat, and the 600-day Mars landing and surface habitat.
- The surplus volumes for both instances of pressurized volumes were visualized in diagrams in order to enable an informed design decision.
- New point design data were calculated for Moon and Mars architectures employing the habitat and crew compartment building blocks; these data are provided in detail in Appendix E.

Conclusions:

- There are two possible ways for design for extensibility:
 - o Point design for one system, design reuse without modification for the other system(s)
 - o Modularization on the subsystem / component level to satisfy all requirements, but (generally) no single requirement exactly
- The two approaches represent different weightings of designs: for the design reuse approach, the requirements for one system are weighed significantly

- stronger than those of the other systems. For the approach that employs modularization on the subsystem level, all requirements have equal weight.
- The two approaches are not mutually exclusive, but can be used synergistically to search for optimal building blocks across designs.
 - Though presented here for the design of extensible manned spacecraft, the two approaches represent a ***generalizable process for the design of extensible systems*** (see Figure 5-3). The process consists of two major sub-processes: options for extensibility can only be identified by analyzing existing architectures. Therefore, in the left-hand side of Figure 5-3, a sub-process for point design precedes the sub-process solely devoted to design for extensibility. In the section “Thesis overall summary” at the end of this chapter, a notional guideline is presented for selecting approach one or two on the basis of the degree of clustering of functional attributes (see below).
 - The work in this thesis represents one iteration of the entire process.

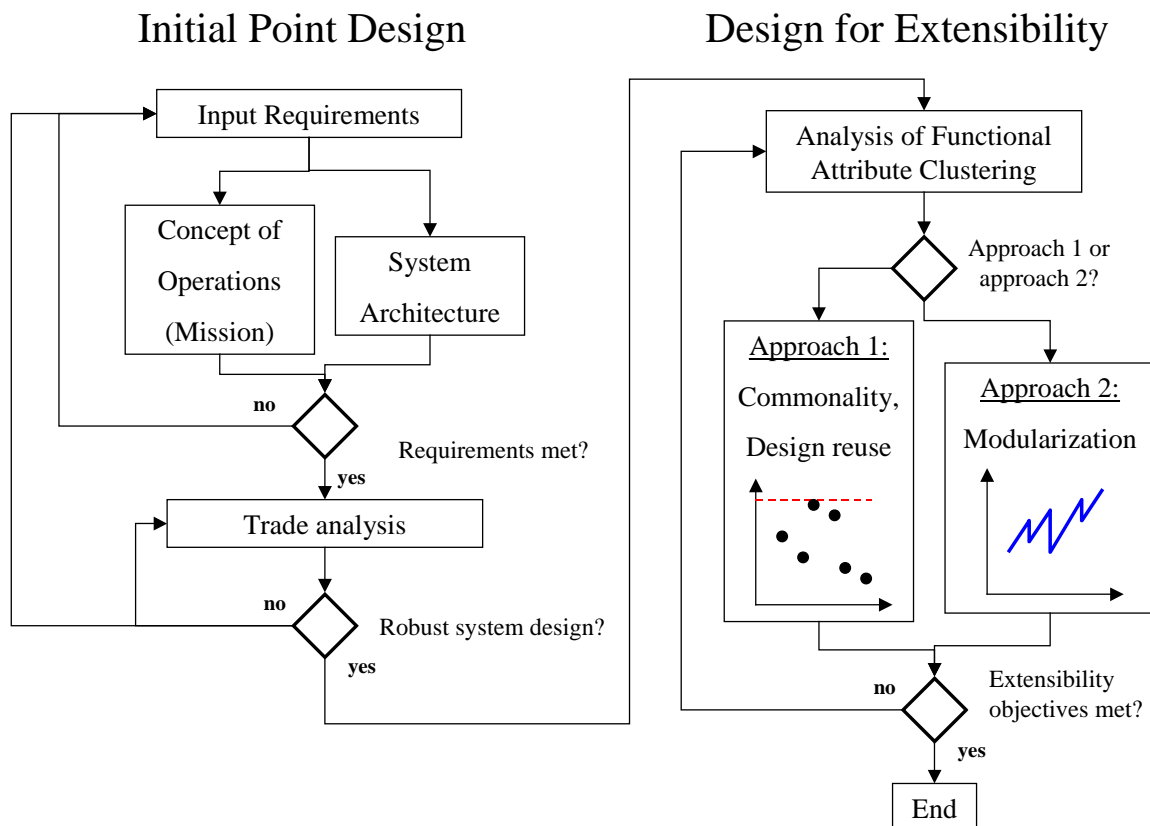


Figure 5-3: Process for the design of extensible systems, consisting of two sub-processes: (1) point design as a basis for (2) design for extensibility (for all elements / subsystems / components)

- For the pressurized volumes of small crew compartments, two possible building blocks exist:
 - o One with approximately 12.5 m³; this would necessitate a Soyuz-like design with two pressurized modules for the Earth Entry Vehicle and the lunar orbiter, but would also create the least surplus volume. Only one of

the two modules needs to have a heat shield to reenter the Earth's atmosphere; this results in a mass saving.

- One with approximately 22 m³; this would provide one-module designs for all crew compartments (Apollo), create, however a bigger surplus.
- It was decided to choose the one-module solution.
- For the surface habitats, it was decided to choose the building block with 114 m³; this necessitates up to three building blocks for the surface habitats (exactly three for the long Mars mission surface habitat, see Section 4.2).
- The building block can also be used for the in-space habitats, albeit with potentially different subsystems attached. Also, the structural requirements would potentially be different; it is, however, assumed that the in-space loads are less stringent than the landing loads.
- The choice of the crew compartment building block expands the concept of operations for the CEV: the CEV now goes to the surface on Moon and Mars, and is used actively during lunar landing and ascent, and for the Mars ascent. These different instances of the CEV design will have many identical subsystems (Structure, ECLSS, EPS, etc.), but also some that are custom-designed for the individual missions (Avionics, Thermal Control, etc.).
- The CEV has a heat shield as lunar orbiter and Earth Entry Capsule, but not as lunar lander and Mars ascent vehicle. The heat shield therefore needs to be structurally independent from the pressure vessel. A potential solution for this could be inflatable heat shields, which would also introduce a considerable mass saving [Messerschmid, 2000].

Further work:

- Detailed analysis of the suitability of individual CEV subsystems to be used for the four different operational concepts described above.
- Sensitivity analysis of the building block choices for crew compartments and habitats for varying crew sizes.

5.3.2 Commonality Between Propulsion Stages (Section 4.2)

Results:

- For the identification of propulsion stages with closely similar requirements, the impulses (propellant mass times exhaust velocity) delivered, rather than the velocity change of these stages are decisive.
- Based on the new designs employing the volume building blocks, the impulses were calculated for all propulsion stages employing liquid methane / liquid oxygen (i.e. all stages except those used for launch, TMI and TLI). Based on the results, two propulsion stages from the point design for the long Mars mission were chosen as building blocks.
- Based on these two propulsion stages, the mass for the architectures using only the habitat, crew compartment, and propulsion stage building blocks were computed and compared to the architectures only using the pressurized volume building blocks: the overall normalized increase in IMLEO was calculated to be

- about 6 %. The Moon architectures using Mars hardware are called ‘Lunar Variants’.
- A hardware development roadmap for the individual components needed for manned Moon and Mars exploration was created based on the spiral development approach used by NASA’s Exploration Systems Mission Directorate.

Conclusions:

- The comparison of propulsion stage impulses is a very useful tool for the identification of options for commonality.
- The increase of IMLEO due to commonality (the penalty of modularization), is very small compared to the overall IMLEO. For individual lunar missions, however, the mass overhead can be quite significant (up to 39 % for a 14-day lunar mission, see Table 4-3). As these missions contribute significantly less mass than the Mars missions to the total cumulative IMLEO of the mission type network, the total mass overhead is still quite small; the Mars missions “drive” the mass overhead.
- It is possible and beneficial to combine the LOI and TEI stages for lunar missions into one stage, as in the Apollo Service module.
- The technology development suggests that all in all, three propulsion stages engines have to be developed in order to carry out Moon and Mars missions (see Section 4.3):
 - The TMI/TLI stage building block (modularization / commonality analysis is part of future work), employing LH₂ / LOX
 - Propulsion stage 1 (deeply throttleable engine), employing LCH₄ / LOX
 - Propulsion stage 2 (deeply throttleable engine), employing LCH₄ / LOX
- After completion of spiral three of the hardware development cycle, several alternate missions are possible: manned missions to Near Earth Objects, Mars flybys, and potentially manned missions visiting Phobos
- The hardware for Moon and for Mars missions is identical except for aerocapture heat shields. As the development of heat shields for Mars is not assumed to take a decade, **there actually does not need to be a long gap between manned Moon and Mars missions.**
- Heavy lift capability (around 100 tons to LEO) is desirable. One possible way to achieve this could be a HLLV using SRBs and the external tank of the STS, however not the orbiter (see Shuttle-C concept, [MIT 16.89 Course, 2004]).

Further work:

- In-depth assessment and quantitative analysis of launch and on-orbit assembly strategies for the case that heavy lift is not available.
- Confirmation of preliminary results with detailed subsystem models.
- Application of commonality mapping to other architecture combinations, e.g. for ISPP.

5.3.3 Modularization of Propulsion Stages (Section 4.3)

Results:

- In this section, the second of the above approaches was applied: weighting all requirements equally, and identifying the best building block.
- The modularization was carried out simultaneously for the fuel volumes (coupled to the oxidizer volumes), and the thrust of the rocket engines, also only for the liquid methane / liquid oxygen stages.
- The number of tank building blocks per stage was limited to eight (4 fuel, 4 oxidizer), and the number of rocket engines to five.
- A sensitivity analysis was carried out for the “optimal” building block sizes, to quantify the impact of perturbations regarding
 - o Modeling parameters
 - o Number of missions and mission types
 - o Singularities: one mission type is not executed at all.
- A preliminary hardware development roadmap was built, organized according to the spiral development approach favored by NASA.

Conclusions:

- It is possible to find tank and engine building blocks that can be used for all liquid methane / LOX stages with a comparatively small IMLEO overhead (ca. 10 %) compared to the point designs with modularized crew compartments and habitats.
- The preliminary IMLEO overhead for subsystem modularization is larger than that for propulsion stage commonality (10 % vs. 6 %), because the latter uses two propulsion stage “building blocks”, and can therefore approximate the requirements more closely than the modularization with only one building block.
- Only two new propulsion stages need to be developed: the modularized stage with up to eight tanks in two layers of four tanks, and the TMI / TLI stage.
- The modular propulsion stage is expected to be more challenging in design than a point-designed one; this indicates that for this case the development and design effort will be more intense in spiral one and two, than in the remaining spirals.
- The sensitivity analysis indicates small sensitivity to perturbations of parameters in the equations modeling propulsion stage structure and engine dry mass (high sensitivity, however, for the specific impulse). This confirms that interface costs for tank and engine modules do not have a significant influence on the building block choice.
- The short Mars mission is the driver for the “optimal” tank and engine building block sizes, because it introduces the largest propellant mass requirement. Not including this mission in the mission type network therefore has a strong impact on the building block choice. The differences in IMLEO overhead for building block choices both with and without the short Mars mission seem to be small. It is therefore recommended to modularize also for the short Mars mission, to preserve the option to execute this mission without any additional hardware development. It is acknowledged, however, that this will be a policy, rather than a design decision.
- Heavy lift capability (around 100 tons to LEO) is desirable.

Further work:

- From the hardware / technology development roadmaps, schedule and funding flows for the individual hardware elements have to be derived.
- In-depth assessment and quantitative analysis of launch and on-orbit assembly strategies for the case that heavy lift is not available.
- Confirmation of preliminary results with detailed subsystem models.
- Analysis of the impact of using TEI stages with equal tank sizes for the short Mars mission.
- Analysis of the impact of combining the TEI and LOI stages for lunar missions.
- Application of commonality mapping to other architecture combinations, e.g. for ISPP.

5.3.4 Modularization of ECLSS and EPS Equipment (Section 4.4)**Results:**

- The equipment masses of the ECLSS and EPS systems of the CEV were calculated for the four different operational concepts, based on the scaling relationships described in Section 2.2.
- For both subsystems, calculations were carried out to identify the “optimal” equipment building block; the selection criterion was equipment mass.
- Interface masses necessary to connect the modularized building blocks to the rest of the spacecraft were accounted for by a fixed mass associated with every building block, independent of the building block size.
- A sensitivity analysis was carried out for the impact of interface mass perturbations on the building block choice.
- The impact of the introduction of a 4-crewmember CEV concept of operations on the building block choice was assessed.

Conclusions:

- Structures similar to racks used on Spacelab, Spacehab, and the ISS could be used to accommodate subsystem modules; this would facilitate module insertion and swapping, also in flight.
- The equipment mass of the ECLSS and EPS subsystems, in a top-level approximation, scales linearly with the crew size. This scaling law also applies to other subsystems (crew accommodations, etc.)
- Due to this scaling law all equipment mass requirements could be satisfied exactly by having one unit per crewmember if no interface masses were necessary.
- This underlines the importance of accurate interface mass estimation.
- For low interface masses, smaller building blocks used in large numbers are more attractive, and vice versa.
- Introducing a 4-crewmember CEV in addition to a 3- and 6-crewmember CEV makes smaller building blocks appear to be more attractive; this is intuitively expected, because smaller building blocks can approximate an increased number of requirements more accurately. Again, the interface mass has a significant influence on the building block choice.

Further work:

- Confirmation of observations through detailed analysis for all CEV and habitat subsystems, based on actual conceptual subsystem design, as opposed to scaling laws.
- Mechanical design of CEV structure and interior to assess geometrical constraints.

5.4 Thesis Overall Summary

The analysis of manned extensible system architectures in the vicinity of Moon and Mars presented in this work produced results regarding many aspects of system architecture, on different levels of system hierarchy. Recommendations for Mars system architecture choices based on minimal IMLEO and risk have been presented. From these architectures, lunar variants using the very same hardware necessary for the Mars architectures were derived, and preliminary modularization of subsystems and components was carried out.

A process for extensible system design was developed and exercised, spanning architecture modeling and generation, point design, and modularization and commonality mapping. Although the process was exercised on manned space systems, it employed principles and methods of engineering design [Pahl, Beitz, 1997; NASA, 1995], which apply to the design of systems from all fields of engineering. The process for extensible design through commonality mapping and subsystem / component modularization is generalizable to general system design.

During the application of the generalized process shown in Figure 5-3, it has to be decided which of the two approaches described above should be employed to identify and implement options for extensibility. In general, this will strongly depend on the distribution of the requirements for the functionality in question. In Figure 5-4, two extreme cases are shown:

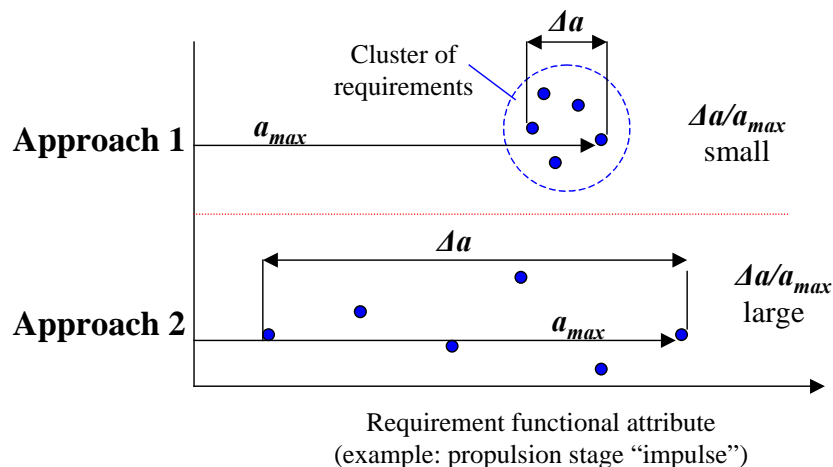


Figure 5-4: Rationale for the selection of approach one or approach two for the extensible design of elements, subsystems, or components

In the case depicted on top, all the functional requirements of the point designs (e.g. the impulse of all LCH₄ / LOX propulsion stages) have values within a certain interval, and

the variation from the largest value to the smallest value is small in comparison to the absolute magnitude of the requirements. This characteristic can be captured by the normalized maximum “design distance” δ , which is defined as the ratio of the maximum difference between the requirement values to the maximum requirement (see Figure 5-4, Equation 5-1):

$$\delta \equiv \frac{\Delta a}{a_{\max}} \quad \text{Equation 5-1}$$

If the design distance is small (i.e. close to zero), then approach one should be chosen: a common building block should be designed for the most stringent requirement, and reused for all other requirements. As the difference between the requirements is small, the penalties due to over-design are small.

In the lower half of Figure 5-4, a requirement distribution with a large design distance is shown: the requirements cover a wide range of values, which leads to a design distance close to one. In this case, the modular building block approach is more desirable: within certain constraints (see Sections 4.2 and 4.4), the building block value with the lowest overall penalty can be selected, and used once or several times for each design. The actual size and number of optimal building blocks depends on the interface penalty (see Section 4.4); the larger the interface penalty, the fewer the number of building blocks employed.

It should be noted again (see Section 4.1) that the two approaches are not mutually exclusive: if, for example, the interface cost is so high that only one module can be employed, then approach two and approach one are identical. Also, the number of building blocks can make a significant difference in terms of the penalty function: in Section 4.2, commonality between LCH₄ / LOX propulsion stages was introduced by choosing two point designed stages from the Mars exploration system as building blocks. In Section 4.3, one optimal modular building block (for tanks and engines each) was determined to be used in all the LCH₄ / LOX propulsion stages. Although the distribution of requirements (see Table 4-2) definitely shows a large “design distance”, approach one with two building blocks is superior to approach two with one modular building block only.

The most important conclusion regarding Moon and Mars exploration systems is that there is ample opportunity for commonality and modularity, which can significantly reduce the development cost, and can significantly shorten, if not eliminate, the development “gap” between Moon and Mars missions. It is highly desirable to design the CEV so that it can also serve (with adapted avionics and crew accommodations) as a lunar lander / ascender crew compartment and as a Mars ascent vehicle crew compartment.

6. Bibliography

General References

Bush, President G.W., A Renewed Spirit of Discovery: The President's Vision for U.S. Space Exploration, January 2004, www.nasa.gov

Clark, M., et al., Dictionary English-German, German-English, Dudenverlag, Mannheim, Germany, 1992

Pahl, G., Beitz, W., Konstruktionslehre – Engineering design, Berlin, Springer, 1997

Rade, L., Westergren, B., Mathematische Formeln, Berlin, Springer, 2000

Astronautics

Adams, C., McCurdy, M., Pauly, K., Optimized Space Mission and Vehicle Design, SAE Technical Papers Series, 2000-01-2332

Bate, R., Mueller, D., and White, J., Fundamentals of Astrodynamics, New York, Dover 1971

Cassenti, B., Trajectory Options for Manned Mars Missions, AIAA 2002-3787

Clark, B., Risk-Aversion Design Drivers For Human Exploration, AIAA-2000-5204

Davis, S., Station Architecture: a Transhab Derived Resort, AIAA-2000-5263

Eckart, P., The Lunar Base Handbook: An Introduction to Lunar Base Design, Development, and Operations, Space Technology Series, W.J. Larson (ed.), New York: McGraw-Hill, 1999

Germany, D., Saucier, D., Extended Duration Orbiter, AIAA-90-3533-CP

Heberling, J., Palaro, H., The Modularization Approach to Living and Working in Near Earth Space, NASA Manned Spacecraft Center, NASA Marshall Spaceflight Center, MSC-04326

Larson, W. J. and Pranke, L. K. (editors), Human Spaceflight – Mission Analysis and Design, New York, McGraw-Hill 2000

Mayer, R., MOSES (Manned Orbital Escape System) – A Hypothetical Application, General Electric, AIAA 1981

Messerschmid, E., Bertrand, R., and Pohlemann, F., Raumstationen – Space Stations, Berlin, Springer 1997

Messerschmid, E., Fasoulas, S., Raumfahrtssysteme, Berlin, Springer 2000

Reynerson, C., Human Space System Modeling: a Tool for Designing Inexpensive Moon and Mars Exploration Missions, Proceedings of ASME DETC Conference, 2003, Chicago, Illinois (DETC2003/DAC-48717)

Thomson, W. T., Introduction to Spaceflight Dynamics, New York, Dover 1961

Braeunig, R.A., <<http://www.braeunig.us/space/index.htm>>, 2001

Mark, W., <<http://www.astronautix.com/>>, 2004

NASA, www.nasa.gov, 2004

NASA's Exploration Systems Mission Directorate, www.exploration.nasa.gov, 2004

European Space Agency, www.esa.int, 2004

System Architecture

Crawley, E. and de Weck, O., Extensibility in Space Transportation, Presentation at NASA Headquarters, October 21, 2003

Dori, D., Object-Process Methodology, Berlin, Springer, 2002

Enright, J., Jilla, C., Miller, D., Modularity and Spacecraft Cost, Journal of Reducing Space Mission Cost, **1**: 133-158, 1998

Gonzalez-Zugasti, J., Otto, K., Baker, J., A Method for Architecting Product Platforms with an Application to Interplanetary Mission Design, Proceedings of 1998 DETC: 1998 ASME Design Automation Conference, Atlanta, GA

Lamassoure, E., Hastings, D., Generalized Metrics for Optimization of Space Systems Cost-Effectiveness, AIAA 2000-5323

National Aeronautics and Space Administration, NASA Systems Engineering Handbook, NASA SP-610S, 1995

Schulz, A. and Fricke, E., Incorporating Flexibility, Agility, Robustness, and Adaptability Within the Design of Integrated Systems - Key to Success, AIAA/IEEE Digital Avionics Systems Conference-Proceedings (1999), 1.A.2-1–1.A.2-8.

Schulz, A. and Fricke, E., et al, Design for Changeability of Integrated Systems within a Hyper-Competitive Environment, INCOSE “Systems Approach to Product Innovation and Development in Hyper-Competitive Environment” Conference, Denver, Colorado, March 2000

Springmann, P., de Weck, O., Parametric Scaling Model for Nongeosynchronous Communications Satellites, Journal of Spacecraft and Rockets, Vol. 41, No. 4, 2004

Simpson, T., Product Platform Design and Optimization: Status and Promise, Proceedings of ASME DETC Conference, 2003, Chicago, Illinois

De Weck, O., Chang, D. et al., Quantitative Assessment of Technology Infusion in Communications Satellite Constellations, AIAA 2003-2355

De Weck, O., Neufville, R. de, Chaize, M., Staged Deployment of Communications Satellite Constellations in LEO, Journal of Aerospace Computing, Information, And Communication, Vol. 1, March 2004

Lunar Exploration Architectures

Von Braun, W., Conquest of the Moon, The Viking Press, New York, 1953

Farquhar, R. W., et al., Utilization of Libration Points for Human Exploration in the Sun-Earth-Moon System and Beyond, 54th International Astronautical Congress, Oct. 2003

Gavin, J.G., The Apollo Lunar Module (LM); A Retrospective, 53rd International Astronautical Congress, Oct. 2002

Harford, J., Korolev, New York, Wiley & Sons, 1997

Houbolt, J.C., Manned Lunar-Landing through use of Lunar-Orbit Rendezvous, volume 1., NASA-TM-74736, 1996

NASA, Orbital Aggregation & Space Infrastructure Systems (OASIS), The Revolutionary Aerospace Systems Concepts Preliminary Architecture and Operations Analysis Report, NASA, 2002

NASA, First Lunar Outpost, NASA, 1992

NASA Public Affairs Office, Apollo 11 Press Kit, NASA, 1969

NASA Public Affairs Office, Apollo 17 Press Kit, NASA, 1972

Wingo, D., Moon Rush, Apogee Books, Burlington, Canada, 2004

Mars Exploration Architectures

Benjamin, P., Hester, J. (editors), Project Ares - Manned Mars Mission, MIT systems engineering design study, 1965

Von Braun, W., The Mars Project, Urbana, Illini Books, 1991

Donahue, B., Architecture Selection: the Key Decision for Human Mars Mission Planning, A01-34140

Goodwin, R., The NASA Mission Reports – Mars, Volume 1, Apogee Books, 2000

Hoffman, S. and D. Kaplan (eds.) The Reference Mission of the NASA Mars Exploration Study Team, NASA Special Publication 6017, Johnson Space Center, Houston, Texas, July 1997

McConaghy, T., Longuski, J., Byrnes, D., Analysis of Broad Class of Earth-Mars Cyclor Trajectories, AIAA-2002-4420

Ransom, S., Mars Mission Design Examples, EADS Space Transportation, presented at Summer School, Alpenbach 2003

Walberg, G., How shall we go to Mars? – A Review of Mission Scenarios, Journal of Spacecraft & Rockets, Vol. 30, No. 2, March – April 1993

Zubrin, R., Weaver, D., Practical Methods for Near-Term Piloted Mars Missions, <http://nw.mars.net>

Zubrin, R., The Case For Mars, New York, Touchstone, 1997

Personal Communication

Prof. Edward Crawley, MIT Department of Aeronautics & Astronautics / Engineering Systems Division

William Nadir, MIT Space Systems Lab

Prof. Jeffrey Hoffman, MIT Department of Aeronautics & Astronautics

Willard Simmons, MIT Space Systems Lab

Prof. Olivier de Weck, MIT Department of Aeronautics & Astronautics / Engineering Systems Division

Paul Wooster, MIT Space Systems Lab

7. Appendices

7.1 Appendix A: Systematical Architecture Generation

Appendix A provides an overview of the 30 architectures generated in Section 2.1.3. For every architecture, the design vector, a schematical diagram, an architecture description, and (if existing) examples from the literature are provided. Section 7.1.1. contains architectures with crew transfers only in destination orbit or on the destination surface, section 7.1.2 the architectures with crew transfers in transit. For the Morphological Matrix showing the design variables with associated options, the rules for the generation of “legal” architectures, and the legend for the schematical architecture diagrams, please refer to Section 2.1.3.

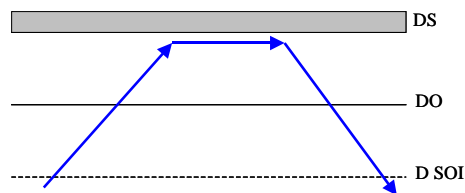
The information given in Appendix A provides qualitative descriptions for all 30 architectures generated in Subsection 2.1.3. Please note that all the architectures with crew transfers in destination orbit or on the destination surface can be used for any proposed Moon and Mars landing mission, for a wide range of technology and trajectory choices. The architectures with crew transfers in transit require special trajectories and are therefore not generally applicable; a comprehensive quantitative discussion of these architectures is beyond the scope of this thesis and has to be considered as future work.

Also, the descriptions given here do not specify how the crew ascends to Earth orbit, and how the crew is transported back to the Earth’s surface at the end of the mission. The assumptions made for the quantitative analysis in Chapter 3 are provided there.

At the end of each architecture description information is provided about the locations at which the vehicles remain after the mission. This information is interesting for the accretion of assets in space.

7.1.1 Architectures with Crew Transfers in Orbit and on the Surface

Design Vector (0, 1, L, N, N, N, N)



Architecture Description:

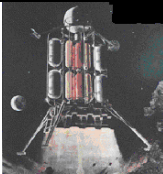
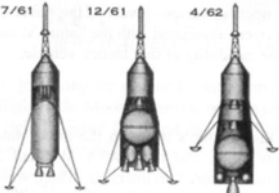
This architecture is the most straightforward one conceivable: the crew always stays in one habitat / crew compartment, from the outset of the mission in LEO to the return to Earth. No rendezvous of any kind is needed. The crew can go into orbit at the destination before landing, or can land directly out from the transfer trajectory. Especially for Mars, this is considered unlikely, because of possible atmospheric conditions (dust-storms) that are averse to landing.

Interesting characteristics of this architecture are

- That no crew transfer is needed (no rendezvous, hence lower risk)
- That the crew travels always with all the consumables needed for the full mission duration
- That only one manned vehicle has to be designed, that could potentially be used for Moon and Mars missions (lunar missions are more demanding from a velocity change point of view, because there is no atmosphere to slow the spacecraft down)
- That the architecture is the most mass-effective, if ISPP is available on Mars surface (see Appendix C, Subsection 7.3.1), but the most inefficient otherwise.
- That every Moon / Mars landing mission can go to a new location, completely independent of the previous missions
- That one very large crew compartment has to be accelerated through all maneuvers
- That no second pressurized habitat is available for contingency situations (this risk could be retired by a modular habitat design not unlike in a conventional ship)
- That the resulting vehicle is very large, and will therefore necessitate extensive on-orbit assembly
- That the habitat needs to be designed for microgravity and partial-g operation

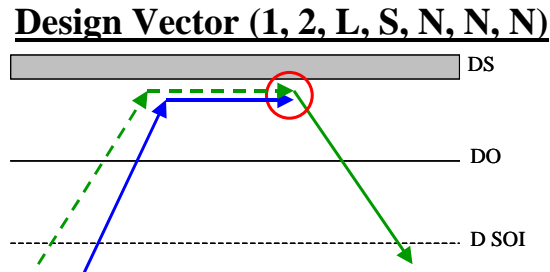
Architecture Examples:

The one-vehicle architecture has actually been proposed several times in the context of lunar landing missions. The table below shows example architectures; for in-depth information please refer to the literature sources given in the table.

	<p>Wernher v. Braun Moon Lander, 1953 [v. Braun, 1953]</p>
	<p>Gemini Lunar Survival Rescue Spacecraft, 1966 [www.astronautix.com, 2004]</p>
	<p>Combined Apollo CSM / Lunar lander, 1961 [Wingo, 2004]</p>

 <p data-bbox="402 415 618 445">FLO manned spacecraft</p>	<p data-bbox="824 289 1393 359">First Lunar Outpost without surface habitat [NASA, 1992]</p>
--	--

Table 7-1: Sample architectures from literature for the (0, 1, L, N, N, N, N) architecture



Architecture Description:

This architecture involves two vehicles: the first one is used by the crew to travel from Earth orbit to Mars vicinity, and into orbit around the destination planet. A direct landing from the interplanetary trajectory could also be performed (see preceding architecture). The first vehicle is also used for the duration of the surface stay on the destination planet. The second vehicle transports the crew from the destination surface back to the Earth; the architecture could therefore also be labeled as “Direct Return”. Vehicle two is assumed to be prepositioned on the destination surface. After the end of the mission, vehicle one remains on the destination surface.

Interesting characteristics of this architecture are

- That only one crew transfer on the destination surface is required
- That the second vehicle can be predeployed and its operational readiness assessed before the crew leaves Earth
- That this architecture offers substantial savings if ISPP is available (see Appendix C, Subsection 7.3.1)
- That the crew travels initially with all the resources needed for the interplanetary transfer and the surface stay
- That used habitats are accreted on the destination surface
- That, once in destination orbit, the crew needs to land in order to return back to Earth
- That the crew needs to land within a certain distance to the predeployed asset on the destination surface (pinpoint landing)
- That the first habitat (and possibly also the second) needs to be designed for microgravity and partial-g operations.
- That, for safety reasons, the next Earth return vehicle is prepositioned so that the crew currently on Mars can access it; this constrains the choice of landing sites

Architecture Examples:

The “Direct Return” architecture has been proposed by Robert Zubrin and others for Mars landing missions as the so-called “Mars Direct” architecture. The table below shows a picture featuring both spacecraft for “Mars Direct”, the transfer & surface habitat and the Earth return vehicle that is prepositioned. For more information please refer to the literature source and to Appendix C, Subsection 7.3.1.

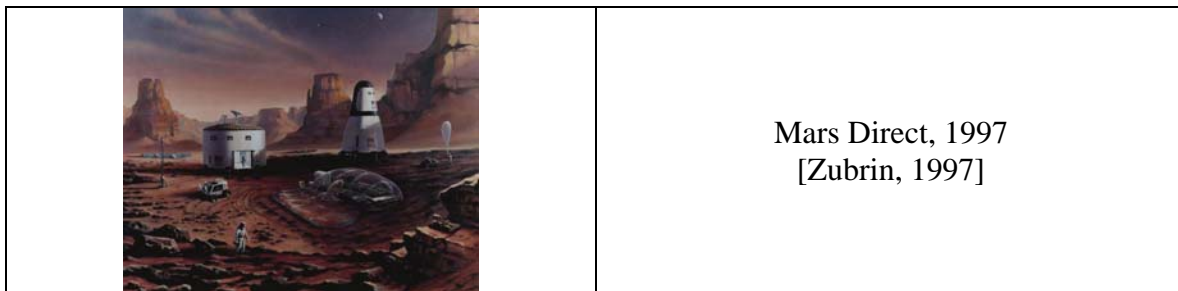
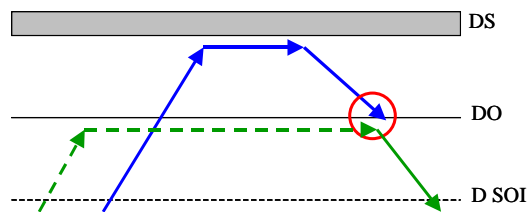


Table 7-2: Sample architecture from literature for the (1, 2, L, S, N, N, N) architecture

Design Vector (1, 2, L, O, N, N, N)



Architecture Description:

This architecture also involves two vehicles: the first vehicle is used by the crew to travel to the destination planet, either go into orbit and then land or land directly on the destination surface, during the surface stay and for the ascent to orbit. The second vehicle is prepositioned in orbit around the destination planet. The crew transfers to this vehicle after the surface stay, and then performs the Trans-Earth-Insertion (TEI) to go home. Vehicle two is assumed to be prepositioned in destination orbit. After the end of the mission, vehicle one remains in destination orbit.

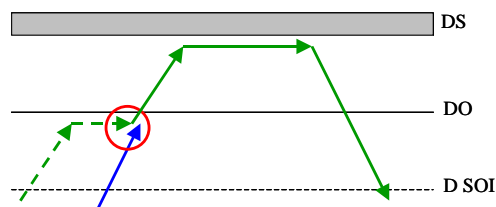
Interesting characteristics of this architecture are

- That the crew travels with all the consumable needed for the interplanetary transfer and surface stay
- That the crew can abort to orbit at any time during descent, landing and the surface stay
- That the operational readiness of the predeployed second vehicle can be assessed before the crew leaves the Earth
- That a different surface landing location can be chosen for every mission
- That with ISPP, the overall mission mass is low (see Appendix C, Section 7.3.1)
- That used habitats are accreted in destination orbit

- That the second habitat can be designed for operations solely in microgravity
- That a crew transfer in orbit, i.e. a rendezvous in orbit has to be achieved for the crew to return to Earth
- That a heavy habitat has to be accelerated through the ascent to orbit maneuver
- That, at least for the surface stay, no second pressurized volume is available for contingency reasons
- That no direct return to the Earth from the surface of the destination planet is possible; this is of special importance for polar lunar missions, where the second vehicle either will be parked in a polar lunar orbit (see trades, Chapter 3) or at the EM-L1

To the best of the author's knowledge, no example designs have been proposed for this architecture.

Design Vector (1, 2, O, L, N, N, N)



Architecture Description:

This architecture can be viewed as a kind of mirror image of the preceding one: one vehicle delivers the crew to destination orbit, where the crew transfers to the second one. This vehicle is used by the crew to land on the destination surface, provide habitable conditions on the surface, ascend to destination orbit again, perform TEI and sustain the crew during the voyage from the destination planet to Earth. Vehicle two is assumed to be prepositioned in destination orbit. After completion of the mission, vehicle one remains in destination orbit.

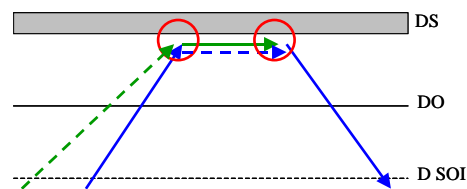
Interesting characteristics of this architecture are

- That, as soon as the crew is in the second vehicle, an abort to Earth or to the second vehicle in orbit is always possible (except for ISPP, i.e. when the vehicle does not contain all the propellant)
- That used habitats are accreted in destination orbit
- That, as soon as the crew performs transfer in destination orbit, all the resources needed for the surface stay and the return to Earth are immediately available to the crew
- That, for ISPP, the architecture has a low overall mass (see Appendix C, Section 7.3.1)
- That the operational readiness of the second vehicle can be assessed before the crew leaves Earth

- That the first habitat can be designed for operations solely in microgravity
- That a crew transfer, and possibly a rendezvous, have to be performed in destination orbit
- That a heavy habitat is accelerated through the ascent to orbit and TEI burns
- That from the beginning of the landing to arrival at Earth no second pressurized volume is available to the crew (see above)

To the best knowledge of the author, no example designs have been proposed for this architecture.

Design Vector (2, 2, L, S, S, N, N)



Architecture Description:

This architecture is related to the one-vehicle architecture described above. One vehicle delivers the crew to the destination surface. There, the crew transfers to a second vehicle, which provides a habitable environment during the surface stay. Then the crew transfers back to the first vehicle and returns to Earth. Vehicle two is assumed to be prepositioned on the destination surface. After the end of the mission, vehicle two remains on the destination surface.

Interesting characteristics of this architecture are

- That, for lunar missions, the crew can abort to Earth at any time in the mission.
- That the operational readiness of the second vehicle can be assessed before the crew leaves Earth
- That the second habitat can be designed solely for operations in partial gravity
- That crew transport to and from the surface, and the surface stay are decoupled; for lunar missions, the same vehicle 1 can be used for different surface stays (extensibility)
- That one surface habitat can be prepositioned at an ideal location, and then be visited by several crews
- That used habitats are accreted on the destination surface
- That, for Mars missions, the habitat for the return trip to Earth has to be lifted to orbit and inserted toward Earth; due to the long transit (at least 180 days), this habitat will be quite heavy
- That, if both vehicles travel separately, no second pressurized volume is available during the transfer to and from the destination
- That the first vehicle will be heavy, necessitating either an HLLV or on-orbit assembly
- That, for Mars missions, the crew needs to land in order to access the resources necessary for the stay in Mars vicinity

- That, in case a surface habitat is visited several times, always the same landing site needs to be visited

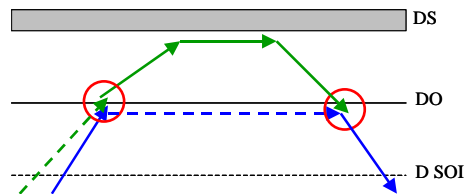
Architecture Examples:

This architecture has been proposed by two sources: by NASA as the so-called “First Lunar Outpost” which features limited hardware commonality with the NASA Mars Design Reference Mission (see below), and by Robert Zubrin, as a derivate of Mars Direct: “Moon Direct”. For more information, please refer to the literature sources given in the table below.

 <p>FLO manned spacecraft</p>	 <p>FLO lunar surface habitat</p>	<p>NASA’s First Lunar Outpost [NASA, 1992]</p>
		<p>Moon Direct, 1997 [Zubrin, 1997]</p>

Table 7-3: Sample architectures from literature for the (2, 2, L, S, S, N, N) architecture

Design Vector (2, 2, O, L, O, N, N)



Architecture Description:

This architecture is the first truly symmetrical one: the manned operations for a vehicle begin and end at the same location. One vehicle delivers the crew to destination orbit. The crew transfers to the second vehicle, which is used to land on the destination surface, to sustain the crew during the surface stay, and to ascend to orbit again. The crew then transfers back into the first vehicle, which transports them back to Earth. This was the architecture of choice for the US and Soviet manned lunar landing missions. Vehicle two is assumed to be prepositioned in destination orbit, or brought along with vehicle one, as in Apollo. After the mission, vehicle two remains in destination orbit.

Interesting characteristics of this architecture are

- That, for lunar missions, that no rendezvous is needed to abort to Earth before crew transfer in lunar orbit
- That, if the vehicles travel together (Apollo), a 'life-boat' is available during coast (Apollo 13)
- That crew transfer in orbit reduces the overall mass compared [Houbolt, 1961]
- That the first habitat can be designed solely for in-space operations
- That the crew can always abort to orbit from the surface, because all the resources needed for the rest of the mission duration are in vehicle 2 or in orbit
- That, if the second vehicle is predeployed, it can be checked out before the crew leaves Earth
- That the landing site can be chosen entirely independent of the previous ones
- That used habitats are accreted in destination orbit; also, theoretically, the ascent stage of vehicle two could be reused
- That the landing and surface habitat has to be accelerated through ascent to orbit
- That two crew transfers, and a rendezvous in destination orbit are needed
- That, for polar lunar missions, abort to Earth at any given time can be difficult (see trades, Chapter 3)

Architecture Examples:

As mentioned above, the Apollo system and the Soviet lunar landing system were both designed for this architecture. The table below gives an overview of both systems. Please refer to Chapter 2.1 and the literature sources given below for more information.

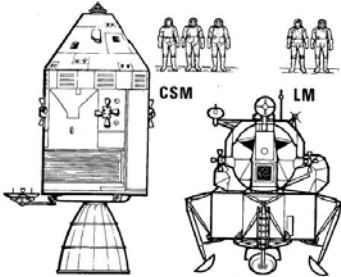
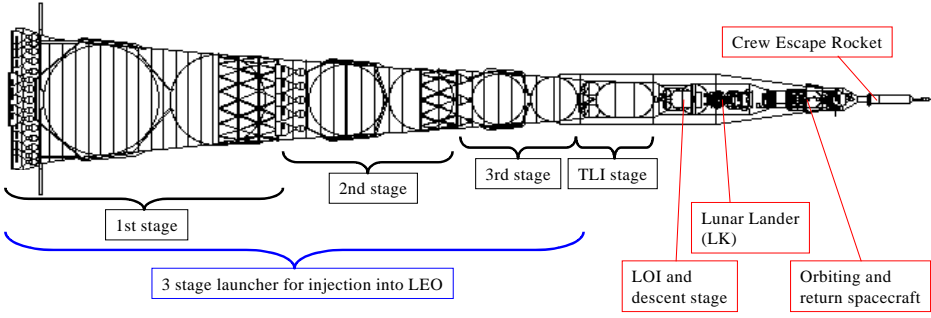
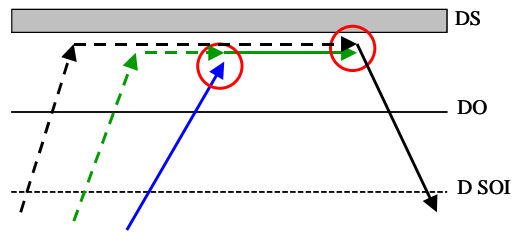
	<p>Apollo [NASA, 1969]</p>
	<p>Soviet Lunar Landing mission [Harford, 1997, www.astronautix.com, 2004]</p>

Table 7-4: Sample architectures from literature for the (2, 2, O, L, O, N, N) architecture

Design Vector (2, 3, L, S, S, N, N)



Architecture Description:

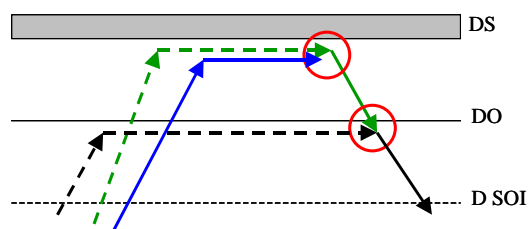
This architecture involves three vehicles: the first vehicle delivers the crew to the surface of the destination planet. After landing, the crew transfers to a prepositioned habitat (vehicle 2), which sustains the crew for the length of the surface stay. At the end of the stay, the crew transfers to a third vehicle, which provides the functions of ascent to orbit and TEI, and sustains the crew during the trip back to Earth. Both vehicles two and three are assumed to be prepositioned on the destination surface. After the mission, vehicles one and two remain on the destination surface.

Interesting characteristics of this architecture are

- That the operational readiness of both prepositioned vehicles can be assessed before the crew leaves Earth
- That two pin-point landings are required to carry out the nominal mission
- That, for lunar missions, after landing on the surface, an abort directly to Earth is always possible
- That two used habitats are accreted on the destination surface
- That, for ISPP, low overall masses can be achieved (see Appendix C, Section 7.2.1)
- That 3 habitats are available to the crew during the surface stay
- That three different manned vehicles have to be designed
- That the crew has to land on the destination surface in order to get back to Earth
- That a surface rendezvous is needed for the return to Earth
- That the return habitat is accelerated through the ascent to orbit burn
- That, for safety reasons, vehicle 3 for the following mission should be accessible for the current crew on the destination surface; this constrains the choice of landing sites; this is a desirable operational feature, not compulsory.

To the best knowledge of the author, no example designs have been proposed for this architecture.

Design Vector (2, 3, L, S, O, N, N)



Architecture Description:

This architecture also employs three vehicles: the first vehicle serves the crew as a transfer habitat from Earth to the destination planet, and also as landing and surface habitat. At the end of the surface stay, the crew transfers to the second vehicle, and ascends to destination orbit. There, the crew transfers into the third vehicle, performs TEI and goes back to Earth. Vehicle two is assumed to be prepositioned on the destination surface, and vehicle three in destination orbit. After the end of the mission, vehicle one remains on the destination surface, and vehicle two in destination orbit.

Interesting characteristics of this architecture are

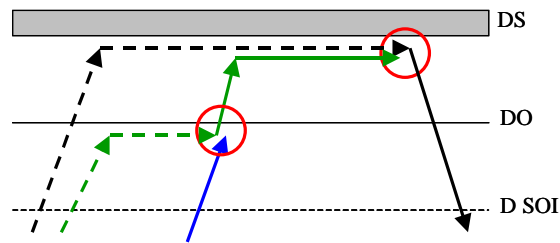
- That this architecture is very mass-efficient under different conditions (ISPP / no ISPP, Moon / Mars), see Section 3.2, Appendix C, Subsection 7.3.1
- That the crew travels with a large part of its resources, which reduces risk
- That, once the descent is initialized, the crew has to accomplish a landing within a certain distance of the ascent vehicle to get home. This requirement can be relaxed if there is a campaign of missions, so that the vehicles of the next mission, which travel at the same opportunity (for Mars) as the crew, are available in case of contingencies.
- That, after the mission, a large habitat is accreted on the surface, and can possibly be reused as a pressurized compartment
- That this architecture provides opportunity to employ ISPP for vehicle two; the savings, however, are rather small (see Appendix C, Subsection 7.3.1)
- That all three vehicles travel completely separately, i.e. can be assembled separately in LEO (if necessary)
- That the operational readiness of both prepositioned vehicles can be assessed before the crew leaves Earth
- That the crew compartment of the Mars ascent vehicle can serve as Earth reentry vehicle for the crew
- That abort to surface is the preferred abort mode in destination vicinity
- That this architecture, if employed as Mars architecture, enables missions to the Mars moons and NEOs with vehicle three

Architecture Example:

			<p>NASA Mars Design Reference Mission [Hoffman, Kaplan, 1997]</p>
---	---	---	---

Table 7-5: Sample architecture from literature for the (2, 3, L, S, O, N, N) architecture

Design Vector (2, 3, O, L, S, N, N)



Architecture Description:

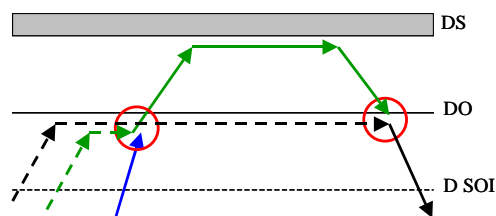
This architecture employs three manned vehicles. The first vehicle transports the crew from the Earth to destination orbit. There, the crew transfers to vehicle two, which is used for the descent to the destination surface, and for the surface stay. At the end of the surface operations, the crew transfers to vehicle three, ascends to orbit, and performs the TEI burn for the voyage home. Vehicle two is assumed to be prepositioned in destination orbit, and vehicle three on the destination surface. After the mission, vehicle one remains in destination orbit, and vehicle two on the destination surface.

Interesting characteristics of this architecture are

- That both prepositioned vehicles can be checked out before the crew leaves Earth
- That one habitat is accreted on the surface, one in destination orbit
- That pinpoint landing capability is required in order to return to Earth, once in destination orbit
- That the crew lands with all consumables for the surface stay
- That, after rendezvous in destination orbit, and prior to landing all the consumables for the surface stay are available to the crew, enabling an orbiting rescue mission
- That if ISPP is available, considerable savings can be achieved, because the large habitat for ascent to orbit and return to Earth is accelerated with ISPP-generated fuel

To the best of the author's knowledge, no example designs have been proposed for this architecture.

Design Vector (2, 3, O, L, O, N, N)



Architecture Description:

This architecture uses three vehicles, and requires two crew transfers. Vehicle one transports the crew from the Earth to destination orbit. There, the crew transfers to

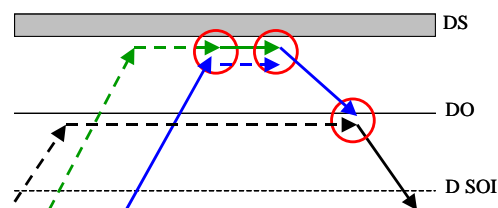
vehicle two. Vehicle two is used for the landing, the surface stay and the ascent to destination orbit. Then, the crew transfers to vehicle three, performs TEI and goes back to Earth. Both vehicles two and three are assumed to be prepositioned in destination orbit. After completion of the mission, vehicle one and two remain in destination orbit.

Interesting characteristics of this architecture are

- That the operational readiness of the two prepositioned vehicles can be assessed before the crew leaves Earth
- That, once the crew is in destination orbit, at least one rendezvous in orbit is required to return to Earth
- That two habitats are accreted in destination orbit, though not necessarily in the same orbit (destination space stations, could be used as communications relays)
- That the crew travels always with substantial amounts of consumables (there is no vehicle that only transports crew from the orbit to the surface, and / or back to orbit)
- That the architecture is very modular: vehicle two is only manned from destination orbit to the surface and back to orbit (conceptually similar to Apollo LM), vehicle one only transports crew to the destination, vehicle three only back
- That the crew does not have to land in order to survive the mission, because at destination orbit arrival, all consumables are available in orbit
- That the exact landing site can be chosen after arrival of the crew at the destination
- That, for lunar missions, and only if vehicle two is a one-stage design, it could be refueled in destination orbit, and landed again
- That this architecture, if employed as Mars architecture, enables missions to the Mars moons and NEOs with vehicle three

To the best of the author's knowledge, no example designs have been proposed for this architecture.

Design Vector (3, 3, L, S, S, O, N)



Architecture Description:

This architecture requires three vehicles and three crew transfers between vehicles. Vehicle one transports the crew from the Earth to the destination surface. After landing, the crew transfers to the predeployed vehicle two, which serves as a surface habitat. At the end of the surface stay, the crew transfers back to vehicle one, and ascends to destination orbit. There, the crew transfers to vehicle three, performs TEI, and goes back to Earth. Vehicle two is assumed to be predeployed on the destination surface, vehicle

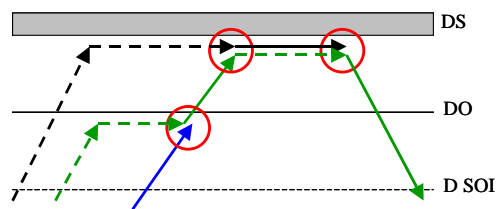
three in destination orbit. After the mission, vehicle two remains on the destination surface, and vehicle one in destination orbit.

Interesting characteristics of this architecture are

- That the crew has to land, because for long surface stays, a considerable amount of consumables is prepositioned on the surface
- That the operational readiness of the two prepositioned vehicles can be assessed before the crew leaves Earth
- That pinpoint landing and orbital rendezvous are required to return to Earth
- That there are potentially great savings by using ISPP, because the heavy habitat of vehicle one has to be accelerated to orbit again
- That the extension and improvement of the surface habitat is completely decoupled from the other elements of the architecture (increase of crew size, duration)

To the best of the author's knowledge, no example designs have been proposed for this architecture.

Design Vector (3, 3, O, L, S, S, N)



Architecture Description:

This architecture requires three vehicles and three crew transfers. Vehicle one takes the crew to destination orbit. There, the crew transfers to vehicle two, and lands on the surface. After the landing, the crew transfers to vehicle three, which is used as a surface habitat. At the end of the surface stay, the crew transfers back to vehicle two, ascends to orbit, performs TEI, and goes back to Earth. Vehicle two and three are assumed to be prepositioned on the destination surface. After the mission, vehicle one remains in destination orbit, vehicle three on the destination surface.

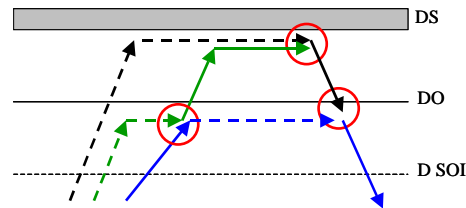
Interesting characteristics of this architecture are

- That the crew has to land, because for long surface stays, a considerable amount of consumables is prepositioned on the surface
- That the operational readiness of the two prepositioned vehicles can be assessed before the crew leaves Earth
- That for Mars missions, a pinpoint landing is required in order to return to Earth, once the descent is initiated (required consumables are on the surface)
- That ISPP is uninteresting (too risky), because vehicle two cannot be filled up with ISPP-generated propellants before the crew leaves Earth; this, however, is regarded as one of the key safety factors for the use of ISPP
- That one habitat is accreted in destination orbit, and one on the surface

- That the surface habitat is extensible separately from the other elements of the architecture

To the best knowledge of the author, no example designs have been proposed for this architecture.

Design Vector (3, 3, O, L, S, O, N)



Architecture Description:

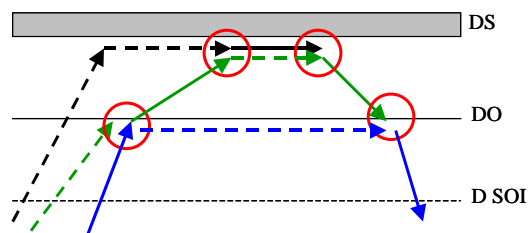
This architecture requires three vehicles and three crew transfers between them. The first vehicle is used by the crew for the voyage from Earth orbit to destination orbit. There, the crew transfers to vehicle two, and lands on the surface. Vehicle two also serves as surface habitat. At the end of the surface stay, the crew transfers to vehicle three, and ascends to orbit. There, the crew transfers back to vehicle one, performs TEI and goes back to Earth. Vehicle two is assumed to be prepositioned in destination orbit, vehicle three on the destination surface. After the mission, vehicle two remains on the destination surface, and vehicle three in destination orbit.

Interesting characteristics of this architecture are

- That, once rendezvous in destination orbit is achieved, the crew does not have to land, but can survive the mission in destination orbit
- That the operational readiness of the two prepositioned vehicles can be assessed before the crew leaves Earth
- That the two long-duration habitats on vehicles one and two can be point-optimized: vehicle one for in-space operations, vehicle two for landing (very short) and surface operations
- That this architecture is easily extensible towards the NASA Mars DRM architecture, thereby leaving more time for Mars architecture decision-making
- That the crew lands with all the consumables needed for the surface stay
- That one habitat is accreted on the surface
- That this architecture, if employed as Mars architecture, enables missions to the Mars moons and NEOs with vehicle one

To the best of the author's knowledge, no example designs have been proposed for this architecture.

Design Vector (4, 3, O, L, S, S, O)



Architecture Description:

This architecture requires three vehicles and four crew transfers. Vehicle one transports the crew to destination orbit. There, the crew transfers to vehicle two, which is used to land on the destination surface. After landing, the crew transfers to vehicle three, which serves as a surface habitat. At the end of the surface stay, the crew transfers back to vehicle two and ascends to orbit. There, the crew transfers to vehicle one, performs TEI, and travels back to Earth. Vehicle two is assumed to be prepositioned in destination orbit, vehicle three on the destination surface. After the mission, vehicle two remains in destination orbit, and vehicle three on the destination surface.

Interesting characteristics of this architecture are

- That the crew has to do a pinpoint landing to access all the consumables needed for the nominal mission
- That the operational readiness of the two prepositioned vehicles can be assessed before the crew leaves Earth
- That the two long-duration habitats on vehicles one and three can be point-optimized: vehicle one for in-space operations, vehicle three for landing surface operations
- That one habitat is accreted on the surface
- That, as vehicle two is significantly smaller than vehicles one and three, vehicles one and two can travel together
- That the crew compartment of vehicle two can be used as Earth entry vehicle
- That the surface habitat is separately extensible from the other elements of the architecture
- That four crew transfers are required for the nominal mission
- That, theoretically, abort to orbit from the surface is always possible
- That this architecture, if employed as Mars architecture, enables missions to the Mars moons and NEOs with vehicle one
- That this mission is completely symmetric, and hence most modular of all the ones investigated here: vehicle one is only an in-space transportation vehicle, vehicle two is only used as a shuttle from orbit to the surface back to orbit, vehicle three is only used as a surface habitat.

Architecture Examples:

Several example designs have been proposed for this architecture. Two prominent examples include the Mars design proposed by Wernher v. Braun in 1972, and the Aurora Human Mission to Mars design study by ESA in 2004. Both combine vehicles two and three into one vehicle with two habitats; this basically means that both vehicles travel together to the destination surface (see Subsection 2.1.3, rules). For more information on the example designs, please refer to the literature sources given below.

	<p>ESA Aurora Human Mars Mission design study [ESA, 2004]</p>
	<p>v. Braun, 1972 [Goodwin, 2000]</p>

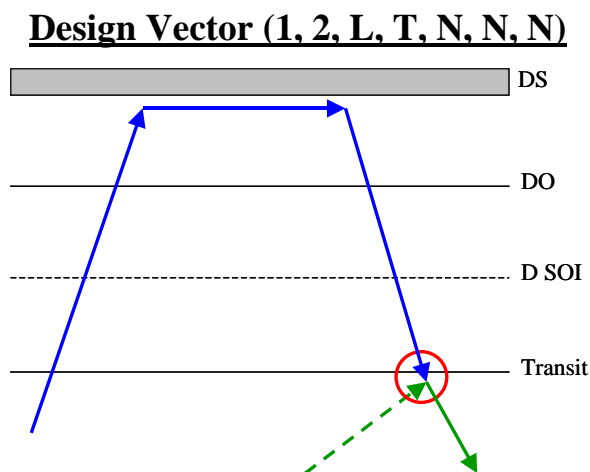
Table 7-6: Sample architectures from literature for the (4, 3, O, L, S, S, O) architecture

7.1.2 Architectures with Crew Transfers in Transit

Architectures with crew transfers in transit have one distinctive feature in comparison with the ones previously described: the spacecraft that is abandoned by the crew is not in an orbit bound to the destination planet. Unless special cycling trajectories are employed, which visit the destination planet again [McConaghy], the abandoned spacecraft cannot be used furtherly.

Architectures with crew transfers in transit can employ regular trajectories (conjunction, fast conjunction); for architectures with crew transfers in transit on the way back to Earth, either free-return trajectories can be employed for the transiting vehicle, or a large maneuver has to be performed to bring the crew back to Earth.

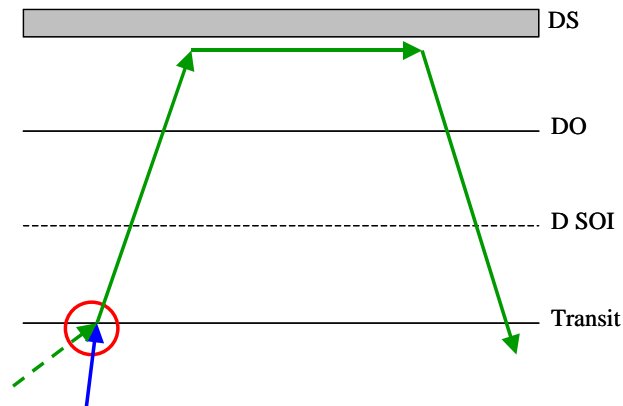
For crew transfers in transit on the way back to Earth, there is only one opportunity to insert into the trajectory needed to achieve rendezvous with the transiting trajectory. This has significant implications for the mission risk. This risk has to be weighed against the possible benefits that arise, because the transiting vehicle does not need to be braked into an orbit, which either requires heavy heat shields or a significant amount of propellant.



Architecture Description:

This architecture requires two vehicles and one crew transfer. Vehicle one is used to transport the crew to the destination surface. It also serves as a surface hab, ascent vehicle and TEI stage. After TEI, the crew intercepts vehicle two, which is on a destination flyby trajectory. The crew then transfers to vehicle two, and returns to Earth. Vehicle two is deployed on the flyby trajectory. This trajectory can either be a true free-return trajectory, which requires no additional major maneuvers, or an adjustment maneuver can be performed after the crew transfer (see above). After completion of the mission, vehicle one remains on an interplanetary trajectory.

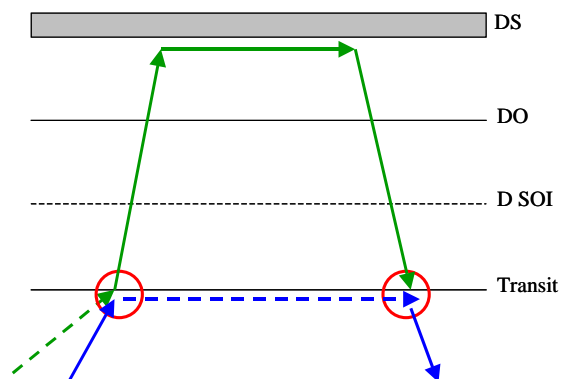
Design Vector (1, 2, T, L, N, N, N)



Architecture Description:

This architecture requires two vehicles and one crew transfer. Vehicle one is used by the crew for the transfer between Earth and the destination planet. In the vicinity of the destination, the crew transfers to vehicle two, and lands on the surface. Vehicle two serves as habitat for ascent, TEI, and the trip back to Earth. In order to ensure the crew transfer, vehicle one and two are assumed to set out together. After completion of the mission, vehicle one remains in an interplanetary trajectory.

Design Vector (1, 2, T, L, T, N, N)

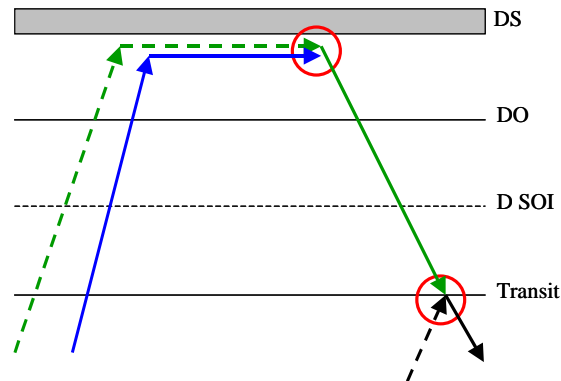


Architecture Description:

This architecture requires two vehicles and two crew transfers. It is related to the Apollo architecture. The crew sets out from the Earth in vehicle one. Sometime before arrival at the destination planet, the crew transfers into vehicle two, and accelerates towards the destination planet, lands, and performs the surface mission. At the end of the surface stay, the crew ascends to orbit again, and intercepts the transiting vehicle one. After rendezvous is achieved, the crew transfers to vehicle one, performs any additional maneuvers needed to get onto a trajectory back to Earth, and returns home. Vehicle two

is abandoned on an interplanetary trajectory. For safety reasons, vehicle one and two set out together.

Design Vector (2, 3, L, S, T, N, N)

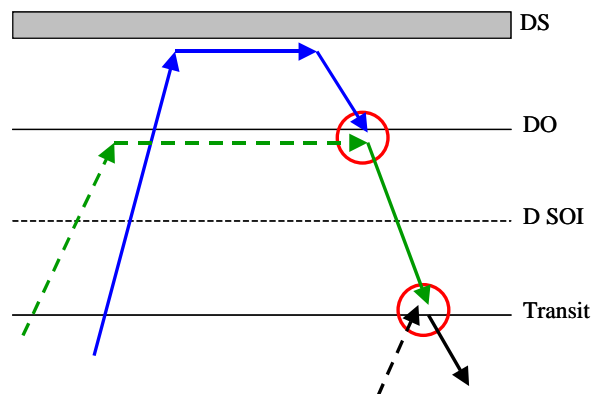


Architecture Description:

This architecture requires three vehicles, and two crew transfers. The crew is transported to the destination surface in vehicle one. This vehicle also serves as surface habitat. At the end of the surface stay, the crew transfers to vehicle two, and ascends to orbit. Then, at the proper time, the crew inserts on a trajectory that intercepts vehicle three. After the rendezvous and docking, the crew transfers to vehicle three, and returns to Earth.

Vehicle two is assumed to be prepositioned on the destination surface, and vehicle three is placed on a flyby trajectory. At the end of the mission, vehicle one remains in destination orbit, and vehicle two is on an interplanetary trajectory.

Design Vector (2, 3, L, O, T, N, N)

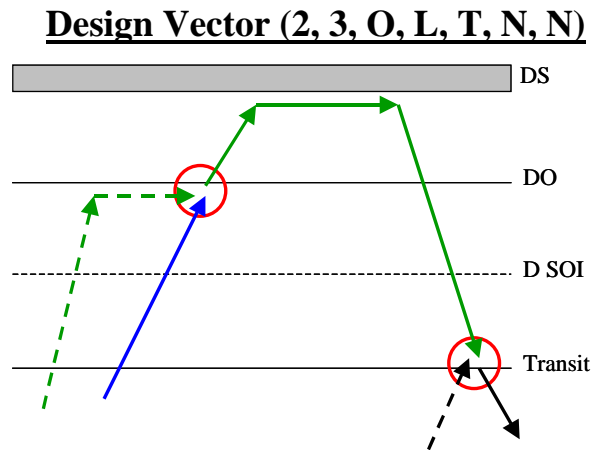


Architecture Description:

This architecture requires three vehicles, and two crew transfers. The crew is transported to the destination surface in vehicle one. This vehicle also serves as surface habitat, and,

at the end of the surface mission, as ascent vehicle to destination orbit. There, the crew transfers to vehicle two, which is used for insertion towards and travel to the transiting vehicle three. After the rendezvous and docking, the crew transfers to vehicle three, and returns to Earth.

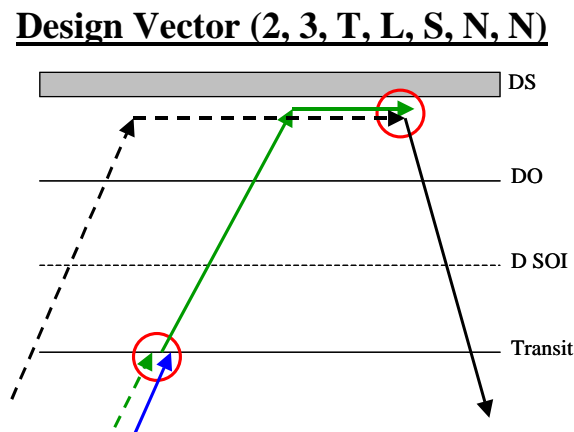
Vehicle two is assumed to be prepositioned in destination orbit, and vehicle three is deployed on a flyby trajectory. At the end of the mission, vehicle one remains in destination orbit, and vehicle two is on an interplanetary trajectory.



Architecture Description:

This architecture features three manned vehicles, and two crew transfers. Vehicle one transports the crew to destination orbit. There, the crew transfers to vehicle two and lands. Vehicle two serves also as surface habitat, and is used for the ascent to orbit, and the interception of the transiting vehicle. After successful interception, the crew transfers to vehicle three and returns to the Earth.

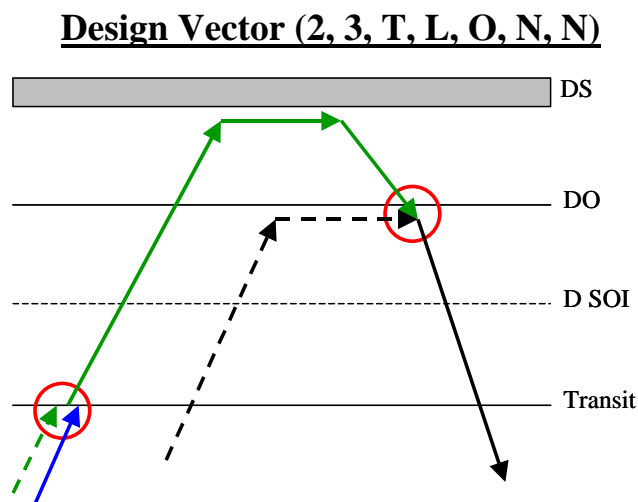
Vehicle two is prepositioned in destination orbit, and vehicle three is deployed on a flyby trajectory. At the end of the mission, vehicle one remains in destination orbit, and vehicle two on an interplanetary trajectory.



Architecture Description:

This architecture requires three vehicles and two crew transfers. Vehicle one is used for the transport between the Earth and the destination planet. Sometime before arrival at the destination, the crew transfers to vehicle two. The crew then lands on the destination planet, and vehicle two is used as a surface habitat. At the end of the surface stay, the crew transfers to vehicle three. Vehicle three is used for ascent to destination orbit, TEI, and the trip back to Earth.

Vehicle three is repositioned on the destination surface. Vehicle one is abandoned on an interplanetary trajectory, and vehicle two remains on the surface. For safety reasons, vehicles one and two set out together.

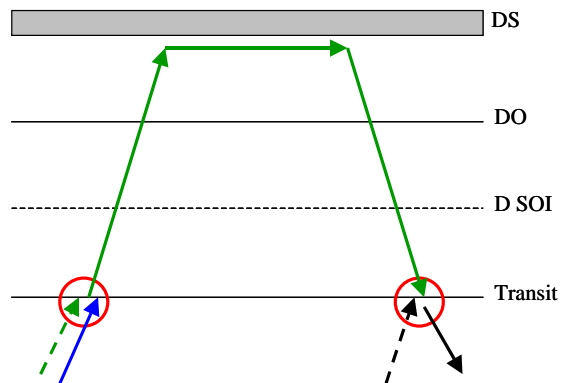


Architecture Description:

This architecture requires three vehicles and two crew transfers. Vehicle one is used for the transport between the Earth and the destination planet. Sometime before arrival at the destination, the crew transfers to vehicle two. Vehicle two also serves as surface habitat and ascent vehicle to destination orbit. There, the crew transfers to vehicle three, performs TEI and travels back to Earth.

Vehicle two sets out with vehicle one for safety reasons; vehicle three is prepositioned in destination orbit. At the end of the mission, vehicle two remains in destination orbit, and vehicle one on an interplanetary trajectory.

Design Vector (2, 3, T, L, T, N, N)

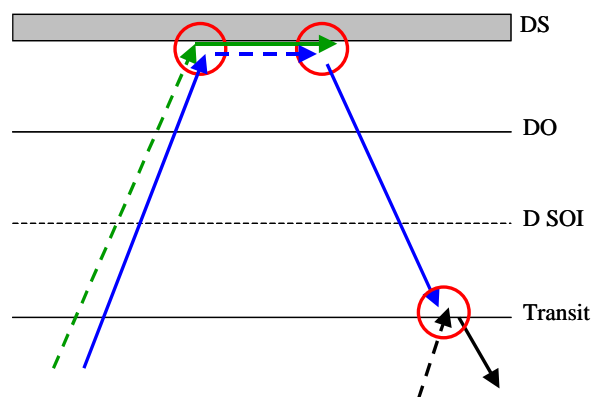


Architecture Description:

This architecture requires three vehicles and two crew transfers. Vehicle one is used for the transport between the Earth and the destination planet. Sometime before arrival at the destination, the crew transfers to vehicle two. Vehicle two lands on the destination surface. It also serves as surface habitat, as ascent vehicle to destination orbit, and is used for the interception of the transiting vehicle three. After successful interception, the crew transfers to vehicle three and return to the Earth.

No vehicles are prepositioned in this architecture. For safety reasons, vehicles one and two set out together. Vehicle three is placed on the flyby trajectory. At the end of the mission, vehicles one and two remain on different interplanetary trajectories.

Design Vector (3, 3, L, S, S, T, N)



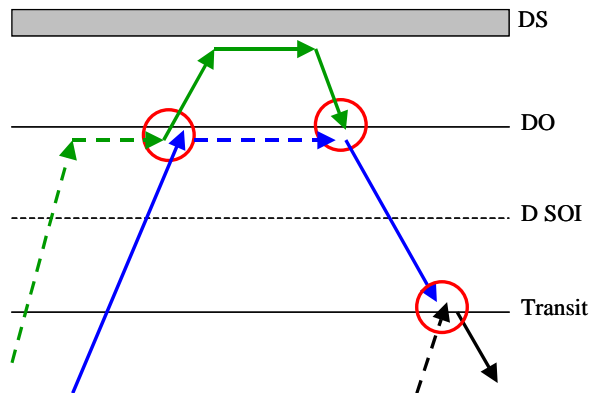
Architecture Description:

This architecture features three vehicles and three crew transfers. It has a certain resemblance to NASA's First Lunar Outpost architecture.

Vehicle one transports the crew to the destination surface. There, the crew transfers to vehicle two, which serves as surface habitat. At the end of the surface stay, the crew

transfers back to vehicle one, ascends to orbit, and intercepts the transiting vehicle three. After successful interception, the crew transfers to vehicle three and returns to Earth. Vehicle two is prepositioned on the destination surface, and vehicle three is placed on a flyby trajectory. At the end of the mission, vehicle one remains on an interplanetary trajectory, and vehicle two on the destination surface.

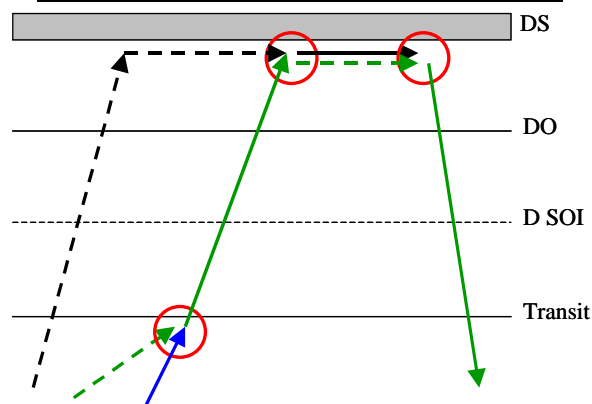
Design Vector (3, 3, O, L, O, T, N)



Architecture Description:

This architecture requires three vehicles and three crew transfers. It resembles the Apollo architecture, albeit with more vehicles. Vehicle one takes the crew to destination orbit. The crew then transfers to vehicle two, and lands. Vehicle two also serves as surface habitat, and for the ascent into destination orbit. There, the crew transfers back to vehicle one, and performs the maneuver necessary to intercept vehicle three in transit. After successful interception, the crew transfers to vehicle three and returns to Earth. Vehicle two is prepositioned in destination orbit, and vehicle three is placed on a destination flyby trajectory. At the end of the mission, vehicle one remains in an interplanetary trajectory, and vehicle two in destination orbit.

Design Vector (3, 3, T, L, S, S, N)

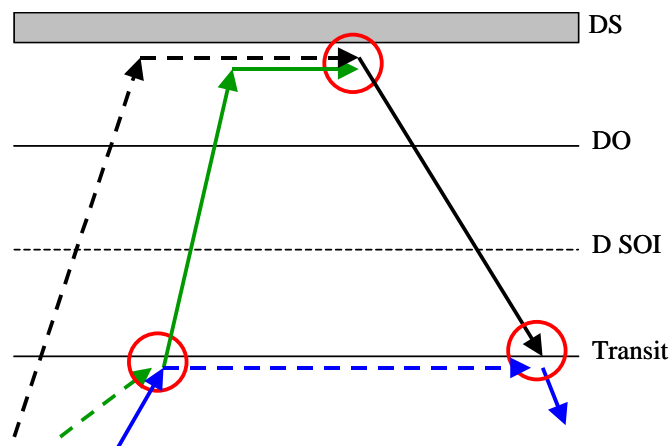


Architecture Description:

This architecture features three vehicles and three crew transfers. It also has a certain resemblance to NASA's First Lunar Outpost architecture. Vehicle one is used for the transport between the Earth and the destination planet. Sometime before arrival at the destination, the crew transfers to vehicle two. Vehicle two is used to land on the destination surface. Once on the surface, the crew transfers to vehicle three. At the end of the surface stay, the crew transfers back to vehicle two, ascends to orbit, performs TEI and returns directly to Earth.

Vehicles one and two set out together for safety reasons, and vehicle three is prepositioned on the destination surface. After completion of the mission, vehicle one remains in an interplanetary trajectory, and vehicle three on the destination surface.

Design Vector (3, 3, T, L, S, T, N)

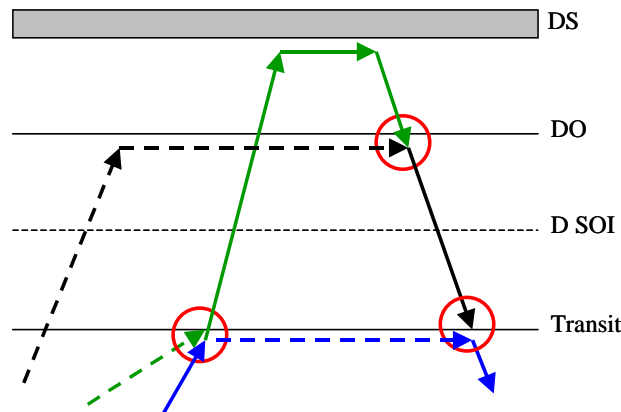


Architecture Description:

This architecture requires three vehicles and three crew transfers. This architecture resembles the "Blend" architecture proposed above. The crew departs Earth in vehicle one. Sometime before arrival at the destination planet, the crew transfers to vehicle two, and accelerates towards the target planet by means of a propulsive maneuver. The crew lands in vehicle two, which is also used as the surface habitat. At the end of the stay, the crew transfers to vehicle three, ascends to orbit and performs the maneuver to intercept vehicle one in transit. After successful interception, the crew transfers to vehicle one, performs any additional maneuvers needed to return home, and goes back to Earth.

Vehicles one and two set out together for safety reasons. Vehicle three is prepositioned on the destination surface. At the end of the mission, vehicle two remains on the destination surface, and vehicle three on an interplanetary trajectory.

Design Vector (3, 3, T, L, O, T, N)

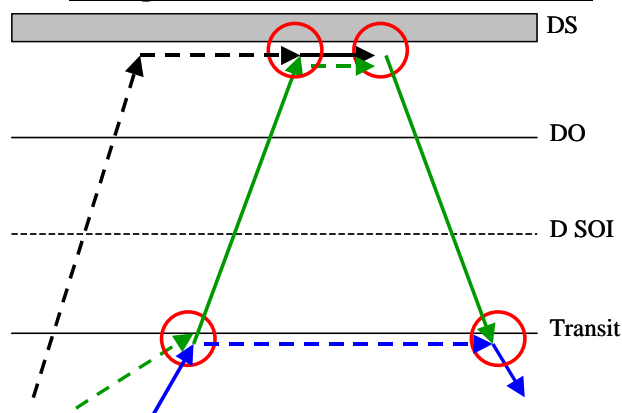


Architecture Description:

This architecture features three vehicles and three crew transfers. The crew departs Earth in vehicle one. Sometime before arrival at the destination planet, the crew transfers to vehicle two, and accelerates towards the target planet by means of a propulsive maneuver. The crew lands in vehicle two, which is also used as the surface habitat. At the end of the stay, the crew ascends to orbit and transfers to vehicle three. The crew then performs the maneuver to intercept vehicle one in transit. After successful interception, the crew transfers to vehicle one, performs any additional maneuvers needed to return home, and goes back to Earth.

Vehicles one and two set out together for safety reasons. Vehicle three is prepositioned in destination orbit. At the end of the mission, vehicle two remains in destination orbit, and vehicle three on an interplanetary trajectory.

Design Vector (4, 3, T, L, S, S, T)

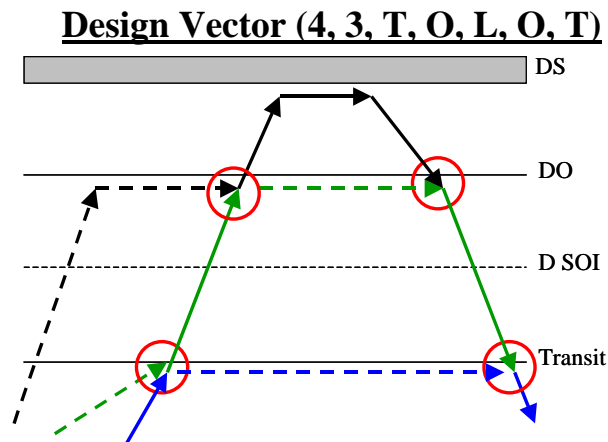


Architecture Description:

This architecture requires three vehicles and four crew transfers. It resembles the Apollo + surface habitat architecture. The crew departs Earth in vehicle one. Sometime before

arrival at the destination planet, the crew transfers to vehicle two, and accelerates towards the target planet by means of a propulsive maneuver. The crew lands in vehicle two, and then transfers to vehicle three, which serves as a surface habitat. At the end of the surface stay, the crew transfers back to vehicle two, ascends to orbit and performs the maneuver to intercept the transiting vehicle one. After successful interception, the crew transfers back to vehicle one and returns to the Earth.

Vehicle one and vehicle two set out together for safety reasons. Vehicle three is prepositioned on the destination surface. After completion of the mission, vehicle three remains on the destination surface, and vehicle two in an interplanetary transfer orbit.



Architecture Description:

This architecture requires three vehicles and four crew transfers. It resembles the Apollo architecture. The crew departs Earth in vehicle one. Sometime before arrival at the destination planet, the crew transfers to vehicle two, and accelerates towards the target planet by means of a propulsive maneuver. Vehicle two goes into destination orbit, where the crew transfers to vehicle three. Vehicle three is used for the landing, the surface stay, and the ascent to orbit. There, the crew transfers back to vehicle two, and performs the maneuver necessary to intercept the transiting vehicle one. After successful interception, the crew transfers to vehicle one and returns to Earth.

For safety reasons, vehicle one and two set out together. Vehicle three is prepositioned in destination orbit. At the end of the mission, vehicle two remains on an interplanetary trajectory, and vehicle three in destination orbit.

7.2 Appendix B: Δv Values, C_3 Energy, and Trip Times for Moon and Mars Transportation

Appendix B provides reference data on velocity changes, flight times, and C_3 energies for Moon and Mars transportation. These data were either taken from literature, or computed by using simplified analytical models. The basic approximation enabling simplified analytical calculation of trip times and velocity changes for planetary missions is the so-called patched-conics approximation.

7.2.1 The Patched-Conics Approximation

The Solar system consists of 10 major bodies (the sun, and the nine planets), as well as of many smaller bodies (asteroids, comets, moons of planets). A spacecraft that travels in the solar system therefore is subject to many different gravitational forces, as well as to atmospheric drag, solar radiation pressure, and, for very high velocities, also to relativistic effects. To calculate the exact trajectory, velocity changes and trip time, it is therefore necessary to solve a complex n-body-problem, which can only be solved analytically for $n < 3$ [Bate, Mueller, White, 1971]. For generalized trajectory analysis and mission design, numerical calculations are necessary. In the early mission design phases, however, the numerical analysis of every possible option would be prohibitively time-consuming. Therefore, the concept of patched conics was introduced, which reduces computation time, but still provides reliable first-order data on trip times and velocity changes [Bate, Mueller, White, 1971].

The concept of patched conics is best explained by analyzing a two-body system, where one body has a much bigger mass than the other (see Figure 7-1): $\text{Mass 2} / \text{Mass 1} \ll 1$. An example of this situation would be the Earth-Moon system ($\text{Mass 2} / \text{Mass 1} = 1 / 81.3$).

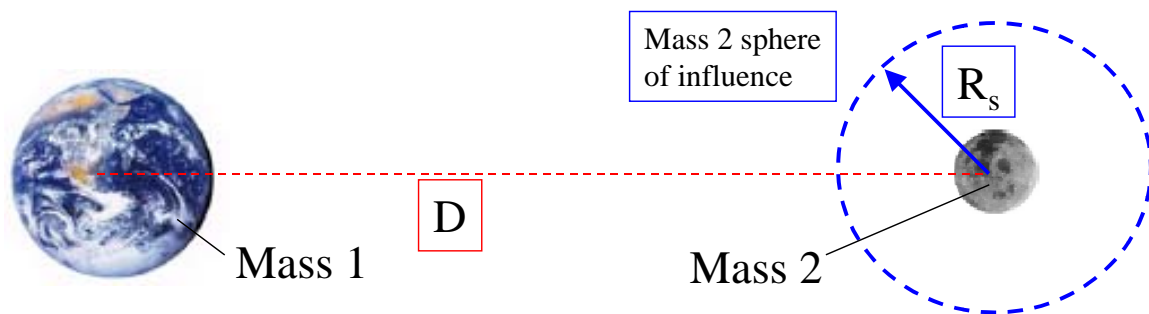


Figure 7-1: Illustration of the concept of the Sphere of Influence (SOI) in the Earth-Moon system

We now insert a third body into the system; the mass of the third body shall be negligible compared to mass 1 and mass 2 (this situation is called a restricted three-body-problem). The gravitational force acting on this body will be dominated by mass 1 for nearly all locations in the system, except when the small body comes very close to mass 2. It appears therefore that the gravitational influence of mass 2 dominates in a certain

contained region of space, which is called the Sphere of Influence (SOI) of mass 2 (see Figure 7-1). It is important to mention that, due to the relative motion of the masses and the characteristics of Newton's law of gravitation, the region is actually not a sphere, but an ellipsoid; it is, however, commonly approximated by a sphere [Bate, Mueller, White, 1971].

The radius of the sphere of influence is given by [Bate, Mueller, White, 1971]:

$$R_s = D \cdot \left(\frac{M_2}{M_1} \right)^{\frac{2}{5}} \quad \text{Equation 7-1}$$

For a detailed derivation of this equation please see [Bate, Mueller, White, 1971]. The sphere of influence of mass 1 is considered to be infinite in all directions. Table 7-7 provides an overview of the radii for the SOI of major solar-system bodies computed by using the above relationship:

Body	R_s [km]	R_s / D [%]	System
Moon	66163.4	17.21212	Earth-Moon
Mercury	112133.2	0.193667	Sun-Mercury
Venus	616477	0.569757	Sun-Venus
Earth	925035	0.618339	Sun-Earth
Mars	576653.5	0.252918	Sun-Mars
Jupiter	48239215	6.197227	Sun-Jupiter
Saturn	54531640	3.82544	Sun-Saturn
Uranus	51726868	1.802079	Sun-Uranus
Neptune	86847356	1.92947	Sun-Neptune
Pluto	3091271	0.052394	Sun-Pluto

Table 7-7: Radii of the SOI for solar system bodies

The radii shown in Table 7-7 are based on the semi-major axes of the orbit of the planet around its central body [Messerschmid, 1997]. As the orbits of the Moon, Mercury, Mars and Pluto have a significant eccentricity, the numbers should be considered as average values.

In the patched-conics models, the concept of spheres of influence is employed in the following way: the trajectory of a spacecraft in a multi-body force field is computed by determining what sphere of influence the craft is located in; this defines the central body. The trajectory of the craft is then treated as a two-body conic section relative to this central body. The characteristics of the conic section are determined by the initial conditions relative to the central body. If the spacecraft leaves the SOI of one body, and enters the SOI of a different one, then the latter becomes the new central body, etc. At the crossover-point, where the craft leaves one SOI and enters another, velocity and location are transformed from the old coordinate system to the new. At this point, the two conic sections relative to the two different central bodies are literally "patched" together; hence the name of the method.

For example, a spacecraft that travels from the Earth to Mars is inserted into a hyperbolic trajectory relative to an Earth-centered system. When the craft is crossing the Earth's SOI relative to the sun, its trajectory becomes an elliptical orbit around the

sun. When the craft is finally crossing the Martian SOI, it is on a hyperbolic trajectory relative to Mars. For a more in-depth treatment of patched conics, please refer to [Bate, Mueller, White, 1971].

Another important concept for the patched-conics approximation is the so-called C3-energy. Figure 7-2 illustrates the concept:

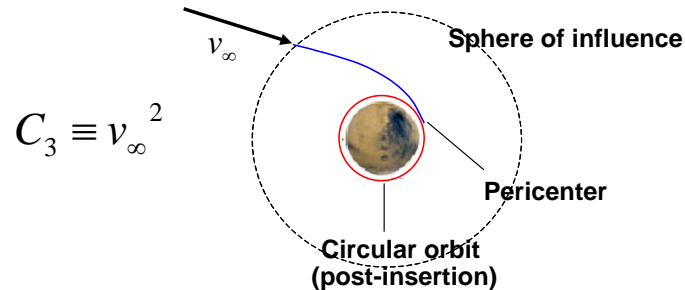


Figure 7-2: C_3 energy in the context of planetary arrival

The motion of a spacecraft inside the SOI of a central body is a classic example of a restricted two-body-problem: the mass of the central body is much bigger than the mass of the spacecraft; therefore, the presence of the spacecraft does not influence the central mass. In the restricted two-body-problem, a conservation law applies for the specific kinetic and potential energy e of the spacecraft relative to the central mass [Bate, Mueller, White, 1971]:

$$\frac{1}{2}v_1^2 - \frac{\mu_{cb}}{r_1} = \frac{1}{2}v_2^2 - \frac{\mu_{cb}}{r_2} = e \quad \text{Equation 7-2}$$

If the spacecraft is in an elliptical or circular orbit around the central body, e is negative. For parabolic trajectories, e is zero, and for hyperbolic trajectories, e is positive. In the restricted two-body-problem, the spacecraft can never fully escape the gravitational influence of the central body. In the patched-conics approximation, however, the influence of the central body vanishes when the spacecraft leaves the SOI. The C_3 energy is defined as the square of the hyperbolic excess velocity of the spacecraft when leaving the SOI see Figure 7-2. As the spacecraft is quite far from the central body when it crosses the SOI, its potential energy can be neglected. The C_3 energy then becomes a direct measure for e .

The reason for using C_3 energies to describe transfer trajectories instead of velocity changes for orbital insertion or injection maneuvers is that the latter always are valid only for a certain orbit around the target body. The C_3 energy provides information about the arrival conditions independently of the arrival orbit. For a given radius r of the circular insertion orbit around a planet, however, the velocity change necessary to brake into this orbit can be easily calculated from the C_3 energy using the vis-viva theorem [Messerschmid, 2000]:

$$\Delta v = \sqrt{C_3 + 2 \cdot \frac{\mu_{cb}}{r}} - \sqrt{\frac{\mu_{cb}}{r}} \quad \text{Equation 7-3}$$

Table 7-7 shows the radii of the spheres of influence for bodies of the solar system in absolute numbers, and also as a percentage of the mean distance between the dominating body and the minor body. It can be seen that for Earth and Mars (in fact, for all the inner planets) this relative radius is below 1 %. Under this condition, it is justified to neglect the radius of the SOI for approximate calculations of the interplanetary transfer trajectory: the trajectory starts on the Earth's orbit and ends in Mars orbit. This simplifies calculation of the interplanetary transfer trajectory significantly. This simplification assumes that the Earth and Mars are "switched on" gravitationally exactly when the spacecraft is on their orbits (in heliocentric coordinates). The Earth departure and Mars arrival C3 energies can then be determined by calculating the relative velocity vectors of planet and spacecraft at encounter on the planet's orbit.

7.2.2 Transportation in the Earth-Moon System

Reference data on trajectories and transportation in the Earth-Moon system has been published by various sources. Table 7-8 provides an overview of all the velocity changes and trip times used for the calculations in this in this thesis.

<u>Starting point</u>	<u>End point</u>	<u>Start exit velocity change [m/s]</u>	<u>End enter velocity change [m/s]</u>	<u>Trip time [d]</u>	<u>Source</u>
LEO (188 km)	LLO	3150	850	3.5	[Farquhar, 2003]
LLO (110 km)	LEO	850	(3150) Aerobraking	3.5	[Farquhar, 2003]
LEO	EM-L1	3100	750	3.5	[Farquhar, 2003]
EM-L1	LEO	750	(3100) Aerobraking	3.5	[Farquhar, 2003]
LEO	EM-L2	3150	350	9	[Farquhar, 2003]
EM-L2	LEO	350	(3150) Aerobraking	9	[Farquhar, 2003]
LEO	ES-L2	3230	900	15	[Farquhar, 2003]
ES-L2	LEO	900	(3230) Aerobraking	15	[Farquhar, 2003]
LEO	ES-L1	3230	900	15	[Farquhar, 2003]
ES-L1	LEO	900	(3230) Aerobraking	15	[Farquhar, 2003]
EM-L1	LLO	248	632	3.5	[NASA, 2002]
LLO	EM-L1	632	248	3.5	[NASA, 2002]
<u>Mission / Spacecraft</u>	<u>DV descent from 110 km LLO [m/s]</u>		<u>DV ascent to 110 km LLO [m/s]</u>	<u>Source</u>	
Apollo 11 LM	2083		1871	[NASA, 1969]	
NASA RLL	1897		1884	[NASA, 2002]	

Table 7-8: Reference data from literature on Earth-Moon transportation

In addition to the data presented in Table 7-8, velocity changes and trip times calculated were calculated using a patched-conics model.

For the Moon, the relative radius of the SOI is about 17 % (see Table 7-7). Though this is a significant fraction of the distance between the Moon and the Earth, we can neglect this radius for preliminary calculations of Moon arrival C3 and time of flight from LEO. The following calculations are based on the assumption that the Moon is "switched on" exactly when the spacecraft intersects the Moon's orbit.

The following is a brief description of the calculation process for the velocity changes and C3 energies. The nomenclature was taken from [Thomson, 1961].

The input parameters for the calculation are the perigee height and the perigee velocity at Earth. From these two, the specific angular momentum of the conic section relative to the Earth can be calculated:

$$h_t = v_p \cdot r_p \quad \text{Equation 7-4}$$

With this, and the gravitational parameter of the central body, the semi-major axis transfer ellipse can be computed:

$$a_t = \frac{1}{\frac{2}{r_p} - \frac{v_p^2}{\mu_E}} \quad \text{Equation 7-5}$$

With the semi-major axis, the eccentricity of the transfer ellipse is known:

$$\varepsilon_t = 1 - \frac{r_p}{a_t} \quad \text{Equation 7-6}$$

In order to determine the time of flight from perigee to the lunar encounter, we need to know the true anomaly of the spacecraft in the ellipse at the time of encounter:

$$\vartheta = \frac{a \cos\left(\frac{h_t^2}{\mu_E \cdot r_{Moon}}\right)}{\varepsilon_t} \quad \text{Equation 7-7}$$

The inertial velocity at encounter is needed for the calculation of the C₃ energy:

$$v = \sqrt{v_p^2 + 2 \cdot \mu_E \left(\frac{1}{r_{Moon}} - \frac{1}{r_p} \right)} \quad \text{Equation 7-8}$$

The flight path angle at encounter is:

$$\beta = a \cos\left(\sqrt{\frac{\mu_E \cdot (1 + \varepsilon \cdot \cos \vartheta)}{r_{Moon} \cdot v^2}}\right) \quad \text{Equation 7-9}$$

Mean orbital velocity of the Moon:

$$v_{Moon} = \sqrt{\frac{\mu_E}{r_{Moon}}} \quad \text{Equation 7-10}$$

The velocity relative to the Moon at encounter can be calculated using the cosine law:

$$v_{rel} = \sqrt{v^2 + v_{Moon}^2 - 2 \cdot v \cdot v_{Moon} \cdot \cos \beta} \quad \text{Equation 7-11}$$

C₃ energy relative to the Moon:

$$C_3 = v_{rel}^2 \quad \text{Equation 7-12}$$

The initial velocity change (initial orbit is circular) is determined by:

$$\Delta v_{EarthOrbit} = v_p - \sqrt{\frac{\mu_E}{r_p}} \quad \text{Equation 7-13}$$

Given the true anomaly at encounter, the transfer time from pericenter to encounter can be calculated by the following expression

:

$$\Delta t = \sqrt{\frac{a_t^3}{\mu_E}} \cdot \left(2 \cdot a \tan\left(\sqrt{\frac{1-\varepsilon}{1+\varepsilon}} \cdot \tan\left(\frac{\vartheta}{2}\right)\right) - \frac{\varepsilon \cdot \sqrt{1-\varepsilon^2} \cdot \sin \vartheta}{1+\varepsilon \cdot \cos \vartheta} \right) \quad \text{Equation 7-14}$$

Figure 7-3 shows the results of this computation as a function of the transfer time between the perigee at Earth and the lunar encounter. The results are for transfers in the Moon's orbital plane (coplanar transfers).

The ideal coplanar Hohmann transfer is at the right-hand end of the curves; it takes about five days to reach the Moon, and requires a velocity change in Earth orbit of slightly above 3100 m/s in LEO. The lunar arrival energy is about 0.7.

The 3.5-day transfer chosen for Apollo [NASA, 1969] also has a velocity change between 3100 and 3200 m/s in LEO, and a lunar arrival energy of about 0.9.

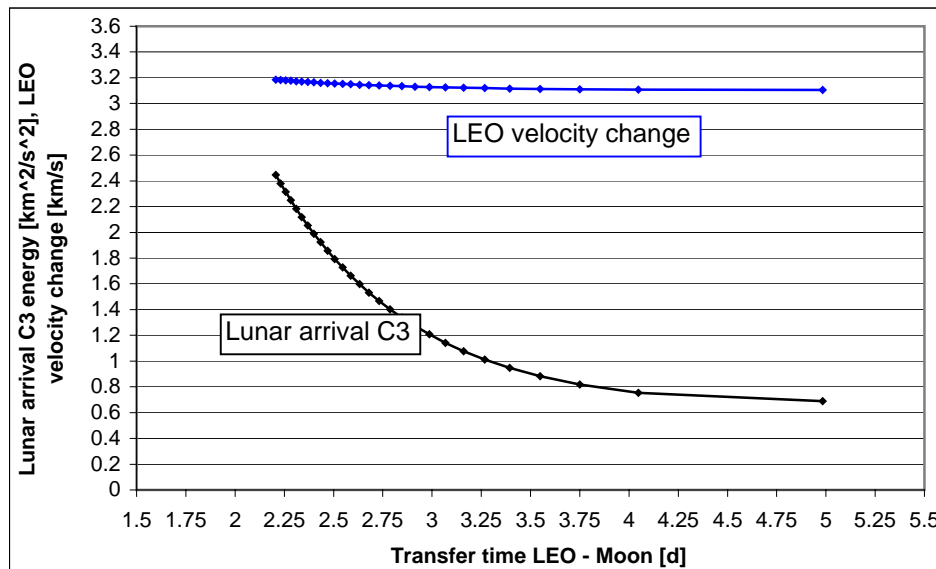


Figure 7-3: Lunar C_3 arrival energy and velocity change in Earth orbit as a function of the time of flight between perigee and Moon encounter

The lunar arrival C_3 can be converted into a velocity change to go into a circular LLO by means of the following equation:

$$\Delta v_{LunarOrbit} = \sqrt{C_3 + 2 \cdot \frac{\mu_{Moon}}{r_{LO}}} - \sqrt{\frac{\mu_{Moon}}{r_{LO}}} \quad \text{Equation 7-15}$$

Figure 7-4 provides a curve for the conversion of lunar arrival energy into velocity change in lunar orbit:

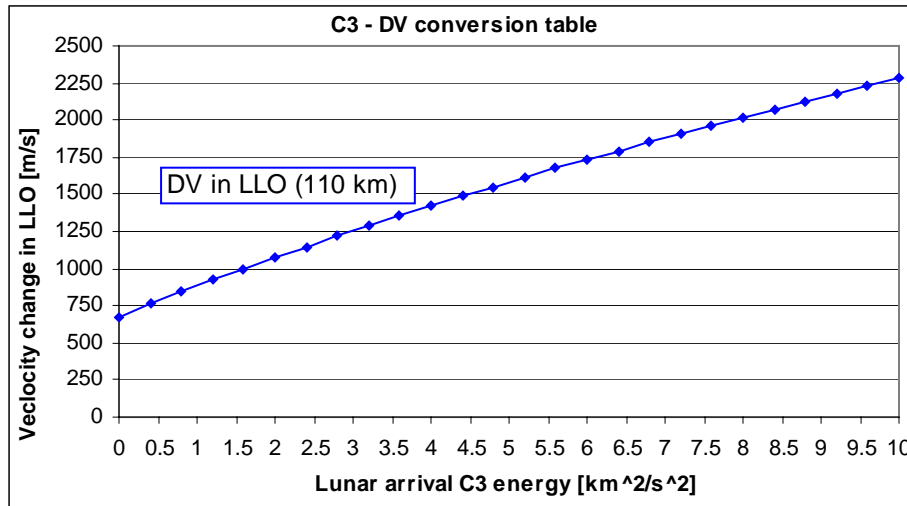


Figure 7-4: Lunar arrival energy to velocity change in LLO conversion table

Calculations using the above equation show that a lunar arrival energy of 0.9 corresponds to a velocity change in LLO of about 860 m/s. This is in very close agreement with the numbers proposed in Table 7-8, thereby proving that the patched conics analysis can be successfully used for the determination of time of flight and velocity changes.

So far, it was assumed that the transfer to the Moon takes place in the Moon's orbital plane; the velocity vector at encounter and the velocity vector of the Moon are located in the same plane. It is very probable, however, that the transfer does not take place in the Moon's orbital plane. For the case of a Hohmann-transfer, the impact of the transfer plane inclination relative to the Moon's orbital plane on the lunar arrival energy shall be investigated.

The lunar arrival energy can be computed by the cosine law; v is the velocity of the spacecraft at encounter, and i is the inclination of the transfer orbit plane (in an inertial system with its origin in the Earth) to the Moon's orbital plane [Bate, Mueller, White, 1971]. Please note: for a Hohmann transfer, the line of nodes for the transfer orbit and the radius vector from the Earth to the Moon are identical at the instant of lunar encounter. The arrival energy can be computed to be:

$$C_3 = \left(v^2 + v_{Moon}^2 - 2 \cdot v \cdot v_{Moon} \cdot \cos i \right) \quad \text{Equation 7-16}$$

The results for this analysis are displayed in Figure 7-5. It can be seen that there is a significant sensitivity of the lunar arrival energy to changes in the inclination. The highest arrival energy is encountered for an inclination of 180 degrees, i.e. when the transfer orbit is retrograde. This is intuitively clear, because in this case the velocity vectors of the spacecraft and the Moon at encounter are pointing in different directions, which causes a high relative velocity, and therefore a high arrival energy.

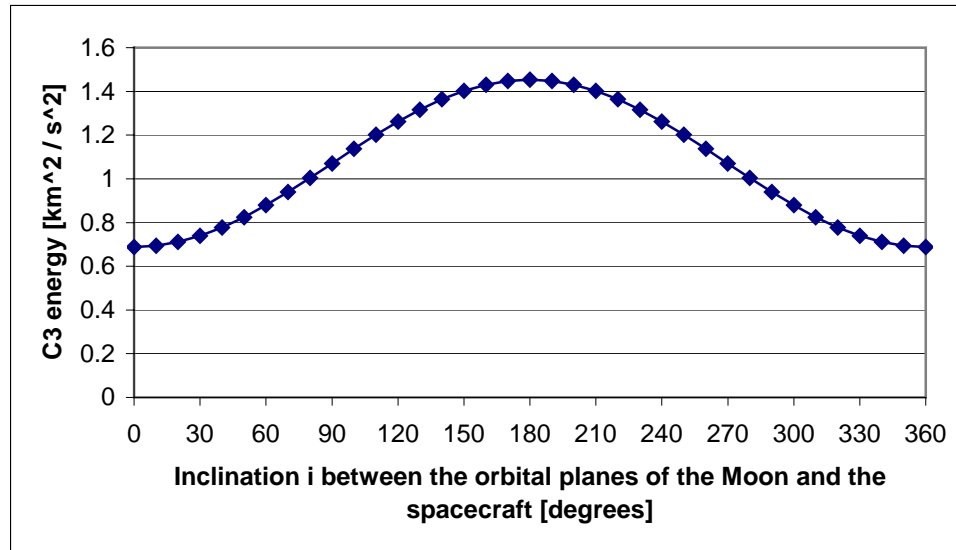


Figure 7-5: Lunar arrival energy as a function of the inclination of the transfer orbital plane to the Moon's orbital plane

7.2.3 Mars Transportation

In addition to the reference data from the literature [Walberg 1993] provided in Section 3.2, a patched conics analysis for transfers between Earth and Mars is described here. The analysis assumes coplanar travel between coplanar, circular Earth and Mars orbits. Especially for Mars, the orbit cannot be assumed to be circular for detailed trajectory calculations; for the validation of the numbers from literature, as well as for the investigation of special trajectory types, a simplified patched conics analysis seems to be appropriate.

The analysis is exactly identical to the one carried out above for transfer trajectories to the Moon. The pericenter of the interplanetary transfer trajectory is the departure point on the Earth's orbit at the beginning of the transfer. As the spacecraft is starting out from the Earth, it is more useful to provide a departure energy similar to the arrival energy at Mars for Earth (and vice versa for the return trajectories from Mars to Earth). This departure energy can be calculated in the following way:

$$C_{3,PlanetDeparture} = \left(v_{Pericenter} - \sqrt{\frac{\mu_{Sun}}{a_{Planet}}} \right)^2 \quad \text{Equation 7-17}$$

Also, it is desirable to know the heliocentric period of the interplanetary orbit, especially for trajectories from the Earth to Mars. The reason is that there are trajectories that have a heliocentric period of 1.5 and 2 years, i.e. they reencounter the Earth after 2 and 1 revolutions (3 and 2 years). These trajectories could be used as free-return trajectories similar to those employed on Apollo. No major maneuvers would be required to return to Earth:

$$P_{\text{InterplanetaryTransferOrbit}} = 2 \cdot \pi \cdot \sqrt{\frac{a_{\text{InterplanetaryTransferOrbit}}^3}{\mu_{\text{Sun}}}} \quad \text{Equation 7-18}$$

The following Figures 7-6 to 7-7 provide the results of the patched conics analysis for Earth-Mars and Mars-Earth transfers. Shown are the departure and arrival energies, as well as the heliocentric orbital periods in months.

It can be seen that there are Earth-Mars trajectories that have an orbital period of 24 months, i.e. 2 years. These trajectories could be used as free-return trajectories; in case of an emergency, they bring the crew directly back to Earth. The Earth departure energy is about 25 as opposed to about 10 for the Hohmann-transfer. As the departure energy is a metric that contains velocity squared, the actual increase in velocity change is quite small (see energy – velocity conversion table in Figure 7-8). The arrival energy at Mars, however, is significantly (one order of magnitude) higher than for the Hohmann-transfer.

Apart from the Hohmann-transfer and the free-return, other interesting trajectories can be identified in Figures 7-6 and 7-7: for crew health reasons, interplanetary transfers could be limited to 180 days. This introduces the so-called “fast-conjunction class” missions that have higher propulsive requirements than Hohmann-missions, but limit the interplanetary transfer times.

Table 7-9 provides reference data for the three mission types used for the trade analysis and the baseline design in Sections 3.3 and 3.4; these values were generated with the patched conics model.

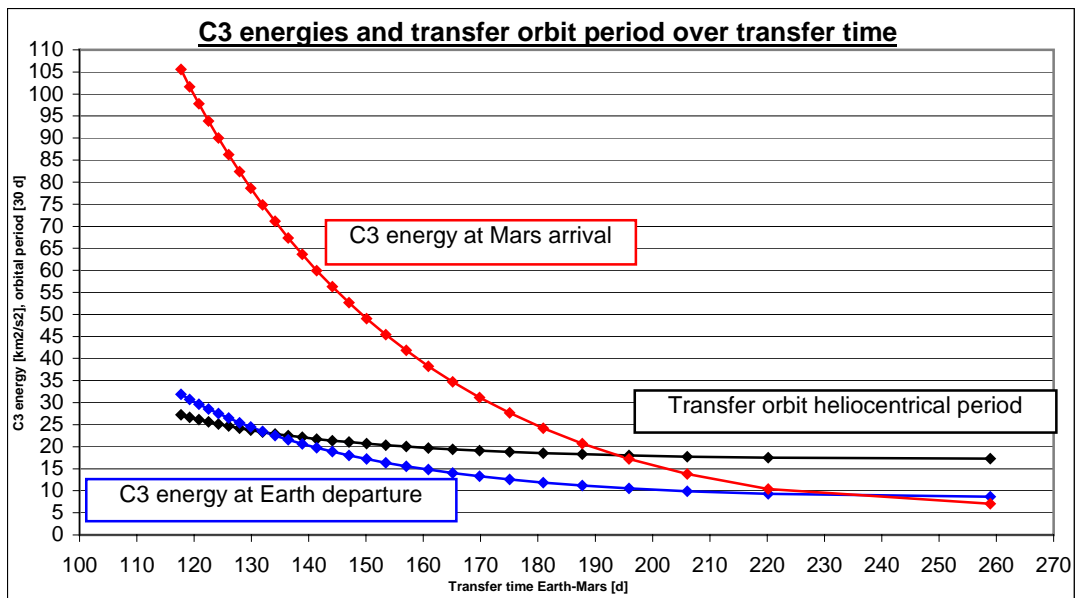


Figure 7-6: Departure and arrival energies, as well as heliocentric orbital periods for Earth-Mars transfers as a function of transfer time

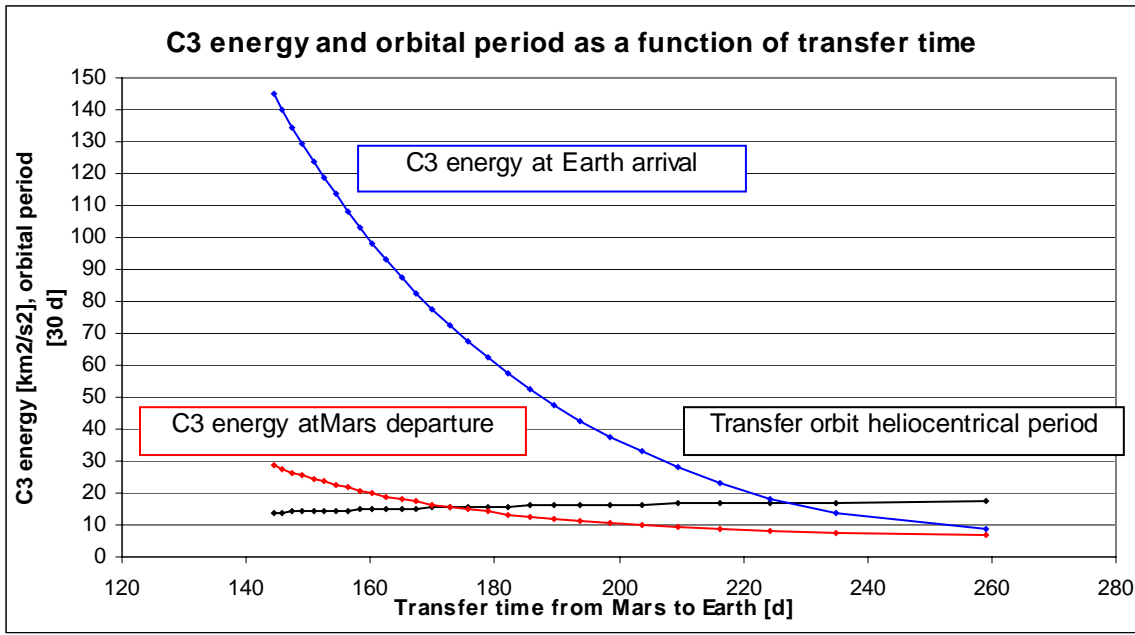


Figure 7-7: Departure and arrival energies, as well as heliocentric orbital periods for Mars-Earth transfers as a function of transfer time

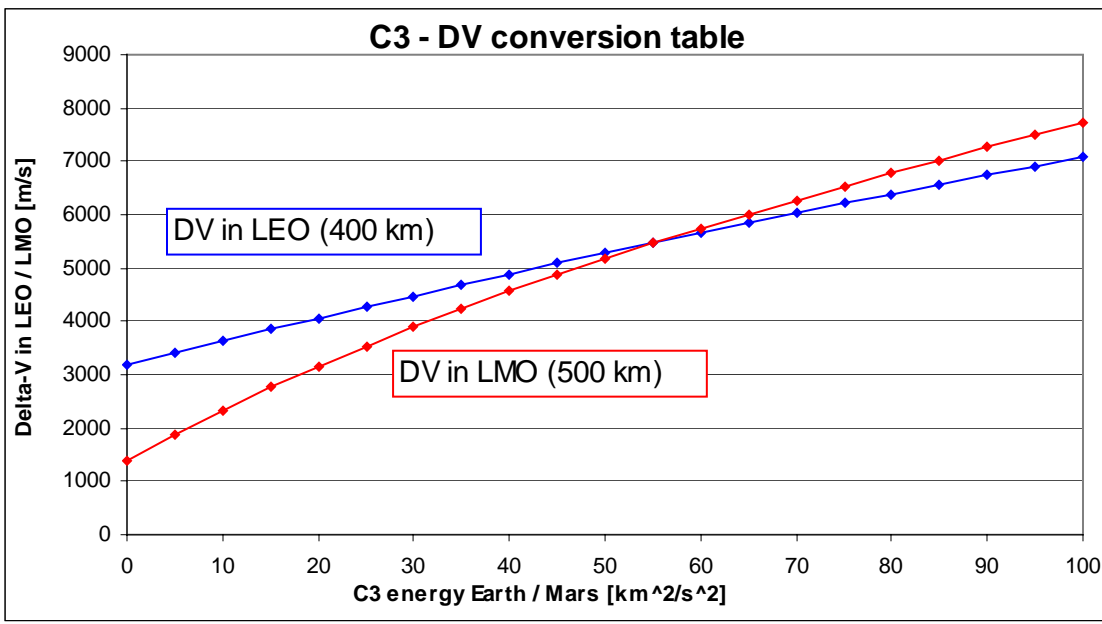


Figure 7-8: Departure / arrival energy to velocity change conversion table for Mars and Earth

Standard Hohmann Mission (ideal)	
Trans-Mars insertion velocity change	3600 m/s
Earth-Mars transit duration	260 d
Velocity change for Mars orbit insertion	2115 m/s
Mars surface stay	500 d
Trans-Earth insertion velocity change	2115 m/s
Earth Entry velocity	11215 m/s
Mars Earth transit duration	260 d
Total duration	1020 d
Fast Conjunction-Class Mars Mission	
Trans-Mars insertion velocity change	3714 m/s
Earth-Mars transit duration	180 d
Velocity change for Mars orbit insertion	3465 m/s
Mars surface stay	660 d
Trans-Earth insertion velocity change	2600 m/s
Earth Entry velocity	Up to 16000 m/s
Mars Earth transit duration	180 d
Total duration	1020 d
Conjunction Class Mars Mission with Free-Return	
Trans-Mars insertion velocity change	4272 m/s
Earth-Mars transit duration	130 d
Velocity change for Mars orbit insertion	6782 m/s
Mars surface stay	710 d
Trans-Earth insertion velocity change	2600 m/s
Earth Entry velocity	16000 m/s
Mars Earth transit duration	180 d
Total duration	1020 d
Descent / Ascent velocity changes	
Mars descent, after aeroentry and parachute	625 m/s
Mars ascent to 500 km circular LMO	4000 m/s

Table 7-9: Three reference conjunction class Mars missions, as well as for Mars descent and ascent, used for trade studies and baseline architectures in Sections 3.3 and 3.4

7.3 Appendix C: Point Design Architecture Data

In Appendix C, the computational methods and results for the point design architectures investigated in Chapter 3 are documented. Section 7.3.1 is focused on the conceptual architecture evaluation carried out in Section 3.2. Subsection 7.3.2 provides reference data on the baseline architectures that incorporate the design options updated and enhanced through trade analysis in Section 3.3, i.e. the upgrading from preferred architectures to baseline architectures.

7.3.1 Architecture Results for In-Situ Propellant Production (ISPP)

As the results for architectures without the use of ISPP have been documented in Section 3.2, only results for architectures employing ISPP are given here. It is assumed that the propellant used by the spacecraft that lifts off the Moon or Mars “appears” on the surface, and can be used. This case represents “best-case” ISPP without any additional equipment mass that needs to be transported to the surface, and without any mass for the fuel transfer interface. The following model was used for the conceptual architecture evaluation in Section 3.2:

- The crew compartment / habitat masses were determined using the empirical equations from Subsection 2.2.1.
- The structure and engine mass for the propulsion stages was assumed to be 15 % of the propellant mass of the stage [Larson, Pranke, 2004]:

$$m_{Structure,Engine} = 0.15 \cdot m_{Propellant} \quad \text{Equation 7-19}$$

- The heat shield mass was assumed to be proportional to the shielded / protected mass (20 % for Earth entry, 15 % for Mars aerocapture and entry):

$$m_{HeatShield,Mars} = 0.15 \cdot m_{Protected} \quad \text{Equation 7-20}$$

$$m_{HeatShield,Earth} = 0.2 \cdot m_{Protected} \quad \text{Equation 7-21}$$

- The masses for parachutes and landing legs were neglected, because they are low (see Section 2.2), and would require an iterative calculation process, as opposed to the analytical one chosen here.
- Trajectory data from Tables 3-1 to 3-3 were used as a source for velocity changes and for the durations of the various mission phases. The assumptions stated in Table 3-4 apply to all Moon and Mars architecture calculations.

The specific impulse for liquid methane / liquid oxygen propellant was assumed to be 394 s [Hoffman, Kaplan, 1997], and the specific impulse for liquid hydrogen / liquid oxygen to be 450 s [Messerschmid, 2000]. The 14 architectures investigated are described qualitatively in Appendix A, Section 7.1. The information provided here and in Section 2.2 permits the duplication of the results presented. The calculation process is based on the conceptual spacecraft design approach outlined in Chapter 12 of [Larson, Pranke, 2000]. With this model, the results in Figures 3-6 to 3-13 and Figures 7-9 and 7-10 (below) were generated: Figure 7-9 shows IMLEO results for a Mars mission with free-return for the case of ‘ideal’ ISPP. The relative ranking of the architectures is significantly different from the one without ISPP. Especially the one-vehicle architecture and the ‘Mars direct’ architecture are now very attractive.

The results for lunar architectures employing ‘ideal’ ISPP (see Figure 7-10) show that the differences between the architectures are more or less evened out; this is also an interesting observation, potentially of relevance for the selection of a transportation architecture for a lunar base. A comprehensive assessment of architecture extensibility is, however, beyond the scope of this thesis. In Figure 7-9 it can be seen that for the NASA Mars DRM and related architectures (“Blend”, Apollo + surface habitat) the use of ISPP has only a small influence on the overall mission mass. This is due to the fact that in all three architectures only the fuel for the ascent into Mars orbit of a small capsule is provided by ISPP, whereas for architectures like “Mars Direct”, large habitats are propelled with ISPP generated fuel, and a large mass saving is achieved.

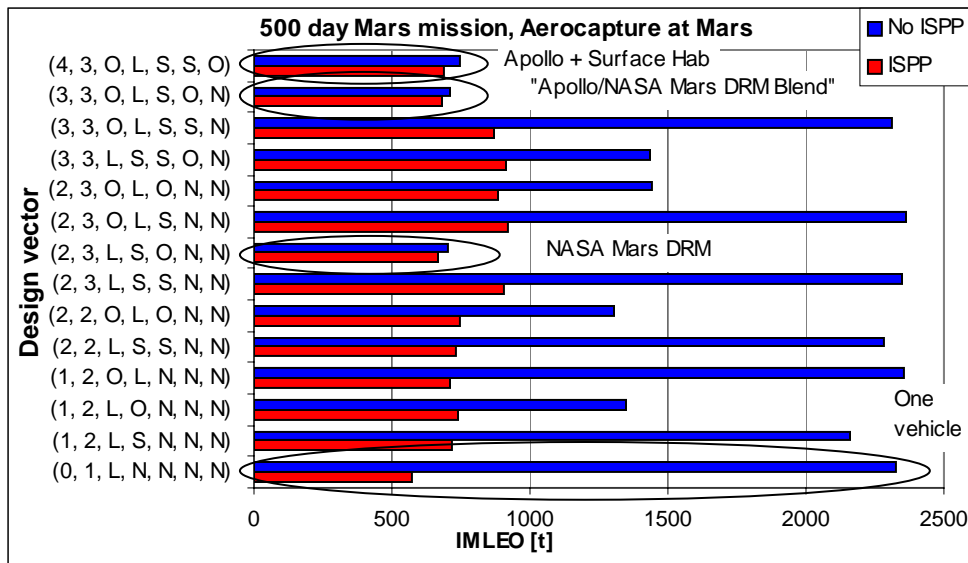


Figure 7-9: Architecture IMLEO requirements for a fast conjunction class mission with free-return for the case of ‘ideal’ ISPP

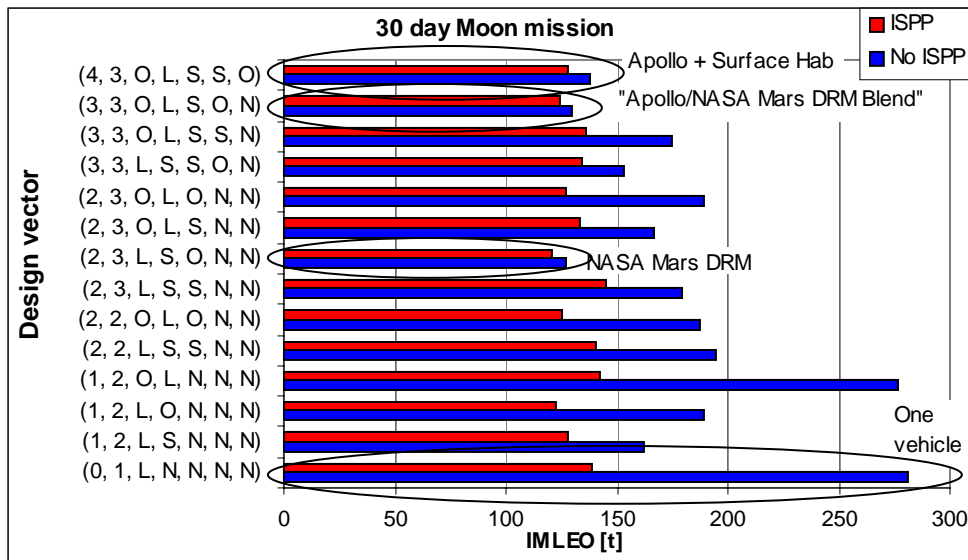


Figure 7-10: Architecture IMLEO requirements for a 30-day lunar landing mission for the case of ‘ideal’ ISPP

7.3.2 Baseline point design Moon and Mars architectures

In this section, reference data for the spacecraft used in the reference architectures are documented. The computational model used to produce these results is somewhat different from the one employed in the previous section, and in Section 3.2. Therefore, a brief description of the calculations is given here, in order to enable the reader to carry out similar computations with different initial conditions.

- The mass of crew compartments was calculated, as in the preceding section, with the empirical equations from Subsection 2.2.1; the masses are a function of the crew size, the amount of time spent in the habitat, the pressurized volume required, and, for flights over 200 days, the resupply factor. The two equations are provided here:

$$m_{CrewCompartment}(\Delta t_{Mission} < 200d) = 592kg \cdot (N_{Crew} \cdot \Delta t_{Mission} \cdot V_{Pressurized})^{0.346} \quad \text{Equation 7-22}$$

$$m_{CrewCompartment}(\Delta t_{Mission} > 200d) = m_{CC}(200days) + (\Delta t_{Mission} - 200d) \cdot N_{Crew} \cdot 9,5 \frac{kg}{d} \cdot \alpha \cdot \eta \quad \text{Equation 7-23}$$

- Heat shields were modeled as above, as constant mass fractions of the mass shielded:

$$m_{HeatShield,Mars} = 0.15 \cdot m_{Protected} \quad \text{Equation 7-24}$$

$$m_{HeatShield,Earth} = 0.2 \cdot m_{Protected} \quad \text{Equation 7-25}$$

- Given the spacecraft mass at the beginning of a maneuver, as well as the initial thrust-to-weight ratio, the thrust required for the burn can be determined. With known thrust, the engine mass (in kg) can be calculated using the following equation from Chapter 2.2.1:

$$m_{Engine} = \left(\frac{T_{max}}{g_0} \right) 0.4189 \cdot (T_{max} [N])^{-0.2236} \quad \text{Equation 7-26}$$

- The structural mass of a propulsion stage (without the engine) is assumed to be 11.3 % of the propellant mass contained in the stage.
- The parachute mass (for Mars landings) is assumed to be 1 % of the suspended mass.
- The landing gear mass is assumed to be a constant fraction of the landed mass (3 % for the Moon, and 7 % for Mars, see Subsection 2.2.1). The landed mass consists of the spacecraft mass before landing minus the descent propellant mass, and also includes the landing gear mass.
- The coupling of the engine mass with the thrust and the initial weight, which is in turn dependent on the engine weight, necessitates iterative, i.e. numerical solution of the calculations for the propulsion stage mass.
- The specific impulse of the propulsion systems is identical to that in the preceding section.

The model outlined here is described in more detail in Subsection 2.2.1. It was validated and benchmarked with data from various spacecraft, including the Apollo LM.

The following Tables 7-10 to 7-13 provide reference data for the baseline architectures, including all the inputs and outputs of the model described above:

<u>Vehicle</u>	<u>Lander / Ascender</u>	<u>Orbiter / CEV</u>	<u>14-day surface habitat lander</u>
Crew size, Duration	3, 5 d	3, 9 d	3, 14 d
Pressurized volume [m ³]	12.32	21.69	32.80
Crew Compartment mass [kg]	3602	5369	7219
Heat shield mass [kg]	-	1122	-
Total crew compartment [kg]	3602	6491	7219
Propellant combination	LCH4 / LOX	LCH4 / LOX	LCH4 / LOX
Initial Thrust / Weight [-]	0.4	0.3	0.4
Engine Thrust [N]	57565	31461	74458
Velocity change [m/s]	3954	1500	2933
Tank / Structure mass [kg]	1062	388	1140
Engine Mass [kg]	212	133	258
Propellant mass [kg]	9396	3438	10010
Mass landing gear [kg]	158	-	266
Total mass propulsion stage [kg]	10828	3959	11674
Sum of total masses [kg]	14430	10450	18975
Propellant combination	LCH4 / LOX	LCH4 / LOX	-
Initial Thrust / Weight [-]	0.3		-
Engine Thrust [N]	95934		-
Velocity change [m/s]	850		-
Tank / Structure mass [kg]	727		-
Engine Mass [kg]	315		-
Propellant mass [kg]	6435		-
Total mass propulsion stage [kg]	7477		-
Sum of total masses [kg]	32357		18975
Propellant combination	LH2 / LOX		LH2 / LOX
Initial Thrust / Weight [-]	0.3		0.3
Engine Thrust [N]	145967		85115
Velocity change [m/s]	1575		1575
Tank / Structure mass [kg]	1681		980
Engine Mass [kg]	436		287
Propellant mass [kg]	14883		8678
Total mass propulsion stage [kg]	17000		9945
Sum of total masses [kg]	49357		28920
Propellant combination	LH2 / LOX		LH2 / LOX
Initial Thrust / Weight [-]	0.3		0.3
Engine Thrust [N]	221827		129549
Velocity change [m/s]	1575		1575
Tank / Structure mass [kg]	2555		1492
Engine Mass [kg]	604		397
Propellant mass [kg]	22617		13209
Total mass propulsion stage [kg]	25776		15098
Sum of total masses [kg]	75133		44018
Total architecture mass [kg]	119151		

Table 7-10: Reference data for the 3-day lunar lander and orbiter, and for the 14-day surface habitat

<u>Vehicle</u>	<u>30-day surface habitat lander</u>	<u>180-day surface habitat lander</u>
Crew size	3, 30 d	3, 180 d
Pressurized volume [m ³]	64.24	168.89
Crew Compartment mass [kg]	11858	30794
Heat shield mass [kg]	-	-
Total crew compartment [kg]	11858	30794
Propellant combination	LCH4 / LOX	LCH4 / LOX
Initial Thrust / Weight [-]	0.4	0.4
Engine Thrust [N]	121850	314528
Velocity change [m/s]	2933	2933
Tank / Structure mass [kg]	1866	4817
Engine Mass [kg]	379	792
Propellant mass [kg]	16513	42625
Mass landing gear [kg]	436	1125
Total mass propulsion stage [kg]	19194	49359
Sum of total masses [kg]	31052	80155
Propellant combination	LH2 / LOX	LH2 / LOX
Initial Thrust / Weight [-]	0.3	0.3
Engine Thrust [N]	139069	358059
Velocity change [m/s]	1575	1575
Tank / Structure mass [kg]	1602	4125
Engine Mass [kg]	420	876
Propellant mass [kg]	14179	36508
Total mass propulsion stage [kg]	16201	41059
Sum of total masses [kg]	47253	121664
Propellant combination	LH2 / LOX	LH2 / LOX
Initial Thrust / Weight [-]	0.3	0.3
Engine Thrust [N]	211372	542955
Velocity change [m/s]	1575	1575
Tank / Structure mass [kg]	2435	6255
Engine Mass [kg]	581	1210
Propellant mass [kg]	21551	55360
Total mass propulsion stage [kg]	24567	62825
Sum of total masses [kg]	71820	184489
Total architecture mass [kg]	146953	259622

Table 7-11: Reference data for the 30-day, and 180-day surface habitats

<u>Vehicle</u>	<u>CEV</u>	<u>Interplanetary Transfer Habitat</u>	<u>Mars Ascent Vehicle</u>	<u>Mars Landing & Surface Habitat</u>
Crew size	6, 4 d	6, 730 d	6, 2.5 d	6, 660 d
Pressurized volume [m ³]	19.82	342	12.49	342
Crew Compartment mass [kg]	4996	61486	3619	61121
Heat shield mass [kg]	999	-	-	-
Total crew compartment [kg]	5995	61486	3619	61121
Sum of total masses [kg]	67481		3619	61121
Propellant combination	LCH4 / LOX		LCH4 / LOX	LCH4 / LOX
Initial Thrust / Weight [-]	0.3		0.6	0.5
Engine Thrust [N]	443154		91775	396225
Velocity change [m/s]	2600		4000	625
Tank / Structure mass [kg]	8331		1135	1362
Engine Mass [kg]	1033		304	947
Propellant mass [kg]	73732		10052	12060
Mass landing gear [kg]	-		-	4810
Total mass propulsion stage [kg]	83096		11491	19179
Sum of total masses [kg]	150577		15110	80300
Propellant combination	-		LCH4 / LOX	-
Initial Thrust / Weight [-]	-		0.5	-
Engine Thrust [N]	-		97740	-
Velocity change [m/s]	-		625	-
Tank / Structure mass [kg]	-		336	-
Engine Mass [kg]	-		319	-
Propellant mass [kg]	-		2975	-
Mass landing gear [kg]	-		1186	-
Total mass propulsion stage [kg]	-		4816	-
Parachute Mass [kg]	1505		199	803
Heat shield mass [kg]	22812		3018	12165
Sum of total masses [kg]	174894		23143	93268
Propellant combination	LH2 / LOX		LH2 / LOX	LH2 / LOX
Initial Thrust / Weight [-]	0.3		0.3	0.3
Engine Thrust [N]	910936		110221	442407
Velocity change [m/s]	2150		1800	1800
Tank / Structure mass [kg]	13485		1417	5688
Engine Mass [kg]	1808		350	1032
Propellant mass [kg]	119338		12540	50336
Total mass propulsion stage [kg]	134631		14307	57056
Sum of total masses [kg]	309525		37450	150324
Propellant combination	LH2 / LOX		LH2 / LOX	LH2 / LOX
Initial Thrust / Weight [-]	0.3		0.3	0.3
Engine Thrust [N]	1610172		178084	712250
Velocity change [m/s]	2150		1800	1800
Tank / Structure mass [kg]	23836		2289	9157
Engine Mass [kg]	2814		509	1494
Propellant mass [kg]	210943		20262	81039
Total mass propulsion stage [kg]	237593		23060	91690
Sum of total masses [kg]	547118		60510	242014
Total architecture mass [kg]	849642			

Table 7-12: Reference data for a fast-conjunction class Mars mission with free return (see Appendix B, Section 3.3)

<u>Vehicle</u>	<u>CEV</u>	<u>Interplanetary Transfer Habitat</u>	<u>Mars Ascent Vehicle</u>	<u>Mars Landing & Surface Habitat</u>
Crew size	6, 4 d	6, 470.5 d	6, 2.5 d	6, 62.5 d
Pressurized volume [m ³]	19.82	342	12.49	222.70
Crew Compartment mass [kg]	4996	56753	3619	29870
Heat shield mass [kg]	999	-	-	-
Total crew compartment [kg]	5995	56753	3619	29870
Sum of total masses [kg]	62748		3619	29870
Propellant combination	LCH4 / LOX		LCH4 / LOX	LCH4 / LOX
Initial Thrust / Weight [-]	0.3		0.6	0.5
Engine Thrust [N]	367479		91775	195728
Velocity change [m/s]	2221		4000	625
Tank / Structure mass [kg]	6167		1135	673
Engine Mass [kg]	893		304	548
Propellant mass [kg]	54576		10052	5957
Mass landing gear [kg]	-		-	2376
Total mass propulsion stage [kg]	61636		11491	9554
Sum of total masses [kg]	124384		15110	39424
Propellant combination	LCH4 / LOX		LCH4 / LOX	-
Initial Thrust / Weight [-]	0.3		0.5	-
Engine Thrust [N]	724265		97740	-
Velocity change [m/s]	2221		625	-
Tank / Structure mass [kg]	12154		336	-
Engine Mass [kg]	1513		319	-
Propellant mass [kg]	107565		2975	-
Mass landing gear [kg]	-		1186	-
Total mass propulsion stage [kg]	121232		4816	-
Parachute Mass [kg]	2456		199	394
Heat shield mass [kg]	37210		3018	5972
Sum of total masses [kg]	285282		23143	45790
Propellant combination	LH2 / LOX		LH2 / LOX	LH2 / LOX
Initial Thrust / Weight [-]	0.3		0.3	0.3
Engine Thrust [N]	1613227		110221	217614
Velocity change [m/s]	2446.5		1800	1800
Tank / Structure mass [kg]	26354		1417	2797
Engine Mass [kg]	2819		350	595
Propellant mass [kg]	233222		12540	24760
Total mass propulsion stage [kg]	262395		14307	28152
Sum of total masses [kg]	547677		37450	73942
Propellant combination	LH2 / LOX		LH2 / LOX	LH2 / LOX
Initial Thrust / Weight [-]	0.3		0.3	0.3
Engine Thrust [N]	3090416		178084	350942
Velocity change [m/s]	2446.5		1800	1800
Tank / Structure mass [kg]	50485		2289	4512
Engine Mass [kg]	4669		509	862
Propellant mass [kg]	446778		20262	39930
Total mass propulsion stage [kg]	501932		23060	45304
Sum of total masses [kg]	1049609		60510	119246
Total architecture mass [kg]	1229365			

Table 7-13 Reference data for a 60-day short Mars mission with a Venus-flyby on the way back to Earth (see Section 3.3)

7.4 Appendix D: Vehicle Propulsion Stages with Equal Tank Sizes (i.e. Propellant Masses)

7.4.1 Two Approaches to the Modeling of Propulsion Stages

For the conceptual design of manned spacecraft that carry out maneuvers with significant velocity changes, a compact model for the structural mass of a propulsion stage is desirable for the analysis of the architectural trade space. Two approaches have been proposed in literature. The first assumes that the structural mass of a propulsion stage is a constant fraction (about 10 %, [Messerschmid, 2000]) of the total vehicle mass, i.e. of the fully fueled propulsion stage in use plus all the other propulsion stages used later, and the payload mass.

$$m_{Structure} = \beta \cdot m_{Stage} = \beta \cdot (m_{Payload} + m_{Propellant} + m_{Structure})$$

Please refer to [Messerschmid, 2000] for a detailed discussion of the model.

The second approach assumes that the structural mass is a constant fraction of the propellant mass contained in the propulsion stage:

$$m_{Structure} = \alpha \cdot m_{Propellant} \quad \text{Equation 7-27}$$

The structural mass is independent of the payload mass, i.e. the mass that is mounted to the propulsion stage and accelerated during the burn [Larson, Pranke, 2000].

Figure 7-11 shows the payload mass fraction for both approaches as a function of the number of stages. The total velocity change is 10000 m/s, and the specific impulse of the propulsion system is 394 s. The proportional constants are assumed to be 10 % and 15 % for approach one and two. It is assumed that the propulsion stages are burned sequentially. Please note: the subjects of this analysis are not the absolute mass fractions, but the nature of the curves presented in Figure 7-11.

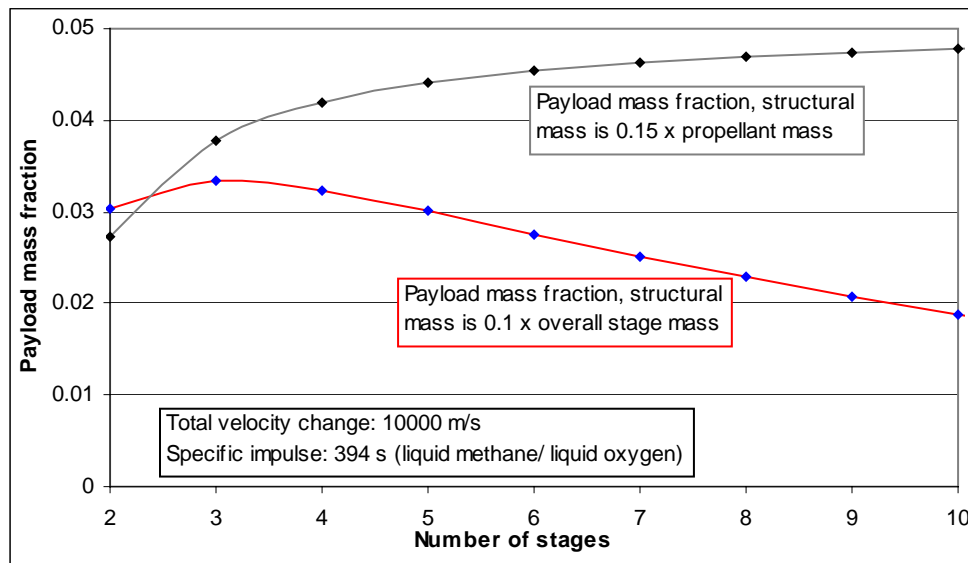


Figure 7-11: Qualitative comparison of the two modeling approaches

Both approaches yield qualitatively very different results: the curve for approach one shows a maximum of the payload mass fraction for a stage number of three. This indicates that there is an optimum stage number for carrying out the maneuver, and that this stage number is actually comparatively low for maneuvers commonly considered for launch and in-space operations. Approach two shows a different trend: the payload mass fraction increases with the number of stages. Every additional stage provides an increase in the payload mass fraction, albeit a decreasing one.

Approach one is commonly used for launch vehicles (see [Messerschmid 2000]); this explains why there has never been a launch vehicle with over four stages.

Approach two is suggested for in-space propulsion for manned spacecraft, and shall therefore be used in this thesis [Larson, Pranke, 2000].

7.4.2 Vehicles with Two Identical Propulsion Stages

Vehicles with several propulsion stages are usually designed to maximize payload mass (or minimize initial mass for a given payload mass). This can be achieved by assigning each propulsion stage the same velocity change [Thomson, 1961]. This, however, yields three completely different propulsion stage designs, because each stage has to carry a different payload.

In the context of extensible design, it is desirable to achieve a high degree of commonality. This can be achieved by designing the propulsion stages to have the same amount of propellant, i.e. to be the same. As the propulsion stages have the same propellant mass, and therefore also structural mass, each provides now a different velocity change, because the payload mass is different. In order to design the common stage for a given propellant combination, the distribution of velocity changes to the stages has to be known. The distribution is a function of the total velocity change, and of the specific impulse.

Figures 7-12 to 7-17 show the distribution of velocity changes and the payload mass fraction as a function of the total velocity change required for three propellant combinations: liquid methane / liquid oxygen (specific impulse 394 s); liquid hydrogen / liquid oxygen (specific impulse 450 s); and the hypergolic propellants used in the Apollo system (specific impulse 311 s). The results are for a vehicle with payload and two propulsion stages.

From the figures, it can be seen that the velocity changes per stage are a non-linear function of the total velocity change required for the vehicle.

In the diagrams for the payload mass fraction, the optimal payload mass fraction for propulsion stages with equal velocity changes is shown for reference. It is noticeable that the payload mass fraction for propulsion stage commonality only shows significant deviations from the optimum for velocity changes in excess of 10000 m/s. The deviations are most significant for hypergolic propellants, i.e. low specific impulse. This indicates that for high specific impulse propulsion, stage commonality is an interesting way to reduce development cost.

The data shown here were calculated numerically using the conceptual model described in Subsection 7.3.1. The approach can be generalized to systems with an arbitrary number of stages.

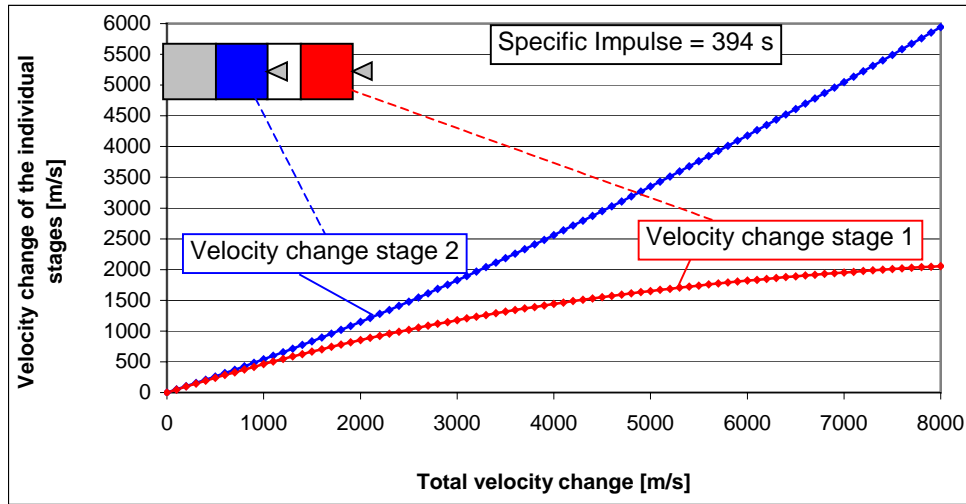


Figure 7-12: Velocity changes for two sequentially used propulsion stages with equal propellant masses (sizes) as a function of the total velocity change (for liquid methane / liquid oxygen propulsion)

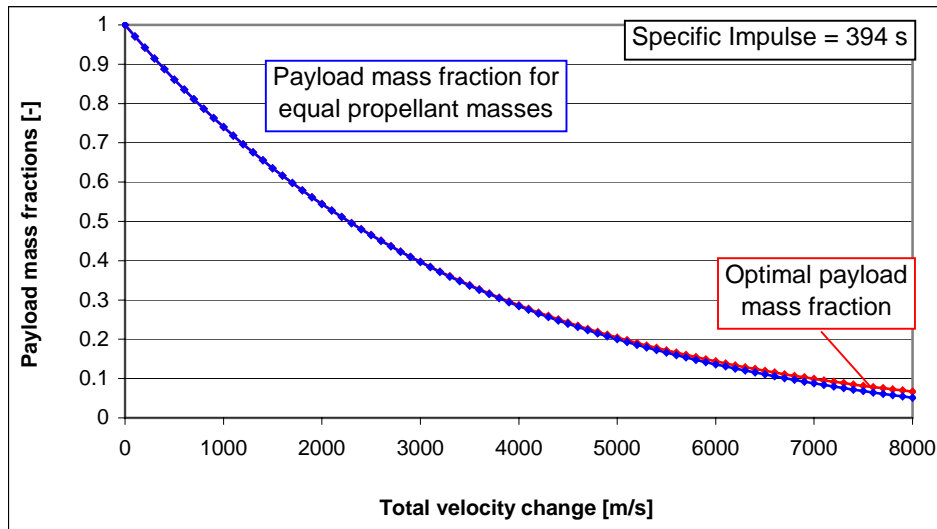


Figure 7-13: Payload mass fraction for two sequentially used propulsion stages with equal propellant masses (sizes) as a function of the total velocity change (for liquid methane / liquid oxygen propulsion) compared to the optimal payload fraction (equal velocity changes)

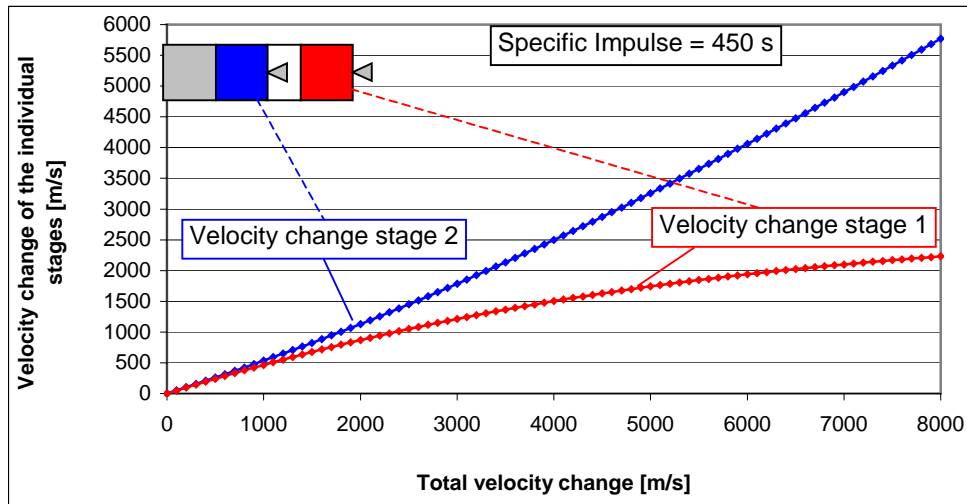


Figure 7-14 Velocity changes for two sequentially used propulsion stages with equal propellant masses (sizes) as a function of the total velocity change (for liquid hydrogen / liquid oxygen propulsion)

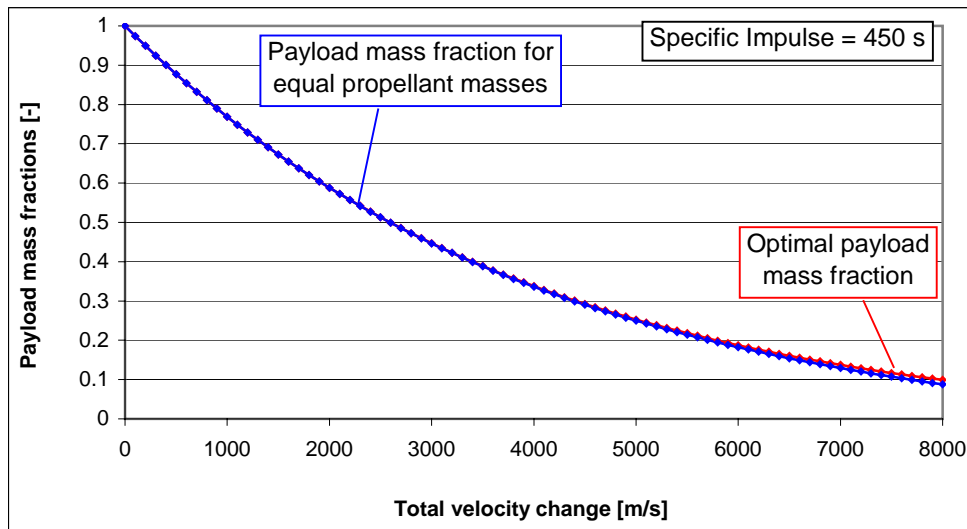


Figure 7-15: Payload mass fraction for two sequentially used propulsion stages with equal propellant masses (sizes) as a function of the total velocity change (for liquid hydrogen / liquid oxygen propulsion) compared to the optimal payload fraction (equal velocity changes)

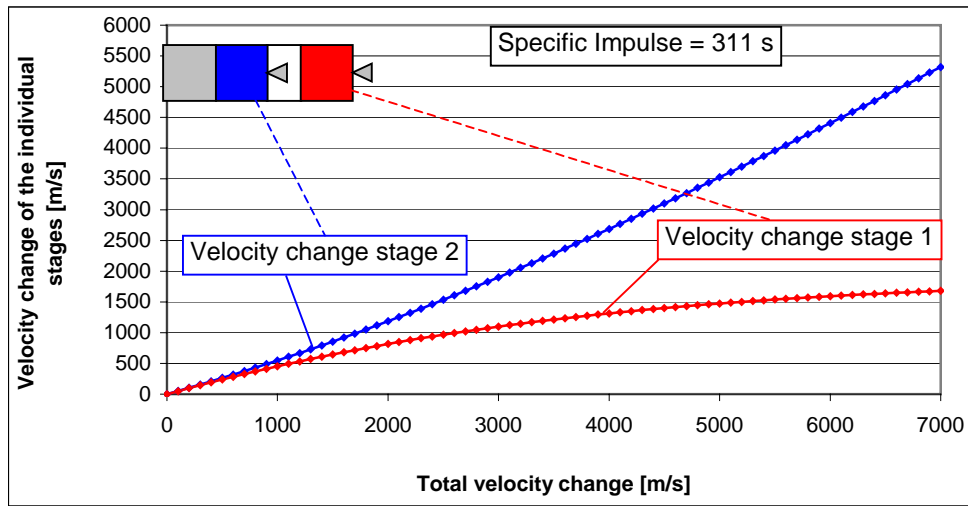


Figure 7-16: Velocity changes for two sequentially used propulsion stages with equal propellant masses (sizes) as a function of the total velocity change (for hypergolic propulsion)

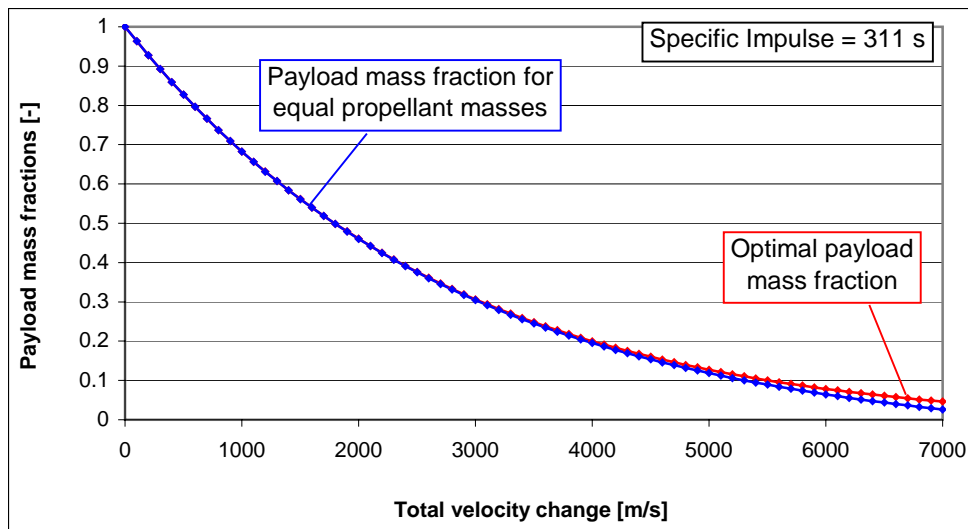


Figure 7-17: Payload mass fraction for two sequentially used propulsion stages with equal propellant masses (sizes) as a function of the total velocity change (for hypergolic propulsion) compared to the optimal payload fraction (equal velocity changes)

7.5 Appendix E: Commonality and Modularization

Appendix E provides reference data for results of the modularization process executed in Chapter 4.

7.5.1 Reference Data for Moon and Mars Architectures and Vehicles with Modularized Pressurized Volumes

This section provides reference data for the architecture configurations with modular crew compartments and habitats developed in Section 4.2. The model used for the calculation of the mass breakdown is identical to that described in Appendix C, Section 7.3.2. The input for the pressurized volumes for crew compartments and habitats is, however, different due to the modularization (see Tables 7-14 to 7-17).

<u>Vehicle</u>	<u>30-day surface habitat lander</u>	<u>180-day surface habitat lander</u>
Crew size	3, 30 d	3, 180 d
Pressurized volume [m ³]	114	228
Crew Compartment mass [kg]	14460	34164
Heat shield mass [kg]	-	-
Total crew compartment [kg]	14460	34164
Propellant combination	LCH4 / LOX	LCH4 / LOX
Initial Thrust / Weight [-]	0.4	0.4
Engine Thrust [N]	148386	348732
Velocity change [m/s]	2933	2933
Tank / Structure mass [kg]	2272	5340
Engine Mass [kg]	442	858
Propellant mass [kg]	20109	47260
Mass landing gear [kg]	531	1248
Total mass propulsion stage [kg]	23354	54706
Sum of total masses [kg]	37814	88870
Propellant combination	LH2 / LOX	LH2 / LOX
Initial Thrust / Weight [-]	0.3	0.3
Engine Thrust [N]	169255	396891
Velocity change [m/s]	1575	1575
Tank / Structure mass [kg]	1950	4572
Engine Mass [kg]	489	948
Propellant mass [kg]	17257	40467
Total mass propulsion stage [kg]	19696	45987
Sum of total masses [kg]	57510	134857
Propellant combination	LH2 / LOX	LH2 / LOX
Initial Thrust / Weight [-]	0.3	0.3
Engine Thrust [N]	257117	601697
Velocity change [m/s]	1575	1575
Tank / Structure mass [kg]	2962	6932
Engine Mass [kg]	677	1310
Propellant mass [kg]	26216	61349
Total mass propulsion stage [kg]	29855	69591
Sum of total masses [kg]	87365	204448
Total architecture mass [kg]	176571	293654

Table 7-14: Reference data for the 30-day and 180-day lunar surface habitats employing the modularized habitat structure (“plugs” + end cones)

<u>Vehicle</u>	<u>Lander / Ascender</u>	<u>Orbiter / CEV</u>	<u>14-day surface habitat lander</u>
Crew size, Duration	3, 5 d	3, 9 d	3, 14 d
Pressurized volume [m ³]	22	22	114
Crew Compartment mass [kg]	4402	5395	11108
Heat shield mass [kg]	-	1079	-
Total crew compartment [kg]	4402	6474	11108
Propellant combination	LCH4 / LOX	LCH4 / LOX	LCH4 / LOX
Initial Thrust / Weight [-]	0.4	0.3	0.4
Engine Thrust [N]	76019	32500	114199
Velocity change [m/s]	3954	1500	2933
Tank / Structure mass [kg]	1402	401	1748
Engine Mass [kg]	263	135	360
Propellant mass [kg]	12408	3552	15476
Mass landing gear [kg]	417	-	408
Total mass propulsion stage [kg]	14490	4088	17992
Sum of total masses [kg]	18892	10562	29100
Propellant combination	LCH4 / LOX	LCH4 / LOX	-
Initial Thrust / Weight [-]	0.3		-
Engine Thrust [N]	114263		-
Velocity change [m/s]	850		-
Tank / Structure mass [kg]	866		-
Engine Mass [kg]	360		-
Propellant mass [kg]	7664		-
Total mass propulsion stage [kg]	8890		-
Sum of total masses [kg]	38344		29100
Propellant combination	LH2 / LOX		LH2 / LOX
Initial Thrust / Weight [-]	0.3		0.3
Engine Thrust [N]	173763		130353
Velocity change [m/s]	1575		1575
Tank / Structure mass [kg]	2002		1501
Engine Mass [kg]	499		399
Propellant mass [kg]	17717		13291
Total mass propulsion stage [kg]	20218		15191
Sum of total masses [kg]	58562		44291
Propellant combination	LH2 / LOX		LH2 / LOX
Initial Thrust / Weight [-]	0.3		0.3
Engine Thrust [N]	263949		198157
Velocity change [m/s]	1575		1575
Tank / Structure mass [kg]	3041		2283
Engine Mass [kg]	691		553
Propellant mass [kg]	26912		20204
Total mass propulsion stage [kg]	30644		23040
Sum of total masses [kg]	89206		67331
Total architecture mass [kg]	156537		

Table 7-15: Reference data for the lunar lander, the lunar orbiter, and the 14-day lunar surface habitats employing the modularized habitat structure (“plugs” + end cones), and the CEV structure (22 m³)

<u>Vehicle</u>	<u>CEV</u>	<u>Interplanetary Transfer Habitat</u>	<u>Mars Ascent Vehicle</u>	<u>Mars Landing & Surface Habitat</u>
Crew size	6, 4 d	6, 730 d	6, 2.5 d	6, 710 d
Pressurized volume [m ³]	22	342	22	342
Crew Compartment mass [kg]	5180	61486	4402	61121
Heat shield mass [kg]	1036	-	-	-
Total crew compartment [kg]	6216		4402	61121
Sum of total masses [kg]	67702		4402	61121
Propellant combination	LCH4 / LOX		LCH4 / LOX	LCH4 / LOX
Initial Thrust / Weight [-]	0.3		0.6	0.5
Engine Thrust [N]	447741		109001	396225
Velocity change [m/s]	2600		4000	625
Tank / Structure mass [kg]	8418		1349	1362
Engine Mass [kg]	1042		347	947
Propellant mass [kg]	74495		11939	12060
Mass landing gear [kg]	-		-	4810
Total mass propulsion stage [kg]	83955		13635	19179
Sum of total masses [kg]	151657		18037	80300
Propellant combination	-		LCH4 / LOX	-
Initial Thrust / Weight [-]	-		0.5	-
Engine Thrust [N]	-		116579	-
Velocity change [m/s]	-		625	-
Tank / Structure mass [kg]	-		400	-
Engine Mass [kg]	-		366	-
Propellant mass [kg]	-		3548	-
Mass landing gear [kg]	-		1415	-
Total mass propulsion stage [kg]	-		5729	-
Parachute Mass [kg]	1516		237	803
Heat shield mass [kg]	22975		3600	12165
Sum of total masses [kg]	176148		27603	93268
Propellant combination	LH2 / LOX		LH2 / LOX	LH2 / LOX
Initial Thrust / Weight [-]	0.3		0.3	0.3
Engine Thrust [N]	919947		131385	442407
Velocity change [m/s]	2150		1800	1800
Tank / Structure mass [kg]	13618		1689	5688
Engine Mass [kg]	1822		402	1032
Propellant mass [kg]	120519		14948	50336
Total mass propulsion stage [kg]	135959		17039	57056
Sum of total masses [kg]	312107		44642	150324
Propellant combination	LH2 / LOX		LH2 / LOX	LH2 / LOX
Initial Thrust / Weight [-]	0.3		0.3	0.3
Engine Thrust [N]	1626068		212174	712250
Velocity change [m/s]	2150		1800	1800
Tank / Structure mass [kg]	24071		2727	9157
Engine Mass [kg]	2836		583	1494
Propellant mass [kg]	213025		24141	81039
Total mass propulsion stage [kg]	239932		27451	91690
Sum of total masses [kg]	552039		72093	242014
Total architecture mass [kg]	866146			

Table 7-16 Reference data for a fast-conjunction class Mars mission architecture employing a free return, and using the modularized habitat structure (“plugs” + end cones), and the CEV structure (22 m³)

<u>Vehicle</u>	<u>CEV</u>	<u>Interplanetary Transfer Habitat</u>	<u>Mars Ascent Vehicle</u>	<u>Mars Landing & Surface Habitat</u>
Crew size	6, 4 d	6, 470.5 d	6, 2.5 d	6, 62.5 d
Pressurized volume [m ³]	22	342	22	228
Crew Compartment mass [kg]	5180	56753	4402	30114
Heat shield mass [kg]	1036	-	-	-
Total crew compartment [kg]	6216	56753	4402	30114
Sum of total masses [kg]	62969		4402	30114
Propellant combination	LCH4 / LOX		LCH4 / LOX	LCH4 / LOX
Initial Thrust / Weight [-]	0.3		0.6	0.5
Engine Thrust [N]	368759		109001	197295
Velocity change [m/s]	2221		4000	625
Tank / Structure mass [kg]	6188		1349	678
Engine Mass [kg]	896		347	551
Propellant mass [kg]	54766		11939	6005
Mass landing gear [kg]	-		-	2395
Total mass propulsion stage [kg]	61850		13635	9629
Sum of total masses [kg]	124819		18037	39743
Propellant combination	LCH4 / LOX		LCH4 / LOX	-
Initial Thrust / Weight [-]	0.3		0.5	-
Engine Thrust [N]	726781		116579	-
Velocity change [m/s]	2221		625	-
Tank / Structure mass [kg]	12197		400	-
Engine Mass [kg]	1517		366	-
Propellant mass [kg]	107938		3548	-
Mass landing gear [kg]	-		1415	-
Total mass propulsion stage [kg]	121652		5729	-
Parachute Mass [kg]	2464		237	397
Heat shield mass [kg]	37340		3600	6021
Sum of total masses [kg]	286275		27603	46161
Propellant combination	LH2 / LOX		LH2 / LOX	LH2 / LOX
Initial Thrust / Weight [-]	0.3		0.3	0.3
Engine Thrust [N]	1618821		131385	219372
Velocity change [m/s]	2446.5		1800	1800
Tank / Structure mass [kg]	26445		1689	2820
Engine Mass [kg]	2826		402	598
Propellant mass [kg]	234031		14948	24960
Total mass propulsion stage [kg]	263302		17039	28378
Sum of total masses [kg]	549577		44642	74539
Propellant combination	LH2 / LOX		LH2 / LOX	LH2 / LOX
Initial Thrust / Weight [-]	0.3		0.3	0.3
Engine Thrust [N]	3101107		212174	353768
Velocity change [m/s]	2446.5		1800	1800
Tank / Structure mass [kg]	50660		2727	4548
Engine Mass [kg]	4682		583	867
Propellant mass [kg]	448323		24141	40251
Total mass propulsion stage [kg]	503665		27451	45666
Sum of total masses [kg]	1053242		72093	120205
Total architecture mass [kg]	1245540			

Table 7-17: Reference data for a 60-day short Mars mission architecture employing a Venus flyby, and using the modularized habitat structure (“plugs” + end cones), and the CEV structure (22 m³)

7.5.2 Modular Building Blocks for the CEV Electrical Power Subsystem Equipment

This section provides results for the modularization of the electrical power subsystem hardware for the CEV. The results are qualitatively of the same nature and indicate the same trends as those for the life support hardware given in Chapter 4.4. This is due to the characteristic that the equipment mass is proportional to the crew size; both the life support and power systems exhibit this characteristic.

In reality, the electrical power need, which sizes the power subsystem consists of two parts: one is proportional to the number of crew (ECLSS, thermal control, communication, etc. power needs), and the other is independent of the crew size (avionics, RCS, etc. power needs). For the analysis here it is assumed that the first group dominates the second.

Hydrogen / oxygen fuel cells with efficiencies comparable to those used for NASA's Reusable Lunar Lander design [NASA OASIS, 2004; Wingo, 2004] are assumed to be employed for the power generation.

The mass overhead due to modularization has two causes:

- Additional equipment mass caused by surplus functionality, and
- Interface masses required to connect the modules to the rest of the system.

The normalized mass overhead in this context is defined by the following equation:

$$\eta = \frac{\sum_i n_i \cdot (m_{BuildingBlock} + m_{Interface}) - \sum_i m_{Point\ Design}}{\sum_i m_{Point\ Design}} \quad \text{Equation 7-28}$$

The index i refers to the different CEV configurations encountered (3-crew, 4-crew, 6-crew). In Figure 7-18, the normalized mass surplus is shown over the building block mass for the 3- and 6-crew cases, in Figure 7-19 for the 3-, 4-, and 6-crew CEVs. As stated in Chapter 4.4 for the life support equipment, in the case of the electrical power equipment it is also desirable to choose the building block size so that the strategic option is preserved to use the CEV with a crew size of four without an undue mass overhead. The optimal building block for the electrical power system would, under these conditions, have a mass of about 200 kg.

The analysis presented here and in Section 4.4 is only preliminary; detailed modeling and modularization of subsystems has to be carried out in the future, including modular EVA systems [Hoffman, 2004; de Weck, 2004].

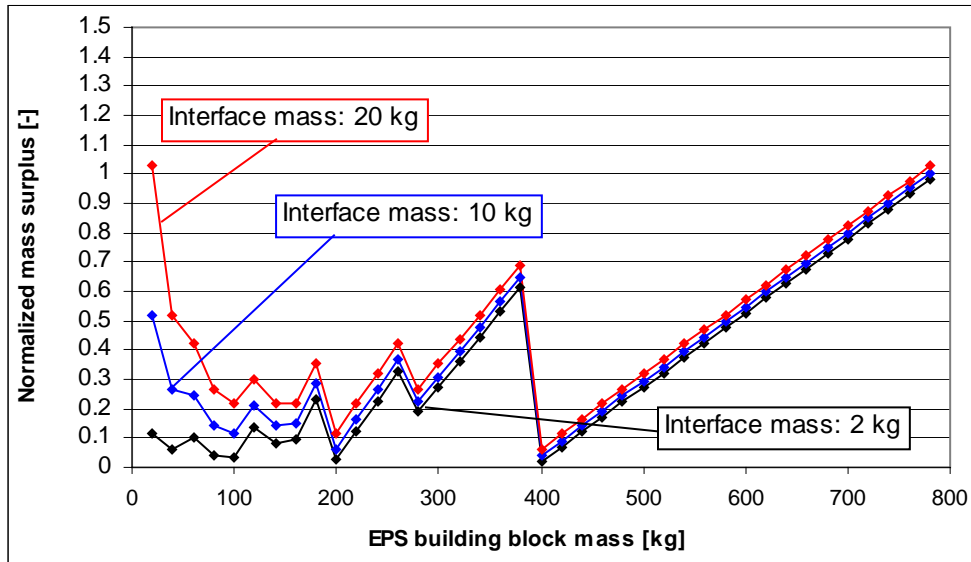


Figure 7-18: Normalized modularization mass penalty for the electrical power equipment dry mass due to interface masses and surplus functionality for a 3-, and a 6-crew CEV

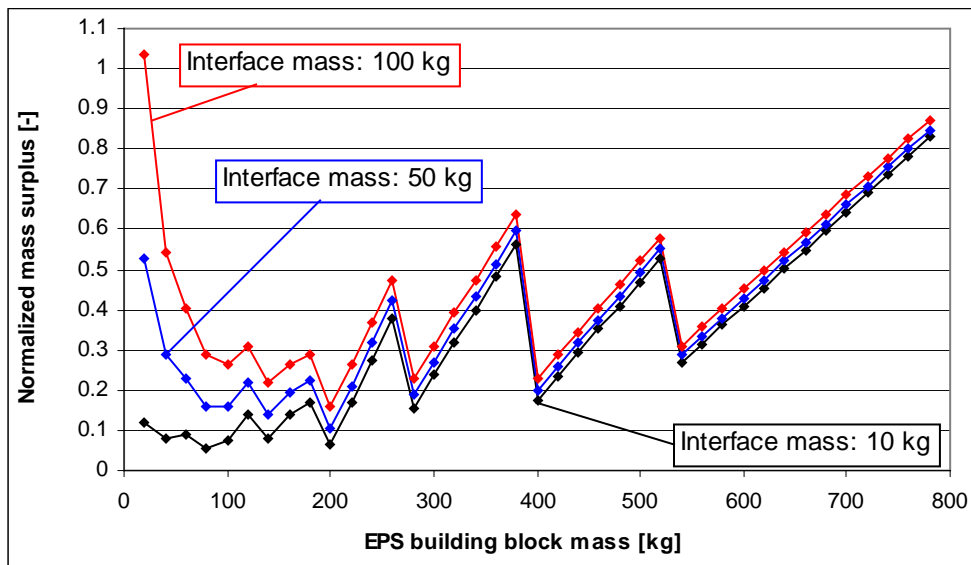


Figure 7-19: Normalized modularization mass penalty for the electrical power equipment dry mass due to interface masses and surplus functionality for a 3-, a 4-, and a 6-crew CEV